Modelling GATA2 Haploinsufficiency Driven Immunodeficiency and Myelodysplastic Syndromes /Acute Myeloid Leukaemia

Ali Abdelfattah

A thesis presented in partial fulfilment of the requirements for the degree of Doctor of Philosophy
At

Cardiff University

College of Biomedical and Life Sciences

School of Biosciences - Biomedicine

November 2020

DECLARATION

Statement 1
This thesis is being submitted in partial fulfilment of the requirements for the degree of PhD.

Signed: Ali Abdelfattah
Data: 30/11/2020

Statement 2
This work has not been submitted in substance for any other degree or award at this or any other university or place of learning, nor is it being submitted concurrently for any other degree or award (outside of any formal collaboration agreement between the University and a partner organisation).

Signed: Ali Abdelfattah
Data: 3011/2020

Statement 3
I hereby give consent for my thesis, if accepted, to be available in the University's Open Access repository (or, where approved, to be available in the University's library and for inter-library loan), and for the title and summary to be made available to outside organisations, subject to the expiry of a University-approved bar on access if applicable.

Signed: Ali Abdelfattah
Data: 30/11/2020

Declaration
This thesis is the result of my own independent work, except where otherwise stated, and the views expressed are my own. Other sources are acknowledged by explicit references. The thesis has not been edited by a third party beyond what is permitted by Cardiff University's Use of Third-Party Editors by Research Degree Students Procedure.

Signed: Ali Abdelfattah
Data: 30/11/2020

Word count of thesis: 38832
Excluding the summary, acknowledgements, declarations, contents pages, appendices, tables, diagrams and figures, references, bibliography, footnotes, and endnotes.

ACKNOWLEDGMENTS

In the first place, I would like to thank and express my greatest appreciation to my supervisor Dr. Neil Rodrigues for offering me the opportunity to work under his supervision and for his valuable suggestions, practical advice, constructive feedback, and continuous help and support throughout this research work. I am also grateful to my co-supervisor Dr. Alex Tonks for his mentor and guidance.

I would like to extend my appreciation to all ECSRI lab members, in particular Dr. Gui Feng, Dr. Juan Menendez, Dr. Alhomidi Almotiri, Leigh-Anne Thomas, and Hamed Alzahrani for their support and helpful advice during these years.

I would like to thank the ECSCRI staff Mark Bishop and Jolene Twomey for their support with flow cytometry. I wholly appreciate Wales Gene Park members Dr. Karen Reed, Dr. Peter Giles, and Shelley Rundle for their assistance with RNA sequencing and bioinformatic analysis. I would also like to be grateful to Heath Park members Kerry Housler, Deborah Adams, Patrick Mason, Roy Davies, Rebecca Underwood, and Matthew Jones for their help with animal husbandry.

I would like to express my special thanks and sincere love to my wife Dua'a Sokker, my children Omar and Salma, my sister and brothers, my nieces and nephews, and all my friends for their love, patience, persistent help, and endless support. I would not have accomplished this project without your encouragement.

Finally, I am extremely grateful to my sponsor The Hashemite University for giving me the opportunity to study at Cardiff University and for their financial assistance, advice, and support.

ABSTRACT

HSCs are entirely responsible for the continuous replenishment of short-lived blood cells to preserve haematopoietic homeostasis. GATA2, a zinc-finger transcription factor, is highly expressed within HSPCs and operates different aspects of HSC functions in the embryonic and adult haematopoietic system. Since either low or high GATA2 expression is involved in leukaemogenesis, the balanced expression of GATA2 is therefore indispensable for retaining normal haematopoiesis. Acquired *ASXL1* mutations are recurrently existent in MDS/AML patients harbouring inherited *GATA2* mutations. While GATA2 haploinsufficiency causes BM failure disorders that can predispose to myeloid malignancies, little information is known about affected HSPC compartments and underlying molecular mechanisms in this context. With the intention to mimic inherited and acquired GATA2 haploinsufficiency disorders, conditional knockout mice models were employed to elucidate the impact of *Gata2* haploinsufficiency on adult HSPCs and haematopoiesis.

Analysis of young *Gata2* haploinsufficient mice utilising a pan haematopoietic Vav-iCre approach revealed a reduction in HSCs, MPPs, MPP4 (LMPPs), early erythroid-progenitors (Pre-MegE/Pre-CFU-E), myeloid-progenitors (Pre-GM/GMP) and megakaryocyte-subpopulations (Pre-MegE/MkPs/megakaryocytes/platelets), but an increase in MPP2. The reduced HSC numbers were associated with increased cellular quiescence and apoptosis rates. The abundance of HSCs, MPPs, LMPPs and CLPs was decreased in aged *Gata2*$^{+/fl}$*;Vav-iCre*$^{+}$ mice although aged HSCs became more proliferative than young HSCs. Acute loss of *Gata2* heterozygote applying the inducible Mx1-Cre model exhibited attenuation in HSCs frequency with an increase in the number of quiescent HSCs. Functionally, acute and chronic ablation of *Gata2* haploinsufficiency resulted in a severe defect in long-term multi-lineage reconstitution and self-renewal capacities of adult HSCs post-transplantation. The DNA damage repair and proinflammatory signalling were the most affected biological pathways in *Gata2* haploinsufficient HSCs. Cooperative haploinsufficient mice of *Gata2* and *Asxl1* (*Gata2*$^{+/fl}$*;Asxl1*$^{+/fl}$*;Vav-iCre*$^{+}$) showed increased HSCs proliferation and decreased HSCs survival, which led to impaired long-term engraftment capability of HSCs and ultimately depleted HSCs pool during stress haematopoiesis. Together, *Gata2* haploinsufficiency interrupts HSCs survival, proliferation, self-renewal, and maintenance. Thus, biallelic expression of *Gata2* is essentially required for preserving adult HSPCs homeostasis.

TABLE OF CONTENTS

LIST OF TABLES

LIST OF FIGURES

ABBREVIATIONS

AGM	Aorta Gonad Mesonephros
ALL	Acute Lymphoblastic Leukaemia
AML	Acute Myeloid Leukaemia
Ang-1	Angiopoietin-1
ASXL1	Additional Sex Combs Like member-1
ATP	Adenosine Triphosphate
BM	Bone Marrow
BMI1	B-lymphoma Mo-MLV Insertion region-1
bp	Base pair
CAR	CXCL12 Abundant Reticular cells
CB	Cord blood
CDK	Cyclin Dependent Kinases
cDNA	Complementary DNA
CEBPα	CCAAT/Enhancer Binding Protein Alpha
CFC	Colony Forming Cell
CFU	Colony Forming Unit
CFU-E	Colony Forming Unit Erythrocyte
CFU-G	Colony Forming Unit Granulocyte
CFU-GEMM	Granulocyte/Erythroid/Macrophage/Megakaryocyte
CFU-GM	Colony Forming Unit Granulocyte/Macrophage
CFU-M	Colony Forming Unit Macrophage
CITED2	CBP/p300 Interacting Transactivators with glutamic/aspartic acid
CLL	Chronic Lymphocytic Leukaemia
CLP	Common Lymphocyte Progenitor
CML	Chronic Myeloid Leukaemia
CMML	Chronic Myelo-Monocytic Leukaemia
CMP	Common Myeloid Progenitor
CT	Cycle Threshold
Cxcl4	Chemokine C-X-C motif ligand-4
DMEM	Dulbecco's Modified Eagle's Medium
DNA	Deoxyribonucleic Acid
DNMT3	DNA (cytosine-5) Methyltransferase-3
E	Embryonic day
ECM	Extra Cellular Matrix

EDTA	Ethylene Diamine Tetra Acetic acid
Ev	Empty vector
EVI1	Ecotropic pro-Viral Integration site 1
FAB	French American British classification
FACS	Fluorescence Activated Cell-Sorting
FBS	Foetal Bovine Serum
FDR	False Discovery Rate
FLT3	Fms Related Tyrosine Kinase-3
g	Gram
GATA	GATA binding protein
G-CSF	Granulocyte Colony Stimulating Factor
GFI1	Growth Factor Independent-1
GMP	Granulocyte/Macrophage Progenitor
GSEA	Gene Set Enrichment Analysis
HOX	Homeobox
HPC1	Haematopoietic Progenitor Cell-1
HPC2	Haematopoietic Progenitor Cell-2
HSC	Haemopoietic Stem Cell
HSPC	Haemopoietic Stem and Progenitor Cell
ICP	Ingenuity Canonical Pathway
iCre	Improved Cre Recombinase
IDH1/2	Isocitrate Dehydrogenase1/2
IL	Interleukin
IL4	Interleukin-4
IL6	Interleukin-6
IMDM	Iscove's Modified Dulbecco's Medium
inv	Inversion
IPA	Ingenuity Pathway Analysis
IPSS	International Prognostic Scoring System
KEGG	Kyoto Encyclopaedia of Genes and Genomes
KO	Knockout
L	Litre
Lineage$^-$(Lin$^-$)	Primitive haematopoietic cells
LMO2	LIM Domain Only-2
LMPP	Lymphoid Primed Multipotent Progenitor
LoxP	locus of X over P1 bacteriophage

LSC	Leukaemic Stem Cell
LTC-IC	Long-Term Culture Initiating Cell
LT-HSC	Long-Term Haemopoietic Stem Cell
LTR	Long Terminal Repeat
MACS	Magnetic Activated Cell Sorting
MDS	Myelodysplastic Syndrome
MegE	Megakaryocyte/erythroid progenitor
MEIS	Myeloid Ectropic Insertion Site
MEP	Megakaryocyte/Erythroid Progenitor
mg	Milligram
Mk	Megakaryocyte
MkP	Megakaryocyte Progenitor
mL	Millilitre
MLL	Mixed Lineage Leukaemia
mM	Millimolar
MPN	Myeloproliferative Neoplasms
MPP	Multipotent Progenitor
mRNA	Messenger Ribo Nucleic Acid
MSC	Mesenchymal Stem Cell
Mx1	Myxovirus dynamin like GTPase-1
NH4Cl	Ammonium Chloride
NMP1	Nucleophosmin-1
PB	Peripheral Blood
PBS	Phosphate Buffered Saline
PcG	Polycomb Genes
PCR	Polymerase Chain Reaction
pIpC	Polyinosinic polycytidylic acid
PLTs	Platelets
PRC1/2	Polycomb Repressor Complex-1/2
Pre CFU-E	Pre-Colony Forming Unit Erythrocyte
Pre-GM	Pre-Granulocyte/Macrophage progenitors
PU.1	Purine Rich sequence 1
qRT-PCR	Quantitative Reverse Transcription-Polymerase Chain Reaction
RBC	Red blood cell
rcf	Relative centrifugal force
RNA	Ribo Nucleic Acid

rpm	Revolutions per minute
RT	Room Temperature
RUNX1	Runt related transcription factor 1
SCA-1	Stem Cells Antigen-1
SCF	Stem Cell Factor
SCFR/c-Kit	Stem Cell Growth Factor Receptor
SCL/TAL1	Stem Cell Leukaemia /T-cell Acute Lymphocytic Leukaemia-1
SDF1	Stromal Derived Factor-1
SEM	Standard Error of-Mean
sh	Short hairpin
SLAM	Signalling Lymphocyte Activation Molecule
SOX17	SRY Related HMG box-17
STAT3	Signal Transducer and Activator of Transcription-3
STAT5	Signal Transducer and Activator of Transcription-5
ST-HSC	Short-Term Haemopoietic Stem Cell
t	Translocation
TET2	Ten Eleven Translocation gene 2
TFs	Transcription Factors
TGF-β	Transforming Growth Factor-β
TPO	Thrombopoietin
TrxG	Trithorax Genes
WBCs	White Blood Cells
WHO	World Health Organisation
WT	Wild Type
ZnF	Zinc Finger
µg	Microgram
µL	Microliter

CHAPTER 1 : Introduction

1.1 Haematopoiesis

1.1.1 Introduction to haematopoiesis

The haematopoietic system is mainly constituted of three types of mature blood cells: Red blood cells ((RBCs), erythrocytes), white blood cells ((WBCs), leukocytes), and platelets ((PLTs), thrombocytes). These cells have separable basic functions including transport indispensable molecules, protection against pathogens, and prevention of bleeding. Although mature blood cells are heterogeneous in their biological function, all cells arise from haematopoietic stem cells (HSCs). HSCs are multifunctional cells that have the competency to differentiate into all other blood cells throughout the process of haematopoiesis. The term haematopoiesis can be defined as a multipart developmental process of blood cell production that includes cell formation, proliferation, differentiation and specialisation into functional mature blood cells that are released from the bone marrow, a centric place of adult haematopoiesis, to the circulation (Rieger and Schroeder, 2012, Orkin and Zon, 2008, Seita and Weissman, 2010).

Mature blood cells have a limited lifespan and must be continuously replaced throughout the organism's life. HSCs provide multi-lineage progenitors to maintain the turnover of the blood formation during the lifetime of an organism (Rieger and Schroeder, 2012, Orkin and Zon, 2008, Seita and Weissman, 2010). Exclusively, HSCs have the potential for both self-renewal (HSCs replication and maintenance) and differentiation (formation of functional blood cells) capacities to sustain HSCs pool size and mature blood cells homeostasis, respectively (Rieger and Schroeder, 2012, Orkin and Zon, 2008, Seita and Weissman, 2010). The capacity of HSCs to either self-renewal or differentiation is tightly regulated by a complicated network of intrinsic (transcription factors) and extrinsic (BM microenvironment (BM niches)) mechanisms as growth factors, cytokines, and signalling pathways (Rieger and Schroeder, 2012, Orkin and Zon, 2008, Seita and Weissman, 2010). Disruptions of these mechanisms

are directly linked to haematological diseases such as anaemia, leukopenia, thrombocytopenia, and different forms of leukaemia.

1.1.2 Origin and development of murine haematopoietic stem cells

Haematopoietic stem cells (HSCs) were discovered by Till and McCulloch in 1961 following a sequence of *in vivo* experiments (Till and McCulloch, 1961). After murine bone marrow cells were transplanted into lethally irradiated recipient mice, colonies of haematopoietic cells were later observed within the spleens of the recipient mice. These colonies were called colony-forming units-spleen (CFU-S) and contained populations of myeloid-erythroid cells. Subsequent experiments revealed that the haematopoietic colonies came from a single originating cell that also possessed a lymphoid capability (Till and McCulloch, 1961, Wu et al., 1968). Furthermore, serial transplantation experiments of spleen haematopoietic cells revealed that CFU-S colonies were able of repopulating haematopoietic cells in the secondary recipient mice (Siminovitch et al., 1963). Together, these experiments outline that HSCs possess the capability for both multi-lineage reconstitution and self-renewal capabilities. Thereafter, investigations in the field of haematopoiesis have been broadly extended to further clarify biological functions of HSCs and haematopoietic progenitors.

Foetal and adult haematopoiesis happens in distinct anatomical places (Figure 1.1). During murine embryogenesis, the evolution of haematopoietic cells commences at embryonic day 7.5 (E 7.5) in the yolk sac blood islands (known as haemangioblasts) that generate primitive erythroid cells and blood vessels (Palis et al., 1999). These cells are incapable of reconstituting long-term haematopoiesis of irradiated hosts (Müller et al., 1994). The definitive haematopoiesis with functional properties of adult HSCs takes place in the Aorto-Gonad-Mesonephros region at E10.5, where these cells are capable of repopulating blood multi-lineage in irradiated recipients (Müller et al., 1994, Medvinsky and Dzierzak, 1996). In this region, HSCs arise from the haemogenic endothelial cells of the dorsal aorta (Eilken et al., 2009). At the same time, HSCs are found in the vitelline and umbilical arteries, and the placenta (de Bruijn et al., 2000). Later, the definitive haematopoietic cells migrate into the foetal

liver, thymus, spleen and in the end to the BM which becomes the central provider of HSCs after birth (Christensen et al., 2004).

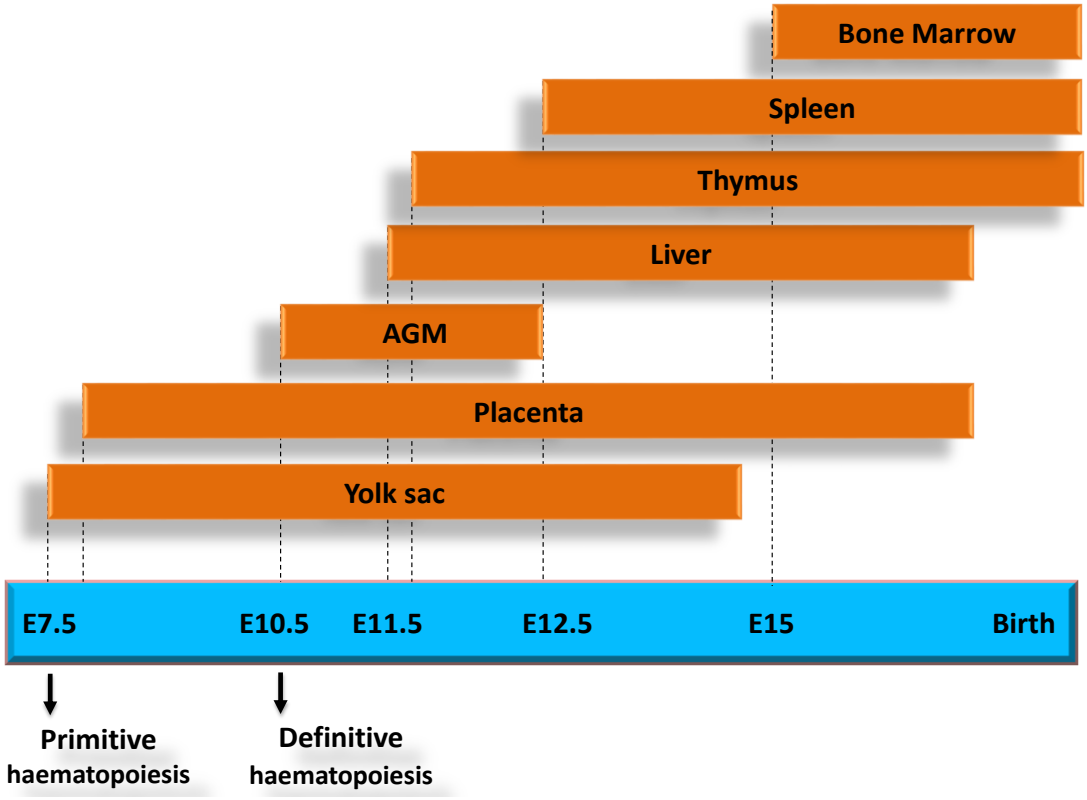

Figure 1-1: Timeline and anatomical sites of murine haematopoiesis development.
The diagram illustrates the generation of haematopoietic stem cells throughout the sequence of embryonic developments. AGM, Aorto-Gonad-Mesonephros; E, embryonic day. (Adapted from (Rieger and Schroeder, 2012)).

Foetal and adult murine HSCs are different in their functional characteristics and immunophenotypic/gene expression. Although foetal HSCs are active in the cell cycle, the majority of adult HSCs are in a quiescent state. Thus, foetal HSCs reconstitute irradiated recipient hosts about five times faster than adult HSCs in transplant experimentations (Harrison et al., 1997). Foetal HSCs switch to adult HSCs and become quiescent at around four weeks after birth to preserve blood production and prevent HSCs exhaustion throughout an organism life (Ye et al., 2013, Kim et al., 2007). The transition to adult HSCs is proposed to be regulated by SRY-related HMG-box-17 (*Sox-17*) and CCAAT/enhancer-binding protein-alpha (*Cebpα*) transcription

factors (Ye et al., 2013, Kim et al., 2007). Deletion of *Sox-17* in foetal haematopoietic cells displayed a severe reduction in definitive HSCs, whereas no difference in the adult HSC numbers was observed in *Sox-17*-null mice (Kim et al., 2007). Switching to adult HSCs was accompanied by a reduction in *Sox-17* expression and a diminution in HSCs proliferation. These results indicate that *Sox-17* is indispensable for the development and maintenance of foetal HSCs. High expression of *Cebpα* is also required during the adult HSCs transition and promotes HSCs quiescence (Ye et al., 2013). Deletion of *Cebpα* in adult HSCs showed an increment in HSC proliferation rates. *Cebpα* expression analysis revealed that the expression of *Cebpα* mRNA was intensively increased in HSCs in four-weeks old mice as compared with two-weeks old mice. Together, *Sox-17* and *Cebpα* transcription factors regulate foetal HSCs switching into adult HSCs.

1.1.3 Murine haematopoietic hierarchy and immunophenotypic characterisations

More recently, several techniques have been used to properly identify the hierarchy of haematopoietic cells such as cell surface marker phenotypes, gene expression and transplantation studies. Haematopoiesis is organised in a hierarchical manner, in which multipotent haematopoietic stem and progenitor cells (HSPCs) differentiate to oligopotent progenitors and subsequently generate restricted precursors and finally segregate into mature blood cells (Figure. 1.2 A). HSPCs are a heterogeneous compartment and contain three subsets of populations: Long-term HSCs (LT-HSCs), Short-term HSCs (ST-HSCs) and Multipotent progenitors (MPPs). The classical model suggests that LT-HSCs have self-renewal potential and give rise to ST-HSCs and MPPs that possess limited self-renewal ability but can differentiate into multi-lineage (Figure. 1.2 A) (Morrison et al., 1997, Okada et al., 1992). In 1988, the prospective purification of HSCs from mouse bone marrow was achieved by using the fluorescence-activated cell sorting (FACS) technology depending on cell surface marker phenotypes (Spangrude et al., 1988). HSPCs are negative for mature cell lineage markers (lineage cocktail antibodies contain: T-cells, CD3; B-cells, B220; T-helper, CD4; T-cytotoxic, CD8; RBCs, Ter119; Monocytes, Mac1; and Neutrophils, Gr1)

and express both stem cell antigen (Sca-1) and stem cell factor (c-kit; CD117) receptors which are known as LSK cells (Lin^-_$Sca\text{-}1^+$_$c\text{-}kit^+$) (Spangrude et al., 1988, Ikuta and Weissman, 1992). LT-HSCs, ST-HSCs and MPPs reside within the LSK compartment. Functionally, LT-HSCs provide long-term reconstitution abilities for all haematopoietic cells of lethally irradiated recipients whereas either ST-HSCs or MPPs only confer short-term repopulation potentials. LSK cells represent around 0.1% of total BM cells and LT-HSCs exist in approximately 10% of the LSK compartment in BM young mice (Morrison et al., 1996, Ikuta and Weissman, 1992, Spangrude et al., 1988). Additional markers are required to identify HSCs within the LSK population. Three distinct subpopulations can be identified using Thy1.1 (CD90) and FMS-like tyrosine kinase 3 (Flt3 (CD135)) cell surface receptors: LT-HSCs, LSK_$CD90^{low}$_$CD135^-$; ST-HSCs, LSK_$CD90^{low}$_$CD135^+$; and MPPs, LSK_$CD90^-$_$CD135^+$ (Christensen and Weissman, 2001). Since the expression of Thy1.1 receptor is restricted to some mouse strains, the CD38 antigen is expressed in all mouse species and provides a suitable marker for the purification of HSPCs (Randall et al., 1996). LT-HSCs are enriched in LSK_$CD34^-$_$CD38^+$ compartments while ST-HSCs are identified as LSK_$CD34^+$_$CD38^-$ compartments.

Further downstream, MPPs give rise to oligopotent progenitors that are committed to either common myeloid progenitors (CMP) or common lymphoid progenitors (CLP) which lose self-renewal capability and differentiate into restricted cell types (Kondo et al., 1997, Akashi et al., 2000). In lymphoid lineages, CLPs reside in Lin^-_$Sca\text{-}1^{low}$_$c\text{-}Kit^{low}$ and express the interleukin-7 receptor α-chain (IL-7Rα; CD127) marker and give rise to B-cell, T-cells and natural killer restricted precursors that ultimately differentiate into mature B cells, T cells and NK cells (Figure 1.1 A) (Kondo et al., 1997). Nevertheless, previous studies showed that Lin^-_$Sca\text{-}1^{low}$_$c\text{-}Kit^{low}$_$CD127^+$ CLPs at most gave rise to B-cells rather than T-cells in transplantation settings (Karsunky et al., 2008). The CD135 antigen is added to robustly purify CLPs. CLPs can be recognised as Lin^-_$Sca\text{-}1^{low}$_$c\text{-}Kit^{low}$_$CD127^+$_ $CD135^+$ and reconstitute both B-cells and T-cells without any lineage-biases (Karsunky et al., 2008). On the other hand, committed myeloid progenitors localise within Lin^-_$Sca\text{-}1^-$_$c\text{-}Kit^+$ cells (Akashi et al., 2000). CMPs are known as LK_$CD34^+$_$CD16/32^-$(Fcγ-II/III receptor) and advance into

megakaryocyte/erythrocyte progenitors (MEP; LK_CD34^{-}_CD16/32^{-}) and granulocyte /macrophage progenitors (GMP; LK_CD34^{+}_CD16/32^{+}) (Akashi et al., 2000). MEPs and GMPs differentiation are committed to megakaryocytes-erythrocytes and granulocytes-macrophages (monocytes, neutrophils, eosinophils, and basophils) mature blood cells, respectively.

Akashi's group has recently redefined the immunophenotype of CMPs (Miyawaki et al., 2015). The new CMPs are LSK_CD34^{+}_CD41^{high} and differentiate into the previous CMPs with robust potency toward myeloid/erythroid lineages (Figure 1.2 E). Additionally, CD150, Integrin subunit alpha-2b (CD41), and Endoglin (CD105) markers are used to further identify myeloid precursors (Pronk et al., 2007). In myeloid-lineages, CMPs segregate into pre-granulocyte/macrophage precursors (Pre-GM; LK_CD150^{-}_CD41^{-}_CD16/32^{-}_CD105^{-}) and then advance to GMPs (LK_CD150^{-}_CD41^{-}_CD16/32^{+}). In erythroid-megakaryocyte lineages, CMPs differentiate into erythroid/megakaryocyte progenitors (Pre-MegE; LK_CD150^{+}_CD41^{-}_CD16/32^{-}_CD105^{-}) that ultimately produce either megakaryocyte-progenitors (MkP; LK_CD150^{+}_CD41^{+}) or erythroid-precursors (Pre CFU-E; LK_CD150^{+}_CD41^{-}_CD16/32^{-}_CD105^{+})(Figure 1.2 D).

Adolfsson et al. demonstrated an alternative model of the haematopoietic lineage commitment (Adolfsson et al., 2005). They recognised a subset known as lymphoid-primed multipotential progenitors (LMPPs) that have the potential to generate both CLPs and GMPs but lose the ability to differentiate into megakaryocytes and erythrocytes, whereas the MEP is directly derived from the ST-HSC/MPP compartments. In this model, CMPs are excluded from the hierarchy (Figure 1.2 B). Thus, LT-HSCs reside in LSK_CD34^{-}_CD135^{-}, ST-HSCs exist in LSK_CD34^{+}_CD135^{-}, MPPs enrich in LSK_CD34^{+}_CD135^{+}, and LMPPs can be isolated by LSK_CD34^{+}_CD135^{High} (Adolfsson et al., 2005, Adolfsson et al., 2001). In addition, both classical and alternative models merge into the composite model because CMPs have already been identified as LK_CD34^{+}_CD16/32^{-} (Adolfsson et al., 2005, Iwasaki and Akashi, 2007). In this model, ST-HSCs advance into CMPs and LMPPs. CMPs together with LMPPs possess the potential to differentiate into GMPs (Figure 1.2 C).

Furthermore, the expression of cell surface receptors of the signalling lymphocyte activation molecule (SLAM) family (CD150 (Slamf1) and CD48 (Slamf2)) is subdivided LSK heterogeneous compartment to four distinct subpopulations: HSCs, LSK_ $CD150^{+}$_$CD48^{-}$; MPPs, LSK_$CD150^{-}$_$CD48^{-}$; HPC1, LSK_$CD150^{-}$_$CD48^{+}$; and HPC2, LSK_$CD150^{+}$_$CD48^{+}$ (Figure. 1.2 F) (Kiel et al., 2005, Oguro et al., 2013). HPC1 and HPC2 compartments are heterogenous committed progenitors in which HPC1 cells possess the potential to differentiate into lymphoid and myeloid progenitors and lose megakaryocytes/ erythrocytes potential, while HPC2 cells give rise to all restricted haematopoietic progenitors and possess less T-lymphoid potential (Oguro et al., 2013). HPC1 cells are extremely close to LMPPs because HPC1 cells are highly positive for Flt3 (approximately 75%) and both HPC1 and LMPPs have lymphoid/myeloid reconstitution potential (Oguro et al., 2013). High expression of CD150 within HSPCs retains their self-renewal potential whereas high expression of CD48 drives HSPCs to lose their self-renewal ability (Oguro et al., 2013). The expression of CD150 in LSK_$CD34^{-}$ compartments determines the self-renewal capability of HSCs and provides insights into myeloid/lymphoid biased HSCs potential (Beerman et al., 2010, Morita et al., 2010). Three subpopulations can be isolated depending on the CD150 expression: Myeloid-biased-HSCs, LSK_$CD34^{-}$_$CD150^{high}$; lymphoid-biased-HSCs, LSK_$CD34^{-}$_$CD150^{-/low}$; and balanced-biased-HSCs, LSK_$CD34^{-}$_$CD150^{intermediate}$. $CD150^{high}$_HSCs are the highest self-renewal potency and possess a robust ability of reconstituting all CD150 fractions in sequential transplantation experiments. in this thesis, slam family markers were utilised to identify murine primitive haematopoietic populations.

However, since the primitive myeloid/lymphoid/erythroid/megakaryocyte progenitors were indistinguishable in the previous models, Pietras et al. have suggested another model of the haematopoietic hierarchy distinguishing myeloid/lymphoid/erythroid/megakaryocytes biased progenitors (Figure. 1.2 G) (Pietras et al., 2015). The Flt3 marker is used in combination with slam markers to dissect HSPCs into five individual sub-compartments: LT-HSCs, LSK_$Flt3^{-}$_ $CD150^{+}$_$CD48^{-}$; ST-HSCs (MPP1), LSK_$Flt3^{-}$_$CD150^{-}$_$CD48^{-}$; MPP2, LSK_$Flt3^{-}$_ $CD150^{+}$_$CD48^{+}$; MPP3, LSK_$Flt3^{-}$_$CD150^{-}$_$CD48^{+}$; and MPP4, LSK_$Flt3^{+}$_$CD150^{-}$_

CD48^{+}. In this model, MPP2 and MPP3 progenitors are myeloid-biased-MPPs with low potency to output lymphoid cells whereas MPP4 progenitors are lymphoid-biased-MPPs and retain their GMP potential. In addition, their results provide additional comprehension of the dynamics of haematopoietic lineages regeneration in lethally irradiated hosts. In the first two weeks post-transplant, rebuilding the haematopoiesis system is characterised by an increase in myeloid-biased-MPPs production, an increment in myeloid cells product via lymphoid-biased-MPPs, and a decline in HSCs self-renewal capability. Subsequently, lymphoid-biased-MPPs restore their lymphoid potential at week 3 following transplantation. The restoration of HSC self-renewal potential occurs at week 4 after-transplant when myeloid-lymphoid cells reach their homeostasis levels. Table 1.1 presents a summary of cell surface markers that characterise murine HSPCs.

Collectively, these conclusions demonstrate that HSCs give rise to all haematopoietic lineages to sustain long-term haematopoiesis throughout the whole life. However, recent evidence has suggested that the haematopoiesis hierarchy is controlled by complicated haematopoietic clones of multipotent progenitors rather than LT-HSCs (Sun et al., 2014, Rodriguez-Fraticelli et al., 2018). Although transplantation assays provide insights into the functional characterisation of BM compartments as repopulation potential and BM homing, the biological features and hierarchical sequences of haematopoietic populations are poorly understood in steady-state haematopoiesis (Sun et al., 2014, Rodriguez-Fraticelli et al., 2018). Sun et al. investigated the native blood cells formation by tracking murine adult haematopoietic compartments utilising *in situ* transposon labelling approaches (Sun et al., 2014). *In vivo* tracking of haematopoietic lineages revealed that about 5% of LT-HSCs were shared clonal origins with MPPs, myeloid progenitors, and mature cells while around 50% of MPPs and myeloid progenitors had similar clonal roots with mature blood cells. These findings indicate that haematopoietic lineages are derived largely from multipotent clones with some contribution from LT-HSCs in steady-state haematopoiesis. Additionally, Rodriguez-Fraticelli et al. further support the idea of the native hierarchy of haematopoietic cells by using the same approach of *in situ* hybridisation (Rodriguez-Fraticelli et al., 2018). Multipotent clones have the potential

to maintain the production of myeloid, lymphoid, and erythroid lineages whereas LT-HSC/MPP2 cells are the major source of megakaryocyte progenitors during steady-state haematopoiesis. These observations signify that MPP clones are supposed to be responsible for sustaining native long-term blood formation.

1.1.4 Human haematopoietic hierarchy and immunophenotypic characterisations

The tools of human HSCs purification are extremely similar to that used for murine HSCs including cell-surface expression analysis and transplantation experiments (Figure. 1.2 H). Immunodeficient mouse models (NOD/SCID/IL2Rγ^{null}; NSG mice) have been used to engraft human BM-cells in order to reduce the xenogeneic rejection (Notta et al., 2011). In contrary to murine HSPCs, human HSPCs are enriched in lin$^-$_CD34$^+$_CD38$^-$ and represent around 0.5–5% of BM and cord blood cells (Notta et al., 2011, Larochelle et al., 1996).

HSCs (Lin$^-$_CD34$^+$_CD38$^-$_CD45RA$^-$_CD90$^+$_CD49f$^+$) differentiate to multipotent progenitors with limited self-renewal (MPPs; Lin$^-$_CD34$^+$_CD38$^-$_CD45RA$^-$_CD90$^-$_CD49f$^-$) that advance into CMPs (Lin$^-$_CD34$^+$_CD38$^+$_CD45RA$^-$_CD135$^+$_CD10$^-$_CD7$^-$) and multi-lymphoid progenitors, (MLPs; Lin$^-$_CD34$^+$_CD38$^-$_CD45RA$^+$_CD90$^-$_CD135$^+$_CD10$^+$_ CD7$^-$) (Notta et al., 2011, Doulatov et al., 2010, Manz et al., 2002). Thereafter, MLPs give rise to macrophage precursors and CLPs (Lin$^-$_CD34$^+$_CD38$^+$_CD45RA$^+$_ CD10$^+$) while CMPs segregate to GMPs (lin$^-$_CD34$^+$_CD38$^+$_CD45RA$^+$_CD135$^+$_CD10$^-$_CD7$^-$) and MEPs (Lin$^-$_CD34$^+$_CD38$^+$_ CD45RA$^-$_CD135$^-$_CD10$^-$_CD7$^-$) oligopotent progenitors (Manz et al., 2002, Galy et al., 1995).

Recently, a two-tier model has been suggested to describe the commitment of human blood cells challenging previous hierarchical models in which oligopotent progenitors are omitted from the hierarchy (Notta et al., 2016). In this paradigm, HSCs/MPPs multipotent cells reside at the top tier and differentiate to unipotent progenitors that are immediately segregated to all types of mature blood cells. Megakaryocytes are exceptional in this model and directly differentiate from HSCs/MPPs compartments.

Along the same lines, several murine reports indicate that megakaryocytes or megakaryocyte/erythrocyte progenitors are anatomically nearby to HSCs and immediately differentiate from HSCs (Pietras et al., 2015, Yamamoto et al., 2013, Bruns et al., 2014). Sanjuan et al. discovered that approximately 60% of HSCs are megakaryocyte-biased-HSCs that express von-Willebrand-Factor with high potential towards megakaryopoiesis (Sanjuan-Pla et al., 2013). Additionally, megakaryocytes secrete essential factors that regulate HSC quiescence and negatively correlate with HSCs activity in the cell-cycle as chemokine C-X-C motif ligand-4 (CXCL4, platelet factor-4), thrombopoietin (TPO), and transforming growth factor-β1 (TGFB1) (Bruns et al., 2014, Nakamura-Ishizu et al., 2014b, Zhao et al., 2014). Conditional ablation of murine *Cxcl4*, *Tpo*, and *Tgfb1* disturbs the HSC dormancy and promotes the proliferation of HSCs. More recently, human cord blood $CD34^-$_HSCs have been purified using CD133 and GPI-80 markers with highly self-renewal potential (Sumide et al., 2018). $CD34^-$_HSCs localise at the top of the human hierarchy and directly segregate into megakaryocyte/erythrocyte progenitors.

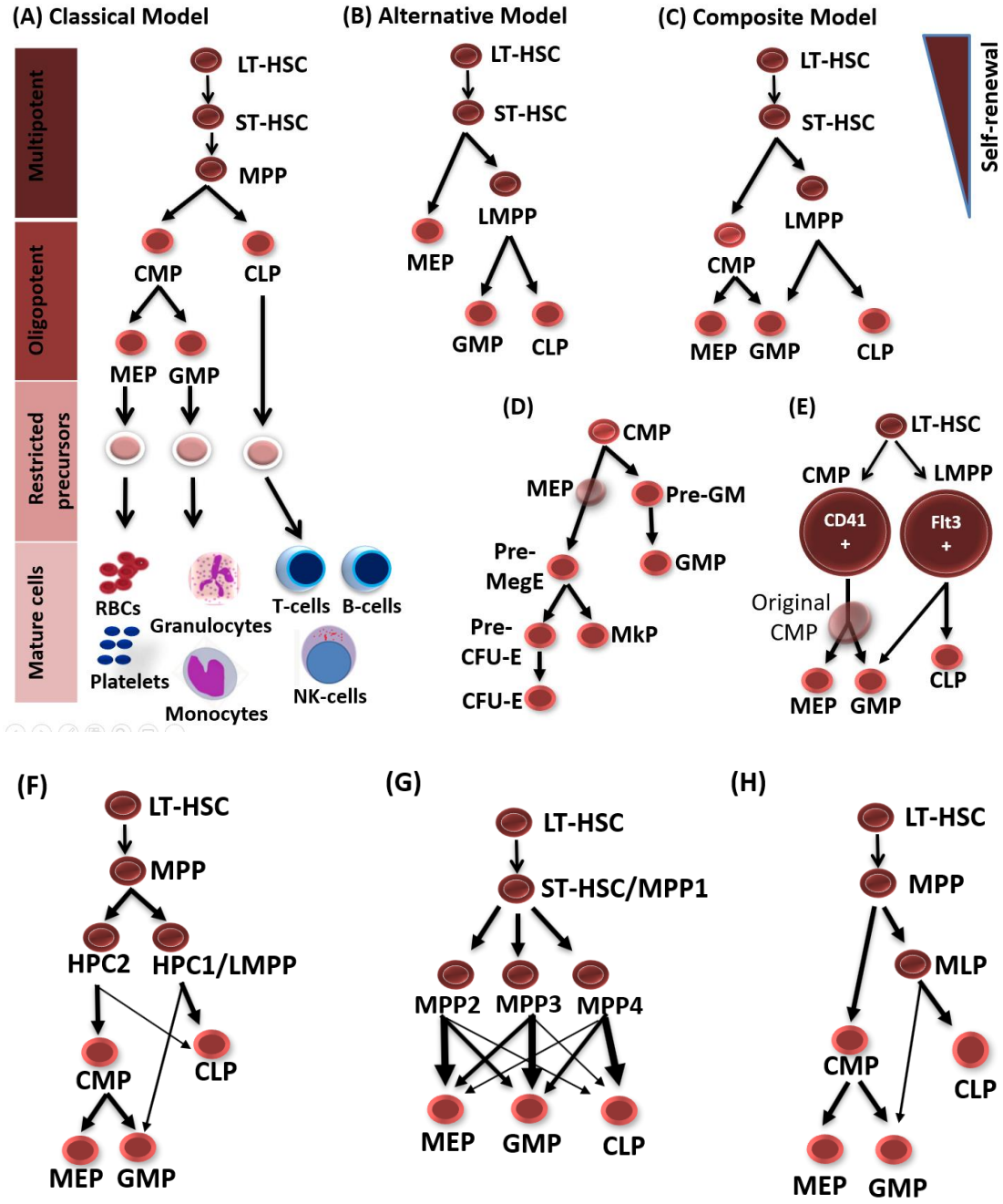

Figure 1-2: Murine and human haematopoietic hierarchy.

Different models have been applied to describe the hierarchical arrangement of haematopoietic compartments: (A) the classical model; (B) the alternative version; (C) the composite paradigm; (D) differentiated scheme of myeloid/erythroid/megakaryocyte progenitors; (E) revised paradigm based on CD41-CMP and Flt3-LMPP; (F) Oguro et al. model; (G) Pietras et al. paradigm; and (H) human hierarchy (Adapted from (Pronk et al., 2007, Pietras et al., 2015, Adolfsson et al., 2005, Oguro et al., 2013, Doulatov et al., 2012, Miyawaki et al., 2015))

Table 1.1: Cell surface markers for murine haematopoietic subpopulations.

LT-HSCs	$Lin^-\_c\text{-}kit^+\_Sca1^+\_CD90^{low}\_CD135^-$ $Lin^-\_c\text{-}kit^+\_Sca1^+\_CD34^-\_CD38^+$ $Lin^-\_c\text{-}kit^+\_Sca1^+\_CD34^-\_CD135^-$ $Lin^-\_c\text{-}kit^+\_Sca1^+\_CD150^+\_CD48^-$ $Lin^-\_c\text{-}kit^+\_Sca1^+\_CD135^-\_CD150^+\_CD48^-$
ST-HSCs MPP1	$Lin^-\_c\text{-}kit^+\_Sca1^+\_CD90^{low}\_CD135^+$ $Lin^-\_c\text{-}kit^+\_Sca1^+\_CD34^+\_CD38^-$ $Lin^-\_c\text{-}kit^+\_Sca1^+\_CD34^+\_CD135^-$ $Lin^-\_c\text{-}kit^+\_Sca1^+\_CD135^-\_CD150^-\_CD48^-$
MPPs	$Lin^-\_c\text{-}kit^+\_Sca1^+\_CD90^-\_CD135^+$ $Lin^-\_c\text{-}kit^+\_Sca1^+\_CD34^+\_CD135^+$ $Lin^-\_c\text{-}kit^+\_Sca1^+\_CD150^-\_CD48^-$
HPC1 LMPP MPP4	$Lin^-\_c\text{-}kit^+\_Sca1^+\_CD150^-\_CD48^+$ $Lin^-\_c\text{-}kit^+\_Sca1^+\_CD34^+\_CD135^{High}$ $Lin^-\_c\text{-}kit^+\_Sca1^+\_CD135^+\_CD150^-\_CD48^+$
HPC2 MPP2	$Lin^-\_c\text{-}kit^+\_Sca1^+\_CD150^+\_CD48^+$ $Lin^-\_c\text{-}kit^+\_Sca1^+\_CD135^-\_CD150^+\_CD48^+$
MPP3	$Lin^-\_c\text{-}kit^+\_Sca1^+\_CD135^-\_CD150^-\_CD48^+$
CMPs	$Lin^-\_c\text{-}kit^+\_Sca1^-\_CD34^+\_CD16/32^-$ $Lin^-\_c\text{-}kit^+\_Sca1^+\_CD34^+\_CD41^{high}$
CLP	$Lin^-\_c\text{-}kit^{low}\_Sca1^{low}\_CD127^+$ $Lin^-\_c\text{-}kit^{low}\_Sca1^{low}\_CD127^+\_CD135^+$
Pre-GM	$Lin^-\_c\text{-}kit^+\_Sca1^-\_CD150^-\_CD41^-\_CD16/32^-\_CD105^-$
GMP	$Lin^-\_c\text{-}kit^+\_Sca1^-\_CD34^+\_CD16/32^+$ $Lin^-\_c\text{-}kit^+\_Sca1^-\_CD150^-\_CD41^-\_CD16/32^+$
MEP Pre-MegE	$Lin^-\_c\text{-}kit^+\_Sca1^-\_CD34^-\_CD16/32^-$ $Lin^-\_c\text{-}kit^+\_Sca1^-\_CD150^+\_CD41^-\_CD16/32^-\_CD105^-$
MkP	$Lin^-\_c\text{-}kit^+\_Sca1^-\_CD150^+\_CD41^+$
Pre-CFU-E	$Lin^-\_c\text{-}kit^+\_Sca1^-\_CD150^+\_CD41^-\_CD16/32^-\_CD105^+$
CFU-E	$Lin^-\_c\text{-}kit^+\_Sca1^-\_CD150^-\_CD41^-\_CD16/32^-$ $\_CD105^+CD71^+\_Ter119^-$
Granulocyte cells	$Mac1^+Gr1^+$
Monocyte/Macrophage cells	$Mac1^+Gr1^-$
Erythroid cells	CD71, Ter119
T-lymphocyte cells	CD3, CD4, CD8
B-lymphocyte cells	B220
Megakaryocytes	CD41, CD42d

1.1.5 Transcription factors in haematopoiesis

HSCs generation, survival, quiescence, self-renewal, and differentiation are under the firm control of multiple transcription factors (TFs) (Rieger and Schroeder, 2012, Orkin and Zon, 2008, Seita and Weissman, 2010). However, dysregulated expression of TFs is frequently associated with leukaemogenesis (Rieger and Schroeder, 2012, Orkin and Zon, 2008, Seita and Weissman, 2010). Haematopoietic TFs can be classified into two main clusters: specific HSCs TFs and multi-lineage TFs. However, many studies have suggested the combinatorial interactions between these TFs in both HSCs specification and multi-lineage differentiation (Rieger and Schroeder, 2012, Orkin and Zon, 2008, Seita and Weissman, 2010). Wilson et al. carried out chromatin immunoprecipitation followed by RNA-sequencing for ten TFs (*SCL/TAL1, LYL1, LMO2, RUNX1, MEIS1, PU.1, ERG, FLI1, GFI1B and GATA2*) that are crucial for the development of HSPCs using murine haematopoietic precursor cell-7 (HPC-7) cell line (Wilson et al., 2010). Findings of this study indicated a combinatorial interaction between *SCL/TAL1, RUNX1, LYL1, LMO2, ERG, FLI1 and GATA2* TFs (Figure 1.3). These seven TFs form the heptad HSCs and have a direct effect on the HSPCs development and differentiation.

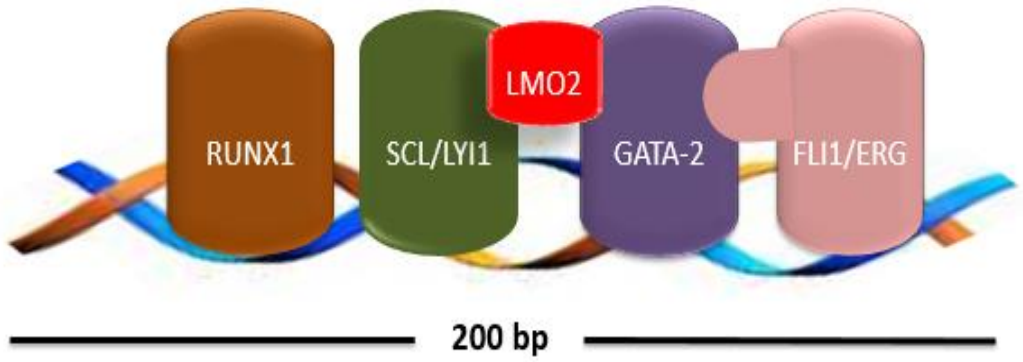

Figure 1-3: Scheme of GATA2 associated protein complexes bound to DNA.
The figure illustrates the combinatorial interactions of seven TFs that regulate the HSPCs genes expression. All of these TFs except LMO2 bind directly to DNA within 200 base pairs or less. Adapted from (Wilson et al., 2010).

The specific HSCs TFs such as SCL/TAL1, RUNX1, LMO2, MLL, FLI1 and GATA2 are essential for the HSCs generation and/or maintenance (Figure 1.4). Stem cell leukaemia /T-cell acute lymphocytic leukaemia1 (SCL/TAL1) which belongs to the basic helix-loop-helix (bHLH) transcription family is essential for the HSCs formation. *Scl/Tal1* knockout (KO) mice are embryonic lethal at E9.5 with severe defects in blood formation at the yolk sac (Robb et al., 1995). Deletion of *Scl/Tal1* in the adult BM mice revealed that *Scl/Tal1* is inessential for adult HSCs maintenance, but prohibits the final differentiation of erythroid/megakaryocyte lineages (Mikkola et al., 2003). Runt-related transcription factor1 (RUNX1, also known as acute myeloid leukaemia-1 (AML1)) is indispensable for HSCs formation in the aorta gonad-mesonephros region and plays an essential role in haematopoietic cells transition from the endothelial cells (Chen et al., 2009). *Runx1* KO mice are unable to form haematopoietic clusters in the AGM region, signifying the roles of *Runx1* in the primitive haematopoiesis. Conversely, conditional deletion of *Runx1* after the definitive haematopoiesis revealed that *Runx1* is dispensable for the HSCs maintenance (Chen et al., 2009). In addition, double *Runx1* and *Gata2* heterozygote mice die at mid-gestation due to a defect in haematopoiesis although either single heterozygote *Runx1* or *Gata2* mice are alive (Wilson et al., 2010). LIM domain protein 2 (LMO2) is vital for the development of both primitive and definitive haematopoiesis. *Lmo2* KO mice are lethal at E10.5 with a particular disruption of yolk sac erythropoiesis (Warren et al., 1994). The LMO2 protein reacts with other proteins as SCL/TAL1, E2A, LDB1 and GATA1 constructing an oligomeric complex. This complex is required for the erythroid differentiation (Wadman et al., 1997). Mixed lineage leukaemia (MLL) is also required for the HSCs formation and maintains the expression of Hox genes that regulate the proliferation of primitive haematopoietic cells. Analysis of *Mll*-null embryonic stem cells revealed a depletion of HSC numbers in the AGM region, indicating the essential role of *Mll* in the HSCs specification and development (Ernst et al., 2004). Friend leukaemia integration1 (FLI1) belongs to the Ets-family of TFs that regulate haematopoiesis by binding to the target gene sequence GGA (A/T). *Fli1*-null embryos are lethal at E12.5 with severe haemorrhage in the AGM region (Spyropoulos et al., 2000). *Fli1* interacts with *Scl/Tall* and *Gata2* forming a triad complex which is essential for the HSCs generation (Pimanda et al., 2007). At the progenitor level, *Fli1* enhances

the differentiation of megakaryocytes. *Fli1* KO mice display thrombocytopenia with a severe reduction of megakaryocyte progenitors (Spyropoulos et al., 2000).

CITED2, EVI1 and c-MYC TFs play crucial roles in HSCs homeostasis. Cbp/P300 Interacting Trans-activator with Glu/Asp-rich Carboxy-terminal domain-1 (CITED2*)* is required for maintaining the survival of adult HSCs. Conditional deletion of *Cited2* in adult haematopoietic compartments exhibited a reduction in HSPC numbers with BM failure phenotypes (Kranc et al., 2009). The c-MYC protein reacts with BM niches to maintain the equilibrium between HSCs self-renewal and differentiation. The *c-Myc* KO mice showed an increase in HSC numbers and a decline in lineage positive cells with an increment in the expression of N-cadherin and other adhesion molecules in BM niches, signifying that *c-Myc* is required to release HSCs from their niches (Wilson et al., 2004). On the other hand, overexpression of *c-Myc* in HSCs displayed impairment in HSCs self-renewal capability and increases the HSC differentiation efficiency (Wilson et al., 2004). Ecotropic viral integration site 1 (EVI1) is also essential for the homeostasis of HSCs. Deletion of *Evi1* in the embryo and adult Haematopoietic cells exhibited a reduction in the number of HSCs and a defect in HSCs reconstitution potential (Goyama et al., 2008). Likewise, low expression of *Evi1* perturbs the proliferation effectiveness of transformed leukaemic cells. Conversely, overexpression of *Evi1* in BM mice showed a weakness in HSCs self-renewal and an increase in the differentiation of multi-lineage cells (Kataoka et al., 2011).

Other transcription factors are required for adult HSCs self-renewal to maintain the HSC pool size and prevent HSCs exhaustion as B-lymphoma Mo-MLV insertion region 1 (BMI1), Translocation-ETS-leukaemia/ ETS Variant 6 (TEL/ETV6), Growth factor independent-1 (GFI1), Homeobox domain B4 (HOXB4), Pre-B-cell leukaemia transcription factor 1 (PBX1). Conditional deletion of *Bmi1*, *Tel/Etv6* or *Gfi1* in adult HSCs revealed a deterioration in HSCs self-renewal potential in serial transplantation experiments (Park et al., 2003, Hock et al., 2004a, Hock et al., 2004b). *Hoxb4* is also essential for HSCs self-renewal and expansion. Overexpression of *Hoxb4* in mice BM cells displayed an increase in HSCs self-renewal potential with an effective repopulation capability for all committed progenitors in recipient hosts (Antonchuk

et al., 2002). Conversely, *Hoxb4*-null mice showed a reduction in HSCs reconstitution potential (Björnsson et al., 2003). *Pbx1* confers HSCs self-renewal and preserves HSCs quiescence through TGF-β signalling pathway (Ficara et al., 2008). *Pbx1*-null mice accompanied by a considerable reduction in HSC numbers and an impairment in HSCs self-renewal potency.

At the lineage-specific level, there are several transcription factors regulating myeloid, erythroid/megakaryocyte and lymphoid cells differentiation such as PU.1, GATA1, CEBPA, GATA2, GATA3, IKAROS, and E2A (Figure 1.4). Purine box-binding protein-1 (PU.1) belongs to the Ets family and has vital roles in the formation of committed myeloid/lymphoid progenitors at the lymphoid-primed multipotential progenitors (LMPPs) stage (Iwasaki et al., 2005, Arinobu et al., 2007). The commitment of HSCs towards myeloid/lymphoid or erythroid/megakaryocyte lineages is controlled by *Pu.1* and *Gata1* TFs, respectively. There is an antagonistic interaction between *Pu.1* and *Gata1*. *Gata1* represses *Pu.1* and confers the development of megakaryocyte/ erythrocyte progenitors, while *Pu.1* suppresses *Gata1* and drives the haematopoiesis towards myeloid/lymphoid populations (Nerlov et al., 2000). Knock-in *Pu.1* locus with a fluorescent reporter protein (GFP) showed *Pu.1* is highly expressed in LMPPs, and *Pu.1*-GFP^{+}_LMPPs differentiate to myeloid/lymphoid lineages with low potential towards erythroid/megakaryocyte cells (Arinobu et al., 2007). *Pu.1* KO mice displayed an impaired repopulating potential of HSCs and a severe defect in the generation of the initial myeloid/lymphoid precursors (Iwasaki et al., 2005). On the other hand, knock-in mice with GFP into *Gata1* promoter exhibited that the level of *Gata1*_GFP^{+} is the highest in primitive common myeloid progenitors (CMPs) that give rise into erythroid/megakaryocyte/ myeloid compartments with losing the lymphoid potency (Miyawaki et al., 2015). CCAAT/enhancer-binding protein alpha (CEBPα) is essential for granulocytes development and guides multipotent progenitors toward myeloid lineages (Radomska et al., 1998). *Cebpα* regulates the transition of the CMPs into granulocyte/monocyte progenitors (GMPs), and inactivation of *Cebpα* in adult mice showed prevention in GMPs formation and accumulation of myeloblasts (Zhang et al., 2004). CEBPα and PU.1 reciprocally antagonise their expression to determine the

mature blood cell fates. Upregulation of *Pu.1* induces monocyte differentiation and inhibits granulocytes maturation, while overexpression of *Cebpα* represses monocytes and promotes granulocyte differentiation (Radomska et al., 1998). GATA1 is required for both embryonic and adult erythrocytes differentiation (Fujiwara et al., 1996). Erythropoiesis is cooperatively regulated by *Gata1, Gata2,* stem cell leukaemia (*Scl*), Kruppel Like Factor-1 (*Eklf1*), and friend of GATA1 (*Fog1*) TFs. The expression of *Gata1, Gata2, Fli1,* and *Runx1 is* necessary for megakaryopoiesis (Orkin and Zon, 2008).

IKAROS is essential for the early commitment of lymphoid progenitors and encourages the differentiation of HSCs towards lymphoid cells. Germline deletion of Ikaros in BM mice showed a severe reduction in B-cells, T-cells and natural killer cells with normal frequencies of erythroid/myeloid cells (Georgopoulos et al., 1994). Low expression of *Ikaros* is associated with a decrease in the expression of Flt3 and IL7Rα signalling receptors in lymphoid cells (Yoshida et al., 2006). In marked contrast to murine, human GATA2 determines the lymphoid-cells fate by regulating the specification of multi-lymphoid progenitors (MLPs) from the primitive HSC/MPP compartments (Doulatov et al., 2012). Knockdown of *GATA2* in MLPs showed normal terminal differentiation of lymphoid cells (Laurenti et al., 2013). These findings signify that *GATA2* regulates the earliest point of lymphoid differentiation without affecting the lymphoid output. E-box binding protein 2A (E2A) is required for the CLP formation and induces transcription factors that are essential for B-cells specification including Early B cell factor (EBF1) and PAX5 (Borghesi et al., 2005). *E2a* null mice showed immature B-cells are arrested at the early stage of B-cells differentiation (pre-pro B-cells) with the absence of mature B-cells (Borghesi et al., 2005). Notch1 signalling and GATA3 arrange the early developmental stage of T-cells. Notch1 signalling regulates the commitment of lymphoid cells. Overexpression of Notch1 in BM mice displayed an increase in T-cell numbers and a reduction in the frequencies of B-cells, whereas *Pax5* promotes B-cells differentiation by repressing Notch1 signalling receptors (Pui et al., 1999, Delogu et al., 2006). *Gata3*-null embryonic stem cells displayed normal frequencies of erythroid, myeloid and B-cells, but showed a deficiency in mature T-cells with a failure in the formation of double-negative thymocytes (Ting et al., 1996).

GATA2 is another important transcription factor for the HSC generation, survival, and maintenance. The role of GATA2 in haematopoiesis is discussed below (section 1.3). In summary, TFs are essential for regulating haematopoiesis, alterations in TFs expression levels (up-regulation or down-regulation) may initiate and/or promote the development of Haematological disorders.

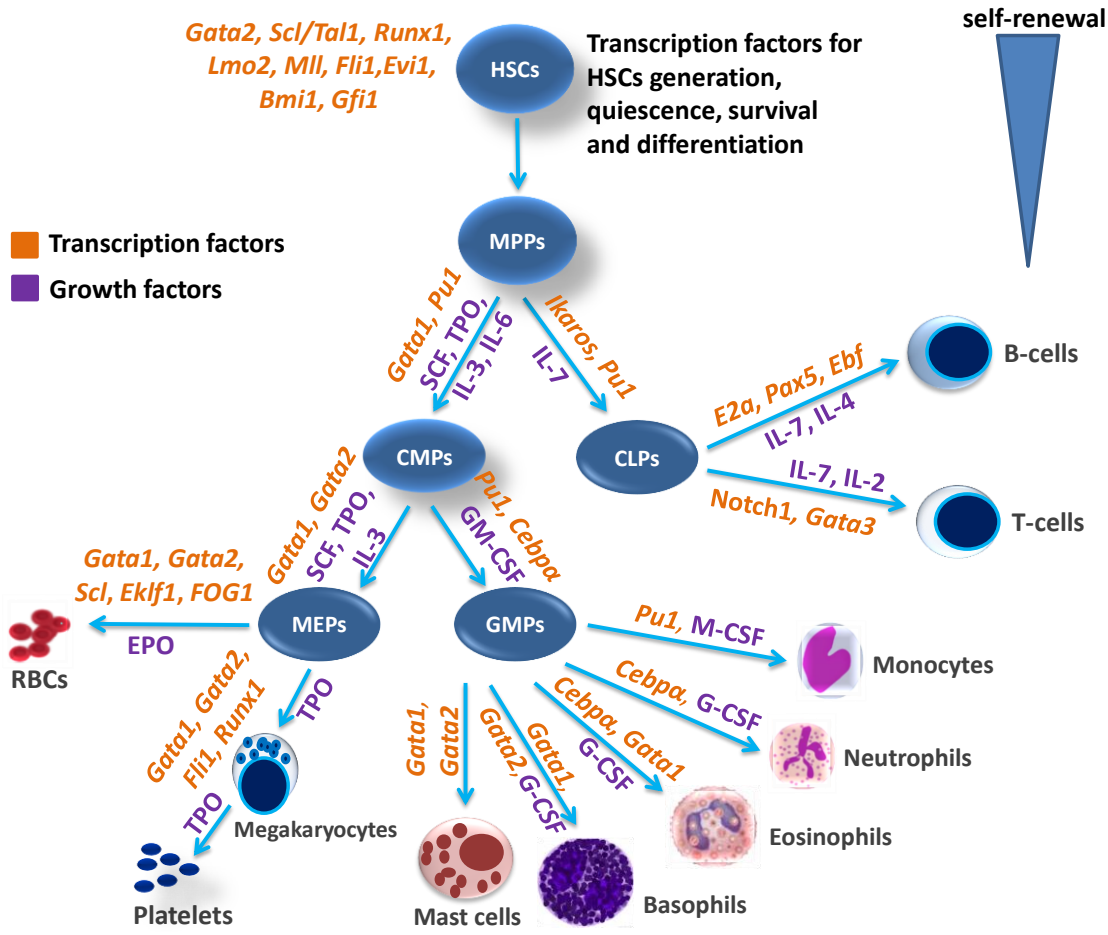

Figure 1-4: Transcription factors in haematopoiesis.
HSCs generation, maintenance and differentiation are regulated by a varied combination of transcription factors, cytokines, and growth factors. CSF indicates colony-stimulating factor; G-CSF, granulocytes-CSF; M-CSF, macrophages-CSF; GM-CSF, granulocytes- macrophages-CSF; IL, interleukin. (Adapted from (Orkin and Zon, 2008, Kaushansky, 2006)).

1.1.6 The cell cycle regulations for HSCs quiescence, self-renewal, and differentiation

The distinct feature of HSCs is their self-renewal potential and the ability to differentiate into all types of mature blood cells. Since HSCs maintain a supply of lineage cells throughout the lifetime of an individual, HSC self-renewal is required for the continual maintenance of HSCs pool size to protect HSCs exhaustion (Seita and Weissman, 2010). The HSC activity within the cell cycle is reflected in the developmental demands of the organism. Foetal HSCs are rapidly divided to support the growth requirements and around 100% of HSCs are activated within the cycle in murine foetal liver (Nygren et al., 2006). Conversely, approximately 75% of adult HSCs are in quiescence and around 25% of HSCs enter the cell cycle to maintain blood homeostasis for a long period in adult life (Cheshier et al., 1999). The equilibrium between quiescence and proliferation is mediated by a complex network of intracellular and extracellular mechanisms that regulate the cells fate. The cell cycle is comprised of interphase and mitosis phases. The interphase is comprised of three sub-phases: G1-phase, S-phase, and G2-phase. Cells grow during the G1 phase, and cells that reach the G1-checkpoint make the decision to enter the S-phase or return to the resting stage (G0-phase, also known as quiescent phase) (Pardee, 1974). In the S-phase, the DNA synthesis takes place and cells continue to grow and prepare for the cell division. During the mitosis phase (M phase), the cell division occurs, and the accuracy of mitosis is assessed at the M-checkpoint. HSCs are divided through the cell cycle and undergo either symmetric or asymmetric division and give rise to daughter HSCs and/or committed progenitor cells (Figure 1.5) (Nakamura-Ishizu et al., 2014a).

The cell cycle regulatory proteins such as cyclin-dependent protein kinases (CDKs) encourage HSCs to enter the cell cycle phases, while cyclin-dependent kinase inhibitors (CKIs) are essential to maintain HSCs in a quiescent state (Morgan, 1997). At each phase of the cell cycle, CDKs bind to their cyclin partner to form an active complex (Figure 1.5). Retinoblastoma family of transcriptional proteins (RB, P107, and P130) repress cells from entering the cell cycle by suppressing of *E2f* TFs (Ho and Dowdy, 2002, Giacinti and Giordano, 2006). To enter the G1-phase, CDK4 and CDK6 interact with cyclin-D to form a cyclin-D_CDK4/6 complex to initiate the

phosphorylation of retinoblastoma proteins (RBPs) that subsequently activate *E2f* TFs and allow cells to continue through the G1-phase (Ho and Dowdy, 2002, Giacinti and Giordano, 2006). At the end of G1-phase, further phosphorylation of RBPs is executed by a cyclin-E_CDK2 complex that requires entry into the S-phase to commence the DNA synthesis (Ho and Dowdy, 2002, Giacinti and Giordano, 2006). The cyclin-A_CDK2 and cyclin-A_CDK1 complexes preserve the progression through the S and G2 phases, respectively. In the last phase, the cyclin-B_CDK1 complex promotes cells to enter the M phase to commence the cell division (Ho and Dowdy, 2002, Giacinti and Giordano, 2006). The deletion of RBPs in adult mice was accompanied by an increase in HSCs proliferation and a reduction in HSCs quiescence (Viatour et al., 2008). The numbers of HSPCs and peripheral red blood cell were significantly reduced in the cyclin-D_CDK4/6 deficient mice during embryogenesis (Kozar et al., 2004, Malumbres et al., 2004).

On the other hand, CKIs regulate the cell cycle during the G1 phase by hindering the activity of CDKs. CKIs are divided into two main categories: The Inhibitor of CDK4/6 (INK4) family (p15, p16, p18 and p19) and the CDK inhibitory protein/kinase inhibitor protein (CIP/KIP) family (p21, p27, and p57), in which INK4 proteins repress the activity of cyclin-D_CDK4/6 complexes whereas CIP/KIP proteins suppress the cyclin-E_CDK2 complex. Both families restrain the cell cycle at G0/G1 phase by inhibiting the phosphorylation of RBPs (Viatour et al., 2008). The B-lymphoma Mo-MLV insertion region 1 (BMI1) represses the expression of p16/p19 proteins to sustain the self-renewal potential of HSCs. *Bmi1* deficient mice exhibited an increase in *p16*/*p19* expression and a significant reduction in cycling HSCs with an impairment in adult HSCs self-renewal (Park et al., 2003). The number of cycling HSCs was increased in *p18* knockout mice with an intact self-renewal capability of HSCs (Yuan et al., 2004). The expression of p21 is prompted by the p53 protein which regulates the quiescence of HSCs. *p53*-null adult mice displayed a depletion in quiescent HSCs and an imperfection in HSCs self-renewal upon serial transplantation experiments (Matsumoto et al., 2011). In addition to the cell cycle regulatory proteins, there are a lot of TFs, growth factors, cytokines, and signalling pathways, that influence the HSCs fate to maintain the adequate level of blood homeostasis. For instance, BM

stromal cells secrete TGFβ and Notch ligands to regulate the HSCs quiescence and self-renewal, respectively (Ezoe et al., 2004).

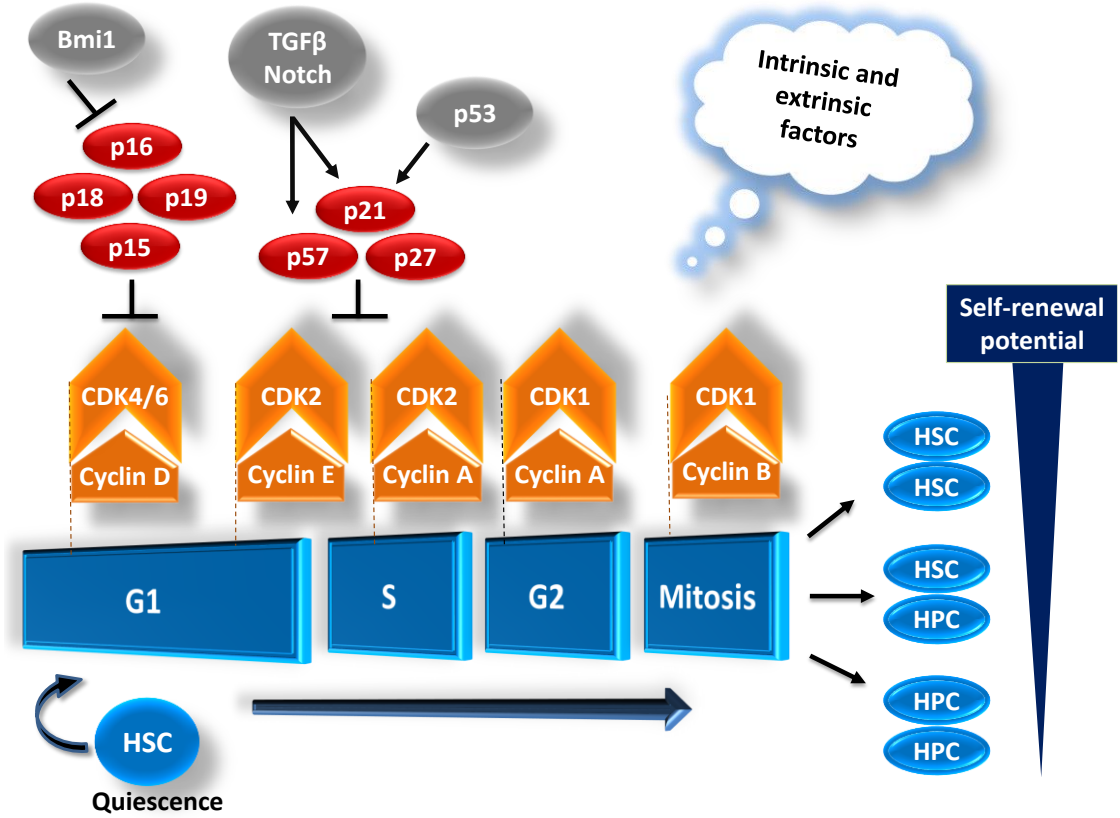

Figure 1-5: The cell cycle regulations of haematopoietic stem cell division.
HSCs undergo either asymmetric divisions, which HSCs advance into new HSCs (self-renewal) and HPCs (haematopoietic progenitors), or symmetric divisions, which HSCs give rise into two identical HSCs (an expanded HSCs pool size) or HPCs (increased production of mature blood cells). HSCs indicate haematopoietic stem cells; HPCs, haematopoietic progenitor cells; and CDK, cyclin-dependent kinase. Adapted from (Ezoe et al., 2004, Nakamura-Ishizu et al., 2014a)

1.1.7 Bone marrow niches

Adult HSCs are anatomically localised in a particular region of the BM microenvironment known as stem cell niches. The fate of HSCs towards self-renewal and differentiation is principally organised by extrinsic factors deriving from BM niches (Morrison and Scadden, 2014, Orkin and Zon, 2008, Crane et al., 2017, Ding et al., 2012). Many types of stromal cells are involved in the construction of BM niches as mesenchymal stem cells, fibroblasts, osteoblasts, endothelial cells, adipocytes, and mature blood cells, and produce substances like glycoprotein, collagen, glycosaminoglycans, cytokines, and growth factors, that create the extracellular matrix (Morrison and Scadden, 2014, Orkin and Zon, 2008, Crane et al., 2017, Ding et al., 2012). Several studies have suggested that the HSC niche localises in an endosteal osteoblastic niche (adjacent to osteoblast cells) and a perivascular endothelial niche (close to blood vessels) (Morrison and Scadden, 2014, Orkin and Zon, 2008, Crane et al., 2017, Ding et al., 2012). HSCs reside in the BM cavity with a hypoxic atmosphere, in which quiescent HSCs locate at the highest area of a hypoxic gradient while cycling HSCs and differentiated haematopoietic cells settle at the lowest area of a hypoxic gradient in BM niches (Parmar et al., 2007).

HSC niches produce soluble growth factors and cytokines that encourage HSCs maintenance such as thrombopoietin (TPO), angiopoietin-1 (Ang1), stem cell factor (SCF) and stromal-derived factor-1 (SDF1, also known as C-X-C chemokine-12 (CXCL12)). TPO binds to the myeloproliferative leukaemia protein (c-MPL) receptor, which is expressed on HSCs. TPO/c-MPL signalling is essential for HSCs self-renewal and megakaryocytes maturation (Kimura et al., 1998). The number of HSCs was decreased in *c-Mpl*-null mice as well as the self-renewal ability of HSCs was attenuated in serial transplantation assays (Kimura et al., 1998). Ang1 interacts with HSCs through the TIE2 receptor, a tyrosine kinase receptor, to preserve HSCs in a quiescent state by maintaining the adhesion of HSCs to the bone (Arai et al., 2004). Both osteoblast and vascular endothelial cells secrete SCF which confers HSCs growth and survival by binding to the c-KIT receptor, a tyrosine kinase receptor. No difference in the HSC numbers was observed in *Scf*-osteoblasts deficient mice while a massive reduction in the HSC numbers was detected in *Scf*-vascular endothelial cells

null mice, and *Scf* knock-in mice experiments revealed that vascular endothelial cells were a major source of SCF in BM niches (Ding et al., 2012). SDF1 is predominantly produced by perivascular stromal cells while endothelial and osteoblast cells express a low level of SDF1, which reacts with HSCs through CXC-chemokine-4 receptor (*CXCR4*) (Ding and Morrison, 2013).

SDF-1/CXCR4 signalling enhances the HSC maintenance, homing, mobilisation and proliferation of myeloid and lymphoid progenitors (Ding and Morrison, 2013, Wright et al., 2002, Sugiyama et al., 2006). Ding et al. investigated whether HSPCs occupy the same BM niches or not by the deletion of *Sdf1* from endothelial cells, osteoblast cells or perivascular stromal cells, and they concluded that HSPCs reside in a different BM microenvironment, and HSCs exist primarily in a perivascular endothelial niche while an endosteal osteoblastic niche is the home of early lymphoid progenitors (Ding and Morrison, 2013). Moreover, CXCL12 abundant reticular (CAR) cells are located in the BM perivascular space and secrete a large amount of CXCL12 (Sugiyama et al., 2006). The majority of HSCs were attached to CAR cells via CXCR4 in both endosteal osteoblastic and perivascular endothelial niches, and these findings suggest that CAR cells are the prominent component in BM niches and play an essential role in the HSCs quiescence (Sugiyama et al., 2006). Cooperatively, these finding showed that BM niches regulate the HSCs fate by conferring the HSCs maintenance, homing, quiescence, self-renewal, and differentiation.

Adipogenesis is a process of MSCs differentiation into adipocytes that form fat cells in the bone marrow niche (Tong et al., 2005, Tong et al., 2000). The expression of CEBPα and peroxisome-proliferator-activated-receptor-γ (PPARγ, adipocytes marker) induce CEBPβ/CEBPδ TFs that stimulate adipocytes differentiation (Tong et al., 2005, Tong et al., 2000). Permanent GATA2/GATA3 expression represses the differentiation of adipocyte-precursors (pre-adipocytes) towards adipocytes and directly inhibit the activity of *PPARγ*-mRNA (Tong et al., 2000). The repression of adipocytes generation is mediated by the interaction of GATA2/GATA3 TFs with adipogenesis regulators (CEBPα/CEBPβ) (Tong et al., 2005). Thus, down-regulated GATA2/GATA3 expression is required for terminal adipocytes formation.

1.1.8 Aged haematopoietic cells

Ageing HSCs are accompanied with several alterations including an incremental increase in HSC numbers, a reduction in the reconstitution potential, an impairment in HSCs self-renewal capability, alterations in HSCs polarity, diminished adaptive immune cells, changes in BM homing efficiency and skewing in HSCs differentiation potential towards myeloid lineages (Morrison et al., 1996, Kim et al., 2003, Pearce et al., 2007, Rossi et al., 2005, Liang et al., 2005).

Despite an increase of HSC numbers in old mice, the repopulation ability of HSCs was reduced upon transplantation experimentations (Morrison et al., 1996, Kim et al., 2003, Pearce et al., 2007). Serial transplants of either BM or HSCs from aged haematopoietic compartments displayed a reduction in B-lymphocytes and an impairment in HSCs self-renewal potential (Kim et al., 2003). The increase in HSC numbers is associated with a rise in HSCs cycling, a decrease in apoptosis level in HSCs and a reduction in genes expression that trigger HSCs apoptosis (Morrison et al., 1996, Pearce et al., 2007). Analysis of expressed genes in old HSCs revealed that genes involved in the stress and inflammation responses were upregulated, whereas genes involved the integrity of genomes and chromatin modifications were downregulated (Chambers et al., 2007). The most likely mechanism that causes imperfections in HSC functions is an accumulation of genomic materials due to a defect in DNA damage repair pathways (Rossi et al., 2007).

Changes in HSCs polarity, an asymmetric distribution of cellular elements, are another characteristic of elderly HSCs. The fluctuation of polarity in aged HSCs is associated with an increase in the expression level of Cell division cycle-42 (*Cdc42*), an essential regulator of extracellular matrix (Florian et al., 2012). Pharmacological inhibitors of *Cdc42* in aged HSCs were accompanied by an increase in HSCs differentiation towards lymphoid cells and improved HSCs self-renewal potential. Thus, aged HSCs rebuild their polarity upon the *Cdc42* downregulation.

Aged HSCs exhibit biased differentiation toward myeloid cells and a reduction in the output of lymphoid cells (Kim et al., 2003, Rossi et al., 2005). The gene expression

analysis of young and aged HSCs displayed an up-regulation of myeloid priming genes and a down-regulation of lymphoid priming genes in old HSCs when compared with young HSCs (Rossi et al., 2005). Aged HSCs are highly expressed genes that associate with the development of myeloid malignancies (Rossi et al., 2005, Signer et al., 2007). In addition, aged BM niches display different biological functions when compared to young microenvironments. Rantes (CCL5), an inflammatory cytokine, is highly secreted by elderly HSC niches and encourages the haematopoiesis towards myeloid lineages (Ergen et al., 2012). Retroviral overexpression of *Ccl5* in murine BM compartments showed an expansion in myeloid cells and a reduction in lymphoid cells. While *Ccl5*-null mice revealed a lymphoid skewing lineage and a profound reduction in myeloid progenitors. Collectively, these data propose that aged HSCs are associated with an increased predisposition to develop clonal haematopoiesis, myelodysplasia, myeloproliferative and acute myeloid malignancies in elderly people.

1.2 Myeloid malignancies

Myeloid neoplasms are clonal illnesses that disturb haematopoietic stem and progenitor cells (HSPCs) characteristics such as proliferation, differentiation, and self-renewal (Arber et al., 2016, Rodak et al., 2013). In general, myeloid malignancies are divided into chronic and acute phases. Chronic phases are slow malignancies progression such as myelodysplastic syndromes, (MDS), myeloproliferative neoplasms (MPN), and MDS/MPN overlapping neoplasms, while acute malignancies progress rapidly as acute myeloid leukaemia (Figure 1.6) (Arber et al., 2016, Rodak et al., 2013).

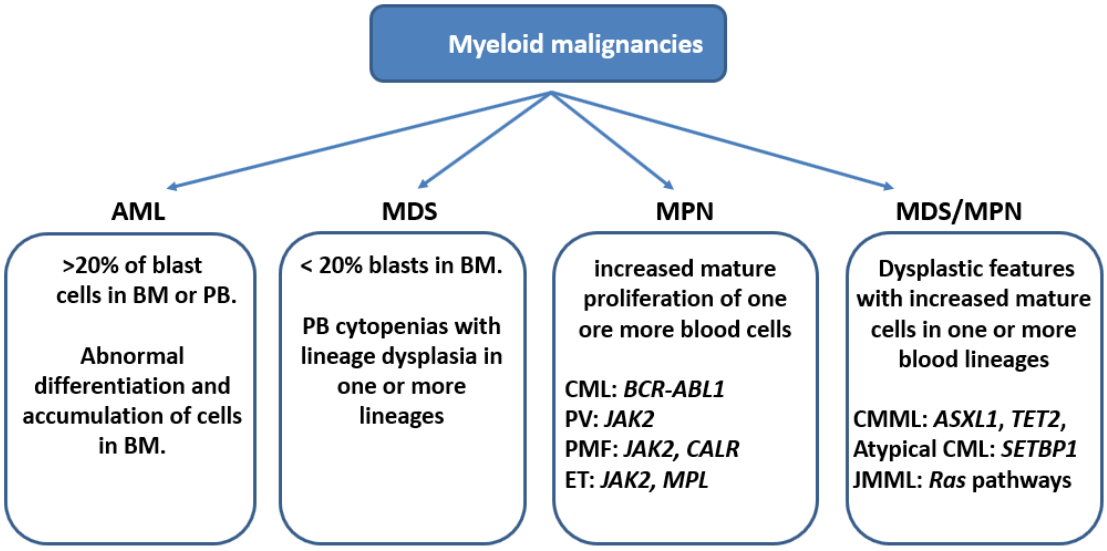

Figure 1-6: Scheme illustrates the clonal myeloid malignancies.

1.2.1 Acute Myeloid Leukaemia

Acute myeloid leukaemia is heterogeneous disorders that lead to clonal growth and accumulation of immature myeloid cells (blast cells; undifferentiated precursor cells) in the bone marrow with extramedullary tissues infiltration (Arber et al., 2016, Rodak et al., 2013). The majority of AML cases are acquired malignancy in previously healthy individuals. AML is the most frequent type of leukaemia in the neonate, but the disease is rare to occur in childhood and adolescence. The incidence of AML is more recurrent in elderly people with a median age of about 65 years (Rodak et al., 2013). The clinical manifestation of AML patients is generally nonspecific but results from

bone marrow failures such as anaemia, thrombocytopenia and neutropenia which advance to the clinical findings of fatigue, bruising and bleeding, and susceptibility to infections, respectively (Rodak et al., 2013). AML patients are treated with chemotherapy, immune regulation therapy and bone marrow transplant (Rodak et al., 2013). Early diagnosis and treatment are significant contributing factors for a better prognosis, and the disease could be lethal if patients were untreated within a few months secondary to infections or bleeding.

1.2.1.1 AML classification

Two main systems are commonly used to classify AML subtypes: the older French American-British (FAB) and the newer World Health Organization (WHO) classifications. The FAB system was proposed in 1976 by a group of French, American, and British haematologists. The FAB system is based on the morphological and cytochemical characteristics of leukaemic cells to distinguish between different types of AML (FAB M0 to M7) (Bennett et al., 1976). In 2001, the WHO published a new classification system in order to replace the old FAB system to become the crucial modality for AML classification as a part of efforts to improve the diagnosis, prognosis and treatment of AML cases (Hossfeld, 2002). The WHO classification of AML contains all FAB categories and further consists of a combination of morphology, immunophenotypes, chromosomal translocations, genetic lesions, and clinical presentation. The FAB system requires approximately 30% blast cells in BM aspiration or peripheral blood for the diagnosis of AML, while the WHO category decreases the blast threshold to 20%. The WHO classification was updated in 2016 and identified six AML major subtypes (Table 1.2) (Arber et al., 2016). Furthermore, based on clinical ontogeny, AML can be subdivided into three groups: 1) *De novo* AML arises in individuals without preceding haematological disorders or leukaemogenic exposures; 2) secondary AML arises in patients who have a clinical history of haematological disorders such as myelodysplastic syndrome (MDS) or myeloproliferative neoplasm (MPN); and 3) therapy-related AML is associated with prior chemotherapy or radiotherapy exposures (Lindsley et al., 2015).

1.2.1.2 AML pathogenesis

The accumulation of chromosomal abnormalities as well as gene mutations results in a clonal population of poorly differentiated myeloid precursor cells. About 40-50% of all AML patients are cytogenetically normal, while cytogenetic abnormalities are found in approximately 50-60% of adult AML, including loss or gain of the whole chromosome, chromosomal deletion, inversion and translocation (Ghanem et al., 2012, Mrozek et al., 2004). Genetic mutations are also identified in more than 90% of AML cases (Patel et al., 2012, Metzeler et al., 2016).

A two-hit model hypothesis has been suggested for categorising the mutations that associate with leukaemogenesis. In this paradigm, class I mutations enhance the cellular proliferation and survival without affecting the cellular differentiation such as receptor-tyrosine kinases upregulation (FLT3 and c-KIT) or signalling pathways (RAS-RAF1-MEK-ERK), whereas class II mutations which comprise genetic alterations in haematopoietic transcription factors cause impairment in haematopoietic cells differentiation as CCAAT/enhancer-binding protein-alpha (CEBPα), core-binding factor (CBF), nucleophosmin1 (NPM1), promyelocytic leukaemia-retinoic acid receptor-alpha (PML-RARα), mixed lineage leukaemia (MLL), and homeobox (HOX) family (Deguchi and Gilliland, 2002, Dash and Gilliland, 2001). According to this model, class I & II mutations must occur together for the initiation of haematological neoplasms. Since AML patients carry other types of mutations that cannot fall within class I or II, class III mutations have been established including mutations of epigenetic modifiers that regulate cellular proliferation and differentiation such as DNA (cytosine-5)-methyltransferase 3A (DNMT3A), Tet methylcytosine dioxygenase 2 (*TET2*), Additional sex combs like 1 (ASXL1), and Isocitrate dehydrogenase 1/2 (IDH1/2) (Metzeler et al., 2016). The mutations of *FLT3*, *NPM1* and *DNMT3A* genes are the most frequent in AML patients, figure 1.7 illustrates the percentages of the most common mutated genes in 664 AML cases (Metzeler et al., 2016).

Table 1.2: The latest WHO classification of AML.
Adapted from (Arber et al., 2016).

AML with recurrent genetic abnormalities • AML with t(8;21)(q22;q22.1);*RUNX1_RUNX1T1* • AML with inv(16)(p13.1q22) or t(16;16)(p13.1;q22);*CBFB_MYH11* • Acute-promyelocytic leukaemia with t(15;17)(q22;q12) *PML_RARA* • AML with t(9;11)(p21.3;q23.3);*MLLT3_KMT2A* • AML with t(6;9)(p23;q34.1);*DEK_NUP214* • AML with inv(3)(q21.3q26.2) or t(3;3)(q21.3;q26.2); *GATA2*, *MECOM* • AML (megakaryoblastic) with t(1;22)(p13.3;q13.3);*RBM15_MKL1* • AML with *BCR_ABL1* • AML with mutated *NPM1* • AML with biallelic mutations of *CEBPα* • AML with mutated *RUNX1*
AML with myelodysplasia-related changes
Therapy-related myeloid neoplasms
AML, not otherwise specified (NOS) • AML with minimal differentiation • AML without maturation • AML with maturation • Acute myelomonocytic leukaemia • Acute monoblastic-monocytic leukaemia • Acute erythroid leukemia • Acute megakaryoblastic leukaemia • Acute basophilic leukaemia • Acute panmyelosis with myelofibrosis
Myeloid sarcoma
Myeloid proliferations related to Down syndrome • Transient abnormal myelopoiesis (TAM) • Myeloid leukaemia associated with Down syndrome

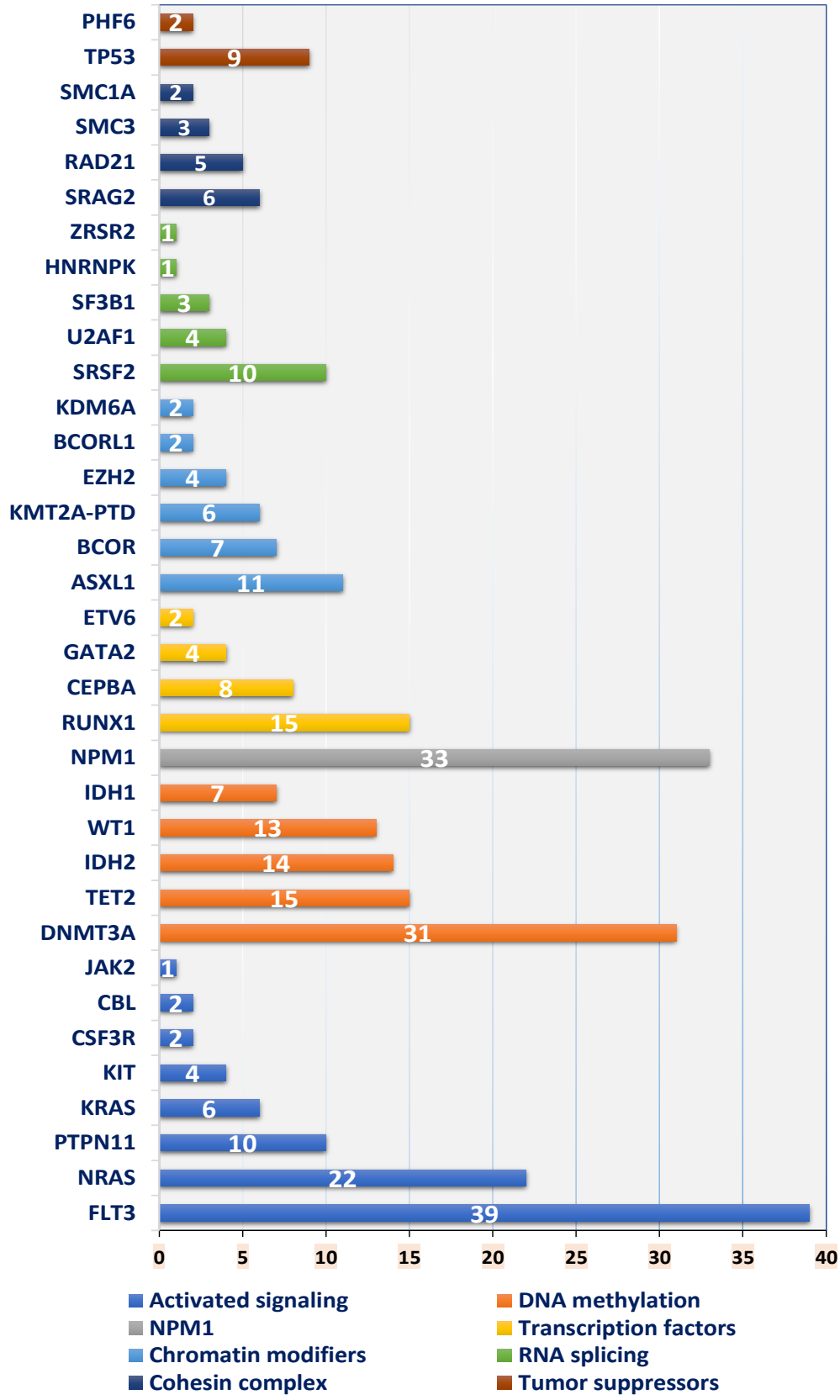

Figure 1-7: The most frequently affected genes in AML patients.
A chart depicts the frequency of mutated genes in 664 AML cases. Adapted from (Metzeler et al., 2016).

1.2.2 Myelodysplastic Syndromes

Myelodysplastic syndromes (MDS), known as preleukaemic phenotypes, are heterogeneous illnesses that characterise by proliferation of myeloid /erythroid/megakaryocyte haematopoietic cells with ineffective differentiation leading to bone marrow failure and peripheral blood cytopenias, reflecting abnormal development of one or more of the blood cell lineages (erythrocytes, platelets, and myeloid cells) (Mufti et al., 2008, Bejar and Steensma, 2014, Mufti, 2004, Rodak et al., 2013). MDS are one of the most common haematological disorders in elderly patients, with a median age at diagnosis of over 65 years, though MDS can occur in younger individuals (Rodak et al., 2013). MDS patients present with clinical manifestations of anaemia, neutropenia, and thrombocytopenia, leading to fatigue, more susceptible to infections, bleeding and bruising and other symptoms (Rodak et al., 2013).

1.2.2.1 MDS classification

There are three classification systems using to classify MDS into subtypes. In 1982, MDS were classified by the FAB classification scheme depending on the percentage of blasts and morphological dysplastic criteria (Bennett et al., 1982). Patients are diagnosed with MDS when the percentage of blasts is about 5-30% of all BM cells and/or dysplastic bone BM is existent. Secondly, the International prognostic scoring-system (IPSS) was introduced in 1997 and is based on a percentage of BM blasts, cytogenetic abnormalities and the number of cytopenias (Greenberg et al., 1997). The IPSS system is useful in predicting rates of survival and transition to AML. According to the IPSS criteria, the increase percentages of blast-cells (less than 5%, 5%-10%, 11%-20% and 21%-30%) indicate the severity of MDS with an elevated risk for AML progression. Finally, the WHO developed a classification system for MDS in 2001, followed by a revised version in 2008. Later in 2016, a newly revised version was released and identified eight MDS-subtypes (Table 1.3) (Arber et al., 2016). The WHO system relies on morphologic features, clinical features, and cytogenetic abnormalities. According to this scheme, patients with 10%-19% BM blast cells are

diagnosed with high-risk MDS, whereas patients with more than 20% of blast cells are diagnosed with AML.

1.2.2.2 MDS pathogenesis

Based on the clinical ontogeny, MDS can be subdivided into two categories: 1) primary MDS/*de novo* MDS occur in previously healthy individuals and 2) Secondary MDS/therapy-related MDS appear in patients who have a clinical history of prior exposure to chemotherapy or radiotherapy to treat another medical illness. Cytogenetic abnormalities are found in about 50% of MDS cases, including monosomy 5 or 7, deletion of the long arm of chromosomes 5, 7 or 20, trisomy 8, translocations, inversions and deletions involving other chromosomes (Bejar et al., 2011). Somatically mutated genes are frequently found in adult MDS patients, including mutations in mRNA splicing factors, epigenetic regulators, TP53, transcription factors, cohesion factors and kinase signalling pathways (Bejar and Steensma, 2014, Sperling et al., 2017). Mutations of genes that encode mRNA splicing and epigenetic regulations are the most frequent in MDS patients and represent around 75% of all cases (Figure 1.8) (Bejar and Steensma, 2014, Sperling et al., 2017). The genetic abnormalities in MDS patients including chromosomal abnormalities, gene mutations, and epigenetic abnormalities are associated with AML transformation (Bejar et al., 2011). About 30% of all patients with MDS evolve AML during the course of the disease (Mufti, 2004).

Table 1.3: WHO categorisation of MDS.
Adapted from (Arber et al., 2016).

MDS with single lineage dysplasia
MDS with ring sideroblasts (MDS-RS) • MDS-RS and single lineage dysplasia • MDS-RS and multilineage dysplasia
MDS with multilineage dysplasia
MDS with excess blasts
MDS with isolated del(5q)
MDS, unclassifiable
Provisional entity: Refractory cytopenia of childhood
Myeloid neoplasms with germ line predisposition

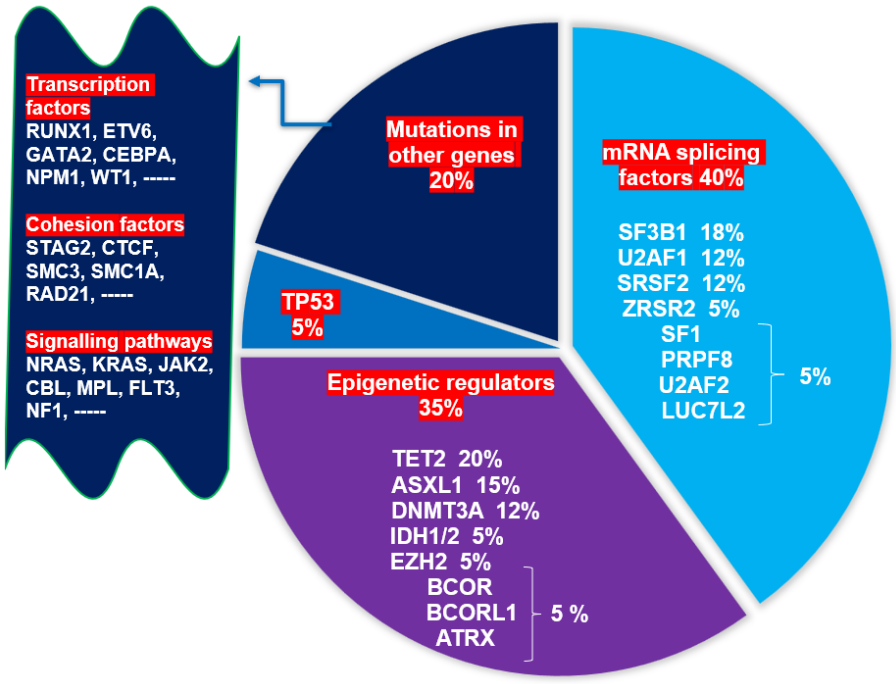

Figure 1-8: The most recurrently affected genes in MDS patients.
Adapted from (Sperling et al., 2017, Bejar and Steensma, 2014).

1.2.3 Familial leukaemia syndromes

There are several hereditary syndromes with systemic anomalies that predispose and develop haematological malignancies such as (1) BM failure syndromes, as severe congenital neutropenia, Diamond-Blackfan anaemia, and congenital thrombocytopenia; (2) DNA-repair deficiency syndromes, as Fanconi anaemia; and (3) tumour suppressor gene syndromes, as Li-Fraumeni syndrome (Owen et al., 2008). However, there are some families without systemic manifestations evolving haematological malignancies known as pure familial neoplasms. Some genes have been identified in non-syndromic MDS/AML predisposition such as RUNX1, CEBPα, GATA2, ETV6, ANKRD26, and DDX41 (Table 1.4) (Song et al., 1999, Arber et al., 2016).

Hereditary leukaemia patients are relatively rare, and they are younger than sporadic MDS/AML cases, with an autosomal dominant inheritance pattern (Owen et al., 2008). Other acquired mutations are required for the MDS/AML transformation. RUNX1 Familial leukaemia, also known as familial platelet disorder, is characterised by thrombocytopenia and platelets dysfunction with an increased propensity of evolving MDS/AML (Song et al., 1999). *CEBPα* mutations are also involved in Familial MDS/AML with similar features in both germline and sporadic cases (Owen et al., 2008). The morphological lineaments consist of FAB M1/M2 subtypes, normal karyotypes, an abundance of Auer rods, misexpression of CD71, and eosinophilia. Haploinsufficiency of GATA2 is another familial MDS/AML predisposition gene with mutations in the second zinc finger domains (Hahn et al., 2011). In addition, these mutations have been also reported in other immunodeficiency syndromes with MDS/AML predisposition as MonoMAC syndrome, DCML deficiency syndrome, and Emberger syndrome with additional systemic abnormalities (reviewed in further details in section 1.3.5) (Dickinson et al., 2011, Hsu et al., 2011, Ostergaard et al., 2011).

Table 1.4: WHO categories of familial neoplasms.
Adapted from (Arber et al., 2016).

Myeloid neoplasms with germ line predisposition without organ dysfunction • AML with germ line *CEBPA* mutation • Myeloid neoplasms with germ line *DDX41* mutation
Myeloid neoplasms with germ line predisposition with pre-existing platelet disorders • Myeloid neoplasms with germ line *RUNX1* mutation • Myeloid neoplasms with germ line *ANKRD26* mutation • Myeloid neoplasms with germ line *ETV6* mutation
Myeloid neoplasms with germ line predisposition and other organ dysfunction • Myeloid neoplasms with germ line *GATA2* mutation • Myeloid neoplasms associated with BM failure syndromes • Myeloid neoplasms associated with telomere disorders • Myeloid neoplasms associated with Down syndrome

1.3 *GATA2* transcription factor

1.3.1 The GATA family of transcription factors

The GATA (Guanine/Adenine/Thymine/Adenine) family is a nuclear zinc-finger (ZnF) transcriptional factors that trigger or suppress the expression of target genes by binding to the DNA sequence WGATAR (W:A/T, R:A/G) through two highly conserved ZnF domains, in which each ZnF domain binds to four-cysteines and forms Cys-X2-Cys-X17-Cys-X2-Cys complexes to stabilise the construction of ZnF domains (Merika and Orkin, 1993, Tsai et al., 1989). The GATA family contains six members. The expression of GATA1, GATA2 and GATA3 is found in haematopoietic cell lineages, while GATA4, GATA5 and GATA6 members are expressed in tissues of mesodermal/endodermal ancestries such as the heart, liver and lung (Figure 1.9) (Laverriere et al., 1994). GATA1 is broadly expressed within the differentiated cells of the erythrocyte, megakaryocyte and eosinophil lineages (Orkin, 2000). Conversely, GATA2 is specifically expressed in adult and embryonic haematopoietic stem and progenitor cells (HSPCs), erythroid-precursor, megakaryocytes and mast cells (Tsai et

al., 1994, Tsai and Orkin, 1997). GATA3 is essential for the T-cells development (Ting et al., 1996). On the other hand, the expression of these GATA members is not only restricted to haematopoietic lineages, in which GATA1 can be expressed in the testis in Sertoli-cells; GATA2 is existent in the central nervous system, endothelial cells and placenta; and GATA3 is found in kidney, central nervous system and skin (Vicente et al., 2012a).

The particular haematological functions of the GATA family members have been widely studied using *Gata*-knockout (KO) mice. The expression of GATA1 is indispensable for the normal maturation of erythroid, megakaryocytes, and mast cells. *Gata1*-KO mice reveal defective erythropoiesis with blocking in the erythroid differentiation at pro-erythroblast phase and die at embryonic day (E) 10.5-11.5 (Takahashi et al., 1998, Fujiwara et al., 1996). Adult *Gata1* heterozygote mice die at 5 months old with serious anaemia and thrombocytopenia due to splenomegaly, in which pro-erythroblast/megakaryocyte precursor cells fail to terminally generate mature erythroid/megakaryocyte cells and accumulate in the spleen (Takahashi et al., 1998). Low expression of *Gata1* is also associated with a defect in mast cells differentiation, while mast cells restore their differentiation potential upon retroviral-derived-*Gata1* overexpression (Migliaccio et al., 2003). *Gata2*-null embryos die at E10-11 of gestation due to severe anaemia and show a defect in HSCs formation (Tsai et al., 1994). GATA3 is a vital contributory factor to thymocytes differentiation and terminal T-cells maturation. *Gata3*-mutant mice die at E11-12 due to internal haemorrhage and display growth malformations in spinal cord and brain (Pandolfi et al., 1995). *Gata3*-null embryonic-stem-cells show a reduction in circulating T-cells due to an impairment in immature thymocytes development (double-negative-thymocytes) with normal differentiation towards myeloid/ erythroid/B-cell populations (Ting et al., 1996). *Gata4*-null embryos die at E8.5-10.5 revealing defects in heart tube formation (Kuo et al., 1997). *Gata5*-KO mice are born healthy but show some genitourinary abnormalities in females (Molkentin et al., 2000). Early embryo lethality is observed in *Gata6*-null mice due to defective extraembryonic development (Koutsourakis et al., 1999).

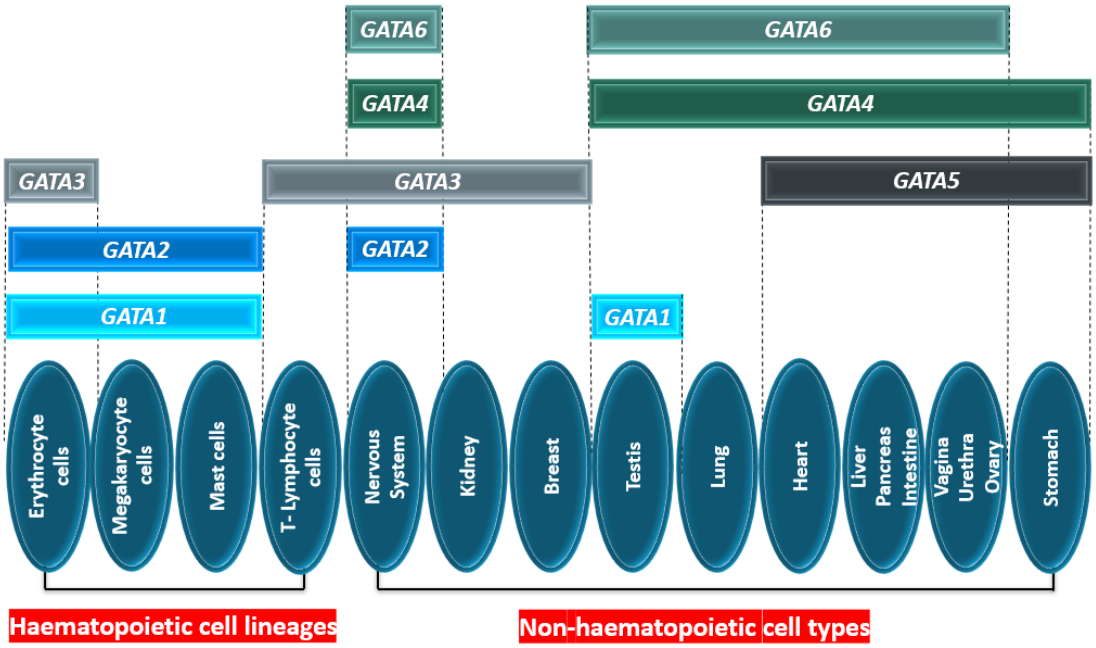

Figure 1-9: The expression of GATA family members.
Adapted from (Lentjes et al., 2016).

1.3.2 *GATA2* gene structure and expression

The *GATA2* gene is situated on the human long arm of chromosome three (3q21.3), while chromosome six includes the murine *Gata2* gene. The human *GATA2* gene contains seven exons and can produce three mRNA transcripts, whereas the murine *Gata2* gene has six exons and can produce two mRNA transcripts (Figure 1.10 A and B) (Lee et al., 1991, Minegishi et al., 1998). The transcripts are identical and only differ at their first untranslated exon, in which the distal IS-exon is specifically utilised in haematopoietic and neuronal compartments while the proximal IG-exon is exploited in all other tissues that express GATA2. About 466–480 amino acids are produced from both murine and human mRNA transcripts with a molecular weight of around 50 KDa. The *GATA2* genome has two fully preserved zinc finger (ZnF) domains that are encoded by exon 4 and 5: N-terminal zinc finger (N-ZnF) which interact with other proteins (protein-protein reciprocal interactions), and C-terminal zinc finger (C-ZnF) which is responsible for the specificity of DNA binding (Trainor et al., 2000, Merika and Orkin, 1993). The *GATA2* non-finger domains encompass of two transactivation

domains (TAD), sited in both terminal regions; a nuclear localisation signal (NLS); and a negative regulatory domain (NRD)(Figure 1.10 C) (Minegishi et al., 2003).

GATA2 expression is controlled by specific cis-acting regulatory elements that distribute throughout the mouse genome such as -77kb, -3.9kb, -2.8kb, -1.8kb, and +9.5 kb, these elements are defined according to their position to the IS-promoter (Grass et al., 2006). These positions are occupied by *Gata2* itself or other transcription factors to regulate the expression of downstream targets. A cis-element −2.8 kb upstream of the 1S-exon is required for *Gata2* expression in haematopoietic stem and progenitor cells (HSPCs), while a −1.8 kb upstream site represses the expression of *Gata2* in early erythroid progenitors (Grass et al., 2006). -77kb-null mice die at embryonic day 14 due to anaemic phenotypes (Johnson et al., 2015). The deletion of -77kb enhancer results in a defect in the differentiation of foetal-liver myeloid/erythroid/megakaryocyte progenitors. A cis-element +9.5kb, an E-box domain, is located in in the fourth intron and regulates HSCs generation by controlling the expression of essential genes that are required for the emergence of HSCs from the haemogenic endothelium (Gao et al., 2013).

The GATA2 transcription factor is modified by post-translational modifications such as phosphorylation, acetylation, sumoylation and ubiquitination, which are essential for *GATA2* activation and repression (Figure 1.10 C). Interleukin-3 phosphorylate GATA2 in haematopoietic progenitor cells by activating the mitogen-activated protein kinase pathway that regulates cellular proliferation and differentiation (Towatari et al., 1995). GATA2 can also be phosphorylated at cyclin-dependent-kinases (CDKs) motifs, indicating the regulated functions of GATA2 in cellular proliferation (Koga et al., 2007). GATA2 can be acetylated at different lysine-residues that enhance the effectiveness of GATA2 DNA-binding capability, and mutations in these sites are associated with a disruption of the GATA2 protein (Hayakawa et al., 2004). Two potential sumoylation sites have been identified in human GATA2 protein (human 221–224 and 388–391 amino acids), and this modification is associated with transcriptional suppression (Chun et al., 2003). Ubiquitination-proteasome-

dependent pathways are responsible for GATA2 protein degradation (Minegishi et al., 2005).

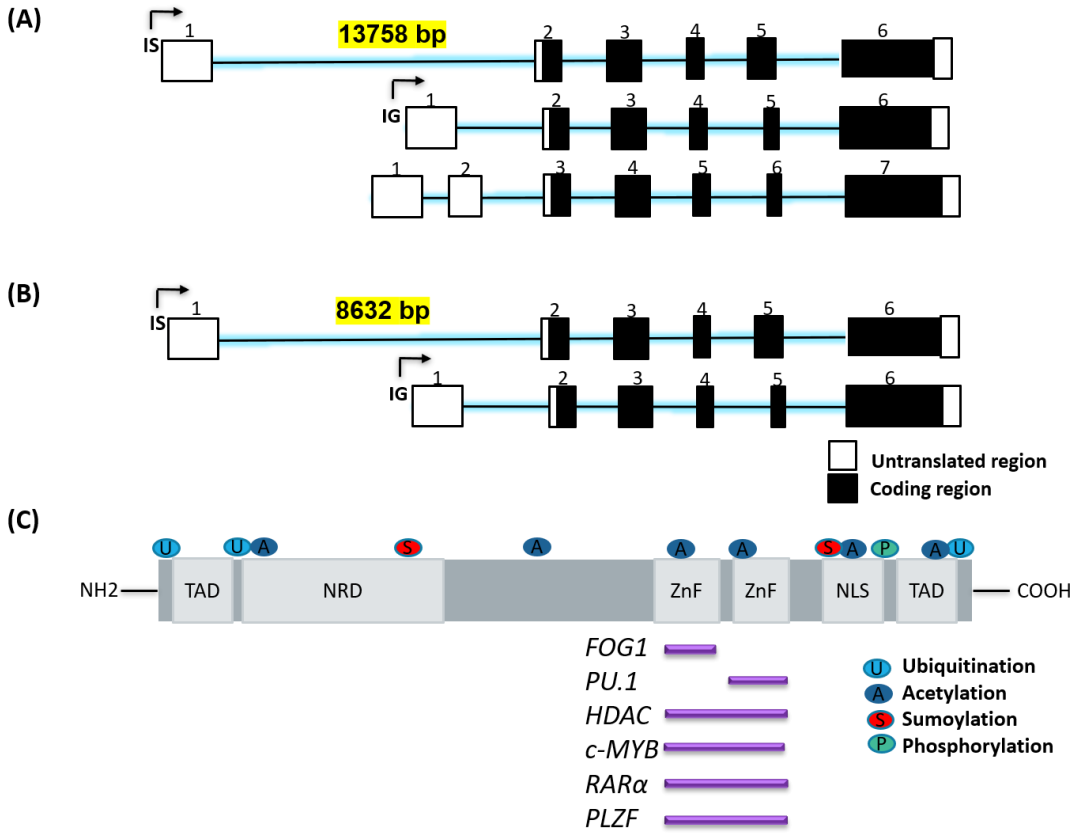

Figure 1-10: Genomic and protein structure of *GATA2*.
(A) The scheme describes the human *GATA2* locus. Arrows show the starter sites for transcription. Additional information is currently unavailable about the third mRNA transcript. (B) Diagram illustrates the mouse *Gata2* locus. Spanning about 8.6 kb. (C) *GATA2* protein has several sites for post-translational modifications. *GATA2* ZnF domains interact with other proteins as *FOG1, PU.1, HDAC, c-MYB, RARα,* and *PLZF* (highlighted in purple). Adapted from (Vicente et al., 2012a, Rodrigues et al., 2012).

1.3.3 GATA2 functions in HSCs specification and maintenance

Many investigational methodologies have been employed to evaluate the function of GATA2 in haematopoietic stem and progenitor cells (HSPCs) and haematopoiesis. GATA2 expression profile displays that *Gata2*-mRNA expression is the highest in HSCs and the mRNA level gradually declines during the cellular development /differentiation into mature blood cells that show the least *Gata2*-mRNA expression (Menendez-Gonzalez et al., 2019b, Orlic et al., 1995, Guo et al., 2013). *Gata2*-reporter knock-in mouse models show that *Gata2* is expressed in primitive haematopoietic cells as early as embryonic-day 7.5 in the yolk sac, placenta, foetal liver, and aortic-endothelial cells and intra-aortic haematopoietic cluster cells of the Aorto-Gonad-Mesonephros region, where definitive haematopoiesis occurs (Minegishi et al., 2003, Kaimakis et al., 2016). Knock-in *Gata2*-Venus fluorescent reporter in *Gata2* locus with typical *Gata2* expression/function shows all HSCs in the AGM region at E11 are expressed *Gata2*-Venus and *Gata2*-Venus-positive cells are able of reconstituting multi-lineage haematopoietic cells in transplant studies, whereas some HPCs are negative for *Gata2*-Venus-reporter (Kaimakis et al., 2016). Colony-forming-cell (CFC) assays illustrate that *Gata2*-Venus-positive cells are bi-potent and/or multipotent progenitors (CFU-GEMM and CFU-GM), while *Gata2*-Venus negative cells (*Gata2* independent HPCs) are mono-potent progenitors as CFU-G, CFU-M and BFU-E.

GATA2 performs an important role in the generation of HSCs from haemogenic endothelium in haematopoietic developmental processes (Figure 1.11) (Gao et al., 2013, de Pater et al., 2013). In this setting, GATA2 expression is initiated by Notch1 and Bmp4 signalling pathways, which then acts together with different haematopoietic TFs, involving FLI1, SCL/TAL1, LMO2 and RUNX1, that cause HSCs to emerge from haemogenic endothelium. Chromatin immunoprecipitation analysis shows Notch1 binds to *Gata2* promoter in murine aortic endothelium cells at E9.5 to initiate the definitive haematopoiesis (Robert-Moreno et al., 2005). Ablation of Notch1 signalling is accompanied by embryonic lethality at E10, entire loss of haematopoietic progenitors, and diminished expression of *Gata2, Runx1*, and *Scl/Tal1* TFs, whereas Notch1 overexpression in mouse cell-lines leads to

upregulation of *Gata2* and inhibits erythrocytes/granulocytes differentiation (Robert-Moreno et al., 2005, Kumano et al., 2001). RUNX1 is a vital regulator for the development of HSCs from endothelial cells in the AGM area. Notch1 signalling activates *Gata2b* expression, *Gata2* ortholog in zebrafish, that ultimately stimulates *Runx1* expression in the haemogenic endothelium to initiate the HSCs emergence, implying that *Gata2* is a key regulator for the HSCs development in the haemogenic endothelium and acts an upstream of *Runx1 (Butko et al., 2015)*. Mouse conditional deletion of *Scl/Tal1* using *Tie2-Cre,* a specific Cre for embryonic/adult stem cells, shows normal HSCs formation, signifying that SCL/TAL1 is necessary for mesodermal cells specification towards the haemogenic endothelium that further differentiates into foetal/adult HSCs (Schlaeger et al., 2005). *Gata2* expression is activated by BMP4 signalling and activates the expression of BMP4, SCL/TAL1 and FLK1, an endothelial cell growth factor, and increases the formation of endothelial cell (Lugus et al., 2007). Moreover, the HSC proliferation is predominantly regulated by the EVI1 Tf, and *Gata2* promoter works as an enhancer for *Evi1* to mediate HSCs proliferation (Yuasa et al., 2005). *Evi1*-null mice die at E10.5 with a reduction in HSCs-pool size and display a minimal expression level of *Gata2*. *Evi1* or *Gata2* overexpression in *Evi1*-null cells reverses the phenotype and enhances HSCs proliferation. Collectively, the expression of GATA2 and FLI1 is controlled by Notch1/BMP4 signalling, later GATA2 and FLI1 regulate the expression of each other and cooperate to trigger expression of SCL/TAL1 and RUNX1.

Constitutive (germline) *Gata2* homozygote deletion ($Gata2^{-/-}$) mice exhibit a defect in the generation of definitive haematopoietic cells, $Gata2^{-/-}$ embryo is anaemic, and dies at E10.5 of gestation before the HSC generation in the AGM region (Table 1.5) (Tsai et al., 1994). Analysis of yolk sac of $Gata2^{-/-}$ embryos show a threefold reduction in HSC numbers (Tsai et al., 1994, Tsai and Orkin, 1997). The roles of $Gata2^{-/-}$ in definitive haematopoiesis were studied in chimeric mice by injecting $Gata2^{-/-}$ embryonic stem (ES) cells into wild-type blastocysts, $Gata2^{-/-}$ ES cells showed an ineffective production in primitive haematopoietic progenitors with normal maturation of macrophage/erythroid cells (Tsai et al., 1994, Tsai and Orkin, 1997), proving that GATA2 is critical for the regulation of the earliest stages of

haematopoiesis. Furthermore, conditional deletion of *Gata2* in vascular endothelial cells utilising vascular-endothelial-cadherin-Cre (Vec-Cre) before the HSCs formation shows a reduction in HSC compartments, indicating that *Gata2* is essential for HSCs generation in the AGM region (de Pater et al., 2013). Vav-Cre mouse models are used to explore the impact of *Gata2* deletion in haematopoietic cells after the HSCs/HPCs generation (Table 1.5), in which the Vav-promoter is expressed in haematopoietic compartments at E11 (de Pater et al., 2013, Stadtfeld and Graf, 2005). *Gata2*$^{fl/fl}$; Vav-Cre^{+} embryos survive until E16 and display a significant reduction in colony forming-cell (CFC) numbers at AGM-E11, foetal liver-E11 and foetal liver-E14 with a twofold reduction in HSCs numbers (de Pater et al., 2013). Foetal liver-E14 HSCs exhibit a threefold increment in annexin V level, an apoptotic marker, and fail to adequately reconstitute haematopoietic lineages upon transplantation experiments, signifying that *Gata2* is indispensable for HSCs survival and maintenance in foetal liver (de Pater et al., 2013). In addition, *Gata2* heterozygote germline (*Gata2*$^{+/-}$) and conditional knockout (Gata2$^{+/fl}$; Vav-Cre^{+}) mouse models have been used to further explore the role of *Gata2* in the HSCs development (Table 1.5). *Gata2*$^{+/fl}$*; Vav-Cre*$^{+}$ embryos display a reduction in HSCs and CFC numbers in foetal AGM and liver (de Pater et al., 2013). *Gata2*$^{+/-}$ embryos have decreased numbers of HSCs in the AGM region, and AGM-HSCs exhibit a reduced efficiency of reconstituting haematopoietic populations with an impairment in HSCs self-renewal potential in competitive serial transplantation experiments, while the number of HSCs appears normal in the *Gata2*$^{+/-}$ yolk sac, foetal liver and BM, but foetal BM-HSCs show an impairment in multi-lineage reconstitution in transplant settings (Ling et al., 2004).

In human cord-blood, knockdown of GATA2 expression in CD34^{+}CB shows a threefold decrease in CFC numbers and reduced frequencies of primitive haematopoietic compartments in long-term-culture-initiating-cells (LTC-IC) experiments (Menendez-Gonzalez et al., 2019b). Another study which utilises twofold knock-down of *GATA2* in CD34^{+}CB exhibits a positive correlation between *GATA2* expression and vital genes that involve in HSCs formation as *KIT, GFI1B,* and *HOXB4*, representing *GATA2* target-genes in CD34^{+}HSPCs (Fujiwara et al., 2012). *GATA2* knockdown in human K562 cell-line which derives from chronic myelogenous leukaemia patients is associated with a

reduction in the expression of *HOXB4*. Chromatin-immunoprecipitation analysis displays that *GATA2* directly interacts with *HOXB4* promoter, an essential regulator of HSCs-pool expansion.

In the adult stage, conditional deletion of *Gata2* in adult mice using inducible Cre ($Gata2^{fl/fl}$; $ER\text{-}Cre^{+}$, induced by tamoxifen treatment) displayed that mice die 7-14 days post tamoxifen injection, peripheral blood cytopenias, BM failure with a whole ablation in primitive haematopoietic populations and a defect in reconstitution potential in BM transplantation experiments (Table 1.5) (Li et al., 2016). In a similar manner, *Gata2* conditional knockout in adult mice employing inducible Mx1-Cre (*$Gata2^{fl/fl}$; $Mx1\text{-}Cre^{+}$,* induced by pIpC) showed an entire reduction in primitive haematopoietic compartments, implying *Gata2* autonomously maintains haematopoietic homeostasis in adult BM mice (Table 1.5) (Menendez-Gonzalez et al., 2019b). Furthermore, analysis of haematopoietic compartments in the germline *$Gata2^{+/-}$* of adult mice revealed that a reduction in the frequency of HSCs with a defect in reconstituting potential upon competitive transplant experimentations, signifying that *Gata2* is indispensable for adult HSCs homeostasis (Rodrigues et al., 2005). An increase in quiescence and apoptosis are observed in *$Gata2^{+/-}$* adult HSCs. The particular level of *Gata2* is tightly required to maintain the survival rate of HSCs. *$Gata2^{+/-}$* HSCs show an increased apoptotic level due to decreased expression of the BCL-xL protein, an anti-apoptotic gene, suggesting that *Gata2* directly influences the HSCs survival (Table 1.5) (Rodrigues et al., 2005). Likewise, adult *$Gata2^{+/-}$* mice exhibited a reduction in LSK populations in another study (Guo et al., 2013). Analysis of single-cell expression in *$Gata2^{+/-}$* LSK-cells displays a reduced expression of megakaryocytes/erythroid genes as *Gfi1b*, *Cd41*, and *Gata1*, while an increased expression of myeloid/lymphoid markers such as *Flt3*, *Sell*, *Cd34*, *Cd53*, and Cebpα (Guo et al., 2013). Table 1.5 demonstrates the crucial roles of GATA2 in haematopoiesis utilising mouse models.

Over-expression models provide more insights into how GATA2 regulates HSPCs proliferation and differentiation. Enforced expression of *Gata2* using a retroviral vector in mice showed that *in vitro* CFC and LTC-IC assays of BM cells exhibit reduced

numbers of haematopoietic progenitor colonies with natural apoptotic levels (Persons et al., 1999). Murine HSPCs display a reduced capability to differentiate when transplanted into irradiated hosts with peripheral pancytopenia (Persons et al., 1999). Overexpression of *Gata2* in murine HSPCs leads to suppression of the expression of c-*Myc* mRNA and accumulation of cell-cycle inhibitors such as p21 and p27 proteins (Ezoe et al., 2002). GATA2 constrains the production of SKP2 and CUL1 proteins and prevents the ubiquitination process of p21 and p27**,** indicating GATA2 works as a regulator of quiescence in HSPCs. Furthermore, xenotransplantation of human $CD34^{+}CD38^{-}$ CB-cells with enforced expression of *GATA2* shows a reduction in LTC-IC and CFC numbers in *in vitro* assays, a defect in HSPCs reconstitution potential, a block in HSPCs differentiation, normal apoptosis, and an increase in HSPCs quiescence (Tipping et al., 2009). The expression level of *GATA2*-mRNA is around threefold higher in quiescent HSPCs than proliferative $CD34^{+}CD38^{-}$ HSPCs. These changes in the cell-cycle status are combined with repression of essential cyclin-dependent-kinase regulators that mediate the cellular proliferation as CDK4, CDK6, and *MCM5* (Tipping et al., 2009). Moreover, murine low-level overexpression of *Gata2* that is physiologically close to leukaemia with GATA2-overexpression revealed that transplantation of *Gata2* overexpressed BM cells enhances the expansion of myeloid progenitor cells and inhibits the differentiation of lymphoid progenitors (Nandakumar et al., 2015). GATA2 induces the proliferation of myeloid cells beyond the GMPs stage via N-MYC and HOXA9 signalling pathways. Collectively, the precise level of GATA2 expression is decisive for regulating the fate decision of HSCs between quiescence, self-renewal, and differentiation to preserve the HSC pool size.

1.3.4 The role of GATA2 in haematopoietic differentiation

GATA2 acts as a decisive regulator for myeloid cell differentiation. The frequency of CMP, MEP and CLP in adult *Gata2* $^{+/-}$ BM is comparable to wild-type mice, while the number of GMP is decreased in *Gata2* $^{+/-}$ BM cells (Rodrigues et al., 2008). *In vitro* colony-forming assay of *Gata2* $^{+/-}$ BM cells reveals a reduction in the numbers of CFU-GM colonies, while the differentiation of other haematopoietic progenitors is unaffected (Ling et al., 2004, Rodrigues et al., 2008). Knockdown of *Gata2* in wild-

type GMP and CMP cells showed the number of CFU-GM is lower in GMP cells compared with CMP cells, demonstrating that the defect in the GMP population is independent of the differentiation defect of HSCs and implying the role of *Gata2* in GMP proliferation and differentiation through the Notch signalling target gene Hairy and enhancer of split homolog-1 (HES1), a regulator of the cell cycle progression of haematopoietic cells (Rodrigues et al., 2008). Since the frequency of dendritic cells (DCs) is commonly reduced in GATA2 haploinsufficiency syndromes, Onodera et al. investigated the roles of GATA2 in DCs formation and differentiation (Onodera et al., 2016). *In vivo* conditional deletion of *Gata2* in adult haematopoietic compartments showed a drastic reduction in CMPs, GMPs, CLPs, common dendritic precursors (CDPs), and peripheral dendritic cells ($Cd11c^{+}$). *In vitro* deletion of *Gata2* in CMPs, GMPs, CLPs, and CDPs after culturing seven-days in BM-feeder environments revealed reduced numbers of $CD11c^{+}$ cells that derived from CMPs and CDPs, implying that *GATA2* has particular roles for DCs differentiation through LSK-CMPs-CDPs axis. Conversely, adult haploinsufficient-*Gata2* ($Gata2^{+/-}$) showed normal differentiation of CDPs and $Cd11c^{+}$ cells.

GATA2 expression plays dosage-dependent functions in HSPCs differentiation, in which the decision of HSCs gives rise to erythroid or myeloid lineages that is determined by the interaction between GATA1/GATA2 and PU.1 TFs, respectively (Figure 1.11) (Zhang et al., 1999). PU.1 is required for myeloid/lymphoid specification (Chou et al., 2009, Arinobu et al., 2007). GATA1/GATA2 interacts with PU.1 through the C-ZnF domain and inhibits PU.1 binding to c-JUN coactivator that is required to initiate myeloid differentiation. PU.1 hinders erythroid differentiation by inhibiting GATA1/GATA2 DNA binding capacity during myeloid differentiation, while overexpression of GATA2 inhibits the transactivation potential of PU.1 resulting in transcriptional repression of myeloid genes (Walsh et al., 2002). Knock-down of *Gata2* in $Gata1^{-}$ megakaryocyte/erythrocyte (G1ME) murine cell line shows a threefold increase in *Pu.1* expression and induces the differentiation towards macrophages (Chou et al., 2009). On the contrary, both GATA2 and PU.1 expression are required for mast-cells development (Walsh et al., 2002). Both GATA2 and PU.1 enhance c-KIT expression that is required for mast-cells differentiation. Mast-cell

differentiation is executed by the GATA-switch mechanism, where GATA2 replaces co-factor friend of GATA1 (FOG1*)* at the *Gata2* locus site resulting in upregulated GATA2 and downregulated FOG1 expression to initiate mast-cells maturation (Cantor et al., 2008). GATA2 expression is required for the terminal differentiation of basophils and mast cells from pre-basophil/mast progenitors (Pre-BMPs) (Li et al., 2015). *Gata2* knockout mice showed a reduction in numbers of basophils/mast-cells, while *Gata2*$^{+/-}$ Pre-BMPs fail to differentiate into mast cells and normally differentiate into basophils. Furthermore, GATA2 is essential for the expression of immunoglobin-E receptor (FcεRI) on the basophil/mast cells surface that bind to IgE to defend against allergens. GATA2 expression is needed to sustain IL4 and IL13 expression in basophils and mast-cells, respectively. *Stat5* directly binds to the *Gata2* promoter and mediates the differentiation of basophils/mast cells.

The expression levels of GATA2 regulate the fate decision alongside erythroid-megakaryocyte differentiation pathways. The expression of GATA1 is crucial for erythroid differentiation (Guo et al., 2016, Tsang et al., 1997). *Gata2* binds to *Gata1* promoter and suppresses the expression of *Gata1* in HSPCs by interacting with *Lsd1* and *Tal1* TFs (Guo et al., 2016). The expression of *Gata2*, *Lsd1* and *Tal1* mRNA is decreased during the differentiation of erythroid cells. In this process, *Lsd1*/*Tal1* complex suppresses *GATA2* expression, and *GATA2* is displaced by *GATA1* from a chromatin site by "GATA-switch" (Guo et al., 2016, Tsang et al., 1997). GATA switching is mediated by the interaction between *Gata1* and *Fog1*, and this *Gata1*/*Fog1* interaction is essential to sustain the erythroid maturation (Tsang et al., 1997). In addition, GATA2 prohibits erythroid differentiation through the regulation of erythropoietin (EPO) expression, which is essential for the development of erythroid progenitors. *Gata2* disturbs the transcriptional activity of *Epo* by binding to the GATA site of the *Epo* gene promoter, inhibiting the erythroid differentiation (Imagawa et al., 1997). On the other hand, elevated level of GATA2 expression is required for the terminal megakaryocyte differentiation (Lulli et al., 2006, Gao et al., 2013). The ETS1 transcription factor regulates megakaryocyte maturation and supports the expression of GATA2 and megakaryocytes downstream genes, providing the critical roles of GATA2 in the megakaryocyte development (Lulli et al., 2006).

GATA2 expression is positively correlated with the formation of megakaryocyte/erythroid progenitors (MegE) and enhances MegE cells formation (Gao et al., 2013). Murine *Gata2* $^{+/-}$ LSK displayed a decrease in *Gata1*-mRNA, *Gfi1b*-mRNA, and MegE cells (Gao et al., 2013). Overexpression of *Gata2* in murine BM-progenitors enhances megakaryopoiesis, while *Gata2*-knockdown reduces colony-forming-megakaryocytes and perturbs terminal megakaryocytes differentiation (Huang et al., 2009).

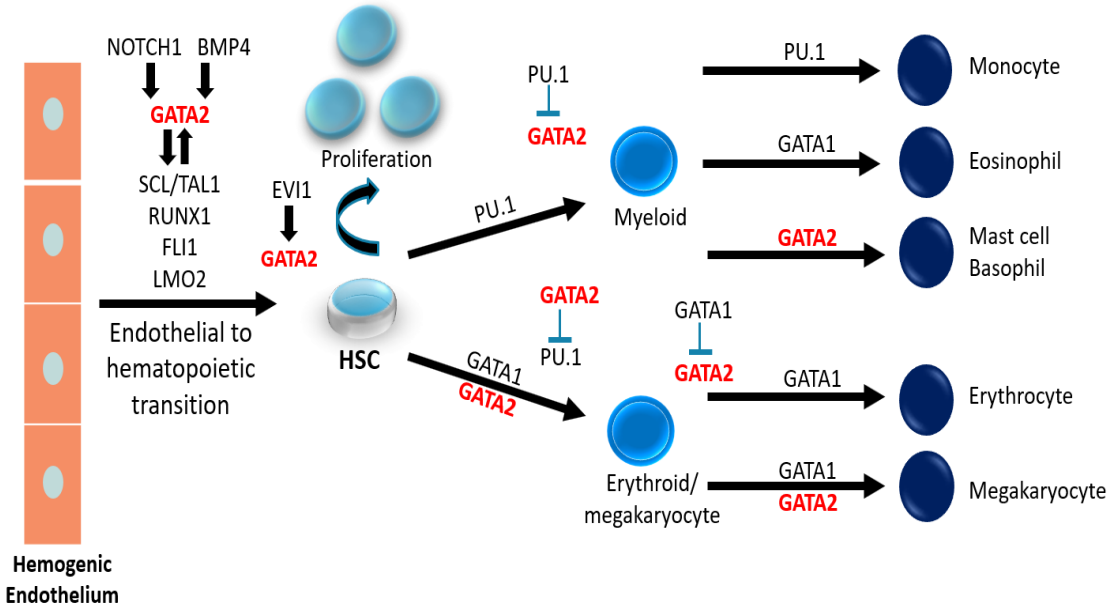

Figure 1-11: The role of GATA2 in haematopoiesis.
GATA2 cooperates with other transcription factors to regulate haematopoiesis. GATA2 is involved in the rise of HSCs from haemogenic endothelium, and later it contributes to the HSCs proliferation. GATA2 and PU.1 have the potential to regulate the decision of HSCs to restrict to erythroid or myeloid lineages. In monocyte and erythrocyte differentiation, *GATA2* is repressed by PU.1 and GATA1, respectively. GATA2 is also essential for the terminal differentiation of megakaryocytes, basophils, and mast cells. (Adapted from (Collin et al., 2015, Hirabayashi et al., 2017)).

Table 1.5: *Gata2* requirements in haematopoiesis utilising mouse models.

Reference	Mouse models	Haematopoietic phenotypes
Foetal haematopoiesis		
(Tsai et al., 1994, Tsai and Orkin, 1997)	*Gata2*-germline-KO (Homozygote)	• Mice die at E10.5 with acute anaemia • Reduced HSC numbers in yolk-sac
	Gata2-germline-KO ESCs-chimera	• Defects in HPCs formation
(Ling et al., 2004)	*Gata2*$^{+/-}$ germline (Heterozygote)	• A reduction in HSC numbers in AGM • A defect in HSCs-AGM in repopulation multi-lineage and self-renewal potential
(de Pater et al., 2013)	*Gata2*-conditional-KO At vascular endothelial (Vec-Cre)	• Mice die at E14 • Decreased numbers of HSCs in AGM.
	Gata2-conditional-KO *Gata2*$^{fl/fl}$*; Vav-Cre*$^{+}$	• Mice die at E16 • A decrease in HSC CFC numbers in AGM & FL with increased apoptosis level
	Gata2-conditional-KO *Gata2*$^{+/fl}$*; Vav-Cre*$^{+}$	• Reduced numbers of HSCs in AGM & FL
Adult haematopoiesis		
(Menendez-Gonzalez et al., 2019b, Onodera et al., 2016, Li et al., 2016)	*Gata2*-conditional-KO *Gata2*$^{fl/fl}$*; Mx1-Cre*$^{+}$ *Gata2*$^{fl/fl}$*; ER-Cre+*	• An entire depletion in LK and LSK compartments
(Rodrigues et al., 2005, Rodrigues et al., 2008)	*Gata2*$^{+/-}$ germline	• A reduction in frequencies of LSK, HSCs, and GMPs • An increase in HSCs quiescence and apoptosis level.

1.3.5 Haematological diseases associated with GATA2 dysregulation

1.3.5.1 GATA2 haploinsufficiency syndromes

The term GATA2 deficiency or haploinsufficiency, a single mutant allele causes decreased GATA2 protein production and/or impaired GATA2 protein functions, has come to be used to describe GATA2 related diseases. *GATA2* mutations were identified in four main clinical syndromes associated with predisposition to evolve MDS and AML: Monocytopenia with *Mycobacterium Avium* Complex (MonoMAC) syndrome; dendritic cell, Monocyte, B-cell and natural killer lymphocytes (DCML) deficiency syndrome; Emberger syndrome; and familial MDS/AML (Figure 1.12) (Dickinson et al., 2011, Hsu et al., 2011, Ostergaard et al., 2011, Hahn et al., 2011). In terms of the mechanisms underlying GATA2 haploinsufficiency, essential amino acid residues that are required for either the DNA binding activity or *cis*-elements effectiveness are disturbed by *GATA2* mutations (Hahn et al., 2011, Katsumura et al., 2018).

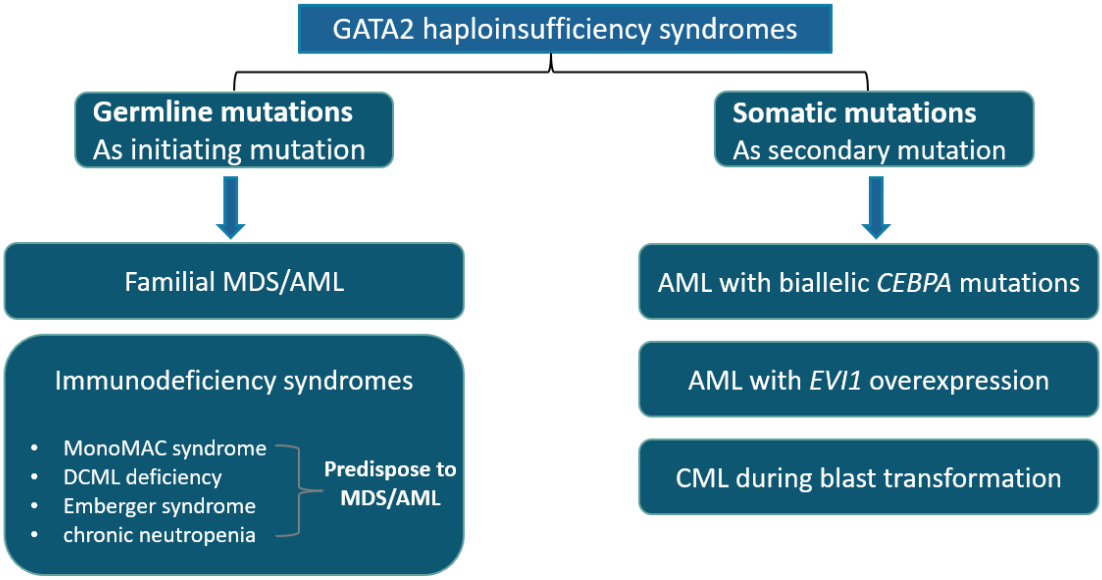

Figure 1-12: Scheme describing GATA2 haploinsufficiency syndromes.

1.3.5.2 *GATA2* mutations

Germline and somatic *GATA2* mutations distribute throughout the *GATA2* locus, and approximately 70% of mutations take place in the zinc finger domains, a DNA binding site (Collin et al., 2015, Wlodarski et al., 2017). N-terminal zinc finger (N-ZnF) and C-terminal zinc figure (C-ZnF) mutations disturb *GATA2* chromatin binding activity and the expression of downstream target genes (Hahn et al., 2011, Katsumura et al., 2018). *GATA2* mutations are mainly categorised into four groups: (1) truncated mutations (nonsense, in-frame-deletion and in-frame-insertion mutations) which represent approximately 60% of haploinsufficient GATA2 cases; (2) around 30% of reported patients are missense mutations; (3) non-coding mutations in intron-4 (+9.5kb cis-element) which form around 10% of cases; and (4) few cases are reported for whole-locus deletions, N/C terminals, and UTR regions (Figure 1.13) (Wlodarski et al., 2017, Collin et al., 2015). The majority of *GATA2* germline mutations are located within the C-ZnF domain, whereas somatic mutations are commonly existent within the N-ZnF domain (Collin et al., 2015). N-ZnF mutations, rather than C-ZnF mutations, affect the expression of target genes and involve in the activation of Ras signalling pathways (Katsumura et al., 2018).

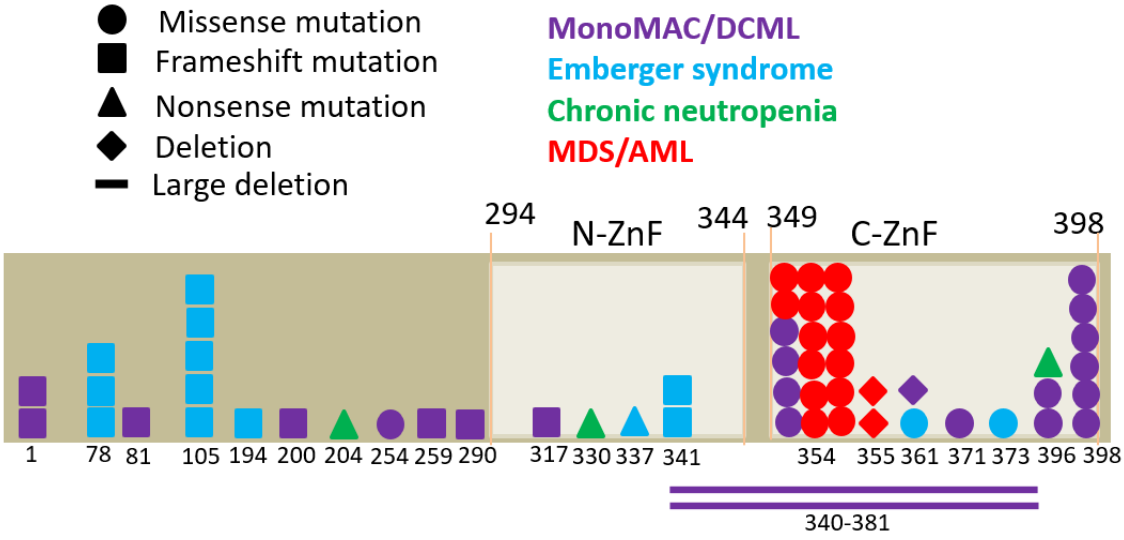

Figure 1-13: GATA2 mutations.
Adapted from (Wlodarski et al., 2017, Hyde and Liu, 2011, Collin et al., 2015)

1.3.5.3 Clinical features of GATA2 haploinsufficiency syndrome

Clinically, GATA2 haploinsufficiency syndromes involve several distinct features to distinguish from sporadic MDS cases including young age at disease onset with a range from 21 to 33 years; unusual disorder in haematological indices; recurrent MDS history within a family (1 in 3); normal haemoglobin, neutrophils, T-cytotoxic cells, and platelets levels in blood; low blood numbers of monocytes, dendritic cells, B-cells, T-helper cells, NK-cells, and CD4:CD8 ratio; a hypocellular BM with diffuse reticulin fibrosis; myeloid/erythroid/megakaryocytes dysplastic features; increased numbers of large granular T-lymphocytes; a depletion in the frequencies of multi-lymphoid progenitors (MLPs), granulocyte-macrophage progenitors (GMPs) and B-lymphocyte/natural killer precursors; normal frequencies of CMPs and MEPs; highly elevated serum Flt3 levels (10 to 100 fold); impaired synthesis of cytokines such as IL6, IL12, TNFα, and IFNγ in peripheral blood; and around 60%-70% of patients have cytogenetic abnormality such as monosomy-7 and trisomy-8 (Collin et al., 2015, Dickinson et al., 2014, Calvo et al., 2011, Bigley et al., 2011).

1.3.5.4 Immunodeficiency syndromes associated with haploinsufficient GATA2

MonoMAC/DCML syndromes are primary immunodeficiency disorders that highly predispose to MDS/AML and characterise by a severe reduction of peripheral monocytes, CD4-lymphocytes, B-cells, NK-cells and dendritic cells (Vinh et al., 2010, Dickinson et al., 2011, Bigley et al., 2011, Hsu et al., 2011). MonoMAC/DCML syndromes present primarily in younger adults and occur as a sporadic or autosomal dominant familial form. Haploinsufficient GATA2 patients are highly susceptible to *Mycobacterium avium* complex infections, human-papilloma virus-infections, fungal-infections, parasite-infections and pulmonary-alveolar proteinosis (GATA2 regulates phagocytosis in pulmonary-alveolar macrophages) with increased propensity to develop MDS/AML. Several cytogenetic abnormalities can develop such as monosomy 7, trisomy 8 or dicentric chromosome 6 with a predisposition to MDS and AML. MonoMAC/DCML patients show a mutation in *GATA2* cis-elements that are required for HSCs generation such as +9.5kb and −2.8 kb sites (Hsu et al., 2013). *GATA2* mutations that are observed in MonoMAC/DCML syndrome include missense

mutations within the C-terminal zinc finger domain (T354M_N371K_R396W_R396Q_R398W), missense mutation outside the fingers domain (P254L), and frameshift mutations (M1del290_G81fs_D259fs_N317fs_R361delRNAN), and a large deletion in both N and C zinc finger domains (Δ340_381). These missense, deletion and frameshift mutations display dominant-negative effects of *GATA2* gene function. Furthermore, Pasquet et al. documented germline *GATA2* mutations in paediatric chronic neutropenia with high risk to acquire MonoMAC syndromes and MDS/AML. Mutations include nonsense mutations in zinc finger domains (R396Q_A372T_M388V_R330X), nonsense mutations outside the DNA domains (R204X_E224X) and a case of whole allele *GATA2* deletion (Pasquet et al., 2013).

Emberger syndrome is an autosomal dominant disorder characterised by primary lymphedema of lower limbs, cutaneous-warts, and deafness with MDS/AML development (Emberger et al., 1979). High levels of GATA2 protein are normally expressed in endothelial cells and lymphatic vessel valves, and haploinsufficiency of GATA2 disrupts the normal lymphatic valve development during embryogenesis (Kazenwadel et al., 2015, Lim et al., 2012). Ostergaard et al. identify *GATA2* mutations in the Emberger syndrome (Ostergaard et al., 2011). These mutations present throughout the genome of *GATA2* and include missense mutations (R361L-C373R), a nonsense mutation (A337X), and frameshift mutations (A78Pfs_L105Pfs_A194Sfs_A341Afs_A341Pfs).

Downregulated GATA2 expression has additionally been observed in aplastic-anaemia, an auto-immune disorder that causes a reduction in HSCs generation and accumulation of fat cells in the BM. GATA2 a pivotal regulator for HSCs proliferation and adipogenesis, in which GATA2 represses adipocytes generation from MSCs through repressing adipogenic marker PPARγ (Tong et al., 2000). Analysing MSCs from aplastic anaemia patients revealed a reduction in *GATA2*-mRNA expression and elevated *PPAR*γ-mRNA as compared with normal individuals, indicating that decreased GATA2 expression leads to fatty marrow accumulation in patients with aplastic anaemia (Xu et al., 2009).

1.3.5.5 GATA2 in familial and sporadic MDS/AML

GATA2 mutations have been detected in familial MDS/AML with an autosomal dominant pattern. Hahn et al. define four families with normal haematological indices having missense mutations at two neighbouring threonines (T354M-T355del) within the C-terminal zinc finger domain of GATA2, which is essential for DNA-binding and protein/protein interactions (Hahn et al., 2011). Molecular modelling proposed that T354 and T355 stabilise the C-terminal zinc-finger of GATA2, and both T354M and T355del mutations show loss of DNA binding activity. *In vitro* studies indicate that the T354M mutant shows dominant-negative effects and the T355del mutant exhibits loss-of-function of GATA2 (Hahn et al., 2011). Acquired monosomy 7, trisomy 8, *ASXL1, EZH2, SETBP1, HECW2, GATA1, NPM1, NRAS,* and *WT1* mutations are the most frequent secondary genetic disorders in MDS/AML cases with *GATA2* germline mutations (Table 1.6) (Fujiwara et al., 2014, Luesink et al., 2012, West et al., 2014, Wlodarski et al., 2017).

Table 1.6: The most recurrent secondary mutations in GATA2 haploinsufficient patients.

Gene/cytogenetic abnormalities	Frequency
Monosomy 7	35-40%
ASXL1	Around 30%
Trisomy *8*	15-20%
EZH2, SETBP1, HECW2, GATA1, NPM1, NRAS, and *WT1*	Rare mutations

On the other hand, somatic *GATA2* mutations were discovered in the acute myeloid transformation of chronic myeloid leukaemia (CML). Zhang et al identified two *GATA2* somatic mutations happening in the blast crisis phase of CML t(9;11): a Δ 341_346 in-frame deletion, which leads to decreased transcriptional activity; and a L359V missense mutation within the C- terminal zinc domain, which in contrast to most *GATA2* mutations observed, acts as a gain-of-function mutation (Zhang et al.,

2008). L359V mutation leads to an increase in the activity of mutant GATA2 protein that binds and inhibits the myeloid transcription factor PU.1, which is essential for the development of monocytes. About 40% of sporadic *GATA2* mutations have been reported in AML patients with both monoallelic and biallelic *CEPBα* mutations (Greif et al., 2012, Green et al., 2013). Approximately 90% of *GATA2* mutations were missense mutations that perturb the transcriptional activity of *CEPBα* within the zinc finger domains including A203P_H258fs _R307W _R308P_A318V_ A318T_ G320A_ G320V _ L321F_ L321P _R330L_R330P_ R330Q_R362Q_P385L.

GATA2 haploinsufficiency was further reported in AML with chromosome-three rearrangements including 3q-inversion inv(3)(q21.3q26.2) or 3q-translocation t(3;3)(q21.3;q26.2). 3q rearrangements include 5' *GATA2*-distal haematopoietic enhancer (-77kb enhancer) moved from 3q21.3 and to become considerably adjacent to EVI1 locus 3q26.2, which triggers GATA2 haploinsufficiency and overexpression of the *EVI1* gene (Yamazaki et al., 2014, Katayama et al., 2017). Retroviral overexpression of *Evi1* in murine BM-cells enhances the leukaemia development, in which *Evi1* restrains the activity of *Pten* through polycomb-repressive complexes, an epigenetic-modifier, and immediately stimulates AKT/mTOR signalling axis, a vital pathway in cellular proliferation (Yoshimi et al., 2011). Katayama et al described the roles of GATA2 in 3q rearrangements in leukaemogenesis (Katayama et al., 2017). The loss of *Gata2* distal haematopoietic enhancer causes about 50% reduction of *Gata2* expression in HSPCs. Haploinsufficiency of *Gata2* with aberrant expression of *Evi1* accelerates the AML development in mouse models. Moreover, haploinsufficient-*Gata2*/high-*Evi1* compound mice exhibit an accumulation of blast cells and aberrant primitive HSPCs differentiation causing an aggressive form of leukaemia (LMPP-like-phenotype). Conversely, high *Gata2*/*Evi1* level enhances leukaemic cells to differentiate into Gr1-myeloid leukaemic cells and delays leukaemogenicity (GMP-like-phenotype).

Although low GATA2 expression has a tumour suppressor function in haploinsufficient GATA2 patients, high expression of GATA2 possesses an oncogenic role in AML patients and correlates with bad progression with low survival rates

(Vicente et al., 2012b, Luesink et al., 2012). Overexpression of GATA2 was significantly correlated with other leukaemic markers such as *FLT3-ITD* and *NPM1* mutations and high expression of both WT1 and EVI1 in normal karyotype cases of adult AML (Vicente et al., 2012b). High GATA2 expression was also found in paediatric AML patients (Luesink et al., 2012). Levels of GATA2 expression returned to normal in patients with complete remission, whereas GATA2 expression stayed high in resistant AML patients. Furthermore, overexpression of GATA2 is associated with poor prognosis among patients receiving chemotherapy treatment (Yang et al., 2017). While high GATA2 expression confers the resistance of AML cells to chemotherapy medications, the leukaemic cells with inhibition of GATA2 expression are less resistant to therapies.

In addition, GATA2 expression promotes the proliferation and survival of AML-cell-lines such as Kasumi-1 (M2/AML; *KIT*/*RUNX1* mutations) and Kasumi-3 (M0/AML; t(3; 7)(q27; q22), high EVI1) (Katsumura et al., 2016). In this paradigm, GATA2 expression is induced by RAS/p38/ERK signalling and ultimately activates CXCR2 and IL1β expressions that sustain AML-cells proliferation and positively auto-stimulate p38/ERK/GATA2 expressions. On the other hand, *GATA2* knock-down in THP1 (t(9;11, MLL-AF9 fusion)), HL60 (M2/AML) and K562 (CML in blast phase) AML-cell-lines that express high GATA2 level shows decreased cellular proliferation and survival (Menendez-Gonzalez et al., 2019a). Consistently, the pharmacological inhibitor K-7174 of GATA2 along with AML chemotherapeutic agents such as Cytarabine (Ara-C) or Etoposide (VP16) in AML-cell-lines expressing a high level of GATA2 decreases the survival rates of leukaemic cells (Menendez-Gonzalez et al., 2019a). Nandakumar et al. studied the effects of low overexpression of GATA2 using a Tamoxifen-inducible mouse model, where the level of *Gata2* expression in this model is comparable to that observed in AML patients (Nandakumar et al., 2015). They found that overexpressed *Gata2* at low level was corroborative of the self-renewal potential of myeloid progenitors and hindered lymphoid differentiation in mouse BM cells, promoting myeloid leukaemic transformation.

Genetic complementation techniques have been exploited to better understand the biological function of *GATA2* mutations (Katsumura et al., 2018). Katsumura et al. assessed the genetic complementation of *GATA2* mutations in null-*Gata2* -77-enhancer (-77$^{-/-}$), an essential *cis*-element for myeloid/ erythroid/megakaryocyte differentiation. Since null -77-enhancer mice die at E14, myeloid/erythroid progenitors (Lineage^{-}_Kit^{+}) from foetal liver were used. Null -77-enhancer Lineage^{-}_Kit^{+} cells expressed low levels of *Gata2*. The induction of empty-vector in null -77$^{-/-}$ Lineage^{-}_Kit^{+} cells showed that the numbers of erythroid and myeloid colonies (CFU-E, BFU-E, and CFU-GM) were notably decreased. The proportions of erythroid/myeloid progenitors were rescued by retroviral-*Gata2* expression in -77$^{-/-}$ Lineage^{-}_Kit^{+} cells. Induced -77$^{-/-}$ cells with R307W or T354M mutations were accompanied by an increment in myeloid progenitors and a severe reduction in erythroid progenitors. The numbers of CFU-GM in R307W or T354M induced cells were approximately three-fold greater than the expression exerted by retroviral-*Gata2,* with remarkably increased granulocytes differentiation in R307W expressing cells. Gene profiles of R307W induced cells were accompanied by an increase in myeloid genes expression (*Mpo*, *Ctsg* and *Elane*), a decline in erythroid genes expression (*Slc4a1*, *Epb4*.9 and *Alas2*), and increased *Myb* expression within HSPCs. These findings suggest that mutations that cause GATA2 haploinsufficiency do not always work as inhibitory of the GATA2 function and perturb the regulation of downstream genes.

Menendez-Gonzalez et al. have recently explored the requirement of GATA2 in leukaemic stem cells utilising *Meis1*/*Hoxa9* mouse models that drive AML initiation (Menendez-Gonzalez et al., 2019b). In this model, *Gata2* was acutely deleted from recipient hosts harbouring *Meis1*/*Hoxa9* overexpression. *Gata2*-KO LSCs showed lateness in the AML development as compared with control LSCs. The mechanism behind decreased LSCs proliferation in *Gata2*-KO is increased apoptosis level due to decreased BCL2 expression, an anti-apoptotic marker. This implies that GATA2 is essential for LSCs survival, maintenance, and self-renewal.

Saida et al. have investigated the leukaemogenesis role of GATA2 in inverted chromosome 16 (inv(16), CBFB/MYH11 fusion oncogenes) M4/AML (Saida et al., 2020). Haploinsufficient GATA2 was observed in relapsed inv(16) AML patients. High GATA2 expression was markedly increased in preleukaemic *Cbfb/Myh11* knock-in mouse models. Acute ablation of *Gata2*$^{+/fl}$*; Mx1-Cre*$^{+}$ in *Cbfb/Myh11; Mx1-Cre* mice displayed a delay in the AML initiation when compared with *Gata2*$^{+/+}$*/Cbfb/Myh11* mice. In transplantation settings, *Gata2*$^{+/fl}$*/Cbfb/Myh11; Mx1-Cre*$^{+}$ BM cells were more aggressive and developed AML three-times faster than *Gata2*$^{+/+}$/*Cbfb*/*Myh11* cells with higher reconstituting potential. Analysing c-kit^{+} LSCs from recipient hosts showed that *Gata2*$^{+/fl}$/*Cbfb*/*Myh11*;Mx1-Cre^{+} leukaemic cells developed new mutations that are well-identified in human leukaemogenesis as *Kras*, *Ptpn11, Bcor*, *Trp53*, and *Kit* mutations, signifying that GATA2 haploinsufficiency initiates different mutations and forms aggressive relapse in inv(16) AML patients.

Although haploinsufficient GATA2 is highly frequent in MDS/AML cases, recent reports have described GATA2 haploinsufficiency in B-ALL patients (Koegel et al., 2016, Novakova et al., 2016, Donadieu et al., 2018). A few cases of MonoMAC patients with haploinsufficient GATA2 predispose into B-ALL that is characterised by reduced numbers of peripheral B-cells, monocytopenia, a profound reduction in B-cell progenitors, and monosomy-7 abnormality. This indicates that a defect in HSCs/multi-lymphoid-progenitors axis could cause an impairment in B-cells differentiation and advances towards B-ALL.

1.4 ASXL1 transcriptional regulator

1.4.1 ASXL family members

The Additional Sex Combs-Like members of proteins (ASXL1_ASXL2_ASXL3) are known as a mammalian paralog of the *Drosophila* Additional-sex-combs (*Asx*) gene (Milne et al., 1999, Schuettengruber et al., 2017, Brock and Fisher, 2005, Asada et al., 2019, Katoh, 2013). The *Asx* gene is a member of the enhancer of trithorax (TrxG) and polycomb (PcG) genes that act as activators or repressors of homeobox genes,

respectively. Thus, the *Asx* gene works as an epigenetic modifier of genes expression throughout the process of chromatin modifications to activate (TrxG) or repress (PcG) homeobox genes, a cluster of developmental embryo genes. Nevertheless, several reports imply that mammalian ASXL members only regulate the expression of polycomb genes in haematological malignancies. Polycomb genes are classified into Polycomb-repressor-complex-1 (PRC1) and Polycomb-repressor-complex-2 (PRC2) depending on their downstream genetic collaborations. ASXL1/ASXL2 proteins are broadly expressed in mammalian tissues as haematopoietic compartments, BM-niches, heart, brain, spleen, liver, skeletal muscle, placenta, prostate, and testes, while ASXL3 expression is limited to brain, eyes, lungs, and lymph nodes (Mozziconacci and Birnbaum, 2011, Asada et al., 2019).

1.4.2 *ASXL1* gene structure

Mammalian *ASXL1* gene localises at the long arm of chromosome twenty (20q11.21), whereas murine *Axsl1* gene is located on chromosome two (Abdel-Wahab et al., 2013, Katoh, 2013, Gelsi-Boyer et al., 2012). Both murine and human *ASXL1* genes are comprised of 12 exons, and ASXL1 protein encompasses around 1541 amino acids with a molecular weight of approximately 170 KDa (Figure 1.14 A). The ASXL protein is commonly constituted from five domains including a N-terminal ASXN domain; an adjacent N-terminal ASXH domain; central ASXM1 and ASXM2 domains; and a C-terminal plant homeodomain (PHD) (Figure 1.14 B) (Katoh, 2013, Gelsi-Boyer et al., 2012, Asada et al., 2019). Structurally, the ASXN-domain is equivalent to the Forkhead-box-domain, a DNA binding motif, and has essential roles in DNA-binding, DNA-repairs, and transcriptional-regulations. The ASXH region is the binding area with other proteins as a deubiquitinase BRCA1-associated-protein-1 (BAP1) and Lysine-specific-demethylase-1A (LSD1/KDM1A). ASXL1 directly interacts with H2A-deubiquitinase-BAP1 forming polycomb-repressive-deubiquitinase (PR-DUB) complex that ultimately represses the ubiquitination activity by initiating H2A mono-ubiquitination (H2AK119-ub) through PCR1 genes and promotes expression of downstream genes. Furthermore, ASXL1 binds to PRC2 genes (*Ezh1_ Ezh2_Eed_Suz12)* and represses histone three by adding tri-methyl groups at lysine-

27 (H3K27me3) and further suppresses the expression of homeobox genes. Upregulation of homeobox genes is a profound marker for haematological neoplasms. ASXM1/ASXM2 domains are involved in the interaction with other proteins as nuclear hormone receptors (NHR). The PHD region is responsible for the histone/DNA-binding and works as a chromatin regulator.

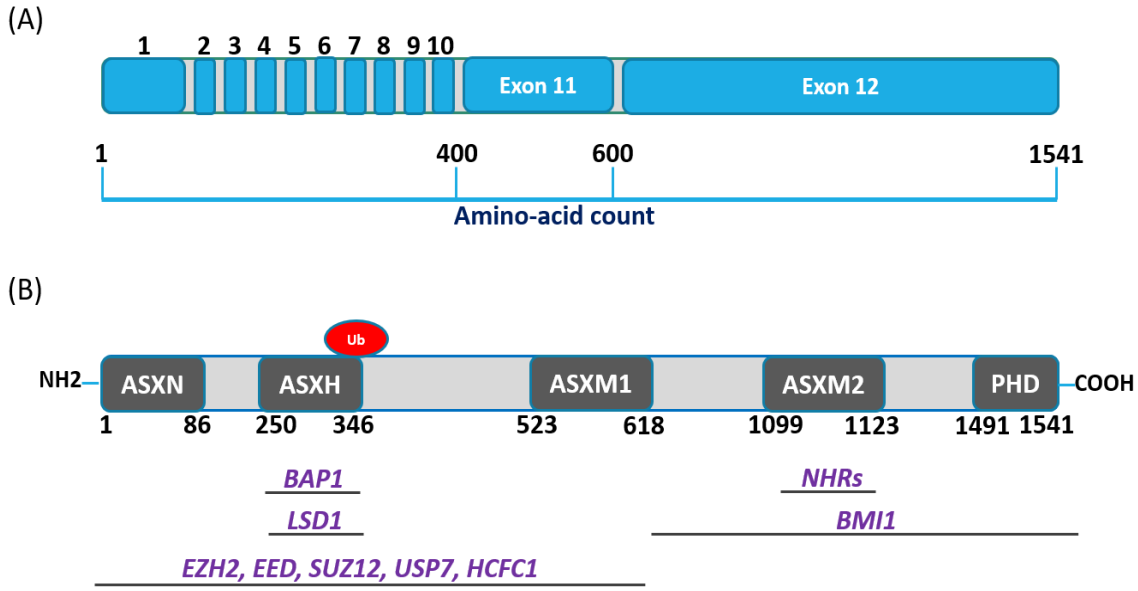

Figure 1-14: Scheme of *Asxl1* locus and protein structure.
(A) Diagram sketches the human *ASXL1* gene. (B) *ASXL1* protein domains with binding regions. The interaction partners are highlighted in purple. Ub indicates ubiquitination. Adapted from (Katoh, 2013, Gelsi-Boyer et al., 2012).

1.4.3 ASXL1 functions in haematopoiesis

Asxl1 knockout (KO) mice have been generated to study the requirements of *Asxl1* in the haematopoietic system by disrupting *Asxl1* wildtype gene. *Asxl1*-mRNA is widely detected in foetal and adult haematopoietic compartments including HSPCs, committed progenitors, and mature blood cells. (Abdel-Wahab et al., 2013, Wang et al., 2014, Fisher et al., 2010). Germline adult *Asxl1*-KO mice (Targeting exon-5) display decreased frequencies of lymphoid-cells in the thymus, a reduction in B-cells numbers in BM/spleen, splenomegaly, an increase in myeloid-cells in BM /spleen, normal leukocytes numbers and morphology, no differences in BM CFC numbers, and

normal HSPCs reconstitution capability in transplantation experiments (Fisher et al., 2010). Constitutive *Asxl1*-KO mice (Targeting exons5-10) are dead at E19.5 with multiple developmental disorders (cleft palates, microcephaly, anophthalmia, and skeletal anomalies), while heterozygote *Asxl1*-KO mice are viable (Abdel-Wahab et al., 2013). Both heterozygote and homozygote animals show normal haematopoietic profiles at E14.5 (Table 1.7).

Conditional homozygote deletion of murine *Asxl1* utilising Vav-Cre (deletion at E11) and inducible Mx1-Cre models exhibits profound haematological phenotypes in adult BM including a reduction in BM/spleen cellularity, peripheral leukopenia and anaemia at 6 months old, a decrease in peripheral B-cells and myeloid-cells, BM erythroid/myeloid dysplasia, increased numbers of erythroblast precursors in BM/spleen, an increment in frequencies of LSK, MPPs, and HSCs in BM, reduced BM CFC numbers and replating capacity, an impairment in HSPCs repopulation and self-renewal potential, increased apoptosis level in MPPs, a reduction in MPPs proliferation, decreased H3K27me3 level, and upregulated expression of *HoxA7* and *HoxA9* in LSK cells (Abdel-Wahab et al., 2013). These phenotypes are highly correlative with human MDS. *ASXL1* mutations are commonly associated with *TET2*, an epigenetic modulator, mutations in MDS patients (Abdel-Wahab et al., 2013). *TET2* is frequently mutated in MDS/AML cases and confers HSCs self-renewal ability in *Tet2*-KO mice (Abdel-Wahab et al., 2013). Analysis of *Asxl1* and *Tet2* double-KO mice shows more aggressive MDS-phenotypes than *Asxl1*-KO mice a, and the deletion of *Tet2* rescues the defect of Asxl1 HSPCs self-renewal capability (Table 1.7) (Abdel-Wahab et al., 2013).

Constitutive ablation of *Asxl1* (*Asxl1*$^{-/-}$) (Targeting exon-1) is 80% embryonic lethal, and the remaining around 20% mice can survive for 42-days with developmental anomalies as body-weight loss, dwarfism, and anophthalmia, whereas constitutive deletion of heterozygote *Asxl1* (*Asxl1*$^{+/-}$) mice are born alive with normal developmental features (Wang et al., 2014). The phenotypes of *Asxl1*$^{-/-}$ and *Asxl1*$^{+/-}$ mice are quite similar to human MDS/MPN. *Asxl1*$^{-/-}$ mice show peripheral cytopenias with myeloid/erythroid dysplasia as hyper-segmented/hypo-segmented neutrophils,

pseudo-Pelger-Huet anomaly, polychromatic RBCs, and Howell-Jolly body, a reduction in numbers of B-cells and neutrophils in PB/BM/spleen, increased numbers of monocytes in PB/BM/spleen, decreased numbers of LK, LSK, MEP in BM, an increment in GMP numbers in BM, an increase in proliferation and apoptosis in LK-cells, a defect in HSPCs reconstitution and self-renewal capability, reduced level of H3K27me3 and H3K4me3 in LK-cells, increased expression of HoxA5, HoxA7, HoxA9, HoxA10, pro-apoptotic BCL2-113, and decreased expression of anti-apoptotic markers such as BCL2 and BCL2-112. *Asxl1*$^{+/-}$ mice display peripheral anaemia, thrombocytopenia, and leukopenia/leucocytosis with myeloid/erythroid dysplastic features, decreased percentages of B-cells/neutrophils and an increased frequency of monocytes in PB/BM/spleen, an insignificant reduction in LSK and LK cells in BM, no differences in CMP, GMP, and MEP numbers in BM, increased apoptosis level and S-G2-M in LK-cells, and decreased donor contribution in primary and secondary transplantation experiments (Wang et al., 2014). In another study, constitutive heterozygote deletion of young Asxl1 mice exhibits normal frequencies of peripheral RBCs, WBCs and platelets, normal numbers of LSK, HSCs and MPPs in BM, decreased BM-CFC numbers, and reduced HSPCs repopulation capacity (Zhang et al., 2018).

ASXL1 knockdown in human CD34^{+} cord-blood-cells exhibits a reduction in CFC-erythroid numbers, increased erythroid dysplastic features as multi-nuclear RBCs, nuclear-budding, and nuclear-bridging, an impairment in RBCs enucleation, increased percentages of erythroblasts, an upregulated expression of HoxA5, HoxA6, HoxA7, HoxA8, and HoxA9 (Abdel-Wahab et al., 2012, Shi et al., 2016). In BM niches, *Asxl1* performs essential roles in adipogenesis. ASXL1 restrains adipocytes differentiation through inhibiting the activity of adipogenic marker PPARγ (Park et al., 2011). Enforced expression of *Asxl1* in murine pre-adipocyte-cells represses the differentiation of adipocyte precursors, while *Asxl1* knockdown promotes adipocytes formation. To conclude, although *Asxl1*-KO mice display different haematological phenotypes, *Asxl1* is an indispensable regulator for normal haematopoiesis.

Table 1.7: *Asxl1* haematological phenotypes utilising mouse models.

NR indicates normal; IN, increase; DC, decrease; and ND, not described.

Reference	Mouse models	Survival	Mature cells PB/BM/spleen	HSPCs phenotypes	Transplant phenotypes of	Gene and histone	Haematological malignancies
(Fisher et al., 2010)	*Asxl1*-germline KO (*Asxl1*$^{-/-}$) (Homozygote)	Partial embryonic lethality	DC B-cells and T-cells. IN myeloid cells. NR morphology.	NR BM CFC numbers.	NR HSPCs reconstitution capability	ND	No MDS/MPN/AML development
(Abdel-Wahab et al., 2012)	germline *Asxl1*$^{-/-}$, *Asxl1*$^{+/-}$	*Asxl1*$^{-/-}$ die at E 19.5	NR erythroid numbers.	NR LSK, MPPs and HSCs numbers.	ND	ND	NR haematological phenotypes at E14.5
	conditional-KO *Asxl1*$^{fl/fl}$; Vav-Cre^{+} & *Asxl1*$^{fl/fl}$; Mx1-Cre^{+}	Alive	DC BM /spleen cellularity. DC B-cells, myeloid-cells. Erythroid/myeloid dysplasia.	IN LSK, MPPs and HSCs. DC BM CFC numbers. IN apoptosis level.	Repopulation and self-renewal defects	DC H3K27me3 level. IN HoxA7 and HoxA9 expressions	MDS-like-disease development at 6-12 months old
(Wang et al., 2014)	Constitutive *Asxl1*$^{-/-}$ KO	20% alive for 42 days	Pancytopenia with Erythroid/myeloid dysplastic features. DC B-cells and neutrophils. IN monocytes numbers	DC LK, LSK, MEPs. IN GMPs. IN apoptosis & proliferation	A defect in reconstitution and self-renewal ability	DC level of H3K27me3 & H3K4me3. IN HoxA5-10 expression.	MDS/MPN-like-disease development
	Constitutive heterozygote *Asxl1*$^{+/-}$	Alive		NR LSK, LK, CMPs, GMPs, and MEPs. IN apoptosis &		ND	MDS/MPN-like-disease at 6-12 months old
(Zhang et al., 2018)	Constitutive heterozygote *Asxl1*$^{+/-}$	Alive	NR RBCs, WBCs, and platelets numbers. NR morphology	NR LSK, HSCs, and MPPS. DC CFU-GM and CFU-E numbers	Decreased HSPCs reconstitution capability	ND	No MDS/MPN/AML Development at 2-4 months old

1.4.4 *ASXL1* mutations in haematological malignancies

ASXL1 expression is broadly widespread in haematopoietic compartments, and ASXL1 misexpression is associated with perturbed HSPCs proliferation and differentiation and enhances the transformation of haematopoietic cells into myeloid malignancies. Heterozygote *ASXL1* mutations are commonly existent in myeloid malignancies, and these mutations are frameshift or nonsense mutations that predominantly localise at exon-12 and cause C-terminal truncated ASXL1 protein and result in loss-of-function of ASXL1 protein (Paschka et al., 2015, Katoh, 2013, Gelsi-Boyer et al., 2012). *ASXL1* mutations affect the ability of ASXL1 to recruit histone-3 repressive PCR2-genes such as *EZH1,* EZH*2*, *EED*, *SUZ12,* and inhibit histone-3 tri-methylation (H3K27me3), and subsequently activate the expression of leukaemogenic *HOXA* genes (Paschka et al., 2015, Katoh, 2013, Gelsi-Boyer et al., 2012). Approximately 90% of *ASXL1* mutations are located at amino-acid 642-685 of exon-12, and the p.Gly646TrpfsX12 mutation represents around 60% of all mutated ASXL1 patients (Paschka et al., 2015, Gelsi-Boyer et al., 2012).

Heterozygote *ASXL1* mutations have been identified in Bohring-Opitz syndrome, a developmental disorder that is characterised by craniofacial anomalies and intellectual disabilities (Hoischen et al., 2011). Somatic heterozygote mutations of *ASXL1* have been discovered in a large scale of myeloid malignancies such as myelodysplastic syndromes (MDS), acute myeloid leukaemia, myeloproliferative neoplasm (MPN) such as primary myelofibrosis (PMF), MDS/MPN overlap disorders such as chronic myelomonocytic leukaemia (CMML), and clonal haematopoiesis, an elderly-related disorder that coexists with one or more somatic mutations that lead to myeloid neoplasms with normal haematological profiles (Paschka et al., 2015, Katoh, 2013, Gelsi-Boyer et al., 2012, Asada et al., 2019). Mutations of ASXL1 are scarcely seen in lymphoid malignancies. *ASXL1* mutations are the highest in CMML patients (about 45%) and represent approximately 15–20% of MDS patients, 35 % of MPN patients, 5-10% of *de novo* AML patients, 30% of secondary AML cases, and 3% of CLL patients (Paschka et al., 2015, Katoh, 2013, Gelsi-Boyer et al., 2012). *ASXL1* mutations are frequently synchronous with other gene mutations such as *GATA2*, *CEBPα*, and *RUNX1* transcription factors; *NRAS*, *JAK2*, *SETBP1*, *NF1*, and *STAG2*

signalling genes; *IDH1*, *IDH2*, and *TET2* DNA-methylation genes; *U2AF1* and *SRSF2*, spliceosome proteins, while *ASXL1* mutations are less frequent with mutations of *NPM1*, *FLT3* and *DNMT3A* genes (Paschka et al., 2015, Katoh, 2013, Gelsi-Boyer et al., 2012, Asada et al., 2019). *ASXL1* mutations are positively associated with disease progression and overall survival (Paschka et al., 2015, Katoh, 2013, Gelsi-Boyer et al., 2012, Asada et al., 2019). Monosomy-7 and trisomy-8 are the most common cytogenetic abnormalities with *ASXL1* mutations (Paschka et al., 2015, Katoh, 2013, Gelsi-Boyer et al., 2012, Asada et al., 2019).

However, some reports have suggested that *ASXL1* mutations are gain-of-function mutations that promote myeloid transformation rather than loss-of-function mutations. Retroviral overexpression of mutant ASXL1 protein (ASXL1-MT) (p.G646TfsX12; derived from human MDS/AML patients) in murine BM exhibits peripheral pancytopenia, increased cellularity in BM/spleen, myeloid/erythroid dysplastic features such as Pelger-Huet anomaly, hyper-segmented neutrophils, Howel-Jolly bodies, and polychromasia at 12 months old (Inoue et al., 2013). Thus, mutant ASXL1 causes MDS-like phenotypes. ASXL1-MT inhibits the function of wild-type ASXL1 and fails to recruit PRC2 genes and ultimately diminishes the level of H3K27me3 and derepresses leukaemogenic *miR152a* and *HoxA* genes. High expression of *miR152a* represses the activity of C-type lectin-domain-family-5-a (*Clec5a*) and subsequently causes impaired myeloid differentiation (Inoue et al., 2013). Conditional knock-in mutant ASXL1 (p.E635RfsX15) in murine (*Asxl1*-MT$^{fl/fl}$; Vav-Cre^{+}) shows age-dependent increased myeloid cells, age-dependent decreased RBCs, increased platelet numbers, increased megakaryocyte progenitors, a reduction in numbers of LSK, HSCs, MPPs and BM CFC-colonies, an increment in MEP frequencies, and impaired HSPCs repopulation potential in transplant experiments (Nagase et al., 2018). Conditional knock-in ASXL1-MT mice fail to develop MDS/AML-like disease for up to 18 months. Similarly, constitutive heterozygote knock-in mutant ASXL1 (p.G643Wfs) in murine (*Asxl1*$^{+/MT}$) did not develop MDS/AML-like disease up to 18 months and showed normal haematological profiles (Hsu et al., 2017). Thus, the type of *ASXL1* mutations (loss-of-function or gain-of-function) is still controversial.

1.4.5 Somatic *ASXL1* mutations in haploinsufficient GATA2 patients

Somatic *ASXL1* mutations represent approximately 30% of MDS/AML cases in haploinsufficient GATA2 patients (Table 1.8) (West et al., 2014). Eight acquired heterozygote *ASXL1* mutations have been reported in GATA2 haploinsufficiency syndromes (West et al., 2014, Bödör et al., 2012). Clinical features of germline GATA2 patients with acquired *ASXL1* mutations involve younger than reported MDS/AML cases (35 +/- 12 years), biased females, recurrent monosomy-7 and trisomy-8 anomalies, and speedy disease evolution with poor survival rates (West et al., 2014, Bödör et al., 2012). Given that acquired *ASXL1* mutations trigger MDS/AML development in familial haploinsufficient GATA2 patients, analysing the interaction between GATA2 and ASXL1 could be beneficial to understand the leukaemic transformation.

Table 1.8: *GATA2*/*ASXL1* mutations in GATA2 haploinsufficient patients.

Adapted from (West et al., 2014, Bödör et al., 2012).

Germline *GATA2* mutations	Acquired *ASXL1* mutations	Cytogenetic abnormalities	Diseases
T354M	G646fs	Monosomy 7	MDS
R398W, G101fs	R693X, G646fs	Normal, Monosomy 7, Trisomy 8	MDS, CMML
R361del	G652S	Monosomy 7, Trisomy 8	MDS
N371K	L817fs	Monosomy 7	MDS
Del340-381	G646fs	t(1;22)	MDS
D367fs, V140fs, R337X	E635fs	Normal, Monosomy 7	MDS
A318fs	E1102D	Monosomy 6	MDS

1.5 Thesis objectives

It is well-known that GATA2 haploinsufficiency causes familial MDS/AML and immunodeficiency disorders such as MonoMAC, DCML, chronic neutropenia, and Emberger syndromes, that can proceed to MDS/AML. Acquired *ASXL1* mutations are highly recurrent in MDS/AML patients harbouring germline *GATA2* mutations (West et al., 2014). However, it remains largely unclear what HSPC compartments are impacted, and what molecular mechanisms are involved in these conditions. Several conditional and constitutive *Gata2* haploinsufficient (heterozygote) murine models exist that may be useful in modelling GATA2 clinical syndromes and progression to MDS/AML. In order to assess the biological impact of *Gata2* haploinsufficiency on the adult haematopoietic system as well as gaining new insights into mechanisms of GATA2 haploinsufficiency driven MDS/AML, this study modelled germline and acquired GATA2 haploinsufficiency syndromes by employing *Gata2*$^{+/fl}$*; Vav-iCre*$^{+}$ and *Gata2*$^{+/fl}$*; Mx1-Cre*$^{+}$ conditional knockout mice models, respectively. There are three primary aims of this project:

1. Evaluate the impact of *Gata2* heterozygote on young (8-12 weeks) and aged (18-20 months) haematopoietic compartments using *Gata2*$^{+/fl}$*; Vav-Cre*$^{+}$ mice. The Vav-iCre promoter is expressed in the developing embryo (E11) and acts as a model to study the chronic loss of *Gata2* haploinsufficiency in young and aged murine, as a model of early- and late-onset disease.

2. Assess the effect of acutely deleted *Gata2* heterozygote on young (8-12 weeks) haematopoietic populations utilising inducible *Gata2*$^{+/fl}$*; Mx1-Cre*$^{+}$ mice. The Mx1-Cre promoter is activated in the adult stage and works as a model to examine the acute loss of *Gata2* haploinsufficiency.

3. Explore the impact of the genetic interaction between *Gata2* and *Asxl1* on the adult haematopoietic system and MDS/AML initiation using *Gata2*$^{+/fl}$*; Asxl1*$^{+/fl}$*; Vav-Cre*$^{+}$ (double heterozygote) mice and lentiviral *Asxl1*-shRNA approaches.

CHAPTER 2 : Materials and Methods

2.1 Transgenic mouse models, husbandry, and tissues isolation

Mice models used in the study were based on Cre-loxP techniques. The Cre-loxP system is commonly used to generate a conditional knockout mouse of specific target genes.

2.1.1 The Cre-lox recombination system

The Cre-Lox system is widely employed to introduce gene deletion, inversion and translocation on specific tissues or cell types (Nagy, 2000, Pathania et al., 1999). Cre-recombinase (cyclisation recombination) is an enzyme from the bacteriophage P1 that belongs to the λ integrase family of site-specific recombinase. Cre-recombinase catalyses the recombination in a specific region that is marked by two 34 base-pairs (bp) loxP sites (locus of X-over P1 bacteriophage). Each loxP-site comprises of two 13bp inverted repeated sequences that are separated by an 8bp spacer region. Each 13-bp region is recognised by a Cre monomer, forming a tetramer. The DNA in the spacer region is cut by the Cre-recombinase. The orientation and location of the loxP sites determine how the product of the recombination reaction will be rearranged: deletion, when the two loxP sites are on the same DNA strand and are in the same orientations; inversion, when the two loxP sites are on the same DNA strand but are in the opposite orientations; and translocation, If the loxP sites are on the different DNA strand. Therefore, if the Cre gene is bound to a specific promoter, the recombination is directed into a specific tissue or a cell type. Several promoters that drive Cre expression have been described, both Mx1 and Vav promoters are able to direct Cre-mediated recombination in all haematopoietic cell types (Stadtfeld and Graf, 2005, Kuhn et al., 1995).

2.1.1.1 Mx1-Cre mouse models

The inducible Myxovirus dynamin-like-GTPase-1 (Mx1) gene participates in the cellular defence to viral infections. The expression of the *Mx1* gene is regulated in an interferon-dependent manner. The *Mx1* promoter is activated following the administration of synthetic double-stranded RNA of Polyinosinic-Polycytidylic acid (pIpC) that activates the expression of Cre recombinase (Kuhn et al., 1995). pIpC mimics viral infections by binding to toll-like-receptor-3 (Tlr3) and triggers the expression of interferon type-1 signalling and promptly activates *Mx1*-promoter expression. The *Mx1* gene is also expressed in mesenchymal stem cells, nestin cells and perivascular cells (Joseph et al., 2013).

2.1.1.2 Vav-iCre mice models

The *Vav* promoter is spontaneously expressed in haematopoietic cells in the middle of embryonic life at around embryonic day E11 (Stadtfeld and Graf, 2005, Shimshek et al., 2002). Both Vav-Cre and Vav-iCre, a codon-improved Cre, have the potency to disrupt floxed genes in foetal haematopoietic cells (Stadtfeld and Graf, 2005, Shimshek et al., 2002). The Vav-iCre promoter is more specific than Vav-Cre, which is designed to limit the epigenetic silencing. In addition, the expression of these promoters is not restricted to the haematopoietic population and they are existent in other tissues. Vav-Cre and the Vav-iCre promoters are expressed in non-haematopoietic cells such as the ovary and the testis, respectively (Joseph et al., 2013).

2.1.2 Experimental mice handling

Mice were generated and maintained at a controlled temperature, humidity and 12-hours light cycle in the Heath hospital animal care unit, Cardiff University. All the animal experiments were conducted in accordance with the Animals Scientific Procedures Act (1986), as amended by the United Kingdom Home Office. (Project license: P6D863C95, Personal license: ID1CBD61D).

2.1.2.1 Breeding strategies

The generation strategy of floxed *Gata2*, floxed *Asxl1*, *Vav-iCre* and *Mx1-Cre* mice were previously described (Stadtfeld and Graf, 2005, Kuhn et al., 1995, Charles et al., 2006, Abdel-Wahab et al., 2013). *Gata2* mice were kindly provided by Dr Julian Downward, Francis Crick Institute. Vav-iCre and Mx1-Cre mice were kindly donated by Dr Kamil Kranc, University of Edinburgh. *Asxl1*, C57Bl/6J (CD45.2) and C57Bl/6J-SJL (CD45.1) mice were purchased from Jackson Laboratory.

Transgenic $Gata2^{fl/fl}$ and $Asxl1^{fl/fl}$ mice were produced as reported previously, resulting in a truncated non-functional protein of GATA2 and ASXL1 (Figure 2.1 A and B) (Charles et al., 2006, Abdel-Wahab et al., 2013). The Vav and Mx1 promoters were used to drive Cre-recombinase expression to excise the floxed *Gata2/Asxl1* allele in the haematopoietic compartments (Stadtfeld and Graf, 2005, Kuhn et al., 1995). $Gata2^{+/+}$, $Vav\text{-}iCre^{+}$ females were bred with $Gata2^{fl/fl}$, $Vav\text{-}iCre^{-}$ males to generate $Gata2^{+/fl}$, $Vav\text{-}iCre^{+}$ (heterozygote) and $Gata2^{+/fl}$, $Vav\text{-}iCre^{-}$ (control) littermates. $Gata2^{+/fl}$, $Mx1\text{-}Cre^{+}$ (heterozygote) and $Gata2^{+/fl}$, $Mx1\text{-}Cre^{-}$ (control) mice were generated by crossing $Gata2^{fl/fl}$, $Mx1\text{-}Cre^{+}$ males or females with $Gata2^{+/+}$, $Mx1\text{-}Cre^{-}$ males or females. For double *Gata2/Asxl1* heterozygote mice, $Gata2^{+/+}$, $Vav\text{-}iCre^{+}$ females were crossed with $Gata2^{+/fl}$, $Asxl1^{+/fl}$, $Vav\text{-}iCre^{-}$ males to generate $Gata2^{+/fl}$, $Vav\text{-}iCre^{+}$ (single *Gata2* heterozygote), $Asxl1^{+/fl}$, $Vav\text{-}iCre^{+}$ (single *Asxl1* heterozygote), $Gata2^{+/fl}$, $Asxl1^{+/fl}$, $Vav\text{-}iCre^{+}$ (double *Gata2/Asxl1* heterozygote mice), and $Gata2^{+/fl}$, $Asxl1^{+/fl}$, $Vav\text{-}iCre^{-}$ (control). Sex-matched 8-12 weeks and 18-20 months old mice were used in this study.

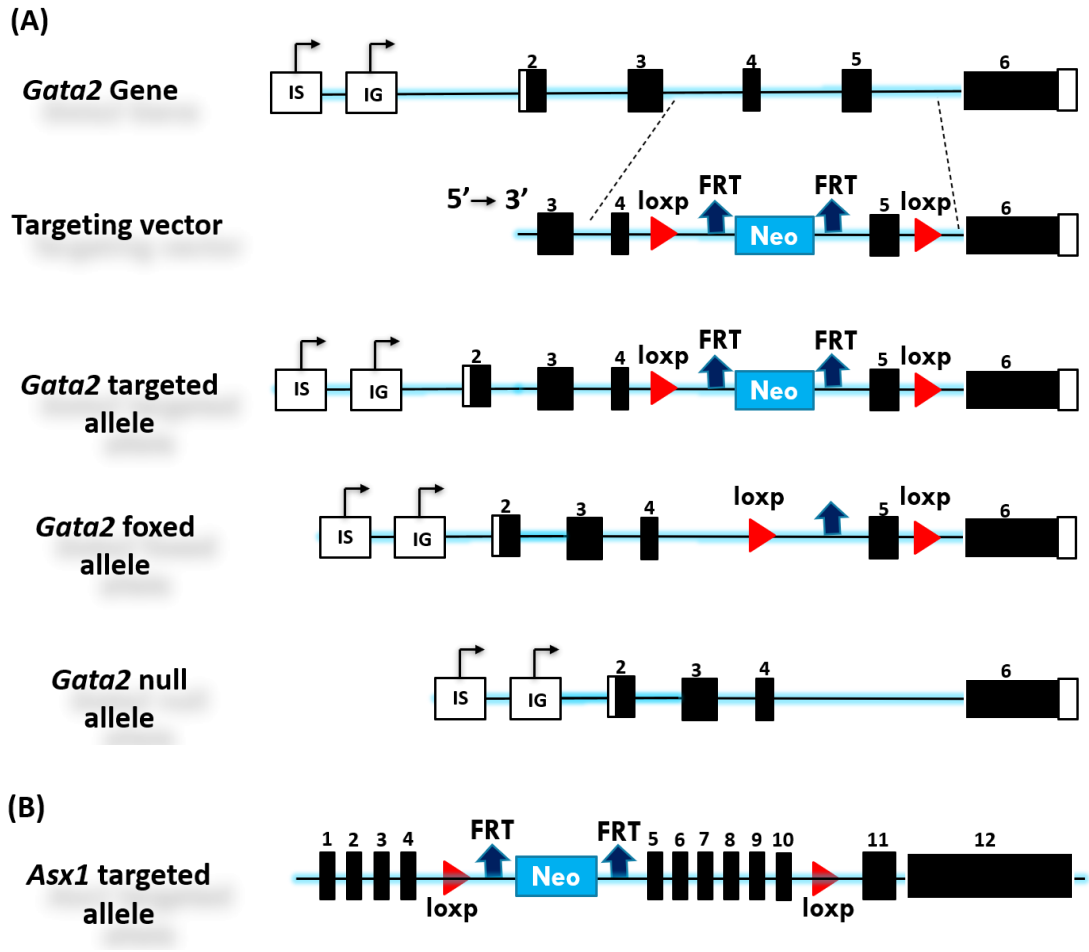

Figure 2-1: The strategy used to produce *Gata2/Asxl1* null alleles.
(A) Generation of floxed *Gata2* alleles. Briefly, the targeting vector was designed to delete the exon 5 of the *Gata2* gene that encodes the C-terminal zinc-figure-domain, a DNA binding part. The targeting vector which comprises of a neomycin resistance gene, FRT sites and loxP sites were inserted between exons 4 and 6 into murine ES-cells. The targeting vector was recombined the wild-type *Gata2* allele in ES cells and followed by ES-cells neomycin resistance selection forming the targeted *Gata2* allele. ES-cells that harbour *Gata2* targeted allele were inserted into C57BL/6 blastocysts to produce $Gata2^{+/fl}$ mouse chimaeras. The neomycin resistance gene was deleted by crossing the $Gata2^{+/fl}$ mouse to Flp-recombinase mouse strains keeping exon 5 flanked with loxp sites. $Gata2^{fl/fl}$ mice were generated by mating $Gata2^{+/fl}$ to $Gata2^{+/fl}$ mice. *Gata2* null alleles were created by crossing $Gata2^{fl/fl}$ mice to Cre recombinase mice under the control of specific promoters. (B) Diagram describes targeted *Asxl1* alleles. Similar to $Gata2^{fl/fl}$ mice, transgenic $Asxl1^{fl/fl}$ mice were produced by inserting a targeting vector for exons 5-10 into (ES) cells. Adapted from (Charles et al., 2006, Abdel-Wahab et al., 2013).

2.1.2.2 Mice identification technique

The punched ear was used for mice identification at 3-4 weeks old. Tissues that removed during ear punching were utilised for mice genotyping. Figure 2.2 describes our identification method.

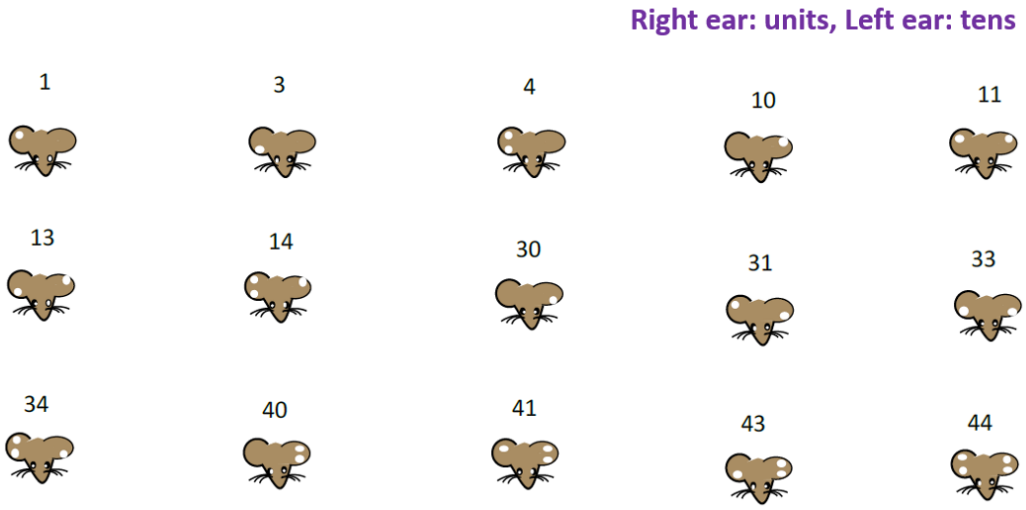

Figure 2-2: Mice ear notch system.

2.1.2.3 pIpC injection

Gata2$^{+/fl}$*, Mx1-Cre*$^{+}$ and *Gata2*$^{+/fl}$*, Mx1-Cre*$^{-}$ mice were given pIpC by intraperitoneal injection every other day for a total of 6 doses. pIpC was dissolved in PBS to form the final concentration of 0.3 mg per dose, GE-healthcare.

2.1.2.4 Mice blood sample collection

Venesection peripheral blood samples were collected from a lateral tail vein in microvette capillary blood collection tubes covered with ethylenediamine- tetra-acetic-acid (EDTA) (Sarstedt). Haematological indices (complete blood count (CBC)) were measured using HemaVet, an automatic counter instrument**.**

2.1.2.5 Isolation of murine haematopoietic cells

Mice were sacrificed by cervical dislocation and then rinsed with 70% Ethanol. Spleen, thymus, and legs were dissected out from a mouse.

2.1.2.5.1 Bone marrow cells isolation

Femurs and tibias were dissected from legs removing muscles and skin tissues. Bones were crushed in a mortar and pestle in 10 mL phosphate buffer saline with 2% foetal bovine serum (2% PBSFBS) solution. The cell suspension was collected into a sterile 50 mL conical tube through a 70 µm cell strainer (Miltenyi Biotec). The small bone fragments were washed with 20 mL 2% PBSFBS solution and the cell suspension was transferred into a collection tube.

2.1.2.5.2 Spleen cells isolation

The spleen was put on a 70 µm cell strainer within a 60-mm sterile Petri dish. Splenic cells were obtained by gently smashing the tissue with a sterile 2 mL syringe plunger in 2 mL 2% PBSFBS solution. The cells were washed with 5 mL 2% PBSFBS solution and the cell suspension was collected into a sterile 15 mL tube.

2.1.2.5.3 Thymus cells isolation

A 70 µm cell strainer was placed in a 60-mm sterile Petri dish. The thymus and 2 mL 2% PBSFBS solution were transferred into the cell strainer. A sterile plunger from a 2 mL syringe was used to mash the thymus. The cells were washed with 2 mL 2% PBSFBS solution and the cell suspension was transferred into a sterile 15 mL conical tube. Harvested cells from BM, spleen, and thymus were then counted utilising the BD Accuri^{TM} machine, an automated cell counter.

2.2 Genomic polymerase chain reaction

2.2.1 DNA extraction

Genomic DNA was used to determine the mouse genotypes. DNA was extracted from ear notch biopsies (25 mg) or bone marrow samples (up to $1x10^7$ cells) according to the manual of Isolate II Genomic DNA kit protocols (Bioline). Briefly, ear samples were placed in a 1.5 microcentrifuge tube with 180 µL lysis buffer-GL, 200 µL lysis buffer-G3, and 25 µL proteinase-K buffer (provided in the kit) at 56°C for 1-3 hours in a heat block, while BM-cells were incubated at 70°C for 10-15 min. 210 µL of 100% ethanol was added, and the mixture was vigorously mixed. Then, the mixture was transferred into Isolate-Genomic-DNA-Spin-Column and centrifuged at 11000 xg for 1 minute. Next, the DNA-Spin-Column was washed with 500 µL wash-buffer-GW1 and 600 µL wash-buffer-GW2 (provided in the kit) and centrifuged at 11000 xg for 1 minute. Lastly, the DNA-Spin-Column was transferred into a 1.5 microcentrifuge tube, and 100 µL of preheated elution buffer (provided in the kit) was added to elute the DNA and centrifuged for 1 minute at 11000 xg. The isolated DNA samples were stored at -20°C. The DNA concentration (final concentration within the range of 20-35 ng/µL) and purity (the DNA absorbance ratio at 260 nm and 280 nm in the range of 1.7-1.9) were determined using the Nanodrop-2000 spectrophotometer (ThermoFisher Scientific).

2.2.2 DNA amplification

A polymerase chain reaction (PCR) was used for the amplification of DNA *in vitro*. PCR was performed according to the manufacturer's guidelines. PCR reaction was performed on 100^{TM} Thermal Cycler (Bio-Rad) in a 25 µL total volume including 12.5 µL of Mango mix (20mM-Tris-HCl, 100mM-KCl, 3mM-MgCl2, 0.002% gelatin, 0.4mM-dNTP mix (dATP, dCTP, dGTP, TTP), 0.06units-Taq DNA Polymerase) (Bioline), 8.3 µL of nuclease free-water (Molecular Probes), and 0.1 µL of each forward and reverse primer (Sigma-Aldrich). Table 2.1 includes primer sequences and PCR conditions.

Table 2.1: PCR primers and thermal conditions.

Primer name	primer sequences		PCR thermal conditions
Gata2	Forward	5' GCCTGCGTCCTCCAACACCTCTAA 3'	Denaturation: 94°C, 1 min Annealing: 60°C, 1 min Extension: 72°C, 1 min Repeat 34 cycles Final cycle: 72°C, 10 min Cooling: 10°C
	Reverse	5' TCCGTGGGACCTGTTTCCTTAC 3'	
Asxl1	Forward	5' ACACCAACCAGCCGTTTTAC 3'	Denaturation: 94°C, 1 min Annealing: 60°C, 1 min Extension: 72°C, 1 min Repeat 34 cycles Final cycle: 72°C, 10 min Cooling: 10°C
	Reverse	5' TCCTTGGATTTTTCTCAGCA 3'	
Excised Asxl1	Forward	5' ACGCCGGCTTAAGTGTACACG 3'	
	Reverse	5' GACTAAGTTGCCGTGGGTGCT 3'	
Vav-iCre	Forward	5' CCGAGGGGCCAAGTGAGAGG 3'	Denaturation: 94°C,40 sec Annealing: 64°C, 40 sec Extension: 72°C, 30 sec Repeat 30 cycles Final cycle: 72°C, 5 min Cooling: 10°C
	Reverse	5' GGAGGGCAGGCAGGTTTTGGTC 3'	
Mx1-Cre	Forward	5' CGTTTTCTGAGCATACCTGGA 3'	Denaturation: 94°C,30 sec Annealing: 55°C, 30 sec Extension: 72°C, 1 min Repeat 30 cycles Final cycle: 72°C, 5 min Cooling: 10°C
	Reverse	5' ATTCTCCCACCGTCAGTACG 3'	

2.2.3 Gel electrophoresis

Agarose gel electrophoresis was performed to visualise the PCR products according to molecular size. 2% agarose gel was prepared, 3 g of agarose powder (Bioline) was mixed with 150 mL 1xTAE buffer (ThermoFisher Scientific) and then microwaved for 3 min at 900 W to polymerise. Next, 5 µL of safeview nucleic acid stain (NBS Biologicals) was added to the content and then poured into a gel tray for 30 min at

room temperature to solidify. The gel tray was transferred into the electrophoresis chamber and covered with 1xTAE buffer. 10 µL of molecular weight ladder (100 bp, BioLabs) and 10 µL of individual amplified DNA samples were loaded onto the agarose gel, the gel was run for 40 min at 94 Volts. DNA fragments were visualised using a UV light device by the ChemiDoc™MP imaging system (Bio-Rad).

2.3 RNA extraction and quantitative PCR analysis

2.3.1 RNA extraction

Up to $5x10^5$ cells were collected for RNA extraction using RNeasy Plus Micro Kit (Qiagen). Cells were put in a 1.5 microcentrifuge tube with 350 µl of 1% β-mercaptoethanol RLT-buffer (Qiagen) and stored at -80 ^oC until extracted. RNA samples were extracted according to the producer's instructions. Briefly, cells were put in gDNA-Eliminator-spin-column and centrifuged for 2 min at 11000 xg. Then, 350 µl of 70% ethanol was added to the flow-through tube and transferred into RNeasy-MinElute-spin-column and centrifuged at 11000 xg for 15 seconds. Next, RNeasy-spin-column was washed with 700 µL W1-Buffer, 500 µL RPE Buffer, (provided in the kit) and 500 µL of 70% ethanol and centrifuged for 15 seconds at 11000 xg. RNA was eluted in 14 µL of RNase-free water. The concentration of RNA was determined using the Nanodrop-2000 spectrophotometer. RNA samples were stored at -80 ^oC.

2.3.2 cDNA synthesis

cDNA was prepared from extracted RNA samples using QuantiTect-Reverse - Transcription Kit (Qiagen) as per manufacturer's guidelines. Briefly, RNA template (up to 1 µg) was mixed with 2 µL gDNA-Wipeout-buffer (provided in the kit) and RNase-free water for a total volume of 14 µL and incubated for 2 min at 42^oC to eliminate the genomic DNA contamination. The mixture was mixed with 1 µL Quantiscript-Reverse-Transcriptase, 4 µL Quantiscript-RT-Buffer, and 1 µL RT-Primer-Mix (provided in the kit) for a final volume of 20 µL and incubated at 42^oC for 15 min. Subsequently, the mixture was incubated for 3 min at 95^oC to stop the activity of Quantiscript-Reverse-Transcriptase. cDNA samples were stored at -20 ^oC.

2.3.3 Real-time quantitative PCR (RT-qPCR)

Quantitative PCR was carried out on the QuantStudioR^{MT} 7-Flex Real-Time-PCR-System (Applied-Biosystems) according to the producer's instructions. A total of 10 µL PCR reaction volume was prepared to contain 2 µL cDNA, 2.5 µL RNase-free water, a 0.5 µL TaqMan primer (Applied-Biosystems), and 5 µL of TaqMan-Universal-PCR-Master-Mix (Applied-Biosystems). Table 2.2 contains TaqMan probes and PCR thermal conditions. Each sample was analysed in three technical replicates. The gene expression level was calculated using the comparative $2^{-\Delta\Delta CT}$ method after normalisation to the *Hprt* housekeeping gene (Schmittgen and Livak, 2008).

Table 2.2: List of RT-qPCR primers and thermal PCR condition.

Gene name	Catalog number	Primer name	PCR thermal conditions
Gata2	4331182	Mm00492301	Samples were amplified for 40 cycles ▪ Initial denaturation: 50°C, 2 min ▪ Denaturation: 95°C, 10 min ▪ Annealing: 95°C, 15 sec ▪ Extension: 60°C, 1 min ▪ Cooling: 10°C
Asxl1	4351372	Mm01240150	
Hprt	4331182	Mm00446968	

2.4 BM colony-forming cell (CFC) assays

As per the manufacturer's protocols, 2x10^4 bone marrow cells were resuspended in 250 µL Iscove's Modified Dulbecco's Medium (IMDM) (StemCell^{TM} Technologies). The cell suspension was added to 2250 µL of semisolid methylcellulose media Methocult^{TM} M3434 that enhances myeloid cells differentiation and supplemented with SCF, IL-3, IL-6, erythropoietin, insulin, and transferrin (StemCell^{TM} Technologies). The mixture was mixed. Then, 1.1 mL of the mixture was plated in duplicate in 35 mm plates using a sterile 16-gauge needle and a 3 mL syringe. Cells were incubated at 37°C with 5% CO2, and colonies were counted after 7-12 days of incubation using a light microscope**.** To quantify B-cell progenitor colonies (CFC-preB), 2x10^5 bone

marrow cells were plated in Methocult™ M3630 that was supplemented with IL-7 (StemCell™ Technologies).

2.5 Magnetic c-kit$^+$ cells enrichment

Bone marrow cells were enriched for c-kit markers using Magnetic Activated Cell Sorting ((MACS), Miltenyi Biotec) according to the company's instructions. Bone marrow suspension (approximately 15 mL) was centrifuged for 5 min at 500 rcf, and the supernatant was removed. Red blood cells were lysed by adding 1 mL of the NH_4Cl lysis buffer for 2 min and subsequently neutralised by 9 mL of 2% PBSFBS and centrifuged for 5 min at 500 xg. After removing the supernatant, the cells were resuspended in 300 µL of 2% PBSFBS with 20 µL of anti c-kit MicroBeads (Miltenyi Biotec) and incubated for 20 min at 4°C in the dark on the rotating shaker. The cells were then washed with 1 mL of 2% PBSFBS and centrifuged for 5 min at 500 xg. Finally, the cells were resuspended in 2 mL of 2% PBSFBS and filtered through a 30 µm Nylon filter (Sysmex) before Auto-MACS separation. Enriched c-kit cells were utilised for HSPCs sorting.

2.6 Fluorescence-activated cell sorting analysis

Fluorescence-activated cell sorting (FACS) analysis was performed on LSR Fortessa™ (Becton Dickinson, Biosciences) flow cytometer. Cells sorting was achieved using a FACSAria™ cell sorter (Becton Dickinson, Biosciences). With a view to diminish prospective spectral-overlap between fluorochromes, manual compensation was carried out in FACS-Diva software, in which single stains were prepared for each fluorochrome in each experiment. Analysis of FACS data was performed with FlowJo 10.6.1 software (Tree Star).

2.6.1 Lineage positive cells staining

About 600 µL of ammonium chloride (NH_4Cl) was added to 12 µL (about $2x10^5$ cells) of peripheral blood samples for 12 min to lyse red blood cells. Around $2x10^5$ cells from PB, BM, spleen and thymus were stained for 30 min at 4°C with fluorochrome cocktails as the following: myeloid cells, Mac1 and Gr1; erythroid cells, Ter119 and CD71; B-cells, B220; and T-cells, CD3, CD4, and CD8 (Table 2.3). Cells were then washed with 2% PBSFBS at 500 xg for 5 min at RT. The cells were resuspended in 200 µL of 2% PBSFBS with 2 µL of 20 µg/mL 4, 6-Diamidino-2-Phenylindole, Dihydrochloride (DAPI) with a final concentration of 0.2 µg/mL to determine live cells. Figure 2.3 describes gating strategies for analysing lineage positive cells. In transplantation settings, CD45.1 and CD45.2 markers were added to fluorochrome cocktails (Figure 2.4).

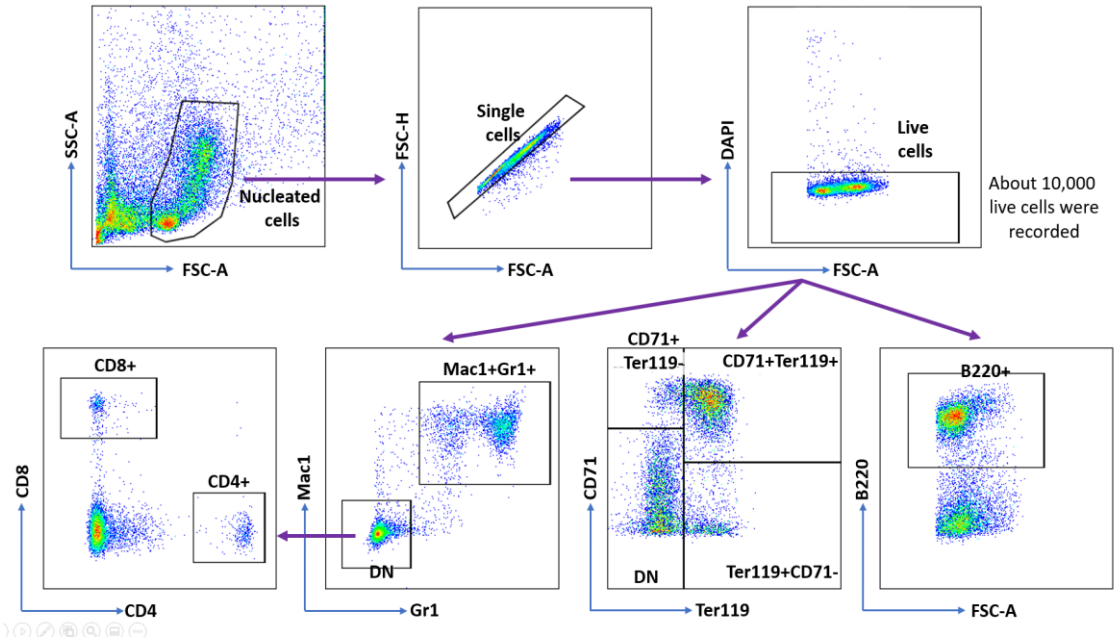

Figure 2-3: Gating strategies for BM lineage positive cells.
Nucleated BM cells were firstly identified by forward scatter and side scatter gating. Cells were then gated for single cells using forward scatter A and H to eliminate doublets and clumps. Next, cells were gated with DAPI negative to exclude dead cells. Finally, all cells were gated from live cells gate.

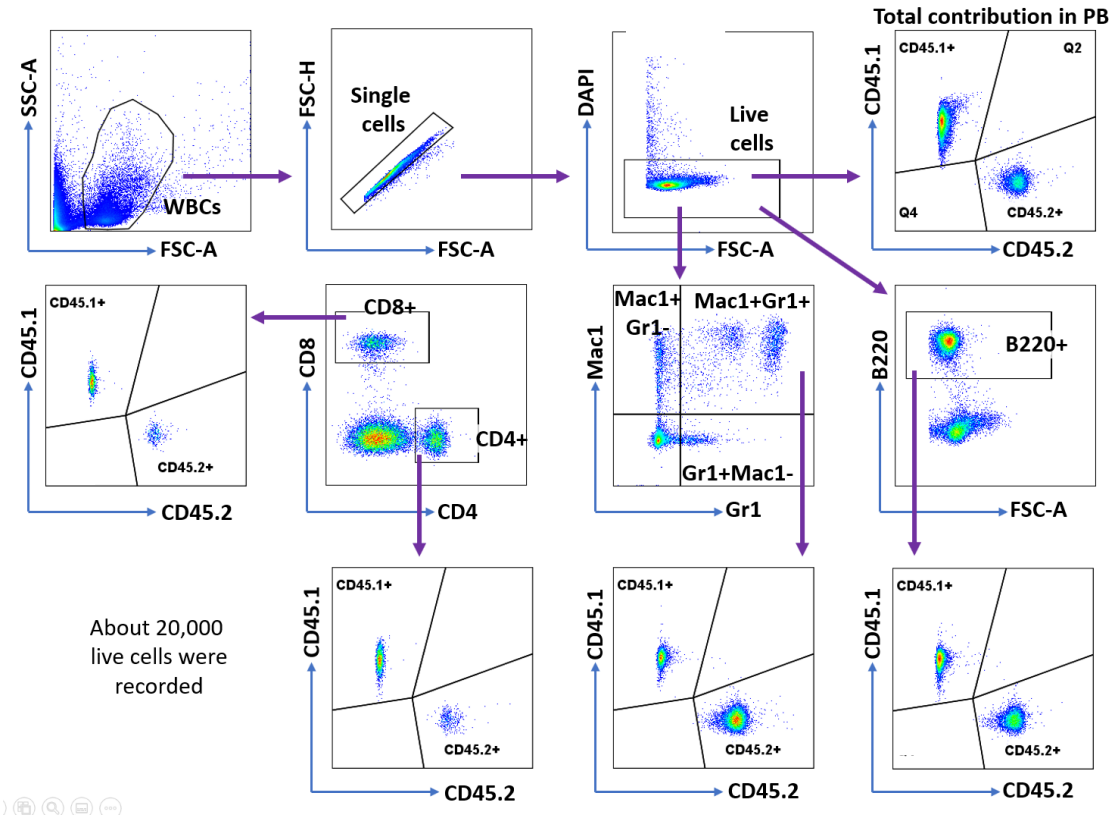

Figure 2-4: Gating strategies for the donor contribution in PB.
WBCs were determined based on forward scatter and side scatter. All mature cells were gated from live cells. In order to measure the donor contribution, CD45.1 and CD45.2 were gated from each population.

2.6.2 Haematopoietic stem and progenitor cells staining

Bone marrow cells were counted and adjusted to $1x10^7$ cells/mL for staining. HSPCs cells were firstly stained with 50 µL Fc-block (CD16/32) and 50 µL antibodies cocktails (biotin-conjugated lineage positive cells (B220_CD3_CD4_CD8a_Mac1_ Gr1_Ter119) and conjugated HSPCs monoclonal antibodies (c-Kit_Sca1_CD48_CD150_CD135 _CD34)), while committed myeloid/lymphoid progenitors were stained with 100 µL of antibodies mix (biotinylated lineage positive cells and conjugated progenitors monoclonal antibodies (c-Kit_Sca1_CD34_CD16/32_CD135_CD127_CD150_CD105 _MAR1_CD41)) (Table 2.3). Stained cells were incubated for 30 min at 4°C. Cells were then washed with I mL of 2% PBSFBS and centrifuged at 500 xg for 5 min at 25°C. Cells were then incubated with streptavidin conjugates at the dark for 20 min at 4°C. Next, cells were washed with 1 mL of 2% PBSFBS and subsequently resuspended in 600 µL

of 2% PBSFBS with 6 µL of 20 µg/mL of DAPI (final concentration of 0.2 µg/mL). Lastly, the cells were passed through a 30 µm Nylon filter (Sysmex) into a FACS tube before being analysed. Figure 2.5 provides a schematic diagram describing HSPCs and restricted progenitors gating methods. In transplant experiments, CD45.1 and CD45.2 markers were added to above staining cocktails and stained with $2x10^7$ cells/mL.

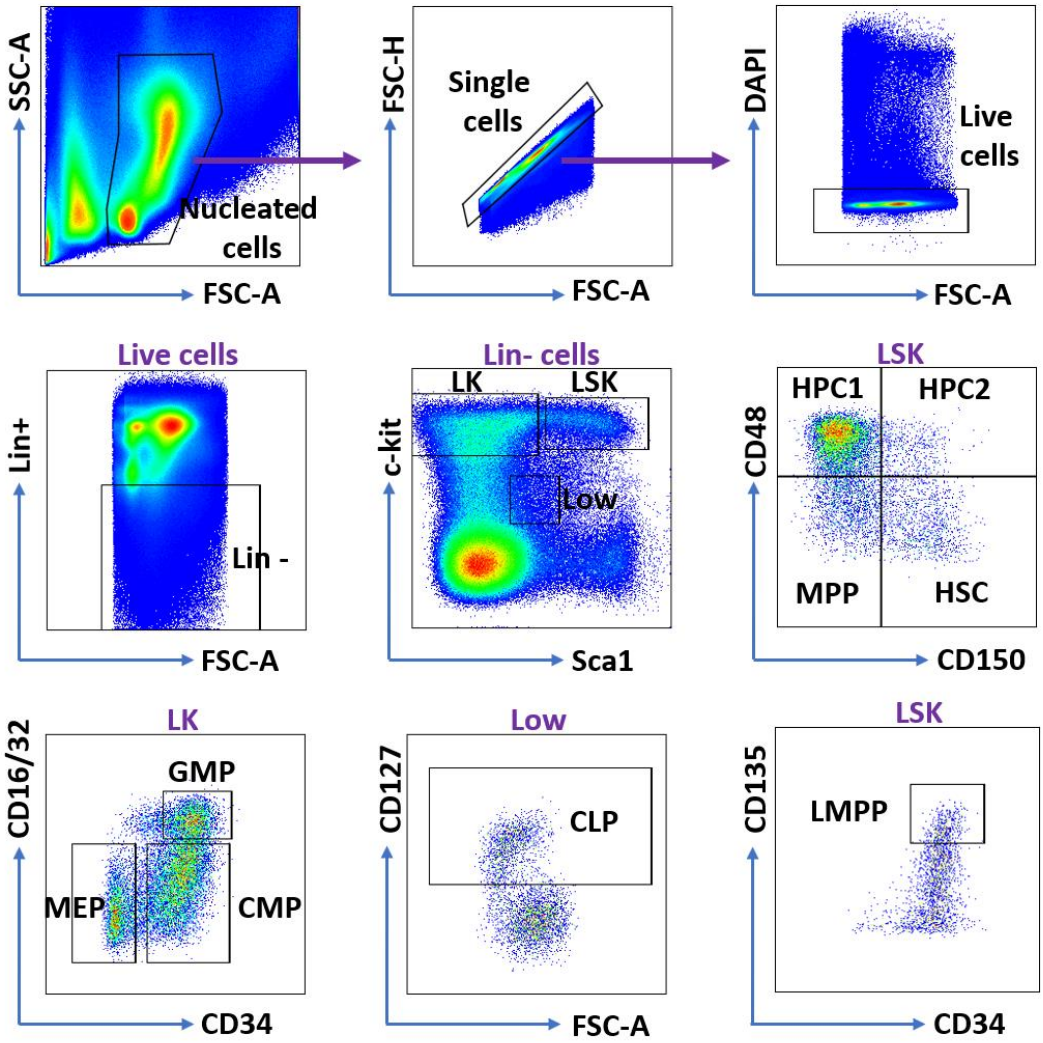

Figure 2-5: HSPCs and restricted progenitors gating strategies.
Lineage (Lin) negative cells were gated from live cells to analyse HSPCs (LSK, HSCs, MPPs, HPC1, HPC2, and LMPPs) and committed myeloid/lymphoid progenitors (LK, CMP, GMP, MEP, and CLP). Around $5x10^6$ nucleated BM cells were recorded.

2.6.3 Apoptosis assay

Annexin-V phospholipid binding-protein staining was utilised to quantify apoptotic cells within a specific population. In the early stage of apoptosis, phosphatidylserine (PS) translocates from the inner to the outer cytoplasmic membrane, which can be detected by fluorescent labelled annexin V that binds to PS. In the late stage of apoptosis, cell plasma membrane becomes permeable and the fluorescent dye DAPI enters the cells and binds to the DNA (Wallberg et al., 2016). Haematopoietic stem and progenitor cells were firstly stained with surface fluorochrome cocktails as described above (section 2.6.2) and then stained with 100 µL of conjugated annexin-V reagent in 1x annexin-V buffer (provided in the kit) in the dark for 30 min at RT (Table 2.3). Cells were then resuspended in 500 µL of 1x Annexin-V buffer with 6 µL of 20 µg/mL DAPI. Cells were filtered through a 30 µm Nylon filter before flow-cytometric analysis (Figure 2.6).

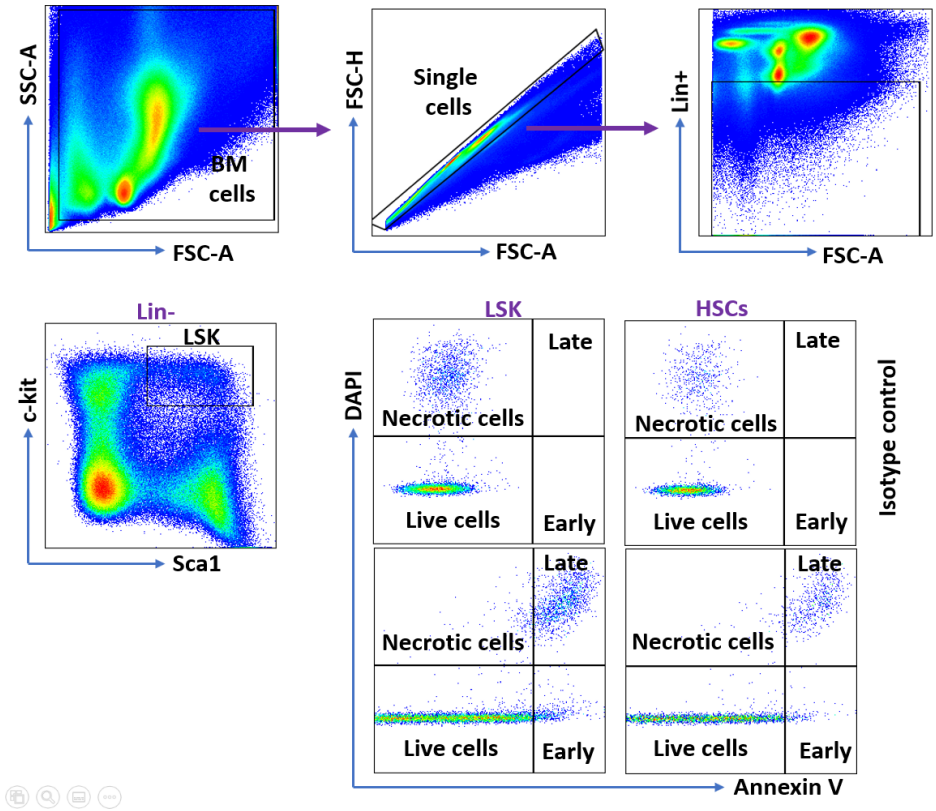

Figure 2-6: Gating methods for apoptosis analysis.
Four populations can be identified using annexin-V and DAPI combination: live cells, annexin-V^-_$DAPI^-$; early apoptosis, annexin-V^+_$DAPI^-$; late apoptosis, annexin-V^+_$DAPI^+$; and necrotic cells, annexin-V^-_$DAPI^+$.

2.6.4 Intracellular staining

Intracellular staining was performed for intracellular proteins as KI-67, γH2AX, BCL2, and BCL-xL. Ki-67 assay is used to assess the cell cycle phases within a specific population. The nuclear Ki-67 antigen is highly expressed in proliferative cells in G1/G2/M phases compared to G0 phase (a quiescent stage) (Gerdes et al., 1984). Surface stained cells were fixed and permeabilised for 15 min at 4°C with PBS 1% paraformaldehyde and PBS, 0.1% saponin, 2% Bovine serum albumin (BSA), respectively. Cells were washed with PBS 0.1% saponin at 500 xg for 5 min at 4°C. Cells were intracellularly stained with 100 µL of Ki-67 antibody in 0.1% saponin 2% BSA in the dark for 30 min and then washed with PBS 2% BSA (Table 2.3). Finally, the cells were resuspended in 600 µL of PBS 2% BSA with 6 µL of 500 µg/mL DAPI (final concentration of 5 µg/mL) and subsequently filtered through a 30 µm Nylon filter and analysed by flow cytometry (Figure 2.7).

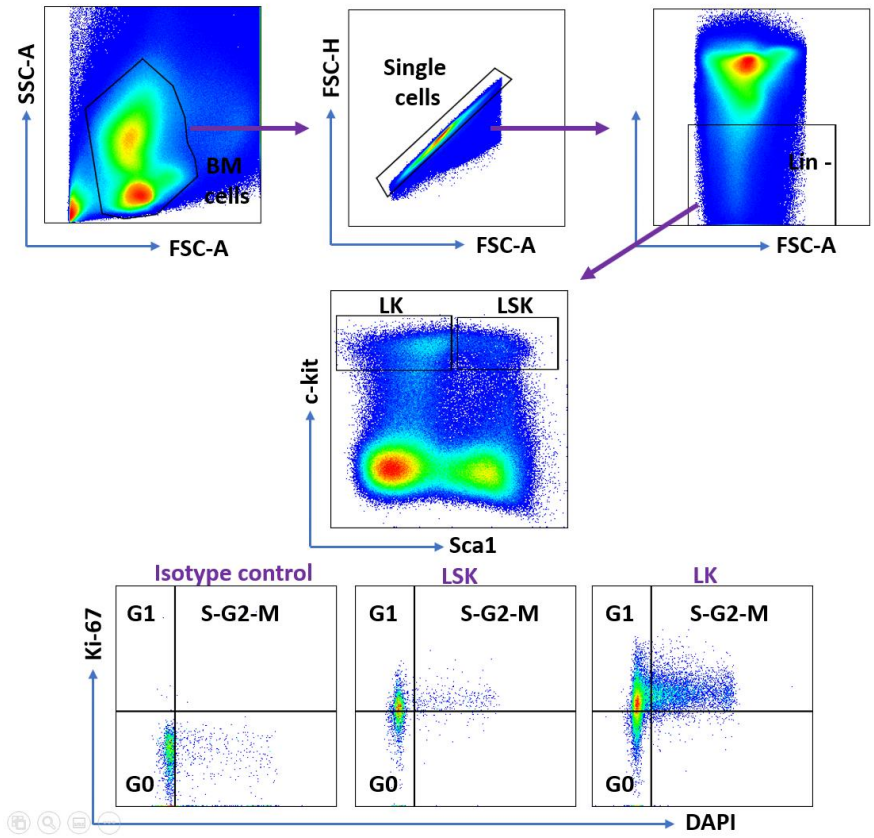

Figure 2-7: Gating strategies for the cell cycle assay.

Cell cycle phases can be distinguished using ki-67 and DAPI staining: G0-phase, ki-67$^-$ DAPI$^-$; G1-phase, ki-67$^+$ DAPI$^-$; and S/G2/M phase, ki-67$^+$ DAPI$^+$.

Table 2.3: List of fluorochromes used for flow cytometric analysis.

Target cells	Cellular marker	Clone	Conjugate	Original Conc	Marker dilution	Company
Lineage positive cells in PB, BM, spleen, and thymus $2x10^5$ cells/ mL	Mac1	M1/70	Biotin, APC, PE	0.2 mg/mL	1/1000	Biolegend
	Gr1	RB6-8C5	Biotin, FITC, PE-Cy7	0.2 mg/mL	1/1000	Biolegend
	Ter119	TER-119	Biotin, APC-Cy7	0.2 mg/mL	1/1000	Biolegend
	CD71	RI7217	PE	0.2 mg/mL	1/1000	Biolegend
	CD3ε	KT3.1.1	Biotin, FITC, APC	0.2 mg/mL	1/1000	Biolegend
	CD4	RM4-5	Biotin, PE-Cy7, PE, PerCP	0.2 mg/mL	1/1000	Biolegend
	CD8a	53-6.7	Biotin, APC-Cy7, PE, BV650	0.2 mg/mL	1/1000	Biolegend
	B220	RA3-6B2	Biotin, FITC	0.2 mg/mL	1/1000	Biolegend
	CD41	MWReg30	FITC, BV510	0.5 mg/mL	1/1000	Biolegend
	CD42d	1C2	PE	0.2 mg/mL	1/1000	Biolegend
	CD45.1	A20	APC, BV650, BV510	0.2 mg/mL	1/1000	Biolegend
	CD45.2	104	PE, FITC, APC-Cy7, BV510	0.2 mg/mL	1/1000	Biolegend
BM HSPCs and committed progenitors $1x10^7$ cells/ml for steady-state analysis $2x10^7$ cells/mL for transplant analysis	c-kit	2B8	APC, PE	0.2 mg/mL	1/100	Biolegend
	Sca-1	D7	APC-Cy7, PE	0.2 mg/mL	1/25	Biolegend
	CD150	TC15-12F12.2	PE-Cy7	0.2 mg/mL	1/100	Biolegend
	CD48	HM48-1	FITC, BV510	0.5 mg/mL	1/50	Biolegend
	CD34	HM34	FITC, PE	0.2 mg/mL	1/25	Biolegend
	CD127	A7R34	BV650	0.2 mg/mL	1/50	Biolegend
	CD16/32	93	PE-Cy7, PE, FITC	0.2 mg/mL	1/25	Biolegend
	CD135	A2F10	PE	0.2 mg/mL	1/50	Biolegend
	CD105	MJ7/18	PE	0.2 mg/mL	1/50	Biolegend
	MAR1	MAR-1	PE-Cy7	0.5 mg/mL	1/50	Biolegend
	Streptavidin	---	PerCP, PB	0.2 mg/mL	1/100	Biolegend, eBioscience
	FC block	93	---	0.5 mg/mL	1/50	Biolegend
HSPCs intracellular staining $1x10^7$ cells/mL	Ki-67	16A8	PE	0.2 mg/mL	1/25	Biolegend
	Annexin V	---	PE	0.2 mg/mL	1/25	Biolegend
	BCL-xL	54H6	PE	0.2 mg/mL	1/100	Cell Signaling Technology
	BCL2	REA356	PE	0.15 mg/mL	1/100	Miltenyi Biotec
	yH2AX	2F3	APC	0.25 mg/mL	1/50	Biolegend
	Isotype PE	REA293	PE	0.15 mg/mL	1/100	Miltenyi Biotec
	Isotype APC	MOPC-21	APC	0.2 mg/mL	1/100	Cell Signaling Technology

2.7 Competitive and serial transplantation experiments

CD45.2 BM cells were harvested, enriched for a c-kit marker, stained with surface HSPCs markers (Lineage positive cocktail, Sca1, c-kit, CD150, and CD48) and sorted for HSCs (Lin^-_$c\text{-}kit^+$_$Sca1^+$_$CD48^-$_$CD150^+$) on FACS Aria as described above. 150 HSCs from either heterozygote *Gata2* or control mice (CD45.2) were mixed with $2x10^5$ competitor BM cells (CD45.1) in 200 µL PBS and transplanted into lethally irradiated (two doses of 500 rads / four hours between the doses) recipient mice (CD45.1) by tail intravenous injection as described previously (Duran-Struuck and Dysko, 2009). For total BM transplant, $1x10^6$ unfractionated BM cells from CD45.2 mice together with $1x10^6$ unfractionated support BM cells from CD45.1 mice were transplanted into lethally irradiated CD45.1-hosts. For aged HSCs experiments, 300 CD45.2 HSCs alongside CD45.1 support BM cells were injected into CD45.1-irradiated recipients. For secondary transplantation, primary recipient mice were sacrificed sixteen weeks after transplantation, and CD45.2 HSCs were purified from *Gata2* heterozygote and control mice. $2x10^5$ CD45.1 competitor BM cells were mixed with 200 CD45.2 HSCs and transplanted intravenously into new CD45.1-lethally irradiated recipients. Recipient mice were placed in an incubator at 37° C for 15-30 min to stimulate the tail vein vasodilation, and the tail vein injection was achieved through a 26g needle with a 1mL syringe. Following the irradiation of recipient mice, the drinking water bottle was supplied with enrofloxacin (10% Baytril oral solution) antibiotic for 30 days.

2.8 RNA-Sequencing

2.8.1 RNA samples preparation

Between $5x10^3$ and $8x10^3$ HSCs (LSK_$CD48^-$_$CD150^+$) were sorted in 350 µl of 1% β-mercaptoethanol RLT-buffer on FACS-Aria, RNeasy Plus Micro Kit (Qiagen) was utilised to perform RNA extraction as described above. RNA samples were stored at -80° C until required for sequencing.

2.8.2 RNA library preparation and sequencing

Library construction and RNA-sequencing were carried out by Wales Gene Park, Institute of Medical Genetics, Cardiff University. Quality assessments were firstly performed to assess total RNA quality and quantity utilising Agilent-2100-Bioanalyser and RNA-Nano-6000 kit (Agilent Technologies). RNA samples with a concentration of 0.5-6 ng and RNA-Integrity-Number (RIN) of more than 8 were used for ribosomal-RNA depletion utilising NEBNext® rRNA-depletion kit (E6310, New England Biolabs®) followed by the library construction using NEBNext® Single-Cell/Low Input RNA Library Prep-Kit for Illumina® (E6420, New England Biolabs®) following the manufacturer's instructions, including total RNA polyadenylated magnetic-beads Purification, cDNA synthesis, cDNA amplification, cDNA purification using Agencourt-AMPure® Beads (Beckman Coulter®), cDNA fragmentations, cDNA adaptor-ligation using NEBNext® Multiplex Oligos for Illumina® (E6440, New England Biolabs®), Adaptor-ligated-DNA cleaning, PCR enrichment, and purification of PCR-product using Agencourt-AMPure® XP beads. Quality tests were carried out to validate DNA libraries as the concentration of the DNA library using a Qubit® fluorometer (Life Technologies) and DNA fragment size using Agilent 4200-Tap-Station (Agilent Technologies). In the last step, the DNA libraries were pooled together and normalised to 4 nM and sequenced using a 75-base-paired-end (2x75bp PE) dual-index-read-format on the Illumina® HiSeq4000 sequencer as per the manufacturer's guidelines.

2.8.3 Bioinformatic analysis of RNA sequencing dataset

Quality tests were firstly performed for RNA sequencing dataset. Trim Galore was used to remove adapter-sequences using a Cutadapt tool, and poor-quality ends of reads were eliminated using a FastQC tool by performing paired-end mode. The GRCm38.p6 mouse-genome was utilised to map trimmed reads (FASTq files) using STAR software with the MultimapNMax=1 flag setting to exclude any reads that mapped to more than one location. The Subread featureCounts Version-1.6.2 software was used to calculate reads counting for both exons and transcripts (Liao et al., 2014). The GENCODE M18 gene-model was employed to determine exon and

transcript locations. Raw data were generated including number of reads that mapped for each gene. The DEseq2 Bioconductor package in R-scripts statistical computing software was used to identify differentially expressed genes (Love et al., 2014), and p-values and adjusted p-values (False Discovery Rate, FDR values) were calculated to diminish false discovery issues (Benjamini and Hochberg, 1995). Above mentioned analyses were performed by Wales Gene Park.

The Ingenuity Pathway Analysis (IPA, Qiagen-Bioinformatics) software was utilised to explore gene ontology and common canonical pathways for transcripts with p-values <0.05 and FDR values < 0.05. Fischer's Exact Test was used to determine enriched pathways. Gene Set Enrichment Analysis (GSEA) was also used to identify significantly enriched pathways with p-values <0.05 and FDR values < 0.05 using hallmark gene-sets and C2-curated (KEGG, Reactome, and BioCarta gene-sets database) gene-sets in the GSEA Molecular Signatures Database (MSigDB, V4.0.2) (Subramanian et al., 2005). Morpheus online software (Broad Institute) was utilised to draw heat-maps for differentially deregulated genes.

2.9 *Asxl1* Knockdown procedures

2.9.1 Plasmids purification

Scramble (Empty-vector, VB150923-10051) and short-hairpin *Asxl1* (*mAsxl1* (shRNA1), VB180515-1197ubr and *mAsxl1*(shRNA2), VB180515-1198gbn) plasmids were bought from VectorBuilder company. psPAX2 and VSV-G plasmids were kindly provided by Dr Kamil Kranc, University of Edinburgh. Figure 2.8 describes vector components and *Asxl1-sh* sequences. All plasmids were cloned in *Stbl3 E. coli* bacteria and preserved in a glycerol stock and stored at -80°C and extracted as per the manufacturer's guidelines. Frozen bacteria were plated on the LB-agar (Invitrogen) plate and incubated overnight at 37°C. A colony of cultured bacteria was picked up and cultured in 200 mL of LB-broth (Invitrogen) media with 200 µg/mL of ampicillin (Gibco) and incubated in a shaking incubator for 4-6 hours at 37°C. DNA plasmids were purified using the EndoFree Plasmid Maxi-Kit (Qiagen) as per manufacturer's instructions and stored at -20°C until required. The Nanodrop-2000

spectrophotometer (Thermo-Scientific) was used to measure DNA purity and concentration.

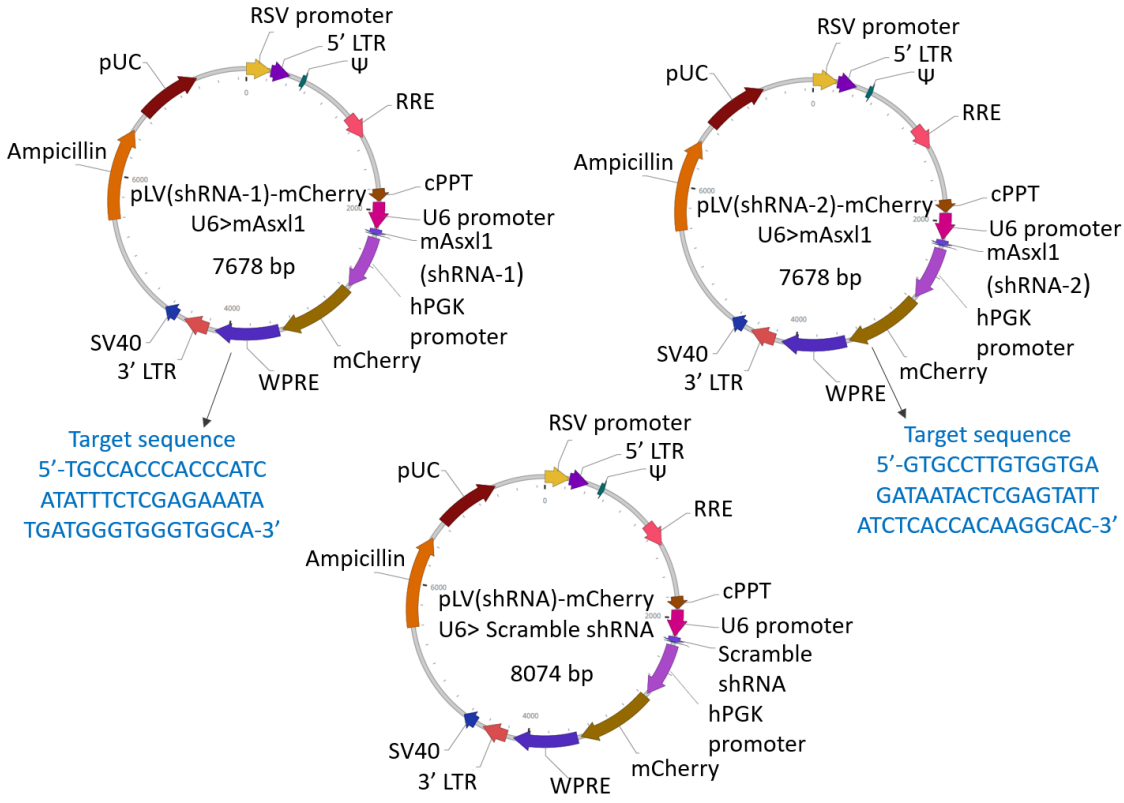

Figure 2-8: *Asxl1* plasmids constructions.
Diagrams illustrate plasmids components. Target sequences of *shAsxl1* plasmids are highlighted in blue. mCherry reporter gene works as a marker to isolate transduced cells by expressing a red fluorescent protein; Rous sarcoma-virus promoter (RSV) promotes viral RNA transcript in packaging-cells; Human U6-small-nuclear-promoter (U6-promoter), a Pol III promoter that drives mRNA expression; Human phosphoglycerate-kinase-1-promoter (hPGK-promoter); Simian virus-40 early-polyadenylation-signal (SV40) enhances mRNA polyadenylation; Ampicillin resistance-gene provides ampicillin resistance; pUC promotes E. coli plasmid replication; Woodchuck-hepatitis-virus-posttranscriptional-regulatory element (WPRE) promotes stability of viral RNA in packaging-cells; HIV-1 packaging-signal (Ψ), viral RNA packaging; HIV-1 Rev-response-element (RRE), viral RNA packaging; Central-polypurine-tract (cPPT) imports HIV-1 cDNA to the nucleus; Long-terminal-repeat (LTR) enhances viral RNA transcription and packaging. Adapted from the VectorBuilder leaflet.

2.9.2 HEK293T cell line

Human embryonic kidney cell line (HEK293T cells, Cell-Biolabs) is widely used in transfection assays. HEK293T cells highly express the SV40 large-T-antigen that enhances the replication of plasmids that originally have the SV40-antigen. HEK293T cells were cultured in Dulbecco's modified Eagles medium (DMEM, Gibco) with 10% foetal bovine serum (FBS, Gibco), 1% L-glutamine (Gibco), and 1% Penicillin/Streptomycin (Gibco). HEK293T cells were plated in 100 mm petri-dish with a density of $1x10^5$-$2x10^5$ cells/mL. The passage of cells was performed every 2-3 days with confluency of 70-90%.

2.9.3 Lentiviral *Asxl1* generation

Lentivirus was produced using the Calcium-Phosphate transfection method that enhances the DNA condensation on the cells surface (Kingston et al., 2003). Plasmids (10 µg/dish of lentiviral shRNA or scramble plasmid, 6.5 µg/dish of psPAX-2 packaging plasmid, and 3 µg/dish of VSV-G plasmid) and 62.5 µL calcium chloride (Sigma) were mixed with free nuclease water for a 500 µL final volume (Figure 2.9). The mixture was slowly added drop by drop to 500 µL 2x-HEPES buffered saline (Sigma) and incubated for 12-15 min at RT. Approximately 60-70% confluent HEK293T cells were used for transfections. 10 mL of fresh media involving 25 µM chloroquine (Sigma) was gently added to HEK293T cells in a 10 mm petri-dish before transfection. The DNA mixture was lightly added to the whole dish and incubated at 37^{o}C for 6-16 hours. Media was exchanged with 8 mL of freshly new media. The lentiviral supernatant was harvested at 24 and 48 hours and filtered through a 0.45 µm filter (Sigma-Aldrich). Ultra-centrifugation was performed for the collected supernatant using Optima XPN-80 Ultracentrifuge (Beckman Coulter) at 2300 xg for 2 hours at 4^{o}C, and generated viral particles were stored at -80 ^{o}C until the next step.

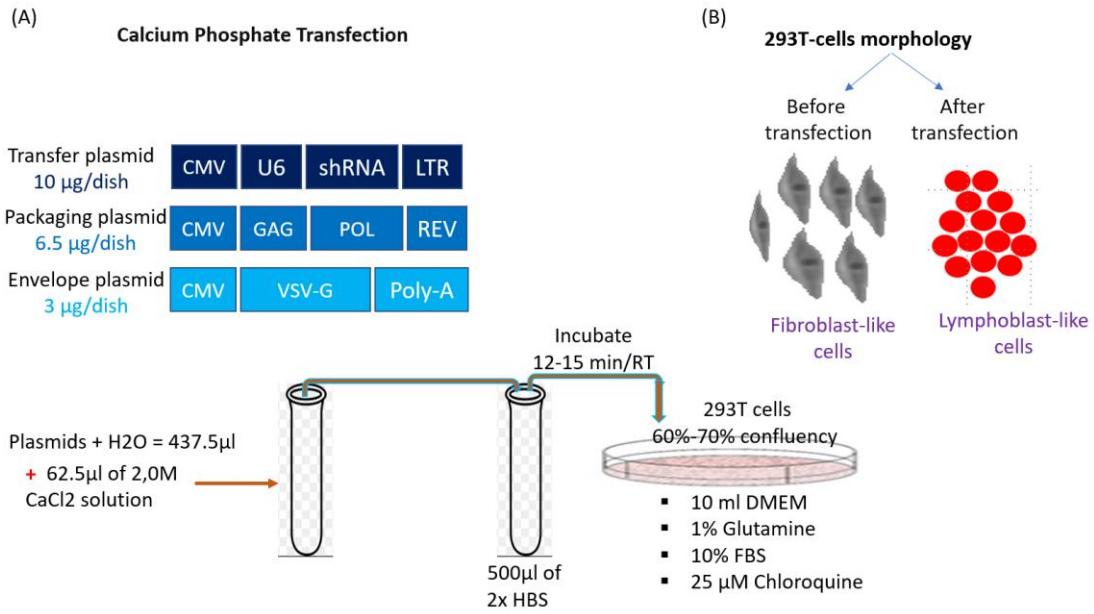

Figure 2-9: Lentiviral *Asxl1* generation.
(A) A diagram describes the production of lentiviral *Asxl1.* (B) The morphology of 293T cells before and after transfection.

2.9.4 Lentiviral *Asxl1* titration

Approximately $5x10^4$ HEK293T cells were seeded in 1 mL of DMEM supplemented with 10% FBS, 1% L-glutamine, and 1% Penicillin/Streptomycin in 12-well plates (Starlab-group) with a different amount of viral particles (1 µL, 0.5 µL, 0.1 µL, 0.05 µL, and 0.01 µL) and incubated for 12-15 hours at 37 °C. The medium was replaced with 1 mL of new media and incubated at 37°C for 72 hours. HEK293T cells were collected and analysed by flow cytometry to determine the expression level of mCherry protein (Figure 2.10). Wells with 5-20% of mCherry positive cells were used to calculate the correct viral titre in order to avoid viral multiple integrations (Fehse et al., 2004). The viral titre was determined by multiplying plated-cell numbers with transduced-cell percentages and divided by the volume of viral particles (mL).

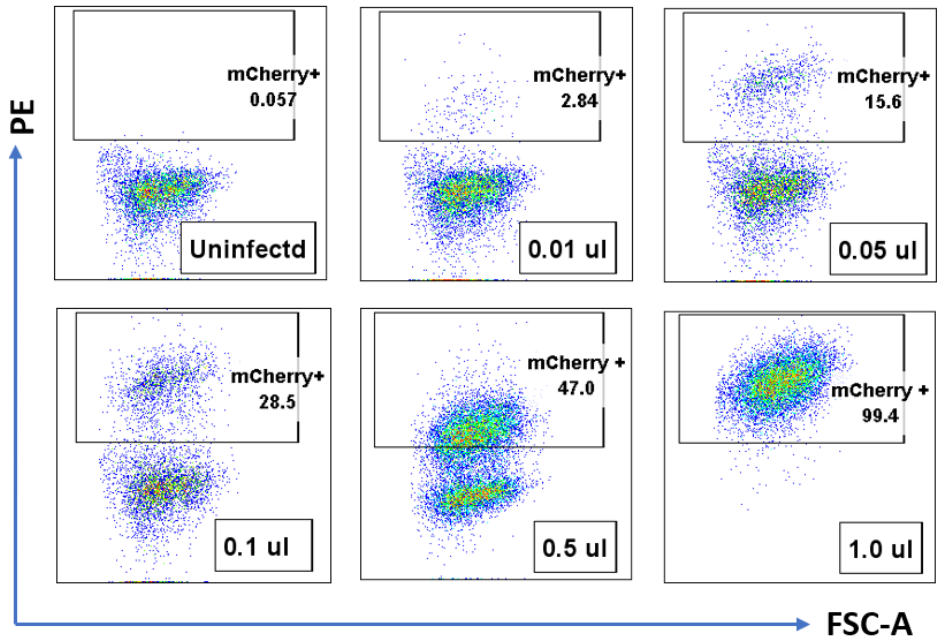

Figure 2-10: Lentiviral *Asxl1* titration.
FACS plots show the frequency of live mCherry$^+$ cells. The viral titre was calculated from wells with 5-20% of mCherry$^+$ cells as follows: numbers of plated cells x percentages of transduced cells / Volume of viral particles (mL), $5x10^4$ X 0.156/0.00005 mL = $156x10^6$ viral particles /mL.

2.9.5 Lentiviral transduction

Retronectin (Clontech) approach was used to transduce murine HSPCs. Retronectin reagent is fragmented recombinant human-fibronectin and facilitates the interaction between cells and lentiviral-transfer-gene. Retronectin reagent is comprised from the cell-binding domain (C-domain), which binds to target cells integrin receptor VLA-5 and VLA-4, and heparin-binding domain (H-domain), which binds to viral particles (Kimizuku et al., 1991). 5 $x10^4$ murine LSK cells were sorted as described above (sections 2.5 and 2.6.2) and pre-stimulated in 200 µl Iscove's Modified Dulbecco's Medium (IMDM) (StemCell™ Technologies) supplemented with 100 ng/mL m-SCF (mouse-stem-cell-factor, Peprotech), 100 ng/mL m-TPO (mouse-thrombopoietin, Peprotech), 100 ng/mL mFlt3L (mouse-Fms-related tyrosine kinase-3-ligand, Peprotech), 10% FBS (Gibco), 1% L-glutamine (Gibco), and 1% Penicillin/Streptomycin (Gibco) and incubated for 3-4 hours at 37°C, 5% CO2 (Holmfeldt et al., 2016, Hosokawa et al., 2010). 96-well culture plates (Starlab) were covered with 200 µl of 100 µg/mL of retronectin and incubated for 2 hours at RT as per manufacturer's

instructions. Following removal of the retronectin reagent, lentiviral particles in 200 µl of IMDM were added to pre-coated 96-well plates with a multiplicity of infection (MOI) of 50, infected cells with enough numbers of viral particles, and centrifuged at 2100 xg at RT for 2.5 hours. Pre-stimulated LSK cells were added to pre-lentiviral-retronectin-coated plates and centrifuged for 5 min at 500 xg at RT and incubated overnight at 37°C, 5% CO_2. The next day, media was gently removed, and cells were collected and washed in IMDM. Cells were next plated with new IMDM supplemented with cytokines as described above in this section and incubated at 37°C, 5% CO_2 for 72 hours (Holmfeldt et al., 2016, Hosokawa et al., 2010). The percentages of mCherry positive cells were evaluated using flow cytometry, and mCherry live cells were sorted for CFC ($1x10^3$ cells were plated in M3434-methylcellulose-media as described above (section 2.4)) or qPCR.

2.10 Statistical analysis

Statistical analysis and graphs were performed using GraphPad Prism 8.3 software (GraphPad Software). Data represent the mean and error bars represent standard error of the mean (SEM). All Data underwent for normality tests using Anderson and Pearson tests before being analysed. Statistical significance was determined using an unpaired 2-tailed t-test, Mann-Whitney U test, or One-Way ANOVA- Tukey's multiple comparisons test unless mentioned otherwise. Differences between samples were considered significant based on the p-value: *, $P < 0.05$; **, $P < 0.01$; ***, $P < 0.001$; ****, $P < 0.0001$.

CHAPTER 3 : The role of *Gata2* haploinsufficiency in young and aged haematopoietic compartments using Vav-iCre mouse models

3.1 Introduction

Self-renewal and differentiation define HSC functions, and the balance between these two processes are critical for the maintenance of blood homeostasis throughout the lifespan of an organism (Orkin and Zon, 2008, Seita and Weissman, 2010). Lineage-specific transcriptional factors are involved in regulating the fate of HSCs. GATA2 is a member of heptad TFs that regulate haematopoietic genes (Wilson et al., 2010). Expression of *Gata2* mRNA is found in embryonic and adult HSPCs, committed myeloid progenitors, erythroid-precursors, megakaryocytes and mast cells (Tsai et al., 1994, Tsai and Orkin, 1997), with the most prevalent expression found in HSCs which declines during differentiation (Menendez-Gonzalez et al., 2019b, Orlic et al., 1995, Guo et al., 2013).

GATA2 is indispensable for the generation of HSCs from haemogenic endothelium in the endothelial-haematopoietic transition process (de Pater et al., 2013). Germline deletion of *Gata2* is embryonic lethal at E10.5 due to severe anaemic complications (Tsai et al., 1994). Conditional knockout (*Gata2*$^{+/fl}$*; Vav-Cre*$^{+}$) and germline deletion (*Gata2*$^{+/-}$) of one allele of *Gata2* in embryos cause a significant reduction in HSC numbers in the AGM region and foetal liver and a defect in AGM-HSCs repopulation potential in transplantation settings (de Pater et al., 2013, Ling et al., 2004). Analysis of adult BM utilising germline knockout mouse models shows that *Gata2*$^{+/-}$ mice have decreased HSCs pool size, increased cellular quiescence and apoptosis of HSCs, reduced number of granulocyte/macrophage progenitors, and a defect in HSCs repopulating capability in competitive transplantation experiments, whereas HSC potential for self-renewal appears to be unaffected (Rodrigues et al., 2005, Rodrigues et al., 2008). GATA2 overexpression mouse models and human CD34^{+} cord haematopoietic cells show an increase in quiescent HSCs coupled with a differentiation block of HSCs (Persons et al., 1999, Tipping et al., 2009). Together,

these findings implying that the precise level of *Gata2* expression is decisive in generating and maintaining HSC functions.

GATA2 haploinsufficiency (heterozygosity) is linked to clinical immunodeficiency syndromes such as MonoMAC syndrome, DCML deficiency syndrome, Emberger syndrome, and congenital chronic neutropenia, that eventually develop into MDS/ CMML/ AML. Germline *GATA2* mutations have been further identified in familial MDS/AML patients (Dickinson et al., 2011, Hyde and Liu, 2011, Hahn et al., 2011, Hsu et al., 2011, Ostergaard et al., 2011). The clinical features of MDS patients with GATA2 haploinsufficiency syndrome comprise that the disease onset between the age of 3 and 78 years; it is more common in young patients with a median age between 21 and 33 years and those patients with a frequent family history of MDS; low blood frequencies of monocytes, dendritic cells, B-cells, NK-cells and CD4:CD8 cells ratio; the normal level of haemoglobin, neutrophils and platelets in peripheral blood; BM hypocellularity; and a reduction in the numbers of multi-lymphoid and granulocyte-macrophage progenitors, and cytogenetic abnormalities represent around 60%-70% of all cases such as monosomy-7 and trisomy-8 (Collin et al., 2015, Dickinson et al., 2014, Calvo et al., 2011, Bigley et al., 2011, Wlodarski et al., 2017).

3.1.1 Aims of this chapter

Although malignant myeloid transformation occurs in approximately 75% of germline GATA2 haploinsufficient patients (Wlodarski et al., 2017), there has been little research about altered HSPC compartments, affected downstream transcriptional pathways, and underlying molecular mechanisms in this context. Additionally, previous studies have not investigated the role of GATA2 haploinsufficiency in aged haematopoietic populations. This study employed conditional knockout mouse models to investigate the role of *Gata2* heterozygote in young (8-12 weeks old) and aged (18-20 months old) HSPCs and haematopoiesis. One allele of the floxed *Gata2* gene was specifically deleted within haematopoietic compartments at E11 utilising the pan-haematopoietic Vav-iCre promoter to mimic germline GATA2 haploinsufficiency syndromes (Stadtfeld and Graf, 2005). Functional, transcriptional and immunophenotypic characteristics of young and aged HSPCs were analysed,

including immunophenotyping analysis of primitive HSPCs, committed haematopoietic progenitors, and mature blood cells; apoptosis assays; cell-cycle assays; colony-forming cell assays; HSCs RNA sequencing, and HSCs repopulation and self-renewal capacities using competitive and serial transplantation experiments.

3.2 Roles of *Gata2* haploinsufficiency in young haematopoietic cells

3.2.1 The generation and validation of *Gata2*$^{+/fl}$; *Vav-iCre*$^{+}$ mouse strains

The Cre-Lox recombination system provides an approach to generate conditional heterozygous *Gata2* mouse models. *Gata2*$^{fl/fl}$ mice were kindly donated by Dr Julian Downward, Francis Crick Institute. Transgenic *Gata2*$^{fl/fl}$ mice were generated as reported previously (Charles et al., 2006). To begin exploring the function of *Gata2* heterozygote in the adult haematopoietic system (Figure 3.1 A), *Gata2*$^{+/+}$; *Vav-iCre*$^{+}$ with *Gata2*$^{fl/fl}$; *Vav-iCre*$^{-}$ were crossed to produce *Gata2*$^{+/fl}$; *Vav-iCre*$^{+}$ (heterozygote) and *Gata2*$^{+/fl}$; *Vav-iCre*$^{-}$ (control) littermates (Figure 3.1 B). *Gata2*$^{+/fl}$; *Vav-iCre*$^{+}$ mice were born in the expected Mendelian ratio and appear phenotypically normal when compared with their control littermates. To verify *Gata2* deletion, genotyping was performed by genomic DNA PCR of ear notch biopsies and BM cells, which confirmed *Gata2* heterozygote and control status (Figure 3.1 C). *Gata2* mRNA expression was assessed in total BM cells and sorted LSK cells in *Gata2*$^{+/fl}$; *Vav-iCre*$^{+}$ and control mice. Expression level of *Gata2* mRNA was similar in BM in both littermates, while a two-fold reduction of *Gata2* mRNA was observed in LSK cells in *Gata2*$^{+/fl}$; *Vav-iCre*$^{+}$ when compared with control mice (Figure 3.1 D). Thus, *Gata2*$^{+/fl}$; *Vav-iCre*$^{+}$ mice demonstrate efficient deletion of a single *Gata2* allele.

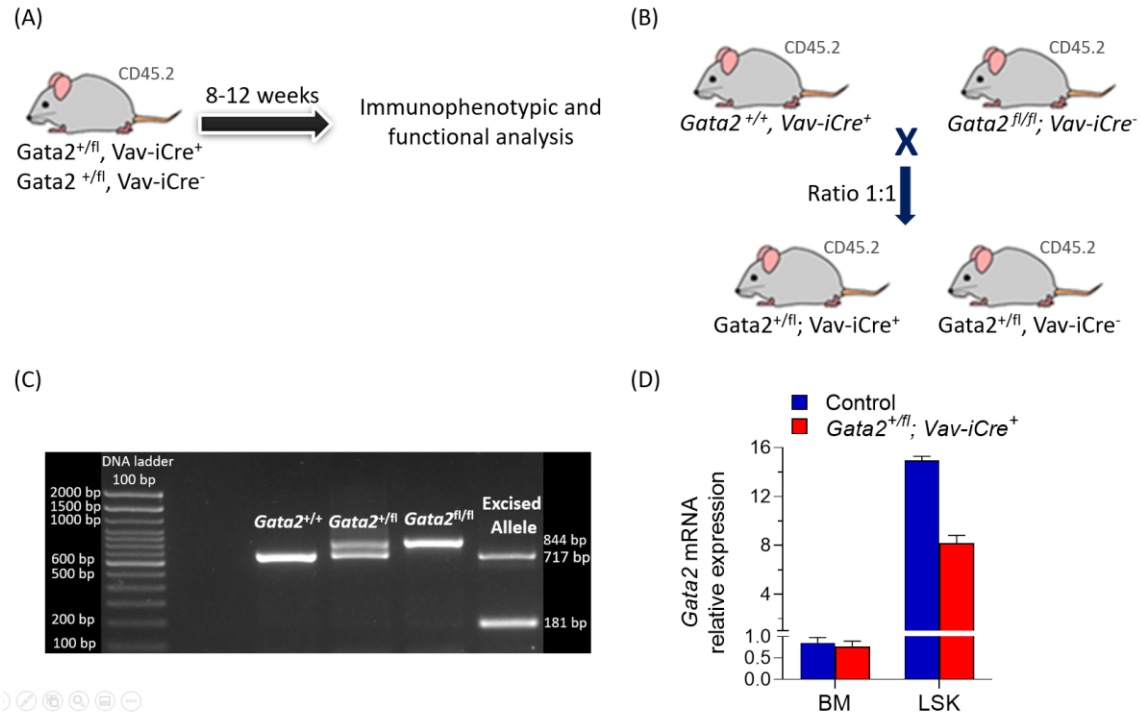

Figure 3-1. *Gata2*$^{+/fl}$*; Vav-iCre*$^{+}$ mice breeding and genotyping.

(A) A scheme describes the experimental design. Control and *Gata2* $^{+/fl}$*; Vav-iCre*$^{+}$ littermates were evaluated at 8-12 weeks old. (B) Breeding scheme of transgenic *Gata2* mice. *Gata2*$^{+/fl}$*; Vav-iCre* and control mice were born in Mendelian ratios. (C) Gel showing PCR products of genomic DNA samples. (+), wild type, 717 bp; (f), floxed allele, 844 bp; and excised allele, 181 bp. (D) Relative *Gata2* mRNA expression compared with *Hprt* mRNA in BM and purified LSK cells from *Gata2*$^{+/fl}$*; Vav-iCre*$^{+}$ and control mice using the comparative $2^{-\Delta\Delta CT}$ method, n= 3 mice for each genotype. Data are presented as mean ± SEM.

3.2.2 *Gata2* haploinsufficiency mice show a decrease in numbers of mature megakaryocytes and peripheral platelets

Peripheral complete blood count (CBC) indices were performed for young (8-12 weeks old) *Gata2*$^{+/fl}$*; Vav-iCre*$^{+}$ and control (*Gata2*$^{+/fl}$*; Vav-Cre*$^{-}$) mice (Figure 3.2 A). No differences in numbers of WBCs, RBCs, and haemoglobin levels were observed in both littermates. However, the number of platelets was significantly decreased in *Gata2*$^{+/fl}$*; Vav-Cre*$^{+}$ mice as compared with the control group. Extensive flow cytometric analysis was performed for lineage-specific haematopoietic cells in the PB BM, spleen, and thymus for both control and *Gata2*$^{+/fl}$*; Vav-Cre*$^{+}$ mice.

The total cellularity of BM, spleen, and thymus cells was comparable between genotypes. We characterised myeloid cells using cell surface protein markers such as Mac1 (Monocytes/Macrophages and granulocyte precursors) and Gr1 (Neutrophils, Eosinophils, Basophils and Monocyte/Macrophage precursors). For erythroid compartments, erythroid cells were categorised into three discrete subpopulations by using CD71 and TER119 proteins expression as 1. Proerythroblasts ($CD71^{+}$ $Ter119^{-/low}$); 2. Early-erythroblasts ($CD71^{+}$ $Ter119^{+}$) and 3. late erythroblasts ($CD71^{-}$ $Ter119^{+}$). T-cell markers (CD4 and CD8) and the B-cell marker (B220) were used to analyse lymphoid cells. Flow cytometric analysis revealed that the frequencies of myeloid, lymphoid, and erythroid cells in the PB, BM, spleen, and thymus were similar in both *Gata2*$^{+/fl}$*; Vav-iCre*$^{+}$ and control mice (Figure 3.2 C, D, E and F). This is consistent with previous studies where terminal differentiation of myeloid/ lymphoid/erythroid blood cells was unperturbed in adult *Gata2* heterozygote mice (Onodera et al., 2016, Rodrigues et al., 2005, Rodrigues et al., 2008).

While GATA2 has been implicated as a key regulator of megakaryopoiesis (Gao et al., 2013, Huang et al., 2009), the role of *Gata2* haploinsufficiency in megakaryopoiesis is unclear. Therefore, this study assessed the frequency of mature megakaryocyte cells in BM and spleen using CD41 and CD42d markers. A significant reduction in the percentages of mature megakaryocyte cells ($CD41^{+}CD42d^{+}$) was noticed in BM and spleen in *Gata2*$^{+/fl}$*; Vav-iCre*$^{+}$ as compared with control mice (Figure 3.2 G). These findings demonstrate that *Gata2* haploinsufficiency perturbs maturation of megakaryocytes, providing an explanation for decreased peripheral platelet numbers observed in *Gata2*$^{+/fl}$*; Vav-iCre*$^{+}$ mice.

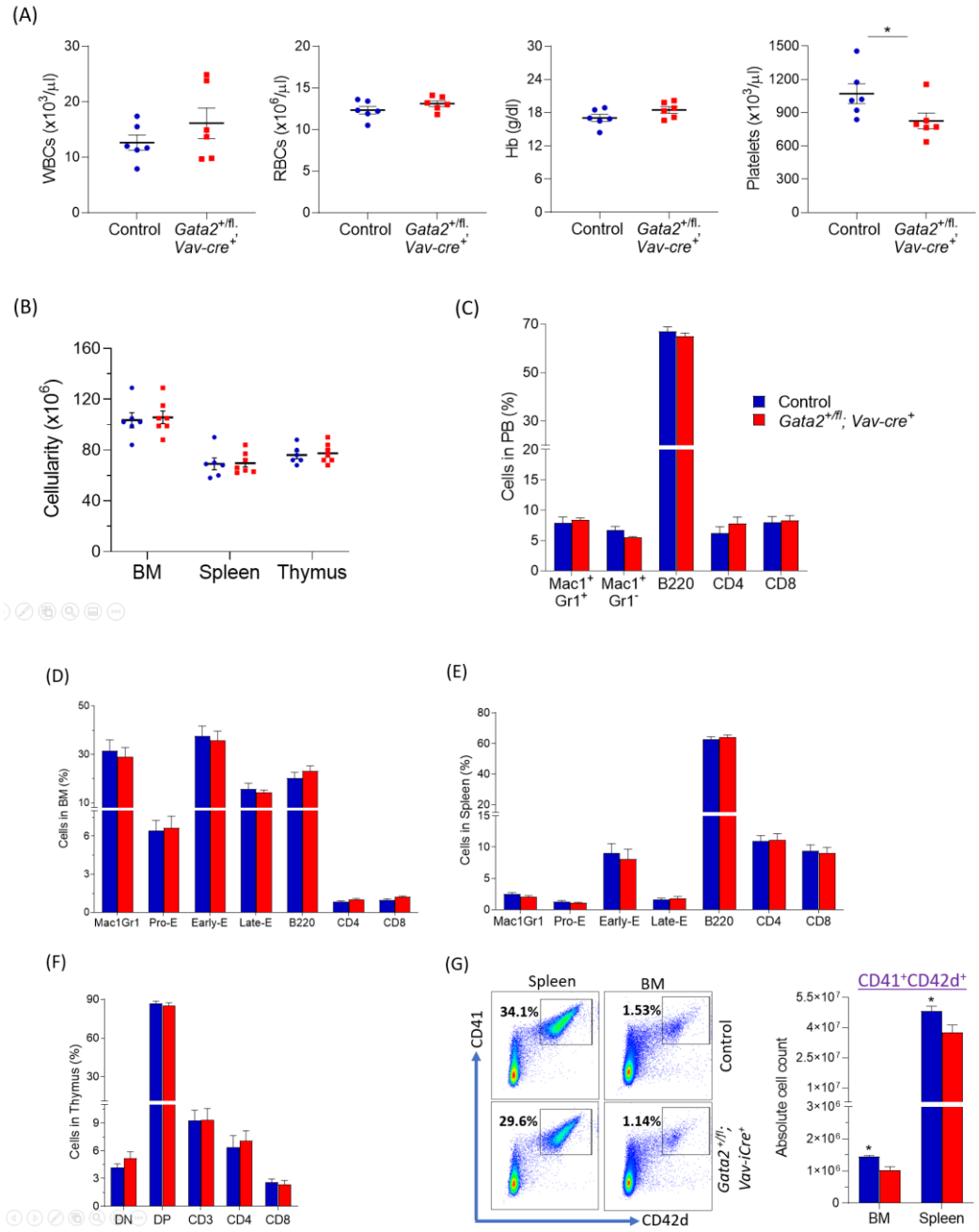

Figure 3-2: Haematopoietic lineage distribution in the PB, BM, spleen, and thymus of *Gata2* haploinsufficient mice.

(A) Absolute numbers of peripheral WBCs, RBC, haemoglobin level, and platelets in control and *Gata2*$^{+/fl}$*; Vav-iCre*$^{+}$ mice. n= 6 per group from two independent experiments. (B) Total cellularity numbers in BM (from two femurs and tibias, (cells/30mL)), spleen (cells/7mL), and thymus (cells/4mL) in control (n=6) and *Gata2*$^{+/fl}$*; Vav-iCre*$^{+}$ (n=7) mice from three independent biological replicates. (C) The frequencies of myeloid (Mac1, Gr1) and lymphoid (B220, CD4, CD8) cells in the PB from control and *Gata2*$^{+/fl}$*; Vav-iCre*$^{+}$ mice. n= 6 for each genotype from three independent experiments. (D, E and F) The percentages of cells in the BM (D), spleen (E), and thymus (F) of control (n=6) and *Gata2*$^{+/fl}$*; Vav-iCre*$^{+}$ (n=7) mice. Data were collected from three independent experiments. Pro-E indicates proerythroblasts (CD71^{+} Ter119 $^{-/low}$); Early-E, early-erythroblasts (CD71^{+}Ter119^{+}); Late-E, late erythroblasts (CD71^{-} Ter119^{+}); DP, CD4^{+}CD8^{+}; and DN, CD4^{-}CD8^{-}. (G) Representative flow cytometric analysis (Left-hand) of the frequency of megakaryocytes (CD41^{+}CD42d^{+}) and absolute numbers (Right) in the BM and spleen from control and *Gata2*$^{+/fl}$*; Vav-iCre*$^{+}$ mice. n= 4 mice per group from a single biological replicate. Presented data are mean ± SEM. Statistical analysis: Mann-Whitney U test *, $P < 0.05$.

3.2.3 *Gata2* haploinsufficiency perturbs cell numbers of myeloid, erythroid, and megakaryocyte progenitors

After observing a reduction in numbers of mature megakaryocytes/platelets in PB/BM/spleen and no difference in the frequencies of myeloid/lymphoid populations in haematopoietic tissues, we next assessed the impact of *Gata2* haploinsufficiency on the frequencies of committed myeloid/lymphoid/erythroid/megakaryocyte progenitors in the BM based on cell surface protein markers. LK (Lin^-_$Sca1^-$_c-Kit^+) cells are comprised from common myeloid (CMP, LK_$CD34^+$_ $CD16/32^-$) and lymphoid (CLP, Lin^-_$Sca1^{low}$_c-Kit^{low}_$CD127^+$) progenitors (Akashi et al., 2000, Kondo et al., 1997). CMPs differentiate to either granulocyte/macrophage (GMP, LK_$CD34^+$_ $CD16/32^+$) or megakaryocyte/erythroid (MEP, LK_$CD34^-$_$CD16/32^-$) restricted progenitors. Flow cytometric analysis showed the frequency of GMPs was significantly reduced in *Gata2$^{+/fl}$; Vav-iCre$^+$* mice, while the proportions of LK, CMPs, MEPs, and CLPs were comparable in both genotypes (Figure 3.3 A). We then used Pronk et al's hierarchy to further analyse myeloid/erythroid/megakaryocyte restricted progenitors (Pronk et al., 2007). In this paradigm, CMPs give rise to either primitive granulocyte/macrophage progenitors (Pre-GM, LK_$CD150^-$_$CD41^-$ _$CD16/32^-$_$CD105^-$) that differentiate into GMPs (LK_$CD150^-$_$CD41^-$_$CD16/32^+$) or primitive erythroid/megakaryocyte progenitors (Pre-MegE, LK_$CD150^+$_$CD41^-$ _$CD16/32^-$_$CD105^-$). Pre-MegE cells segregate into either primitive erythroid forming colonies (Pre-CFU-E, LK_$CD150^+$_$CD41^-$_$CD16/32^-$_$CD105^+$) that differentiate into erythroid forming colonies and pro-erythroblast (CFU-E and Pro-E, LK_$CD150^-$_$CD41^-$ _$CD16/32^-$_$CD105^+$) or megakaryocyte progenitors (MkP, LK_$CD150^+$_$CD41^+$). This study found a significant reduction in the frequencies of Pre-GM, GMP, Pre-MegE, MkP, and Pre-CFU-E in *Gata2$^{+/fl}$; Vav-iCre$^+$* when compared to control mice (Figure 3.3 B). These findings agree with previous studies, in which *Gata2* haploinsufficiency affects GMP numbers (Rodrigues et al., 2005, Rodrigues et al., 2008). In addition, interestingly, *Gata2* haploinsufficiency disrupts early myeloid restricted progenitors (Pre-GM), primitive erythroid (Pre-MegE and Pre-CFU-E), and megakaryocyte progenitors (Pre-MegE and MkP).

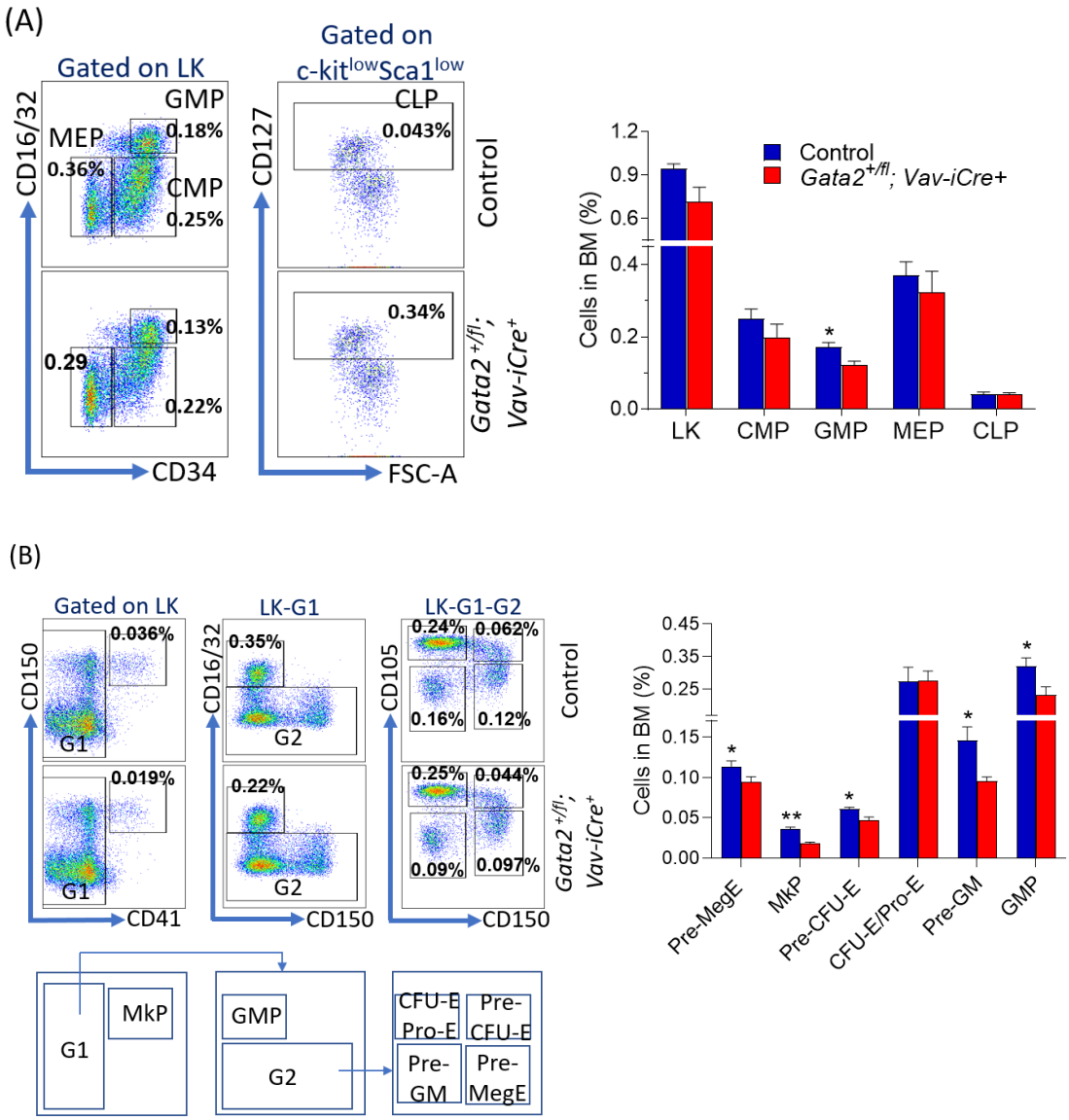

Figure 3-3: Flow cytometric analysis of the BM haematopoietic progenitors in *Gata2$^{+/fl}$; Vav-iCre^{+}* mice.

(A) Representative immunophenotypic analysis (Left-hand) and the frequencies (Right) of committed myeloid/lymphoid/erythroid/megakaryocyte progenitors (LK, CMP, GMP, MEP, and CLP) of control (n=6) and *Gata2$^{+/fl}$; Vav-iCre^{+}* (n=7) mice from three independent experiments. (B) Representative FACS plots (Left-hand) and gating strategy (Left-bottom) and the percentages of myeloid (Pre-GM, GMP), erythroid (Pre-MegE, Pre-CFU-E), and megakaryocyte (Pre-MegE, MkP) progenitors in the BM of control (n=6) and *Gata2$^{+/fl}$; Vav-iCre^{+}* (n=6) mice from two independent experiments. Data represent mean ± SEM. Statistical analysis: Mann-Whitney U test *, $P < 0.05$; **, $P < 0.01$.

3.2.4 *Gata2* haploinsufficient mice exhibit a reduction in the number of BM CFU-GM progenitors

In vitro CFC assays were performed to examine the functional ability of BM progenitor cells from *Gata2*$^{+/fl}$*; Vav-iCre*$^{+}$ mice to proliferate and differentiate to restricted haematopoietic progenitors. BM cells were plated in M3434 media, which promotes myeloid-erythroid cell differentiation, and M3630, a specific media for primitive B-cells differentiation. The total numbers of myeloid-erythroid colonies were comparable in *Gata2*$^{+/fl}$*; Vav-iCre*$^{+}$ and control mice (Figure 3.4 A). However, there was a significant reduction in the number of CFU-GM colonies of *Gata2*$^{+/fl}$*; Vav-iCre*$^{+}$ when compared to control mice, while the numbers of CFU-GEMM, BFU-E, CFU-M and CFU-G, CFU-PreB colonies were comparable in both littermates (Figure 3.4 A and B). These data confirm previous studies in germline *Gata2* heterozygote models and indicate that the number of CFC-GM colonies is specifically reduced in *Gata2* haploinsufficiency mice without impact on other haematopoietic progenitor fates (Rodrigues et al., 2008).

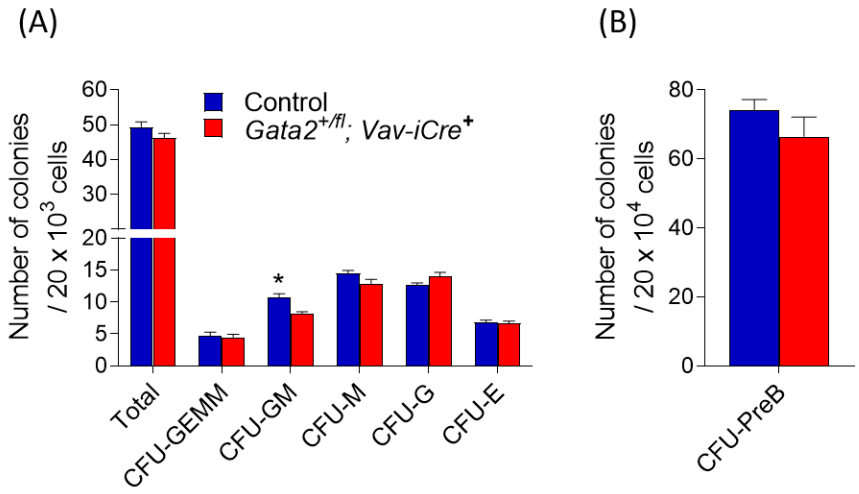

Figure 3-4: CFC assays of total BM cells from *Gata2* haploinsufficient mice.
(A) 20x10^3 BM cells of Gata2$^{+/fl}$; Vav-Cre^{+} and control mice were plated in M3434 semisolid methylcellulose media containing SCF, IL-3, IL-6 and Epo, and colonies were counted after 12 days. n= 6 mice for each genotype from three independent experiments. (B) 20x10^4 BM cells were plated in M36330 media supplemented with IL-7 from *Gata2*$^{+/fl}$*; Vav-Cre*$^{+}$ and control mice, and colonies scored 7days after plating. n= 4 per group from two independent biological replicates. CFU indicates Colony-Forming-Unit; CFU-GEMM, CFU Granulocyte_Erythrocyte_ Macrophage_Megakaryocyte; CFU-E, CFU_Erythroid; CFU-GM, CFU Granulocyte_ Macrophage; CFU-M, CFU Macrophage; and CFU-G, CFU Granulocyte. Presented data are mean ± SEM. Statistical analysis: Mann-Whitney U test *, $P < 0.05$.

3.2.5 Primitive HSPCs are perturbed in young *Gata2* haploinsufficient mice

To assess if the alteration in lineage-specific haematopoietic progenitors was caused by a disruption in the frequencies of primitive BM haematopoietic stem and progenitor cells (HSPCs) in *Gata2* haploinsufficient mice, we analysed the HSPC compartment by flow cytometry. LSK (Lin^-_$Sca\text{-}1^+$_$c\text{-}Kit^+$) and SLAM markers (CD150 and CD48) were used to dissect HSPC compartments as follows: HSC, LSK_$CD150^+$_$CD48^-$; HPC1, LSK_$CD150^-$_$CD48^+$; HPC2, LSK_ $CD150^+$_$CD48^+$; and MPP, LSK_$CD150^-$_$CD48^-$ (Oguro et al., 2013, Kiel et al., 2005). HPC1 progenitors differentiate into lymphoid/myeloid restricted progenitors and are incapable of advancing to megakaryocytes/ erythrocytes, whereas HPC2 cells are able to differentiate to all restricted haematopoietic progenitors (Oguro et al., 2013). Immunophenotypic analysis revealed that the frequencies of LSK, HSCs, MPPs and HPC1 were significantly reduced in BM from *Gata2*$^{+/fl}$*; Vav-iCre*$^+$ when compared to control mice, whereas the proportion of HPC2 was increased at p=0.06 level in *Gata2*$^{+/fl}$*; Vav-iCre*$^+$ as compared with control littermates, suggestive of a differentiation block and progenitor accumulation at the level of HPC2 (Figure 3.5 A).

Akashi's laboratory has suggested an alternative haematopoietic differentiation hierarchy, in which HSCs give rise into LMPPs (LSK_$CD135^{hi}$_$CD34^+$), that possess lymphoid/myeloid potential, and a re-defined primitive CMP (LSK_$CD34^+$_$CD41^{hi}$), which has the potency to differentiate into myeloid/erythroid/megakaryocyte lineages (Miyawaki et al., 2015). Immunophenotypic analysis revealed a significant reduction in BM numbers of both LMPPs and $CD41^+$CMP in *Gata2*$^{+/fl}$*; Vav-iCre*$^+$ as compared to control mice (Figure 3.5 B).

Since HPC1, HPC2, $CD41^+$CMP are heterogeneous committed progenitors, we resolved this heterogeneity using another hierarchical model that distinguishes between myeloid/lymphoid-biased progenitors (Pietras et al., 2015). HSPCs were sub-divided into five compartments using CD135 and slam markers as follows: LT-HSCs, LSK_$Flt3^-$_$CD150^+$_$CD48^-$; ST-HSCs (MPP1), LSK_$Flt3^-$_$CD150^-$_$CD48^-$; MPP2, megakaryocyte/erythrocyte-biased-MPPs (LSK_$Flt3^-$_$CD150^+$_$CD48^+$); MPP3, GMP-biased-MPPs (LSK_$Flt3^-$_$CD150^-$_$CD48^+$); and MPP4, lymphoid/GMP-biased-MPPs

LSK_Flt3^{+}_CD150^{-}_CD48^{+}. The proportions of BM LT-HSC, ST-HSCs, and MPP4 were significantly reduced in *Gata2$^{+/fl}$; Vav-iCre^{+}* mice, while a significant increase in the frequency of MPP2 was observed in *Gata2$^{+/fl}$; Vav-iCre^{+}* as compared with control littermates (Figure 3.6). In agreement with previous data, HSC numbers were reduced in *Gata2* haploinsufficient mice (Rodrigues et al., 2005, Guo et al., 2013). Additionally, these data suggest that *Gata2* haploinsufficiency perturbs the abundance of select adult primitive HSPCs homeostasis including stage-specific effects in MPPs (accumulation of MPP2 and reduction MPP4) as well as differentiation blocks in HPC1, HPC2, LMPPs, and CD41^{+}CMP.

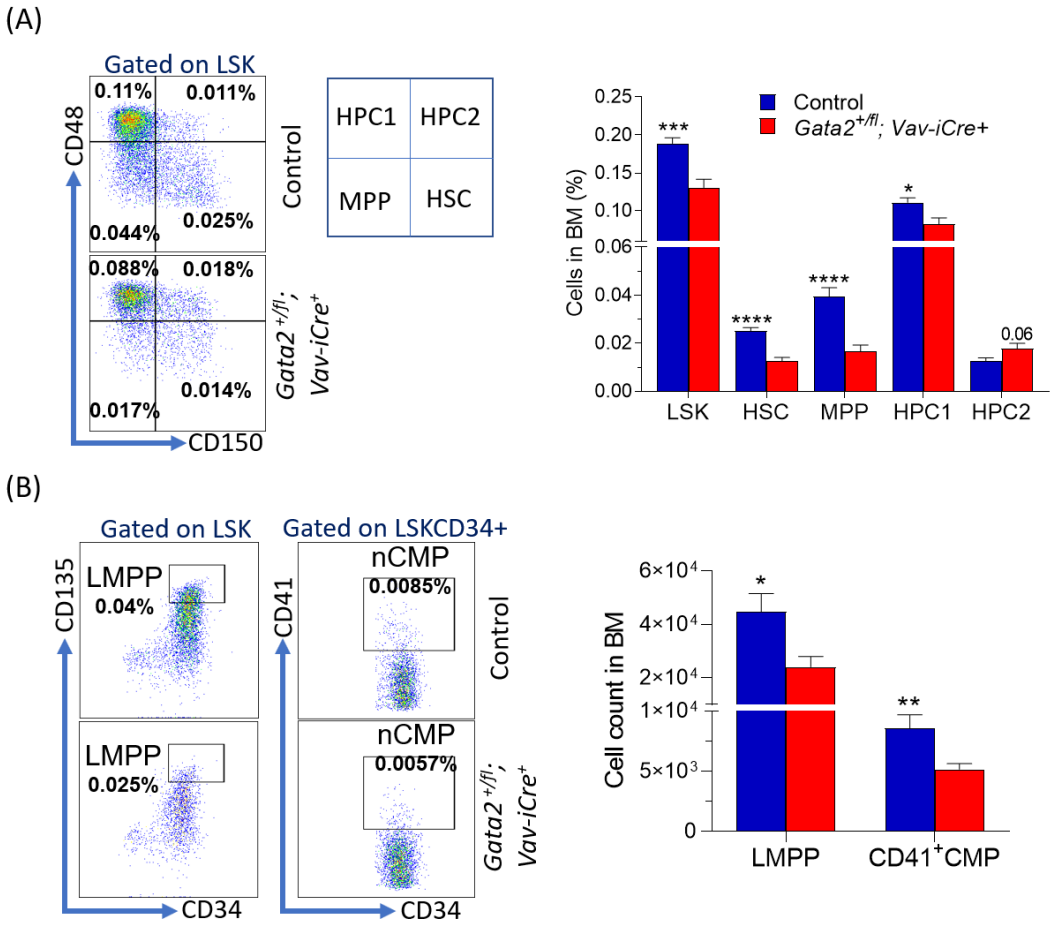

Figure 3-5: Primitive HSPCs are perturbed in young *Gata2* haploinsufficient mice.
(A) Representative immunophenotypic analysis (Lift-hand), gating strategy (Middle) and the frequencies of primitive HSPC compartments (Right) including LSK, HSCs, MPPs, HPC1, and HPC2 in the BM of control (n=9) and *Gata2$^{+/fl}$; Vav-iCre^{+}* (n=10) mice from four independent experiments. Statistical analysis: unpaired, 2-tailed t-test. (B) Representative FACS plots analysis (Left-hand) and absolute numbers (Right) of BM LMPP (n=8 per genotype) and CD41^{+}CMPs (n=6 for each group) from control and *Gata2$^{+/fl}$; Vav-iCre^{+}* mice from two or three separate experiments. Data represent mean ± SEM. Statistical analysis: Mann-Whitney U test *, P < 0.05; **, P < 0.01; ***, P < 0.001; ****, P < 0.0001.

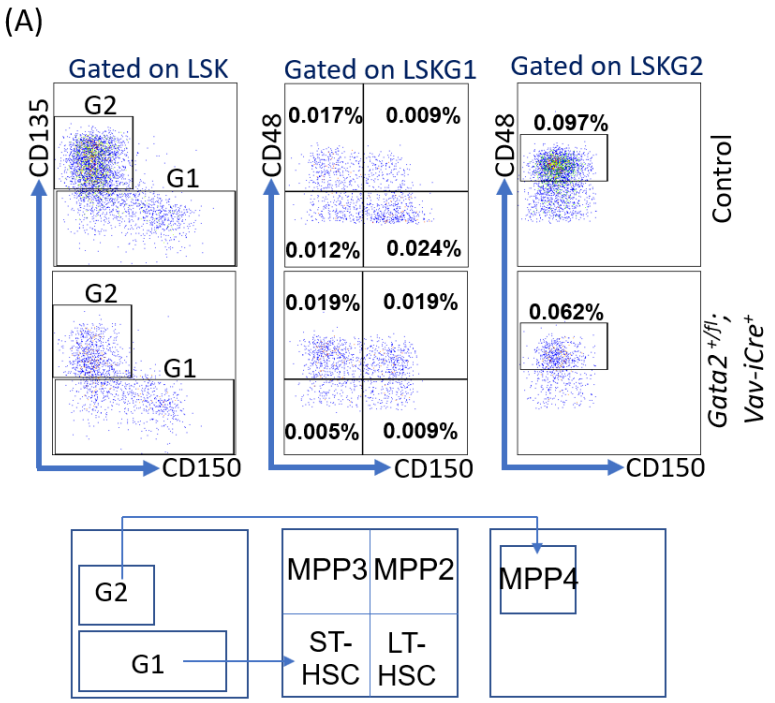

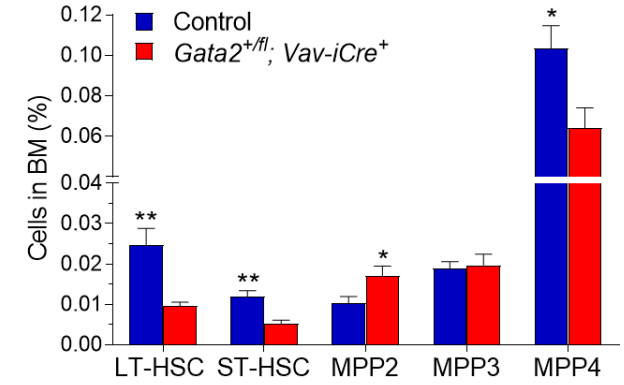

Figure 3-6: *Gata2* haploinsufficiency perturbs adult MPP compartments.
(A and B) Representative FlowJo plots (A), gating methods (A-bottom) and percentages (B) of BM LT-HSCs, ST-HSCs, MPP2, MPP3, and MPP4 from control and *Gata2*$^{+/fl}$*; Vav-iCre*$^{+}$ littermates. n= 6 for each genotype from two independent experiments. Presented data are mean ± SEM. Statistical analysis: Mann-Whitney U test *, $P < 0.05$; **, $P < 0.01$.

3.2.6 Increased apoptosis level in HSPCs of *Gata2* haploinsufficient mice

The preceding data demonstrate *Gata2* haploinsufficiency disrupts the distribution of HSPC compartments. To assess whether differential cell survival was a possible mechanism by which the abundance of HSPCs in *Gata2* haploinsufficiency mice was altered, we conducted annexin V assays. Flow cytometry analysis demonstrated a significant increase in the frequency of total (early plus late) apoptosis in HSCs and MPPs in the BM of *Gata2*$^{+/fl}$*; Vav-iCre*$^{+}$ mice when compared with control mice. There also was an insignificant increase in total apoptosis of HPC1 cells in *Gata2*$^{+/fl}$*; Vav-iCre*$^{+}$ mice. No differences of total apoptosis of LK, LSK, HPC2, CMP, GMP, and CLP were observed in both littermates, suggesting that specific *Gata2* mediated alterations in the abundance of these populations are independent of apoptotic mechanisms (Figure 3.7). These data confirm the association between the reduction of HSC numbers and increased HSCs apoptosis level (Rodrigues et al., 2005, de Pater et al., 2013).

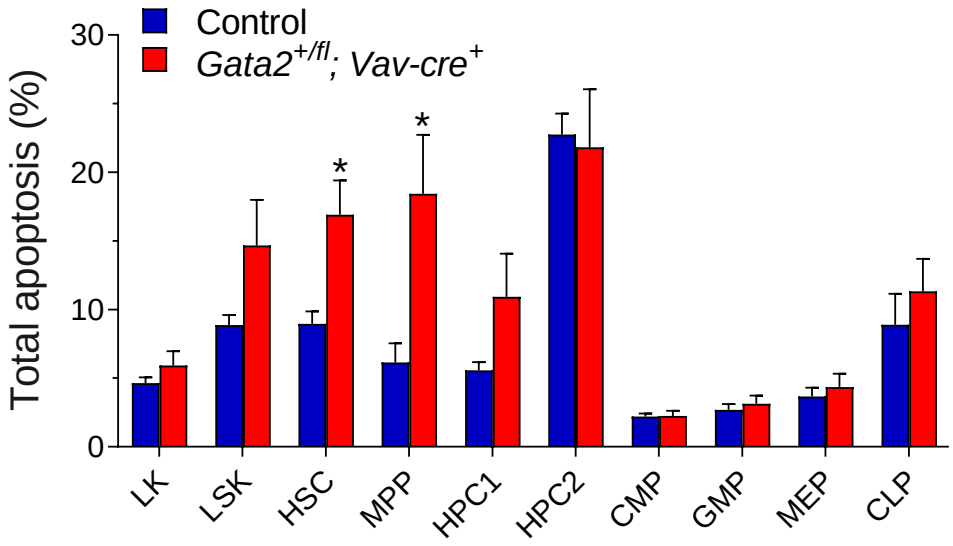

Figure 3-7: Increased apoptosis level in HSPCs of *Gata2* haploinsufficient mice.
The bar chart represents the percentages of apoptotic cells in the BM of control and *Gata2*$^{+/fl}$*; Vav-iCre*$^{+}$ mice. n=6 mice for each genotype from three independent experiments. Annexin V and DAPI were used to stain BM compartments as follows: live, annexin V^{-} DAPI^{-}; early, annexin V^{+} DAPI^{-}; late, annexin V^{+} DAPI^{+}; and necrosis, annexin V^{-} DAPI^{+}. Data represent mean ± SEM. Statistical analysis: Mann-Whitney U test *, $P < 0.05$.

3.2.7 Increased HSCs quiescence in *Gata2* haploinsufficient mice

This study next assessed whether the reduction of HSCs pool in *Gata2*$^{+/fl}$*; Vav-iCre*$^{+}$ mice was also correlated with the cell cycle alterations. The cell cycle status of primitive haematopoietic compartments was evaluated using ki-67 assays. The Ki-67 protein, a nuclear proliferation marker, is highly expressed in G1/G2/M phases compared to G0 phase (Gerdes et al., 1984). The frequency of HSCs in G0 phase was increased in *Gata2*$^{+/fl}$*; Vav-iCre*$^{+}$ when compared to control mice, while the frequencies of MPP, HPC1, HPC2, and GMP cells in G0, G1, and S/G2/M phases were comparable in both littermates (Figure 3.8 A, B, C, and D). These results are in agreement with previous findings, in which GATA2 acts as an indispensable regulator for HSC quiescence (Rodrigues et al., 2005, Tipping et al., 2009).

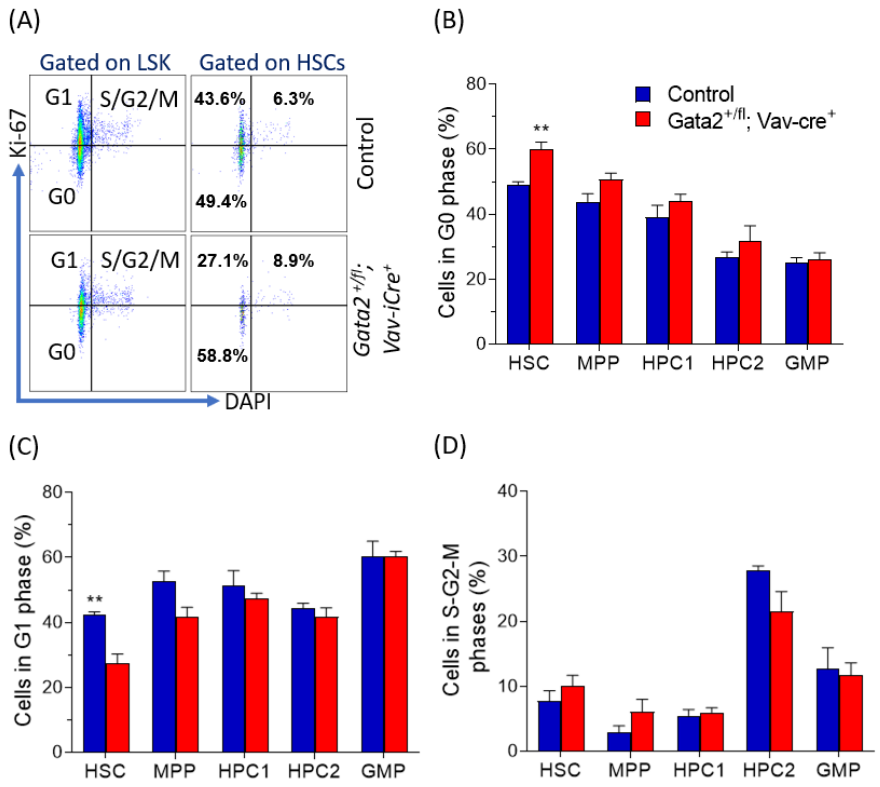

Figure 3-8: Increased HSCs quiescence in *Gata2* haploinsufficient mice.
(A, B, C, and D) Immunophenotypic analysis (A) and percentages of primitive BM cells in G0 phase (B), G1 phase (C), and S-G2-M phases (D) of the cell cycle from control and *Gata2*$^{+/fl}$*; Vav-iCre*$^{+}$ mice. n= 6 per genotype from three independent experiments. Three subpopulations can be recognised using ki-67 and DAPI staining: G0-phase, ki-67^{-} DAPI^{-}; G1-phase, ki-67^{+} DAPI^{-}; and S/G2/M phases, ki-67^{+} DAPI^{+}. Presented data are mean ± SEM. Statistical analysis: Mann-Whitney U test *, $P < 0.05$; **, $P < 0.01$.

3.2.8 *Gata2* haploinsufficient HSCs exhibit a defect in the multi-lineage repopulating potential

In vivo BM transplantation assay is a stringent manner to study HSCs functionality. Transplantation assay is a proliferative stress assay including the transplant of donor cells into lethally irradiated recipient mice to assess the ability of HSCs to differentiate and reconstitute all haematopoietic cell types (Cheng et al., 2013, Harrison et al., 1993, Allsopp et al., 2001). In the first few weeks post-transplantation, the rescue of recipients from death is mediated by multipotent progenitors (MPPs) until fully long-term HSCs reconstituting by week 8 post-transplantation, and HSCs preserve reconstituting for all lineages for more than 16 weeks after transplantation (Cheng et al., 2013, Harrison et al., 1993, Allsopp et al., 2001, Pietras et al., 2015). MPPs firstly rebuild myeloid-cells within the first two weeks after transplant, and lymphoid-cells emerge later, by week 3-4 (Pietras et al., 2015). Serial transplant of HSCs from primary recipients to new irradiated hosts is commonly applied as a measure of HSC self-renewal potential (Cheng et al., 2013, Harrison et al., 1993, Allsopp et al., 2001, Seita and Weissman, 2010). Competitive BM transplantation is used to support reconstitution of recipient mice by co-transplant of donor cells with support (competitor) cells (Cheng et al., 2013, Mercier et al., 2016). Congenic mouse models can be used to distinguish between donor and competitor cell engraftment (Cheng et al., 2013, Mercier et al., 2016). These mice are genetically matching and differ only at the expression of CD45 alleles (CD45.1 and CD45.2).

To stringently assess HSC and progenitor functions, competitive transplantation experiments were performed to test the ability of HSCs for multi-lineage repopulating potential *in vivo*. CD45.2 HSCs were isolated by FACS from either *Gata2*$^{+/fl}$*; Vav-iCre*$^{+}$ or control mice and mixed with competitor BM cells from CD45.1 mice and injected intravenously into irradiated recipient mice (CD45.1) (Figure 3.9 A). PB of recipient mice was assessed at 4, 8, 12, and 16 weeks post-transplant, and BM, spleen, and thymus cells were harvested and analysed at week 16 after-transplantation to test the donor contributions for haematopoietic multi-lineage.
Analysis of PB revealed that the percentages of CD45.2 cells in *Gata2*$^{+/fl}$*; Vav-iCre*$^{+}$ derived cells were significantly decreased as compared to control derived cells, and

this reduction started at week 8 through week 16 (Figure 3.9 B). The frequencies of the donor contribution of *Gata2*$^{+/fl}$*; Vav-iCre*$^{+}$ transplant cells for myeloid (Mac1 and Gr1), T-cell (CD4 and CD8) and B-cell (B220) in PB were reduced at week 16 post-transplantation (Figure 3.9 C). At week 16 post-transplant, we also assessed multilineage reconstitution in BM, spleen, and thymus. These haematopoietic tissues displayed chimerism of CD45.2 *Gata2*$^{+/fl}$*; Vav-iCre*$^{+}$ cells in myeloid, erythroid, T-cell and B-cell lineages that was significantly decreased when compared to control transplant cells (Figure 3.10 A, B and C). Furthermore, we analysed the donor contribution for primitive and committed haematopoietic compartments, and there was a significant reduction in the percentages of *Gata2* haploinsufficient HSCs donor cells for HSPCs (LSK, HSC, MPPs, HPC1, and HPC2, committed/myeloid-progenitors (LK, CMPs, GMPs and MEPs) and committed/lymphoid-progenitors (CLPs) in the BM as compared to control donor cells (Figure 3.10 D). These data are consistent with the previous findings and signify that *Gata2* haploinsufficient HSCs lack competence for multi-lineage repopulation *in vivo* (Ling et al., 2004, Rodrigues et al., 2005).

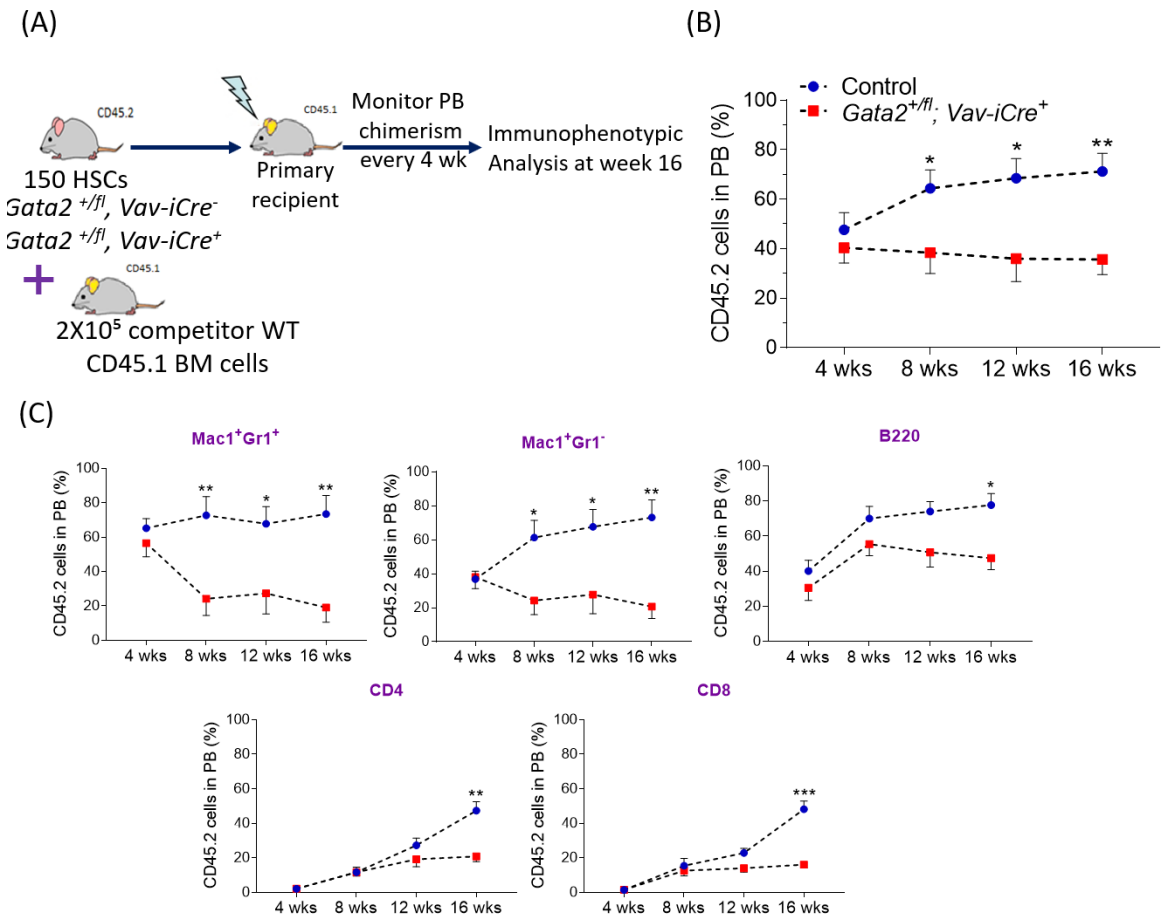

Figure 3-9: *Gata2* haploinsufficient HSCs exhibit a defect in the multi-lineage repopulating potential in PB.

(A) Experimental design for primary HSCs transplant, 150 HSCs from either 45.2$^+$ *Gata2$^{+/fl}$; Vav-iCre$^+$* or *Gata2$^{+/fl}$; Vav-iCre$^-$* (control) mice alongside 2x10^5 support CD45.1$^+$ BM cells transplanted into lethally irradiated CD45.1$^+$ recipient mice. PB was monthly assessed for the donor chimerism. (B and C) Proportions of total CD45.2 cells at 4 weeks basis (B) and donor contribution (C) for myeloid (Mac1$^+$Gr1$^+$, Mac1$^+$Gr1$^-$), B-lymphoid (B220$^+$), and T-lymphoid (CD4$^+$, CD8$^+$) in PB in primary recipients for 16 weeks post-transplantation of *Gata2$^{+/fl}$; Vav-iCre$^+$* or control derived cells. n=8 mice for each group from three independent experiments. Five independent biological donors were used for each genotype. Data represent mean ± SEM. Statistical analysis: Mann-Whitney U test *, P < 0.05; **, P < 0.01; ***, P < 0.001.

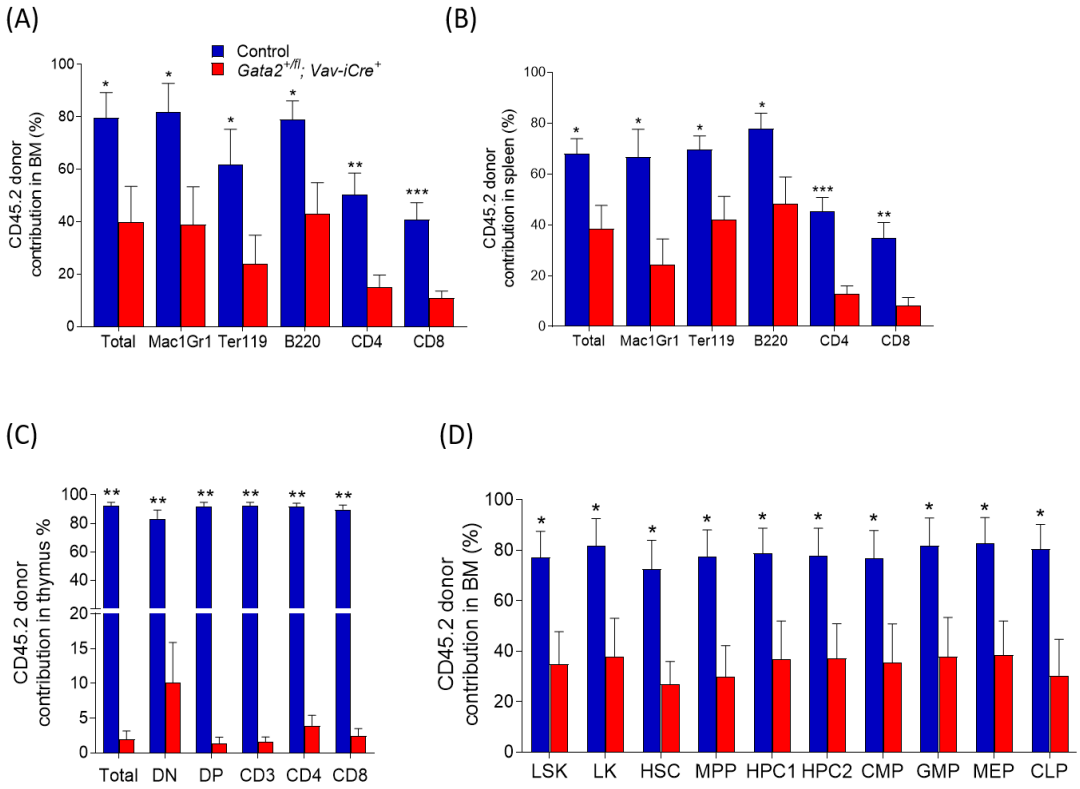

Figure 3-10: *Gata2* haploinsufficient HSCs show a defect in the multi-lineage reconstituting potential in BM, spleen, and thymus.

(A and B) Percentages of total CD45.2 cells and donor contribution in BM (A) and spleen (B) for Myeloid-cells, Mac1$^+$Gr1$^+$; Erythroid-cells, Ter119$^+$; T-cell, CD4$^+$ and CD8$^+$; and B-cells, B220$^+$) at week 16 after transplantation of *Gata2*$^{+/fl}$*; Vav-iCre*$^+$ (n=8) or control (n=8) derived cells from 3 separate experiments. (C) Proportions of total CD45.2 cells and donor contribution in thymus from *Gata2*$^{+/fl}$*; Vav-iCre*$^+$ (n=6) or control (n=6) derived cells from 3 separate experiments. DP indicates CD4$^+$CD8$^+$; and DN, CD4$^-$CD8$^-$. (D) Frequencies of *Gata2*$^{+/fl}$*; Vav-iCre* and control donor contribution cells to HSPCs (LSK, HSCs, MPPs, HPC1 and HPC2) and committed/myeloid-lymphoid progenitors (LK, CMPs, GMPs, MEPs, and CLPs) in BM. n= 8 mice for each genotype. Data were collected from three independent experiments. Five separate donors were used for each genotype. Presented data are mean ± SEM. Statistical analysis: Mann-Whitney U test *, $P < 0.05$; **, $P < 0.01$; ***, $P < 0.001$.

3.2.9 *Gata2* haploinsufficient HSCs show defective self-renewal potential

Serial transplantation is the ideal experiment to examine the self-renewal capability of HSCs (Harrison et al., 1993, Cheng et al., 2013, Seita and Weissman, 2010, Allsopp et al., 2001). This study then assessed the self-renewal potential of *Gata2* haploinsufficient HSCs in serial transplant experiments. At week 16 post-primary transplantation, purified HSCs of *Gata2*$^{+/fl}$*; Vav-iCre*$^{+}$ or control (CD45.2 cells) from primary recipients were mixed with competitor BM cells (CD45.1 cells) and subsequently re-transplanted to lethally irradiated secondary recipient mice (CD45.1 background) (Figure 3.11 A). The donor (CD45.2) derived cells were observed at 2, 4, 8, 12, 16, and 20 weeks in PB. CD45.2 donor contribution cells in BM, spleen and thymus cells were analysed at week 20 post-transplantation. The follow-up of chimerism in PB showed that the percentages of CD45.2 *Gata2*$^{+/fl}$*; Vav-iCre*$^{+}$ donor cells were severely reduced when compared to control donor cells, and the dropping was started at week 2 throughout week 20 post-transplantation (Figure 3.11 B). This observation was extended to BM and extramedullary haematopoietic tissues as spleen and thymus (Figure 3.11 C) in CD45.2 *Gata2*$^{+/fl}$*; Vav-iCre*$^{+}$ donor cells. These results indicate that adult *Gata2* haploinsufficient HSCs are unable of reconstituting secondary recipients in serial transplantation experiments and revealing that *Gata2* haploinsufficiency impacts HSC self-renewal. Together with a defect in the multi-lineage repopulating potential that observed in the primary transplantation experiments, these data provide essential insights into the role of *Gata2* in the adult HSCs self-renewal and differentiation potential.

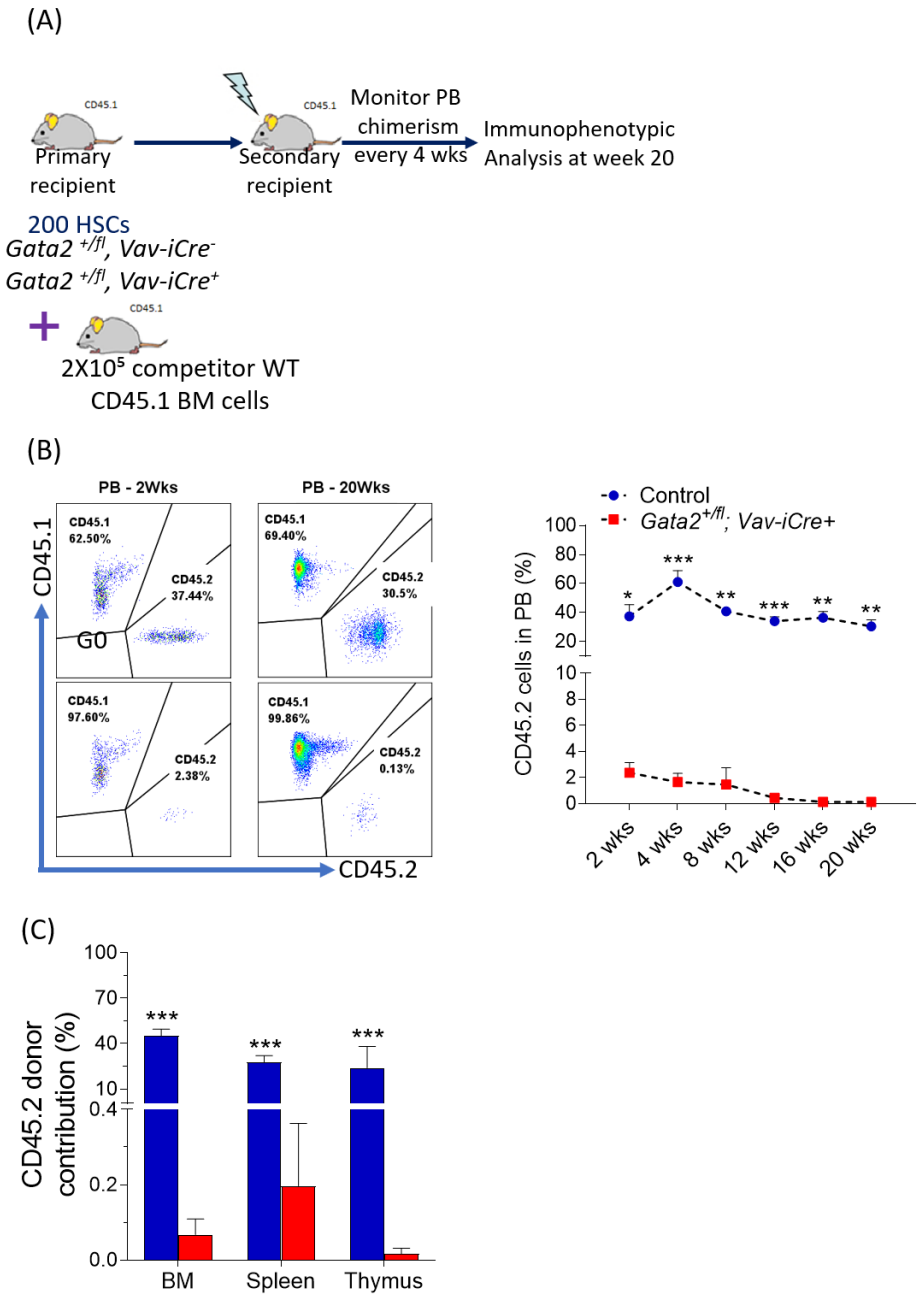

Figure 3-11: *Gata2* haploinsufficient HSCs show a defect in self-renewal potential

(A) Experimental design for secondary transplant experiments, 200 CD45.2 HSCs from either *Gata2*$^{+/fl}$*; Vav-iCre*$^{+}$ or control derived cells from primary recipient mice alongside 2x10^{5} support BM cells transplanted into lethally irradiated secondary CD45.1 recipient-hosts. (B) Representative FACS plots (Left-hand) for the donor contribution (CD45.1 and CD45.2) in PB of Gata2$^{+/fl}$; Vav-Cre^{+} and control (*Gata2*$^{+/fl}$*; Vav-Cre*$^{-}$) transplant cells at week 2 and week 20 post-transplant. Proportions of CD45.2 cells (Right) in PB at 2, 4, 8, 12, 16, 20 weeks after-transplant from *Gata2*$^{+/fl}$*; Vav-Cre*$^{+}$ and control donor cells. (C) Frequencies of CD45.2 cells in BM, spleen, and thymus at week 20 after transplantation of *Gata2*$^{+/fl}$*; Vav-Cre*$^{+}$ and control derived cells. n= 7 mice for each genotype for all experiments. Data were collected from two independent experiments using 3-4 independent biological donors for each genotype. Data represent mean ± SEM. Statistical analysis: Mann-Whitney U test *, P < 0.05; **, P < 0.01; ***, P < 0.001.

3.2.10 Transcriptional signatures associated with *Gata2*$^{+/fl}$*; Vav-iCre* HSCs

To provide insight into the transcriptional mechanisms associated with *Gata2* haploinsufficiency in HSPC compartments, we conducted RNA-Sequencing (RNA-Seq) of purified HSCs (LSK_CD150^{+}CD48^{-}) from both *Gata2*$^{+/fl}$*; Vav-iCre*$^{+}$ and control mice. RNA-Seq data identified that 117 differentially dysregulated genes were identified in *Gata2* haploinsufficient HSCs relative to control HSCs using DEseq2 computing-software based on FDR values (less than 0.05), in which 74 genes were down-regulated and 43 genes were up-regulated (Figure 3.12 A).

Gene ontology (GO) analysis was performed for dysregulated genes to assess molecular and biological functions in *Gata2* haploinsufficient HSCs using Ingenuity Pathway Analysis (IPA) software. IPA analysis indicated that significant genes were associated with cell death and survival, cellular development, cellular proliferation, haematological system development and function, lymphoid tissues development, humoral immune response, immune cell trafficking, cellular morphology, cellular movement, and cell-to-cell signalling and interaction (Figure 3.12 B). Using Ingenuity Canonical Pathway (ICP) and Gene Set Enrichment Analysis (GSEA) Molecular Signatures Database (MSigDB, hallmark gene-sets and C2-curated gene-sets), we also assessed the potential biological pathways that were affected in *Gata2* haploinsufficient HSCs. Several biological pathways were affected in *Gata2* haploinsufficient HSCs such as DNA repair pathways (dsDNA-break repair by homologous recombination and base-excision repair (BER)), cellular immune response pathways (Toll-like receptor signalling, IL-10 signalling, and agranulocyte adhesion/diapedesis), metabolic processes (serotonin degradation), and extracellular matrix components (Glycosaminoglycan-protein biosynthesis and inhibition of matrix metalloproteases) (Figure 3.12 C).

For unbiased analysis, we further performed GSEA to identify biological pathways that were enriched in *Gata2* haploinsufficient HSCs. GSEA analysis revealed that up-regulated genes were enriched in *Gata2* haploinsufficient HSCs for the DNA repair response and IFNy signalling (Figure 3.12 D). IPA was used to identify IFNy target genes that are involved in the recruitment of macrophages including *Ccr1*, *Csf1r*,

Cd23, *Hcar2*, Il1rn, and *Pecam1*. Consistent with the known function of *Gata2* as a regulator of HSPCs development and survival, differentially significant genes were involved in B-lymphopoiesis, accumulation and migration of myeloid cells, cellular survival, cell cycle regulations and DNA repair, and haematological malignancies (Figure 3.13). Furthermore, *Gata2* appears to transcriptionally regulate cellular polarity through actin cytoskeletal organisation and cell adhesion genes that maintain cellular construction and homeostasis (Figure 3.12 C and Figure 3.13).

In summary, in accordance with GATA2 haploinsufficiency syndromes that underlie primary immunodeficiency disorders (Vinh et al., 2010, Dickinson et al., 2011, Bigley et al., 2011, Ostergaard et al., 2011), these results provide new insights into cellular immune response pathways such as IFNy signalling, humoral immune response, Toll-like receptor signalling, IL-10 signalling, immune cell trafficking, and agranulocyte adhesion/diapedesis (Figure 3.12 B, C, and D). In addition, these data suggest that *Gata2* transcriptionally regulates genes involved in the DNA damage response and DNA repair pathways (Figure 3.12 C and D, and Figure 3.13).

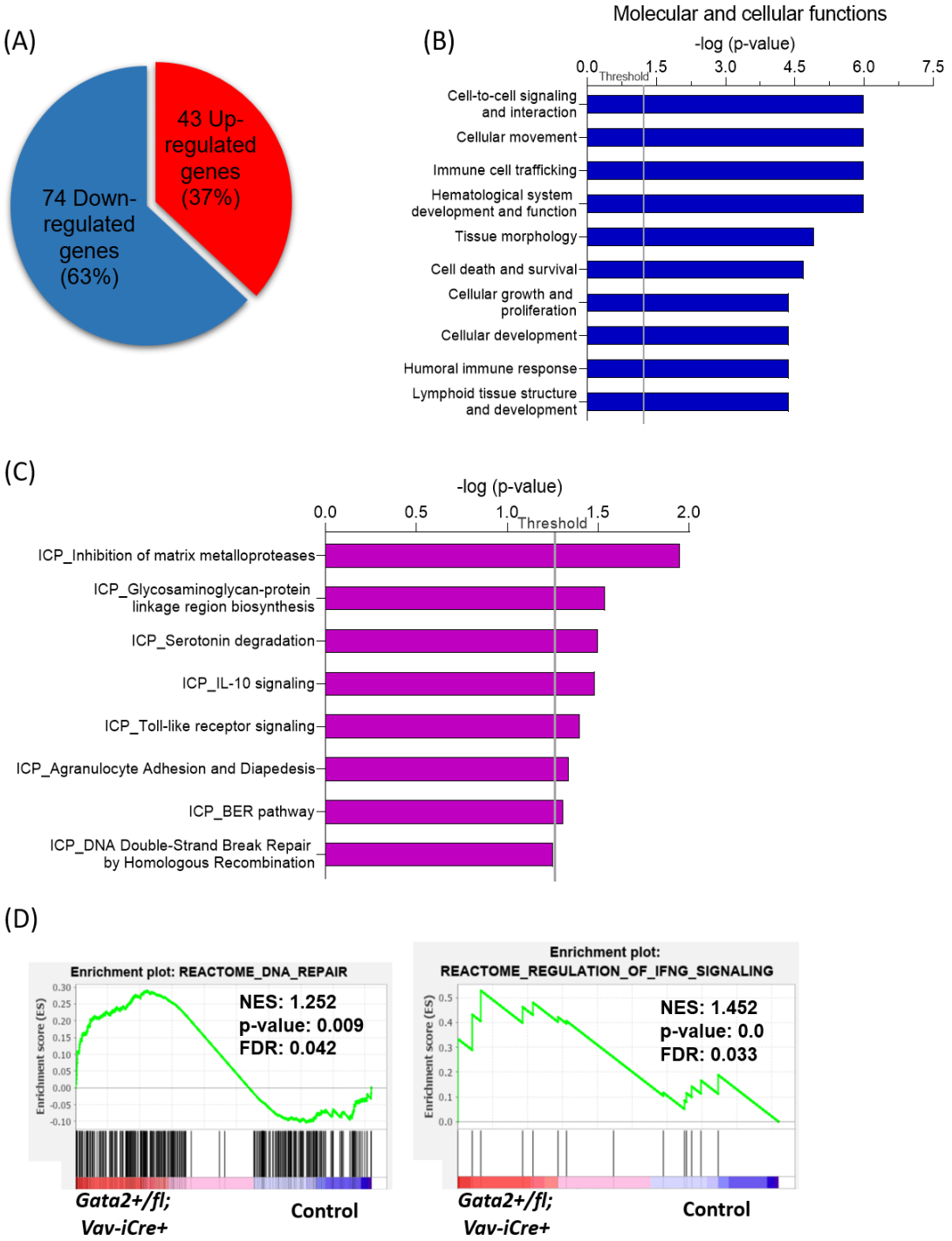

Figure 3-12: Transcriptional signatures associated with *Gata2* haploinsufficient HSCs.
(A) The Venn diagram illustrates significant numbers of differentially dysregulated genes in purified HSCs from *Gata2*$^{+/fl}$*; Vav-iCre*$^{+}$ (n=4) mice as compared to control HSCs (n=4). DEseq2 computing-software was used to identify significant differentially deregulated genes at p-values and FDR-values <0.05 level. (B and C) biological and molecular processes (B) and biological pathways (C) for differentially expressed genes in *Gata2* haploinsufficient HSCs. Given data are presented as $-\log_{10}$ (p-value), and the threshold in the grey colour indicates p-value at 0.05. enriched pathways are determined by Fischer's Exact Test. (D) GSEA plots show enriched pathways for up-regulated genes in *Gata2* haploinsufficient HSCs. Statistical significance is determined by p-values and FDR-values at <0.05 level. NES indicates normalised enrichment score.

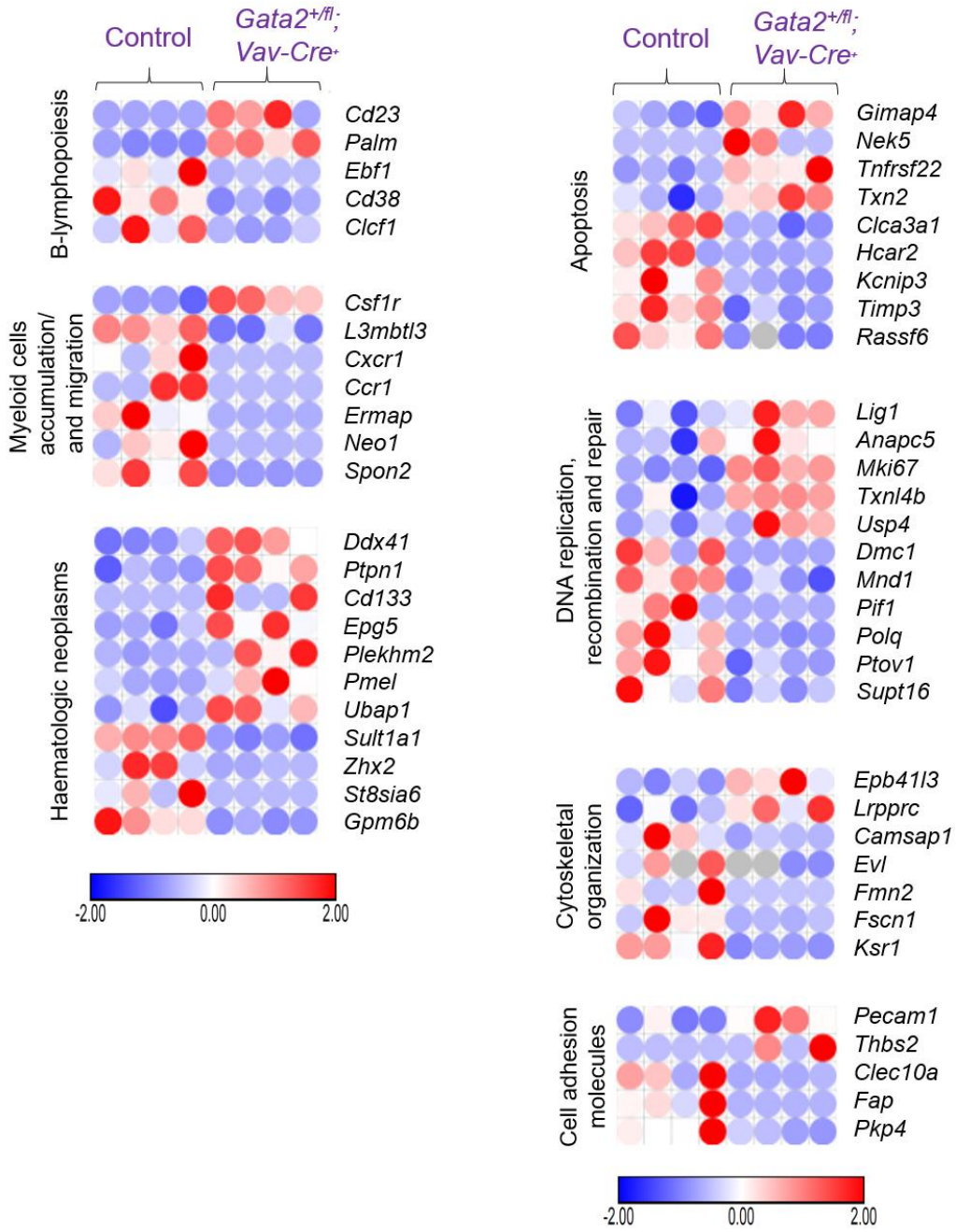

Figure 3-13: Differentially dysregulated genes in *Gata2* haploinsufficient HSCs.
Heat maps of the differentially significant genes in *Gata2* Haploinsufficient HSCs (n=4) compared to control HSCs (n=4). Heat maps are drawn by Morpheus online software showing a Z-score scale. The red colour indicates up-regulated genes; and blue colour, down-regulated genes. The colour gradient represents the intensity of gene expression.

3.2.11 Increased DNA damage response in *Gata2* haploinsufficient HSCs

After observing the upregulation of DNA repair pathways in RNA-seq, this study next validated the DNA damage response in *Gata2* haploinsufficient HSPCs using γH2AX assay. The γH2AX protein, a DNA damage biomarker, is a member of histone H2A family and is phosphorylated at Ser139 following double-stranded DNA breaks and accumulates at locations of the DNA damage to recruit DNA-damage response proteins (Mah et al., 2010). Flow cytometric analysis displayed a significant increase in median fluorescent intensity (MFI) of γH2AX was observed in BM HSPCs and HSCs in *Gata2*$^{+/fl}$*; Vav-iCre*$^{+}$ as compared to control mice (Figure 3.14). Accumulation of the DNA damage and inappropriate DNA damage repair processes affect the normal function of HSCs and positively correlate with human haematological disorders (Biechonski et al., 2017, Mohrin et al., 2010). These results provide crucial insights into the role of *Gata2* in sustaining adult HSC functions and suggest that *Gata2* haploinsufficiency promotes the DNA damage within HSPC compartments.

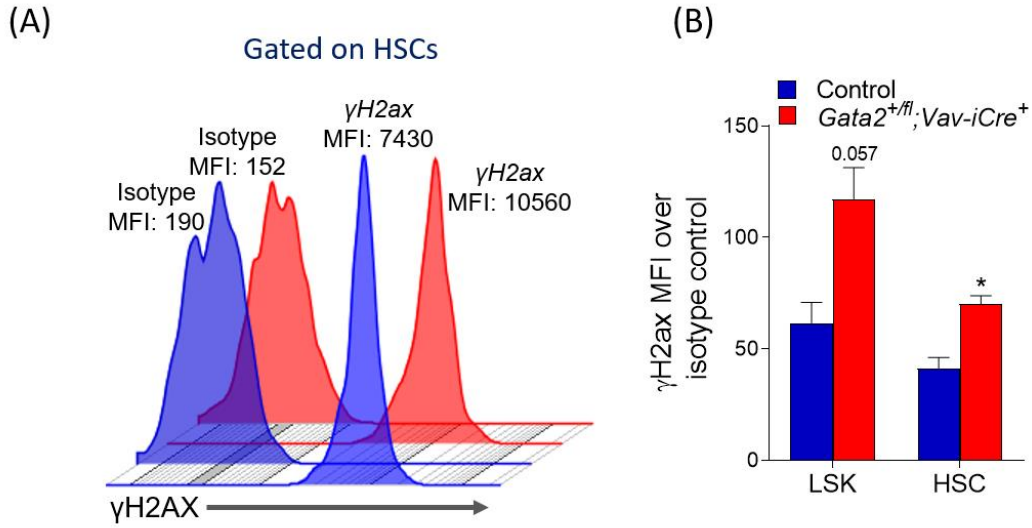

Figure 3-14: Increased DNA damage response in *Gata2* haploinsufficient HSCs.
(A) Representative FACS plot analysis of the median fluorescence intensity (MFI) of γH2AX expression in BM HSCs from control and *Gata2*$^{+/fl}$*; Vav-iCre*$^{+}$ mice. (B) Bar chart analysis of the ratio of γH2ax MFI with respect to fluorescent isotype-control in BM HSPCs in *Gata2*$^{+/fl}$*; Vav-iCre*$^{+}$ mice. n=4 mice for each genotype from two independent experiments. Presented data are mean ± SEM. Statistical analysis: Mann-Whitney U test *, $P < 0.05$; **, $P < 0.01$.

3.3 Roles of *Gata2* haploinsufficiency in aged haematopoietic cells

Given that approximately 90% of GATA2 haploinsufficient patients develop haematological malignancies by the age of 60 years (Wlodarski et al., 2017, Collin et al., 2015). *Gata2* heterozygote (*Gata2*$^{+/fl}$*; Vav-iCre*$^{+}$*)* mice were aged as a model of the late-onset disease to further model the progression of immunodeficiency and developing MDS/CMML/AML that is observed in clinical GATA2 haploinsufficiency syndromes. To investigate the role of *Gata2* haploinsufficiency in aged haematopoietic compartments, *Gata2*$^{+/fl}$*; Vav-iCre*$^{+}$ and control (*Gata2*$^{+/fl}$*; Vav-iCre*$^{-}$) mice were aged for 18-20 months old to correlate with ageing in humans (56 - 69 years old) (Jackson et al., 2017). PB was tested every 2-3 months to analyse the primitive haematopoietic differentiation potential, and BM, spleen, and thymus were harvested at 18-20 months old to assess HSPCs and extramedullary haematopoietic compartments. (Figure 3.15 A).

3.3.1 *Gata2*-mRNA levels in aged haematopoietic compartments

This study firstly assessed the expression level of *Gata2*-mRNA in aged BM wild-type animals including primitive HSPCs (HSC, HPC1, HPC2, LMPP), committed myeloid/lymphoid progenitors (CMP, GMP, MEP, CLP), and mature myeloid/lymphoid lineages. The expression analysis showed that *Gata2* mRNA was broadly expressed in HSPCs and was the highest in HSCs and decreased in differentiated mature blood cells, with a lack of expression in lymphoid lineages, including the CLP (Figure 3.15 B). These results are consistent with the expression levels of *Gata2* mRNA found in haematopoietic populations from young mice (Menendez-Gonzalez et al., 2019b, Orlic et al., 1995, Guo et al., 2013).

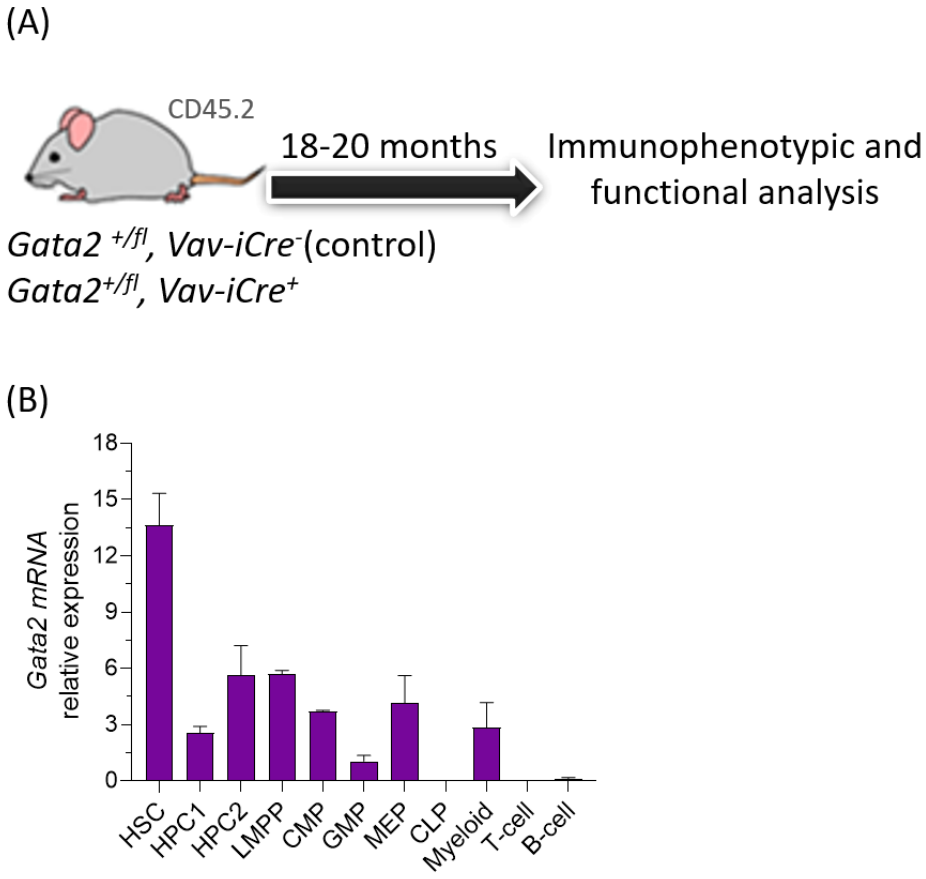

Figure 3-15: *Gata2*-mRNA levels in aged haematopoietic compartments.
(A) A scheme of the experimental design. Haematopoietic tissues were harvested at 18-20 months old. (B) The bar chart shows *Gata2* mRNA expression in purified BM populations of wild-type mice (n=2), including HSCs ($LSKCD150^{+}CD48^{-}$), HPC1 ($LSKCD150^{-}CD48^{+}$), HPC2 ($LSKCD150^{+}CD48^{+}$), LMPPs ($LSKCD34^{+}CD135^{hi}$), CMPs ($LKCD34^{+}CD16/32^{-}$), GMPs ($LKCD34^{+}CD16/32^{+}$), MEPs ($LKCD34^{-}CD16/32^{-}$), CLPs ($Lin^{-}c\text{-}kit^{lo}Sca1^{lo}CD127^{+}CD135^{+}$), myeloid-cells ($Mac1^{+}Gr1^{+}$), T-cells ($CD3_{\varepsilon}$), B-cells (B220). The expression level of *Gata2*-mRNA was normalised to the *Hprt* housekeeping gene, and the relative expression was determined by the $2^{-\Delta\Delta CT}$ equation. Presented data are mean ± SEM.

3.3.2 No differences in the frequencies of multi-lineage haematopoiesis in aged *Gata2* haploinsufficient mice

Firstly, this study evaluated the frequencies of multi-lineage populations in haematopoietic tissues. In accord with literature reports, skewed differentiation capability towards myeloid lineages was observed in both aged *Gata2*$^{+/fl}$*; Vav-iCre*$^{+}$ and control mice (Figure 3.16 A) (Morrison et al., 1996, Kim et al., 2003, Pearce et al., 2007, Rossi et al., 2005, Liang et al., 2005). However, the percentages of myeloid cells (Mac1^{+}Gr1^{+} and Mac1^{+}Gr1^{-}), B-cell (B220^{+}) and T-cell (CD4^{+} and CD8^{+}) were comparable in both *Gata2*$^{+/fl}$*; Vav-iCre*$^{+}$ and control mice during the whole period (between 3-4 months and 18-19 months old) (Figure 3.16 A). No significant difference was observed in the absolute numbers of CBC indices including WBCs, RBCs, haemoglobin, and platelets in both littermates although the number of platelets was insignificantly reduced in *Gata2*$^{+/fl}$*; Vav-iCre*$^{+}$ mice at 18-19 months old (Figure 3.16 B). However, comparing the fold-change of percentages of myeloid/lymphoid cells in PB of aged *Gata2* $^{+/fl}$*; Vav-iCre*$^{+}$ versus young *Gata2* $^{+/fl}$*; Vav-iCre*$^{+}$ mice after normalising with their counterpart control, we noticed an increase in monocyte/macrophage cells (Mac1^{+}Gr1^{-}) in aged *Gata2* $^{+/fl}$*; Vav-iCre*$^{+}$ mice (Figure 3.16 C) in PB. These data demonstrate *Gata2* haploinsufficiency causes steady-state accumulation of monocyte/macrophages in PB during ageing.

The total cellularity numbers were similar in the BM, spleen, and thymus in aged *Gata2*$^{+/fl}$*; Vav-iCre*$^{+}$ as compared with control mice (Figure 3.17 A). No changes were seen in the percentages and numbers of myeloid, erythroid, and lymphoid cells in the BM, spleen, and thymus in both genotypes (Figure 3.17 B, C, and D). Consistent with young multi-lineage haematopoiesis, *Gata2* haploinsufficiency in ageing was largely dispensable for terminal differentiation of multi-lineage blood cells in hematopoietic tissues.

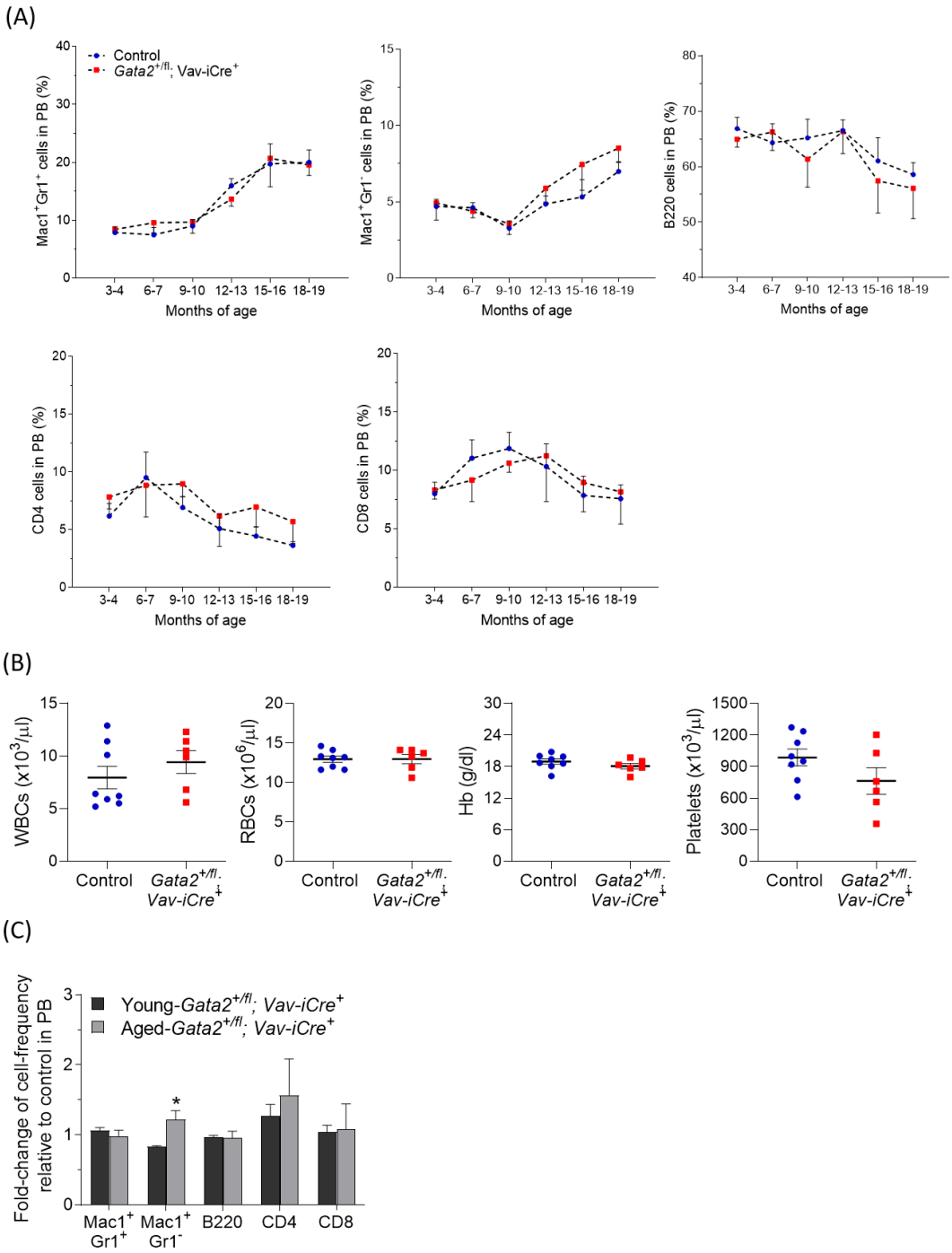

Figure 3-16: No differences on the frequencies of multi-lineage haematopoiesis in the PB of aged haploinsufficient *Gata2* mice.

(A) The frequencies of mature blood cells among 3-4 and 18-19 months old in PB including myeloid (Mac1, Gr1) and lymphoid (B220, CD4, CD8) cells in control (n=9) and *Gata2*$^{+/fl}$*; Vav-iCre*$^{+}$ (n=7) mice from three independent experiments. (B) Absolute numbers of peripheral CBC parameters (WBCs, RBC, haemoglobin, and platelets) from control (n=8) and *Gata2*$^{+/fl}$*; Vav-iCre*$^{+}$ (n=6) littermates at 18-19 months old from two independent biological replicates. (C) Fold-change ratios of cells frequencies in PB of aged *Gata2* $^{+/fl}$*; Vav-iCre* $^{+}$ (n=7) relative to young *Gata2* $^{+/fl}$*; Vav-iCre* $^{+}$ (n=6) mice after normalising with control for each genotype from 3 independent experiments for each group. Presented data are mean ± SEM. Statistical analysis: Mann-Whitney U test *, $P < 0.05$.

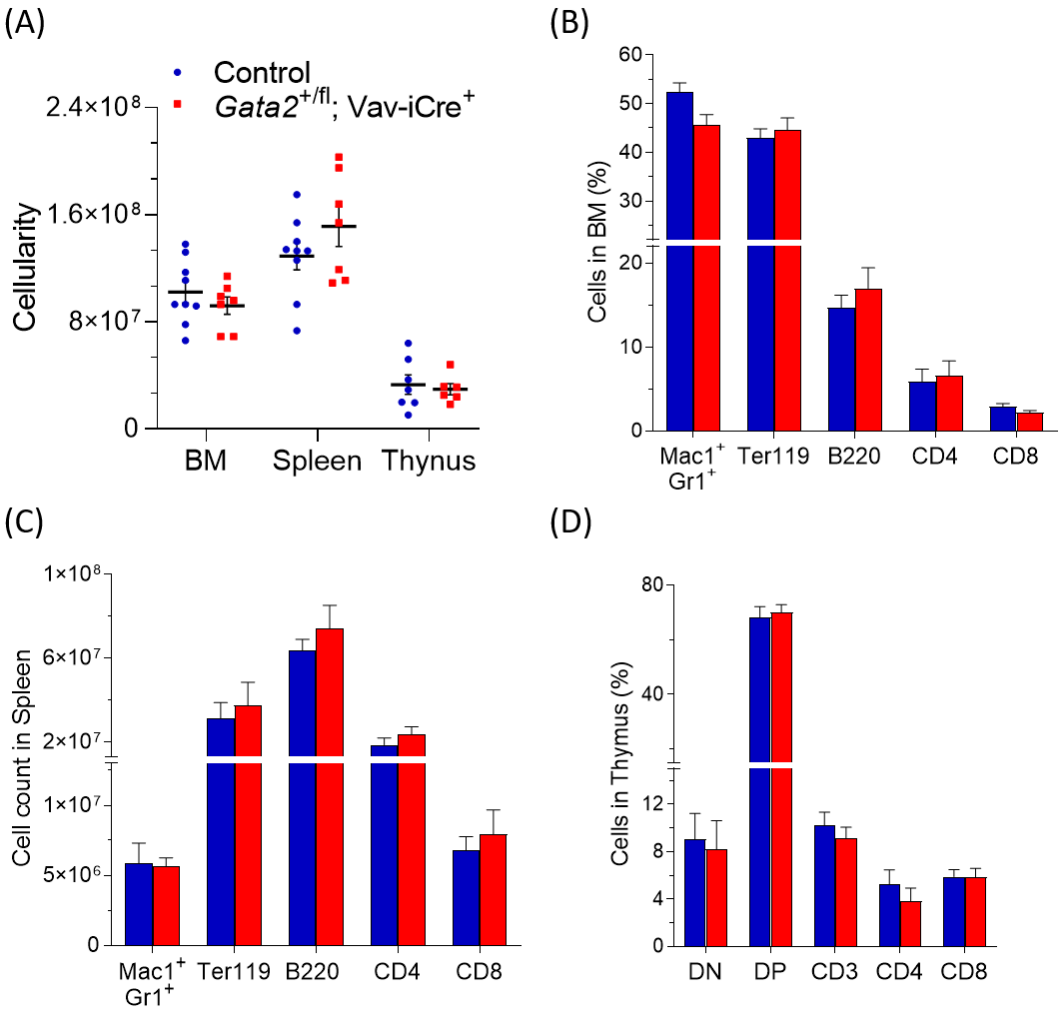

Figure 3-17: No differences on the frequencies of multi-lineage haematopoiesis in the BM, spleen, and thymus of aged *Gata2* haploinsufficient mice.

(A) Live cellularity numbers in BM (from 2-femurs and 2-tibias (cells/30mL)), spleen (cells/7mL), and thymus (cells/4mL) in control (n=7-9) and *Gata2*$^{+/fl}$*; Vav-iCre*$^{+}$ (n=6-7) mice from three independent experiments. (B and C) The proportion of cells in the BM (B) and spleen (C) of myeloid (Mac1Gr1), erythroid (Ter119) and lymphoid (B220, CD4, CD8) from control (n=9) and *Gata2*$^{+/fl}$*; Vav-iCre*$^{+}$ (n=7) mice from three independent experiments. (D) the percentages of lymphoid cells (CD3, CD4, CD8) in thymus in control (n=7) and *Gata2*$^{+/fl}$*; Vav-iCre*$^{+}$ (n=6) mice from three independent biological replicates. DP indicates, CD4^{+}CD8^{+}; and DN, CD4^{-}CD8^{-}. Data are mean ± SEM. Statistical analysis: Mann-Whitney U test.

3.3.3 *Gata2* haploinsufficiency perturbs HSPCs and CLPs during ageing

Subsequently, this study evaluated the ageing impact of *Gata2* haploinsufficiency on the frequencies of primitive HSPCs (HSCs, MPPs, HPC1, HPC2) and committed progenitors (CMPs, GMPs, MEPs, CLPs) in the BM of *Gata2*$^{+/fl}$*; Vav-iCre*$^{+}$ and control mice (Akashi et al., 2000, Kondo et al., 1997, Oguro et al., 2013, Kiel et al., 2005, Adolfsson et al., 2005). In striking contrast to young *Gata2* haploinsufficient committed progenitors (Figure 3.3 A), a significant decline in the frequency of CLPs was noticed in *Gata2*$^{+/fl}$*; Vav-iCre* when compared to control littermates (Figure 3.18 A), whereas the frequencies of CMPs, GMPs, and MEPs were similar in both genotypes. Functionally, *in vitro* CFC assessment of BM myeloid progenitors showed an insignificant decrease in total colony numbers and reduced colonies forming of CFU-GEMM, CFU-GM, and CFU-M in BM of *Gata2*$^{+/fl}$*; Vav-iCre* mice (Figure 3.18 B).

Similar to *Gata2* haploinsufficient young HSPCs, flow cytometry analysis showed that the frequencies of LSK, HSCs, MPPs, and LMPPs were decreased in the BM of *Gata2*$^{+/fl}$*; Vav-iCre* as compared with control mice (Figure 3.18 C). In accordance with published reports, the number/frequency of BM HSCs was expanded in ageing (Morrison et al., 1996, Kim et al., 2003, Pearce et al., 2007, Rossi et al., 2005, Liang et al., 2005), and this was observed in both genotypes. When we normalised young and aged CLP and HSC populations to their control counterparts, we demonstrated an approximate two-fold reduction in CLPs and HSCs in aged *Gata2*$^{+/fl}$*; Vav-iCre* when compared with young *Gata2*$^{+/fl}$*; Vav-iCre* littermates (Figure 3.18 D and E). These findings suggest that *Gata2* is further required to sustain aged HSCs and CLP pool sizes. Furthermore, together with a defect in young *Gata2* haploinsufficient HSCs, these data suggest that *Gata2* may play a distinct role in lymphoid progenitor differentiation which is dependent on ageing.

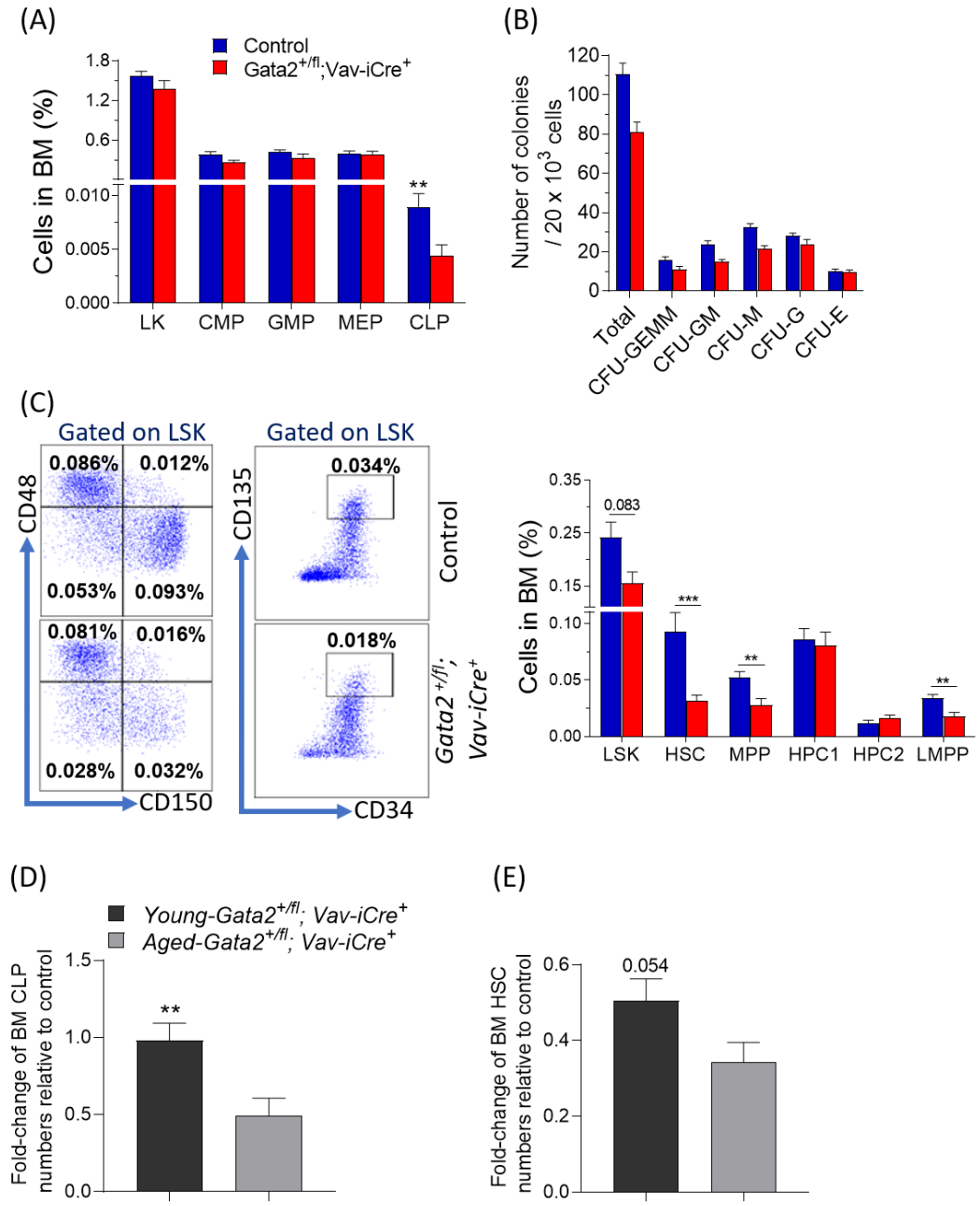

Figure 3-18: Long-term loss of *Gata2* haploinsufficiency perturbs primitive HSPCs and CLPs. (A) The frequencies of committed myeloid/lymphoid progenitors (LK, CMPs, GMPs, MEPs, and CLPs) in BM from control (n=9) and *Gata2*$^{+/fl}$*; Vav-iCre*$^{+}$ (n=7) mice from three independent experiments. (B) CFC numbers of *Gata2*$^{+/fl}$*; Vav-Cre*$^{+}$ and control BM cells after plating in M3434 semisolid methylcellulose media. n= 3 mice per group from two separate experiments. (C) Representative FACS plots (Lift-hand) and frequencies (Right) of the BM primitive HSPCs (LSK, HSCs, MPPs, HPC1, HPC2, and LMPP) in control (n=9) and *Gata2*$^{+/fl}$*; Vav-iCre*$^{+}$ (n=7) mice from three independent experiments. (D and E) Fold change ratios of CLP (D) and HSCs (E) in aged *Gata2* $^{+/fl}$*; Vav-iCre* $^{+}$ (n=7) relative to young *Gata2* $^{+/fl}$*; Vav-iCre* $^{+}$ (n=8) after normalising with wild-type control counterparts from 3 independent experiments for each group. Data represent mean ± SEM. Statistical analysis: Mann-Whitney U test *, $P < 0.05$; **, $P < 0.01$; ***, $P < 0.001$; ****, $P < 0.0001$.

3.3.4 Increased HSC proliferation and altered apoptosis level in aged HSPCs from *Gata2* haploinsufficient mice

To assess the impact of *Gata2* haploinsufficiency on the ageing of HSPCs, the survival of HSPCs was evaluated using annexin V assays. Flow cytometric analysis showed a significant increase in the proportion of total apoptosis (early plus late apoptosis) in BM MPPs of *Gata2*$^{+/fl}$*; Vav-iCre*$^{+}$ mice as compared to control mice, whereas the frequencies of total apoptosis in aged BM HSC and LSK cells were statistically unchanged in *Gata2*$^{+/fl}$*; Vav-iCre*$^{+}$ mice (Figure 3.19 A). This latter result contrasts with young *Gata2* haploinsufficient mice where both HSCs and MPPs display altered cell survival.

GATA2 is an essential regulator of adult HSC quiescence, and this process is required to maintain HSCs pool size and protects the self-renewal potential of HSCs (Rodrigues et al., 2005, Rieger and Schroeder, 2012, Orkin and Zon, 2008, Seita and Weissman, 2010). Thus, in the next set of experiments, the impact of long-term loss of *Gata2* haploinsufficiency on cell cycling of HSPCs was assessed using ki-67 assays. In stark contrast to young *Gata2* haploinsufficient mice, there was a significant decrease of the proportion of HSCs in G0 phase of *Gata2*$^{+/fl}$*; Vav-iCre*$^{+}$ when compared to control mice and together with an increase in the frequency of HSCs in S/G2/M phases from *Gata2*$^{+/fl}$*; Vav-iCre*$^{+}$ mice. No change was noticed in the frequencies of cells in G0, G1 and S/G2/M phases within MPP, HPC1, and HPC2 in both littermates (Figure 3.19 B and C). Thus, aged *Gata2* haploinsufficient HSCs were less quiescent and more proliferative than young *Gata2* haploinsufficient HSCs (Figure 3.19 D).

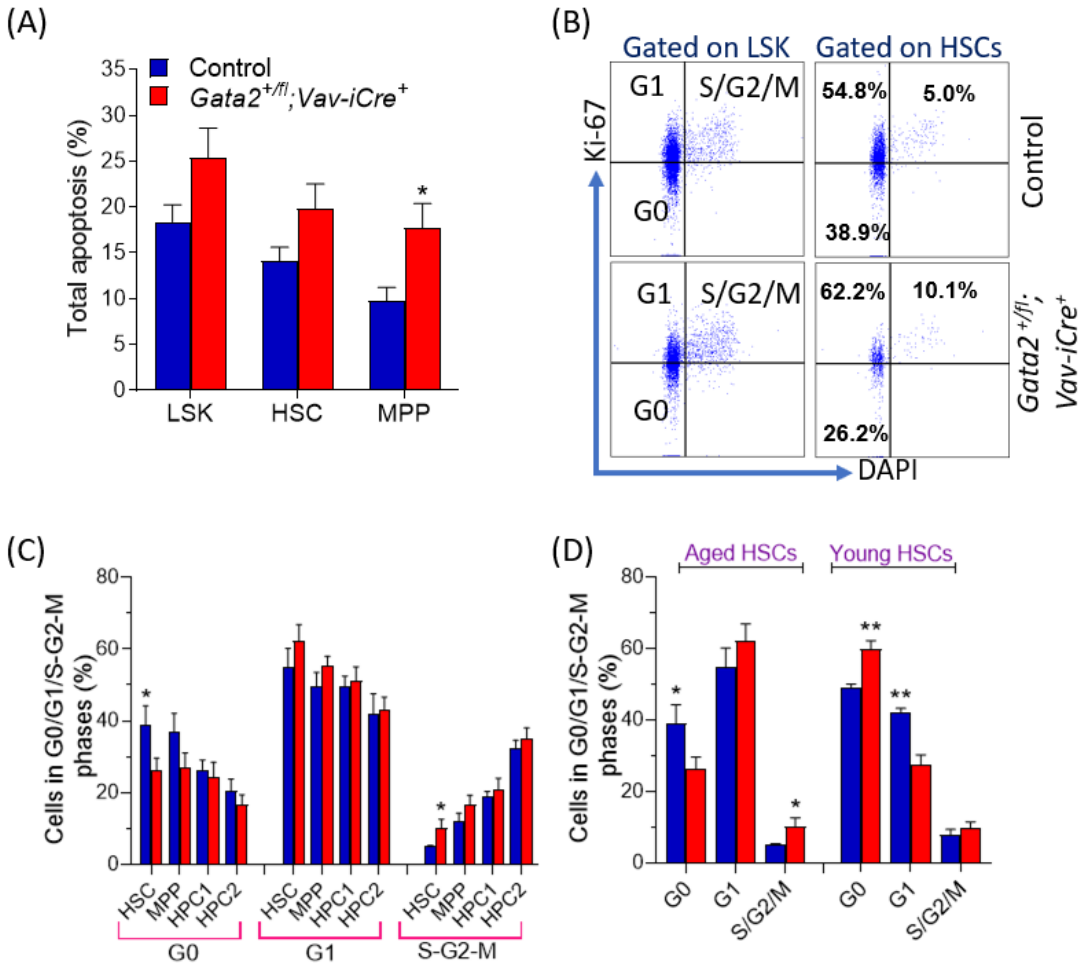

Figure 3-19: Increased HSCs proliferation and altered apoptosis level in aged HSPCs from *Gata2* haploinsufficient mice.

(A) the percentages of total apoptosis in the BM HSPCs of control (n=8) and *Gata2*$^{+/fl}$*; Vav-iCre*$^{+}$ (n=7) mice from three independent experiments. Annexin V and DAPI staining were utilised to stain BM HSPCs. (B and C) FACS plots analysis (B) and proportions (C) of BM HSPCs in the cell cycle phases from control (n=9) and *Gata2*$^{+/fl}$*; Vav-iCre*$^{+}$ (n=7) mice from three separate experiments. G0-phase indicates ki-67^{-}DAPI^{-}; G1-phase, ki-67^{+}DAPI^{-}; and S/G2/M phases, ki-67^{+} DAPI^{+}. (D) The proportion of BM HSCs in G0, G1, and S/G2/M phases of the cell cycle from aged mice (n = 9 control and 7 *Gata2* $^{+/fl}$*; Vav-iCre*$^{+}$) and young mice (n = 6 for each genotype) from 3 independent experiments for each condition. Presented data are mean ± SEM. Statistical analysis: Mann-Whitney U test *, P < 0.05; **, P < 0.01; ***, P < 0.001.

3.3.5 Aged *Gata2* haploinsufficient HSCs lack competence for multi-lineage repopulation

We next performed competitive transplantation experiments to functionally assess the aged HSCs capability of reconstituting multi-lineage haematopoietic populations. To do this, CD45.2 purified aged HSCs from control or *Gata2*$^{+/fl}$*; Vav-iCre*$^{+}$ mice were transplanted into CD45.1-lethally-irradiated recipient hosts (Figure 3.20 A). PB was evaluated every four weeks post-transplant, and haematopoietic tissues (BM and spleen) were harvested at week 16 after-transplant to evaluate the HSCs contribution for multi-lineage repopulation. Flow cytometric assessment displayed that the frequency of total donor contribution (CD45.2 cells) was significantly lower in PB of *Gata2*$^{+/fl}$*; Vav-iCre*$^{+}$ derived-cells as compared with control derived-cells during the whole period post-transplant (Figure 3.20 B). Similarly, there was a significant reduction in the percentages of CD45.2 donor contribution of *Gata2*$^{+/fl}$*; Vav-iCre*$^{+}$ transplant-cells for myeloid (Mac1^{+}Gr1^{+} and Mac1^{+}Gr1^{-}) T-cell (CD4^{+} and CD8^{+}) and B-cell (B220^{+}) in PB at week 16 after-transplant (Figure 3.20 C). When we compared the donor contribution for myeloid/lymphoid cells with young HSCs donor cells in PB, there was about a two-fold increase in myeloid cells and around a two-fold decrease in CD4-cells of aged *Gata2*$^{+/fl}$*; Vav-iCre*$^{+}$ donor-cells as compared with young *Gata2*$^{+/fl}$*; Vav-iCre*$^{+}$ donor-cells (Figure 3.20 F). Thus, *Gata2* haploinsufficiency skews functional myeloid over lymphoid potential in vivo.

Analysing of the donor contribution for haematopoietic multi-lineage in BM and spleen at 16 weeks after transplantation revealed that the frequencies of CD45.2 *Gata2*$^{+/fl}$*; Vav-iCre*$^{+}$ donor-cells for myeloid, erythroid, T-cell and B-cell were diminished when compared with control donor-cells (Figure 3.20 D and E). We next evaluated the frequencies of CD45.2-donor-cells in HSPCs and committed myeloid/lymphoid progenitors. The immunophenotypic analysis showed that a significant decrease was observed in the percentages of CD45.2 *Gata2*$^{+/fl}$*; Vav-iCre*$^{+}$ donor-cells (Figure 3.20 G and H). These results are consistent with young HSCs and imply that aged *Gata2* haploinsufficient HSCs fail to repopulate haematopoietic multi-lineage. Furthermore, aged *Gata2* haploinsufficient HSCs have more myeloid-biased potential as compared to the reconstitution capability of young HSCs.

3.3.6 Increased DNA damage and apoptosis level in aged donor derived *Gata2* haploinsufficient HSCs.

It is a well-known fact that accumulation of DNA damage disturbs normal aged HSC functions and increases the tendency to develop myeloid neoplasms (Rossi et al., 2007, Rossi et al., 2005, Signer et al., 2007). Thus, the γH2AX level in aged CD45.2 HSCs in primary recipient mice was evaluated following transplantation. Immunophenotypic analysis revealed that the γH2AX median fluorescence intensity (MFI) level was higher in *Gata2*$^{+/fl}$*; Vav-iCre*$^{+}$ derived-HSCs as compared with control derived-HSCs (Figure 3.21 A). We next assessed the apoptosis level within CD45.2 derived HSCs. There was a significant rise in the frequency of total apoptosis in BM *Gata2*$^{+/fl}$*; Vav-iCre*$^{+}$ derived-HSCs as compared with control derived-HSCs. (Figure 3.21 B). These results suggest that decreased numbers of *Gata2* haploinsufficient derived HSCs are associated with increased DNA damage and reduced cell survival rates.

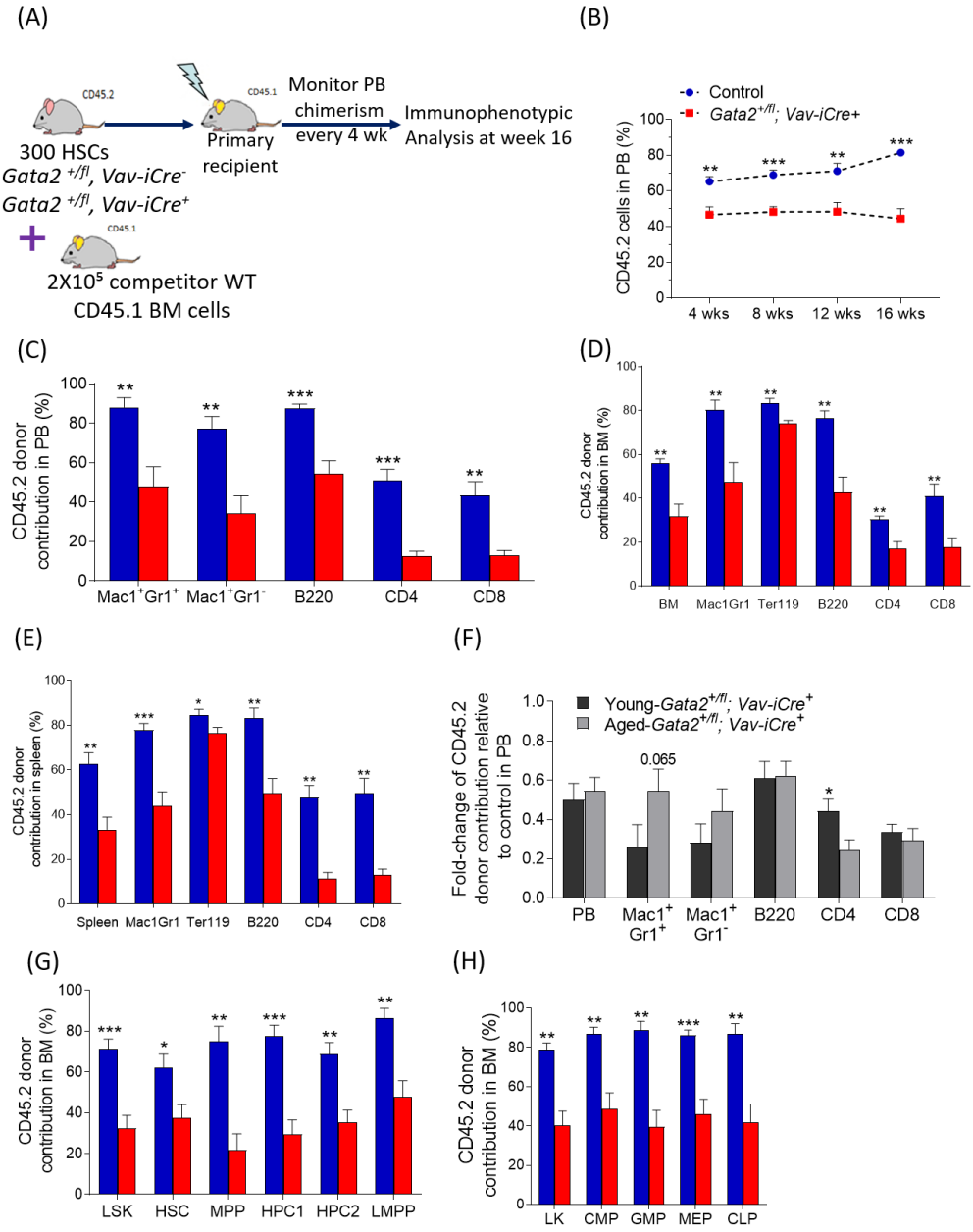

Figure 3-20: Aged *Gata2* haploinsufficient HSCs lack competence for multi-lineage repopulation

(A) Experimental diagram of primary transplant experiments, 300 CD45.2 HSCs from aged *Gata2*$^{+/fl}$*; Vav-iCre*$^{+}$ and control mice were transplanted with 2x10^5 CD45.1 competitor BM cells (8-12 weeks old) into lethally CD45.1-irradiated recipient mice. (B) Proportions of total CD45.2 cells in PB during the whole period post-transplant from control (n=8) and *Gata2*$^{+/fl}$*; Vav-iCre*$^{+}$ (n=8) derived cells from two independent experiments. (C, D and E) Frequencies of CD45.2 donor contribution in PB (C), BM (D), and spleen (E) for myeloid/lymphoid/erythroid cells at week 16 post-transplantation of *Gata2*$^{+/fl}$*; Vav-iCre*$^{+}$ (n=8) or control (n=8) derived cells from two separate experiments. (F) Fold change ratios of CD45.2 donor contributions in PB for myeloid/lymphoid cells of aged mice donor cells (n=8) relative to young *Gata2* $^{+/fl}$*; Vav-iCre* $^{+}$ (n=8) donor cells from 2-3 independent experiments for each group. (G and H) Percentages of CD45.2 donor cells for BM HSPCs (G) and committed progenitors (H) from control (n=8) *Gata2*$^{+/fl}$*; Vav-iCre*$^{+}$ (n=8) derived cells from two independent experiments. Four independent donors were used for each genotype. Data are mean ± SEM. Mann-Whitney U test *, P < 0.05; **, P < 0.01; ***, P < 0.001.

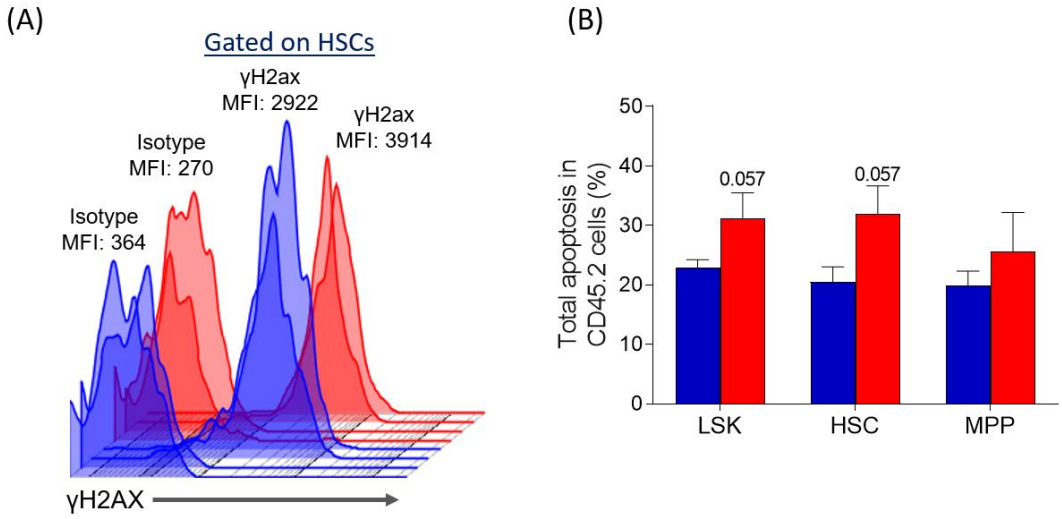

Figure 3-21: Increased DNA damage and apoptosis level in aged donor-derived *Gata2* haploinsufficient HSCs.

(A) Representative histogram plot analysis of the γH2AX median fluorescence intensity (MFI) in *Gata2*$^{+/fl}$*; Vav-iCre*$^{+}$ (n=2) derived-HSCs and control derived-HSCs (n=2) from a single biological experiment. (B) proportion of total apoptosis in BM *Gata2*$^{+/fl}$*; Vav-iCre*$^{+}$ (n=4) derived-HSCs and control (n=4) derived-HSCs from a single experiment. Presented data are mean ± SEM. Statistical analysis: Mann-Whitney U test *, $P < 0.05$.

3.4 Discussion

A mutation of one allele of *GATA2* transcriptional factor impairs the normal functions of HSCs and causes GATA2 haploinsufficiency syndromes that lead to clinical immunodeficiency syndromes with a predisposition to MDS/AML via MonoMAC syndrome, DCML deficiency syndrome, Emberger syndrome, and congenital chronic neutropenia. Monoallelic germline *GATA2* mutations further contribute to familial myeloid neoplastic predisposition (Dickinson et al., 2011, Hyde and Liu, 2011, Hahn et al., 2011, Hsu et al., 2011, Ostergaard et al., 2011).

Until recently, nevertheless, there have been few studies examining perturbed adult HSPC compartments, adult committed myeloid/lymphoid/erythroid/ megakaryocyte progenitors, megakaryopoiesis, aged haematopoietic compartments, and genetic mechanisms in GATA2 haploinsufficiency syndromes. This study employed pan-haematopoietic Vav-iCre promoter to specifically delete one allele of floxed *Gata2* in all haematopoietic tissues (Stadtfeld and Graf, 2005). Given that the Vav-promoter is expressed in the developing embryo at E11, $Gata2^{+/fl}$; $Vav\text{-}iCre^{+}$ mice offer a tractable model to mimic germline GATA2 haploinsufficiency syndromes and offer the opportunity to explore the role of chronic loss of *Gata2* haploinsufficiency in young and aged mice.

This study extensively assessed *Gata2* haploinsufficiency in the young (8-12 weeks) and aged (18-20 months) primitive HSPC compartments. In the first haematopoietic differentiation hierarchy, this study used SLAM (CD150 and CD48) markers to fractionate HSPCs into HSCs, MPPs, HPC1 (lymphoid/myeloid uncommitted progenitors), and HPC2 (myeloid/erythroid/megakaryocyte/lymphoid uncommitted progenitors) subpopulations (Oguro et al., 2013, Kiel et al., 2005). There was a significant decrease in the frequencies of LSK, HSCs, MPPs, and HPC1, but an increase in HPC2 in young haploinsufficient *Gata2* mice (Figures 3.5 A and 3.22 A). In the second haematopoietic differentiation hierarchy, two types of primitive uncommitted progenitors can be identified within LSK compartments based on CD135 (LMPPs, lymphoid/myeloid potential) and CD41 (redefined primitive CMPs, myeloid/erythroid/megakaryocyte potential) expressions (Miyawaki et al., 2015).

The frequencies and numbers of LMPP and CD41^{+}CMP were significantly decreased in young *Gata2* haploinsufficiency mice (Figures 3.5 B and 3.22 B). In aged *Gata2* haploinsufficient HSPCs, this study found a significant reduction in frequencies of HSCs, MPPs, and LMPPs, whereas there were no significant alterations in percentages of HPC1 and HPC2 in aged *Gata2* haploinsufficiency mice (Table 3.1). Consistent with previous studies (Morrison et al., 1996, Kim et al., 2003, Pearce et al., 2007, Rossi et al., 2005, Liang et al., 2005), we noticed that increased HSC numbers and skewed HSCs differentiation towards myeloid cells in both aged *Gata2* haploinsufficient HSCs and control HSCs. However, we found around a two-fold reduction of aged *Gata2* haploinsufficient HSCs when we compared the HSCs numbers between young and aged mice by normalising each one to its counterpart control (Figure 3.18 E). Collectively, these results show that *Gata2* haploinsufficiency disrupts young and aged HSPCs homeostasis. Therefore, *Gata2* has a critical dose-dependent role in the development and maintenance of the young and aged HSCs homeostasis. These results are in agreement with that observed in mouse models of constitutive *Gata2* haploinsufficiency and extend these observations by demonstrating that *Gata2* haploinsufficiency regulates the earliest point of HSC generation and maturation in the embryo with consequences for adult and aged HSPCs homeostasis (de Pater et al., 2013, Ling et al., 2004, Rodrigues et al., 2005, Guo et al., 2013).

In terms of the mechanisms underlying HSPC defects in young *Gata2* haploinsufficient mice, this study found the percentages of HSCs and MPPs compartments undergoing apoptosis were increased in young *Gata2* haploinsufficient mice, signifying that *Gata2* is necessary for the survival of these populations. Similarly, aged haploinsufficient *Gata2* mice showed total apoptosis was significantly increased in MPPs, and apoptosis rates were insignificantly increased in aged HSCs. The present findings seem to be consistent with other research which found the reduction in the frequencies of primitive haematopoietic cells in young *Gata2* haploinsufficient mice may result from an increase in programmed cell death among these cells (de Pater et al., 2013, Rodrigues et al., 2005). Rodrigues at al. highlighted that the decreased HSC survival in the *Gata2*$^{+/-}$ mouse is due to reduced expression of the anti-apoptotic BCL-xL protein (Rodrigues et al., 2005). However, our

group previously analysed anti-apoptotic BCL-xL and BCL2 proteins in *Gata2*$^{+/fl}$*; Vav-iCre*$^{+}$ mice, and no difference was observed in BCL-xL and BCL2 levels in *Gata2*$^{+/fl}$*; Vav-iCre*$^{+}$ mice as compared with counterpart controls (Menendez-Gonzalez et al., 2019b). Thus, it might be that *Gata2* regulates the survival of HSCs in this model independently of BCL family members. In this regard, RNA-Seq analysis showed that differentially dysregulated genes involved in the regulation of cellular survival such as *Clca3a1, Hcar2, Kcnip3, Timp3, Rassf6, Gimap4, Nek5, Tnfrsf22,* and *Txn2*. For instance, our data showed down-regulation of tissue-inhibitor of metalloproteinases–3 (TIMP3), a proapoptotic proteinase inhibitor, which positively regulates cellular survival (Fata et al., 2001). We further noticed insignificant up-regulation of *Trp53* (FDR-value: 0.17 and p-value: 0.002) and caspase-dependent apoptosis genes (*Casp2* (FDR-value: 0.4 and p-value: 0.02), and *Casp7* (FDR-value: 0.3 and p-value: 0.05)) in our RNA-Seq data. Therefore, GATA2 haploinsufficiency may perturb HSCs survival through activation of Trp53 signalling.

In addition, analysis of cell cycle status of young *Gata2* haploinsufficient mice revealed that increases in the percentage of cells in G0 phase within the HSC fraction. These findings further support the idea that GATA2 haploinsufficiency promotes cellular quiescence (Rodrigues et al., 2005). Collectively, the reduction in HSCs numbers in young *Gata2* haploinsufficiency mice was associated with increased cellular quiescence and apoptosis. Increased HSC quiescence may associate with less susceptibility for immune surveillance, attenuated DNA damage repair pathways, and a heightened incidence of haematological neoplasms (Cho et al., 2020, Boyd and Rodrigues, 2018). It is possible therefore that such connections may be present between increased quiescent HSCs and the development of GATA2 haploinsufficiency diseases. In striking contrast to young *Gata2* haploinsufficient HSCs, there was a significant decrease in the G0 phase and an increase in S/G2/M phases in aged *Gata2* haploinsufficient HSCs (Table 3.1). These findings suggest that *Gata2* haploinsufficiency increases the proliferation capacity of aged HSCs and disturbs aged HSCs homeostasis. Since the function of haematopoietic system decreases with age, increased HSCs cycling may result in genomic instability and increased susceptibility to mutations (Cho et al., 2020).

HSCs have both self-renewal and differentiation potential to sustain permanent haematopoiesis (Rieger and Schroeder, 2012, Orkin and Zon, 2008, Seita and Weissman, 2010). Competitive and serial HSCs transplantation experiments were conducted to robustly assess HSCs functional ability for multi-lineage repopulation and self-renewal effectiveness. Analysis of the chimerism in primary transplant experiments showed a reduction of young and aged *Gata2* haploinsufficient donor cells to all haematopoietic compartments. In support of this, *in vitro* CFC assays displayed that numbers of myeloid colonies were decreased in young *Gata2* haploinsufficient BM and severely reduced in aged BM. These findings agree with the results of other research, in which *Gata2* haploinsufficient HSCs are unable of reconstituting multi-lineage haematopoietic cells (Rodrigues et al., 2005, Ling et al., 2004).

Serial transplantation of young *Gata2* haploinsufficient HSCs revealed that *Gata2* haploinsufficient donor cells were severely decreased in PB, BM, spleen, and thymus when compared to control donor cells. Previous studies used germline deletion of *Gata2* heterozygote mouse models concluded that AGM HSCs are impaired in self-renewal potential, while adult BM has normal self-renewal capability in serial transplantation experiments (Ling et al., 2004, Rodrigues et al., 2005). A possible explanation of this difference may be the method of purifying HSCs, in which the HSC surrogate long-term culture-initiating cell (LTC-IC) assay was used to purify HSCs whereas here we purified HSCs with greater homogeneity using FACS with specific markers for HSCs. The present results illustrate for the first time that adult *Gata2* haploinsufficient HSCs are entirely incapable of repopulating multi-lineage haematopoietic compartments of secondary recipients and that *Gata2* haploinsufficiency drives a self-renewal defect in HSCs. In support of this finding, the number of aged *Gata2* haploinsufficient HSCs was decreased when compared to young *Gata2* haploinsufficient HSCs, aged *Gata2* haploinsufficient HSCs were less quiescent with elevated proportions of cycling HSCs than their younger counterparts, and increased DNA damage and apoptosis level were observed in aged donor *Gata2* haploinsufficient derived HSCs. Taken together, primary and secondary

transplantation results demonstrate that *Gata2* plays indispensable roles in the HSCs self-renewal, survival, and maintenance.

Because this study found an expansion in HPC2 cells that contain heterogeneous uncommitted progenitors, we used CD135 and slam markers to further dissect these compartments. Pietras et al. categorised HSPC compartments into five distinct subpopulations: LT-HSCs, ST-HSCs (MPP1), MPP2 (megakaryocyte/ erythroid-biased-MPP), MPP3 (GMP-biased-MPP), and MPP4 (lymphoid/GMP-biased-MPP) (Pietras et al., 2015). Based on these HSPCs categorisation, this study found a significant reduction in LT-HSCs, ST-HSCs and MPP4 and a significant expansion in MPP2 in young *Gata2* haploinsufficient mice, implying that *Gata2* haploinsufficient HSCs induce uncommitted megakaryocyte/erythroid progenitor skewing, and a block at MPP2 stage may exist affecting the differentiation of downstream committed megakaryocyte/erythroid progenitors that ultimately leads to the platelet deficiency observed (Figures 3.6 and 3.22 C). Consistent with these results, analysis of single-cell RNA-Seq of purified BM $CD34^{+}$ cells from MDS patients with familial GATA2 haploinsufficiency results in skewed HSCs differentiation toward megakaryocyte/erythrocyte progenitors (Wu et al., 2020).

The expansion of MPP2 in *Gata2* haploinsufficient BM impaired the differentiation of Pre-MegE progenitors. The reduced numbers of Pre-MegE bipotent progenitors were accompanied by a decrease in frequencies of MkP and Pre-CFU-E committed progenitors. MkP cells generated low numbers of mature megakaryocytes and platelets in BM/spleen and PB, respectively. Pre-CFU-E cells differentiated normally to downstream erythroid precursors (CFU-E, Pro-erythroblast, early and late erythroblast). A well-known fact is that *Gata1* replaces *Gata2* at the chromatin site through “GATA-switch” processes during the erythroid differentiation (Guo et al., 2016, Tsang et al., 1997). Our data suggested that “GATA-switch” may take place in CFU-E cells unimpeded by *Gata2* haploinsufficiency. Analysis of *Gata1* and *Gata2* mRNA expression in Pre-CFU-E and CFU-E is further required to test this hypothesis. These findings highlighted the requirement of *Gata2* in megakaryopoiesis and early erythroid compartments. In support of these results: (1) *Gata2* $^{+/-}$ mice showed that

decreased numbers of MegE compartments and decreased expression level of *Gata1*-mRNA and *Gfi1b*-mRNA within LSK cells; (2) knockdown of *Gata2* in BM LSK exhibited reduced colony-forming-megakaryocyte numbers and decreased peripheral platelets; (3) *Gata2* overexpression in BM LSK resulted in increased colony-forming-megakaryocyte numbers and megakaryopoiesis; (4) BM erythroid /megakaryocytic features of dysplasia were frequently observed in GATA2 haploinsufficiency syndromes; and (5) approximately 20% of GATA2 haploinsufficient patient harbouring MDS/AML had peripheral thrombocytopenia (Gao et al., 2013, Huang et al., 2009, Donadieu et al., 2018, Calvo et al., 2011). Interestingly, megakaryocytes also regulate HSCs cycling and quiescence by secreting important factors as CXCL4, TPO, and TGFB1 (Bruns et al., 2014, Nakamura-Ishizu et al., 2014b, Zhao et al., 2014). Thus, it is possible that MPP2 expansion may positively correlate with HSCs quiescence in *Gata2* haploinsufficient mice.

On the other hand, bipotent MPP4 progenitors from *Gata2* haploinsufficient mice produced low numbers of Pre-GM that ultimately generated a low number of GMPs without affecting CLP numbers. Since MPP4 is functionally similar to LMPPs (Pietras et al., 2015), we confirmed that the reduction of Pre-GM/GMP axis was due to reduced MPP4/LMPP numbers. However, no difference in the frequencies of mature myeloid cells was observed in *Gata2* haploinsufficient mice. These findings might be interpreted by the fact that mature cells express *Gata2*-mRNA at very low levels, and *Pu.1* transcription factor promotes myeloid differentiation by inhibiting *Gata2* expression (Menendez-Gonzalez et al., 2019b, Orlic et al., 1995, Guo et al., 2013, Walsh et al., 2002). In line with reduced GMP population from the hierarchical differentiation of HSCs from *Gata2* haploinsufficient mice, RNA-Seq results showed that genes involved in myeloid cells accumulation and migration were downregulated such as *L3mbtl3, Ccr1, Cxcr1, Ermap, Neo1,* and *Spon2*.

In contrast to young *Gata2* haploinsufficiency mice, CLP numbers were decreased in aged *Gata2* haploinsufficiency mice, while GMP numbers were comparable to control littermates (Table 3.1). No change was observed in the frequencies of myeloid/lymphoid lineage positive cells in aged *Gata2* haploinsufficiency mice. While

Gata2 mRNA was not expressed in the aged CLPs and mature lymphoid cells (Figure 3.15 B), reduced CLP numbers were dependant on the hierarchical differentiation of HSCs due to decreased numbers of LMPPs that highly expressed *Gata2* mRNA. These data suggest that aged *Gata2* haploinsufficient HSCs exhibit a myeloid-biased pattern. In support of these findings, there was a two-fold decrease in aged *Gata2* haploinsufficient CLPs when compared to young *Gata2* haploinsufficient CLPs, normal frequency of aged *Gata2* haploinsufficient GMPS, the proportion of monocyte/macrophage cells was increased by a half-fold in aged *Gata2* haploinsufficiency mice as compared with young *Gata2* haploinsufficient monocyte/macrophage cells, and donor derived-cells from aged *Gata2* haploinsufficient HSCs showed around a two-fold increase in myeloid cells and a two-fold reduction in CD4-cells as compared with young counterparts. Additionally, increased myeloid numbers in aged *Gata2* haploinsufficient mice support these earlier findings, in which elderly *Gata2* hypomorphic mutant mice that express about 20% of GATA2 level show peripheral granulomonocytosis with myeloid/erythroid/megakaryoid dysplastic features and develop equivalent haematological phenotypes to human CMML (Harada et al., 2019).

Collectively, the above findings describe the impact of *Gata2* haploinsufficiency on HSPCs and haematopoiesis. *GATA2* mutations impair a -77kb cis-element, which causes immunodeficiency due to perturbed HSCs generation, and +9.5kb cis-element, which associates with myeloid neoplasms (Johnson et al., 2015, Gao et al., 2013, Hsu et al., 2013). With regards to GATA2 haploinsufficiency roles in leukaemogenesis as a transcriptional repressor, some genes involved in haematological malignancies were upregulated in RNA-Seq data such as *Ddx41, Ptpn1, Cd133, Epg5, Plekhm2, Pmel, and Ubap1*. In agreement with the notion that GATA2 haploinsufficient HSCs cause immunodeficiency disorders (Vinh et al., 2010, Dickinson et al., 2011, Bigley et al., 2011, Ostergaard et al., 2011), RNA-Seq analysis disclosed dysregulation of biological pathways involved in the regulation of immune response processes as IFNy signalling, IL-10 signalling, Toll-like receptor signalling, humoral immune response, and Agranulocyte adhesion/diapedesis. Recent reports suggest B-lymphocytopenia that arises due to differentiation defects in B-cells from

HSCs/multi-lymphoid-progenitors axis is the early sign of GATA2 haploinsufficiency syndromes (Koegel et al., 2016, Novakova et al., 2016, Donadieu et al., 2018). While we did not observe defects in B-cells in our model, RNA-Seq data displayed that *Ebf1, Cd38, Clcf1, Cd23,* and *Palm* genes that involved in B-lymphopoiesis were dysregulated.

Upregulation of IFN-γ signalling was also observed in young *Gata2* haploinsufficient HSCs. IFN-γ is a proinflammatory cytokine and has essential roles in the regulation of HSCs fate. Previous findings utilising both murine and human cord-blood HSCs have reported that IFN-γ decreases HSCs proliferation and ultimately perturbs HSCs pool size and causes a defect in HSCs self-renewal and multi-lineage repopulating activities (de Bruin et al., 2013, Yang et al., 2005). Other reports have suggested that IFN-γ increases HSCs proliferation and differentiation (mainly macrophages) and leads to HSCs exhaustion and a self-renewal defect (Baldridge et al., 2010, Smith et al., 2016). Additionally, IFN-γ is highly expressed in the BM of aplastic-anaemia patients (Zoumbos et al., 1985). Given that GATA2 haploinsufficiency is associated with the aplastic-anaemia development (Tong et al., 2000), the emerged haematological phenotypes of IFN-γ are highly coordinated with *Gata2* haploinsufficient HSCs phenotypes. In this regard, *Gata2* haploinsufficient HSCs exhibited a reduction in HSC numbers, a multilineage defect in competitive transplant experiments, impaired self-renewal capacity in secondary recipient hosts, increased proliferative activity of aged HSCs, and increased monocyte/macrophage frequencies in aged *Gata2* haploinsufficiency mice as compared with young counterparts. Taken together, these findings provide some evidence to suggest that it is possible that *Gata2* haploinsufficient HSCs cause immunodeficiency through upregulation of IFN-γ signalling.

It is a well-known fact that accumulation of the DNA damage impairs HSCs homeostasis and enhances leukaemogenesis (Biechonski et al., 2017, Mohrin et al., 2010). GSEA analysis displayed that up-regulated genes were associated with DNA repair pathways. We further observed dysregulation of genes such as *Dmc1, Mnd1, Pif1, Polq, Supt16, Lig1, Anapc5, Txnl4b,* and *Usp4* involved in dsDNA-break repair by

homologous recombination and base-excision repair pathways. Increased DNA damage was observed in young *Gata2* haploinsufficient HSCs and aged *Gata2* haploinsufficient HSCs that were transplanted. Given that damaged DNA in quiescent HSCs is managed by the nonhomologous end-joining (NHEJ) repair pathway that potentially enhances mutagenesis, it is possible that enhanced quiescence in young *Gata2* haploinsufficient HSCs makes them more susceptible to transformation (Mohrin et al., 2010). Collectively, these results suggest that GATA2 haploinsufficiency impairs genomic integrity in HSPCs and likely increases the probability of developing secondary somatic genetic disorders, such as *ASXL1*, that lead to haematological malignancies.

Table 3.1: Haematological characteristics of young and aged *Gata2$^{+/fl}$; Vav-iCre^{+}* mice.

	Young *Gata2$^{+/fl}$; Vav-iCre^{+}*	Aged *Gata2$^{+/fl}$; Vav-iCre^{+}*
HSPCs	↓ HSCs, MPPs, HPC1, and LMPPs ↑ HPC2	↓ HSCs, MPPs, and LMPPs
Committed progenitors	↓ GMPs	↓ CLPs
Mature cells (PB)	↓ Platelets	No difference
Lineage positive cells (BM and spleen)	↓ Megakaryocytes	Not assessed
Lymphoid cells (thymus)	No difference	No difference
Cell cycle status	↑ HSCs frequency in G0 phase ↓ HSCs frequency in G1 phase	↓ HSCs frequency in G0 phase ↑ HSCs frequency in S/G2/M phases
Apoptosis level	↑ HSCs and MPPs	↑ MPPs
HSCs repopulation potential	A multi-lineage defect	A multi-lineage defect
HSCs self-renewal potential	A defect in HSCs self-renewal	Not assessed

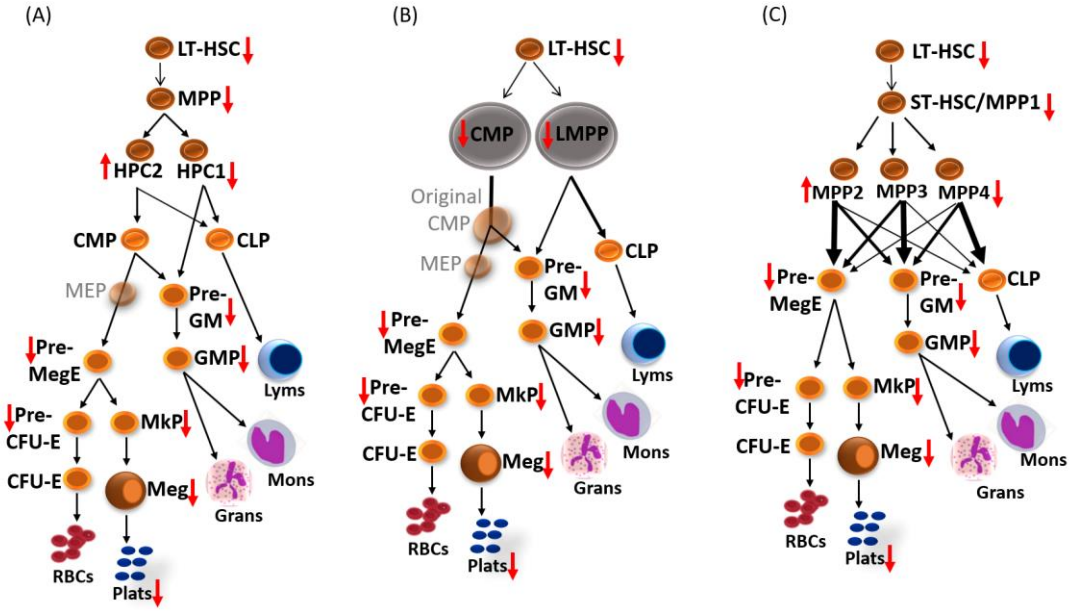

Figure 3-22: Haematopoietic hierarchy phenotypes in young *Gata2*$^{+/fl}$; *Vav-iCre*$^{+}$ mice.

CHAPTER 4 : Examining the role of acute induction of *Gata2* haploinsufficiency in the adult haematopoietic system

4.1 Introduction

Somatic mutations of *GATA2* as a secondary genetic disorder are observed in AML patients with blast transformation of CML and inherited *CEPBα* mutations, and they are implicated in the pathogenesis of myeloid neoplasms (discussed in section 1.3.5.5) (Zhang et al., 2008, Greif et al., 2012, Green et al., 2013). However, little is known about the biological effects of the acute induction of *Gata2* haploinsufficiency on adult HSPCs activity. Following the assessment of the effect of chronic loss of *Gata2* haploinsufficiency in adult and aged haematopoietic compartments, we therefore employed Mx1-Cre mouse models to evaluate the impact of acute induction of *Gata2* haploinsufficiency in adult haematopoiesis.

The expression of Mx1 promoter is triggered in an interferon-dependent manner by administering of synthetic double-stranded RNA of Polyinosinic-Polycytidylic acid (pIpC) (Kuhn et al., 1995). Given that the Mx1 promoter is expressed not only in the haematopoietic cells but also in the BM microenvironment cells (BM niches) (Joseph et al., 2013), there are two available experimental approaches to evaluate the acute induction of *Gata2* haploinsufficiency: a cell-autonomous experiment, in which the Mx1-Cre promoter induces the floxed *Gata2* allele deletion specifically within the haematopoietic cells, and the non-cell-autonomous experiment, in which the Mx1-Cre promoter broadly induces *Gata2* heterozygote deletion in both haematopoietic populations and BM niches. With a view to mimicking what happens on induction of sporadic GATA2 mutations clinically, this chapter will therefore assess the impact of acute induction of *Gata2* haploinsufficiency on HSPCs in these settings.

4.1.1 Objectives

The aims of this chapter are:

1. To elucidate the impact of acute induction of *Gata2* haploinsufficiency on the adult haematopoietic system in non-cell- and cell-autonomous manners.
2. To assess the self-renewal capacity of acutely induced *Gata2* haploinsufficient HSCs in serial transplant experiments.
3. To reveal transcriptional signature after acute induction of *Gata2* haploinsufficiency in HSCs by RNA-sequencing.

4.2 Acute induction of *Gata2* haploinsufficiency in the adult mouse haematopoietic system

4.2.1 Generation of *Gata2$^{+/fl}$; Mx1-Cre^{+}* mice

To interrogate the role *Gata2* haploinsufficiency in the adult mouse haematopoietic system, we generated *Gata2* heterozygote (*Gata2$^{+/fl}$; Mx1-Cre^{+})* and control (*Gata2$^{+/fl}$; Mx1-Cre^{-})* littermates by crossing *Gata2$^{+/+}$; Mx1-Cre^{+}* and *Gata2$^{fl/fl}$; Mx1-Cre^{-}* mice (Figure 4.1 A). To excise the floxed *Gata2* allele, 7-8 weeks old *Gata2$^{+/fl}$; Mx1-Cre^{+}* and *Gata2$^{+/fl}$; Mx1-Cre^{-}* mice were exposed to 6 doses of pIpC. Since the administration of pIpC is associated with an increase in HSPCs proliferation, the recovery period from the induced interferon type 1 response is 8-10 days (Velasco-Hernandez et al., 2016). Mice were analysed 14 days post the last pIpC injection (Figure 4.1 B). The deletion of the floxed *Gata2* allele was confirmed by PCR from genomic DNA of total BM and c-kit^{+} cells; gel analysis revealed that the deletion was efficient (Figure 4.1 C).

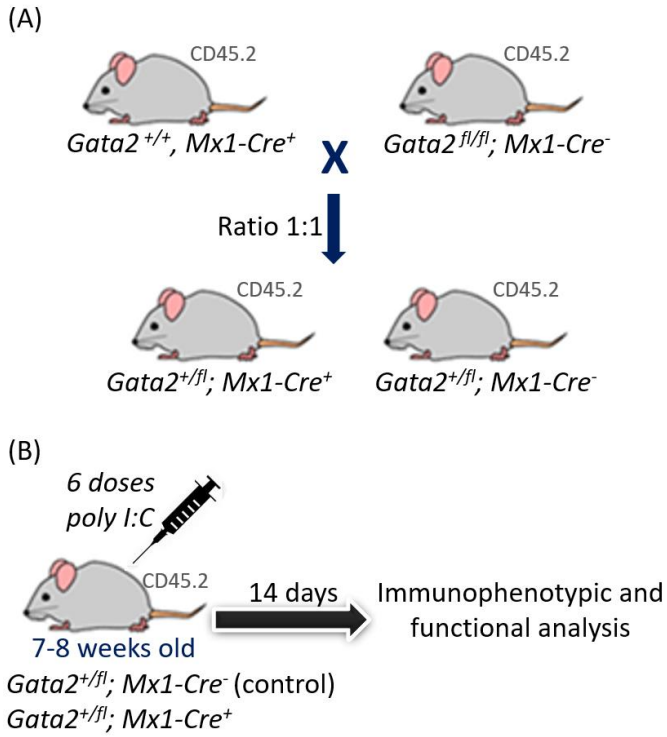

Figure 4-1: Generation of *Gata2 $^{+/fl}$; Mx1-Cre^{+}* mice.

(A) Schematic diagram of the breeding strategy used to produce *Gata2* heterozygote (*Gata2 $^{+/fl}$; Mx1-Cre^{+})* and control (*Gata2 $^{+/fl}$; Mx1-Cre^{-})* littermates. Both animals were normally born in Mendelian ratios. (B) Experimental design, 7-8 weeks old mice had received 6 doses of pIpC every other day by intraperitoneal injection over 10 days (0.3 mg per dose). Immunophenotypic analysis was performed 14 days post the last dose. (**C**) Representative gel analysis of genomic DNA samples of the BM and c-kit+ cells from *Gata2 $^{+/fl}$; Mx1-Cre^{+}* mice. ($^{+}$) indicates wild-type, 717 bp; (^{f}), floxed allele, 844 bp; and excised allele, 181 bp.

4.2.2 Acute induction of *Gata2* haploinsufficiency is dispensable for terminal mature blood cells differentiation

Haematopoietic cell lineages were assessed in the PB, BM, and spleen of adult (11-12 weeks old) *Gata2* heterozygote (*Gata2$^{+/fl}$; Mx1-Cre^{+})* and control mice (*Gata2$^{+/fl}$; Mx1-Cre^{-})* at 14 days after the final pIpC dose. Immunophenotypic analysis revealed no differences in the frequencies of myeloid (Mac1^{+}Gr1^{+} and Mac1^{+}Gr1^{-}), T-lymphocytes (CD4 and CD8), and B-lymphocytes (B220) in the PB of *Gata2$^{+/fl}$; Mx1-Cre^{+}* when compared to control mice (Figure 4.2 A). Total cellularity numbers in BM and spleen were similar in control and *Gata2$^{+/fl}$; Mx1-Cre^{+}* mice (Figure 4.2 B). Likewise, the percentages of myeloid, lymphoid, and erythroid (Ter119) cells in the BM and spleen were comparable between the two littermates (Figure 4.2 C and D). These results indicate that the acute induction of *Gata2* haploinsufficiency does not affect the terminal differentiation of linage positive haematopoietic cells.

4.2.3 Acute induction of *Gata2* haploinsufficiency causes a reduction only in BM HSC numbers

This study next evaluated the impact of acute induction of *Gata2* haploinsufficiency on the frequencies of HSPCs (LSK, Lin^{-}_Sca-1^{+}_c-Kit^{+}; HSCs, LSK_CD150^{+}_CD48^{-}; MPPs, LSK_CD150^{-}_CD48^{-} ; HPC1, LSK_CD150^{-}_CD48^{+}; HPC2, LSK_ CD150^{+}_CD48^{+}; and LMPPs, LSK_CD34^{+}_CD135^{hi}), committed myeloid/lymphoid progenitors (LK, Lin^{-}_Sca1^{-}_c-Kit^{+}; CMPs, LK_CD34^{+}_ CD16/32^{-}; GMPs, LK_CD34^{+}_CD16/32^{+}; MEPs, LK_CD34^{-}_CD16/32^{-}); and CLPs, Lin^{-}_Sca1^{low}_c-Kit^{low}_CD127^{+}) in the BM of acutely deleted *Gata2* haploinsufficient mice (Oguro et al., 2013, Kiel et al., 2005, Akashi et al., 2000, Kondo et al., 1997, Adolfsson et al., 2005). There was a significant decline in the numbers of BM HSCs in *Gata2$^{+/fl}$; Mx1-Cre^{+}* when compared to control mice, whilst the numbers of uncommitted progenitors (MPPs, HPC1, HPC2, and LMPPs) were comparable in both genotypes (Figure 4.3 A and B). At committed progenitor levels, no significant differences in the numbers of myeloid/lymphoid progenitors were noted in both littermates (Figure 4.3 C). Moreover, *in vitro* functional assessment of BM progenitor cells to proliferate and differentiate was examined by performing colony-forming cell (CFC) assays. The numbers of CFU-GEMM, BFU-E,

CFU-GM, CFU-M and CFU-G colonies were indistinguishable in both *Gata2* heterozygote and control BM cells (Figure 4.3 D). Together, these findings imply that acute deletion of *Gata2* haploinsufficiency exclusively disrupts adult HSCs pool size.

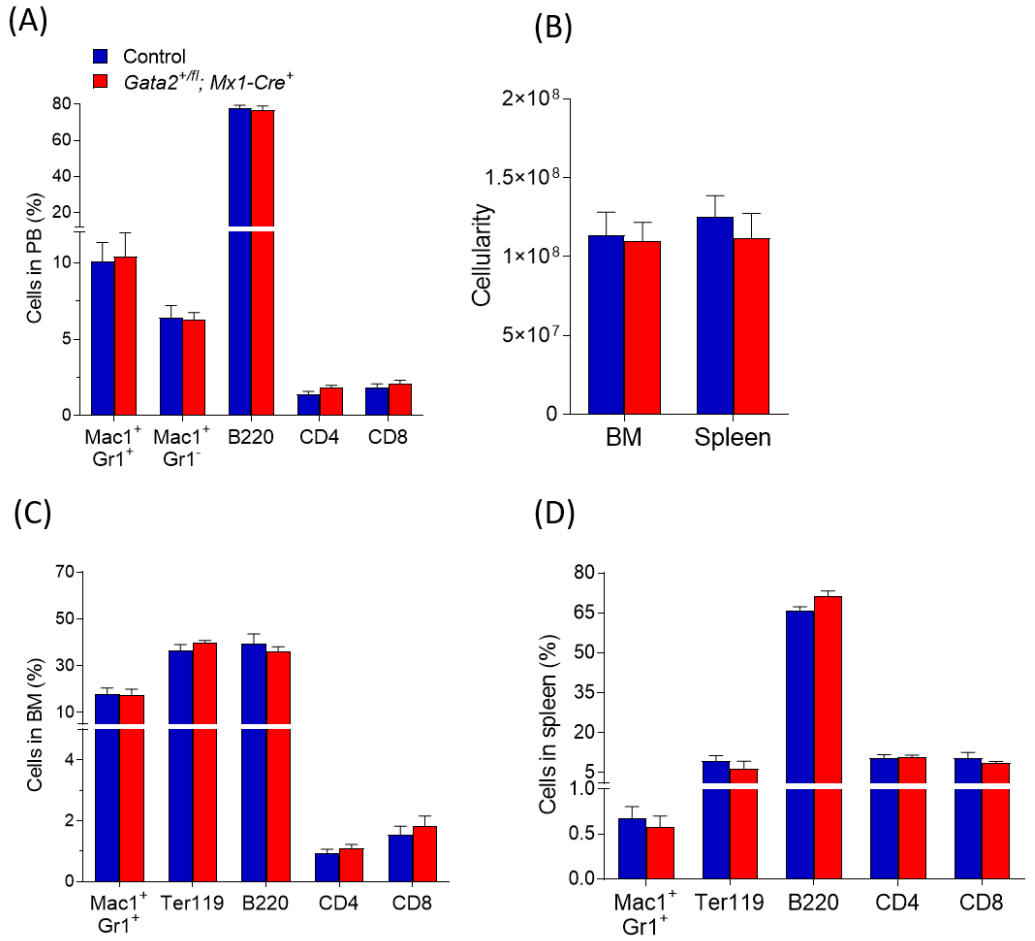

Figure 4-2: Acute induction of *Gata2* haploinsufficiency has no impact on terminal mature blood cell differentiation.

(A) The percentages of myeloid ($Mac1^+Gr1^+$_$Mac1^+Gr1^-$), and lymphoid cells (CD4_ CD8_B220) in PB of control (n=6) and *Gata2*$^{+/fl}$*; Mx1-Cre*$^+$ (n=6) mice from two independent experiments. (B) Total cell numbers in BM (from two-femurs and two-tibias (cells/30mL)) and spleen (cells/7mL) and from control (n=6) and *Gata2*$^{+/fl}$*; Mx1-Cre*$^+$ (n=6) mice from two separate experiments. (C and D) Proportions of lineage positive cells in BM (C) and spleen (D) from control (n=6) and *Gata2*$^{+/fl}$*; Mx1-Cre*$^+$ (n=6) mice from two independent biological experiments. Presented data are mean ± SEM. Statistical analysis: Mann-Whitney U test.

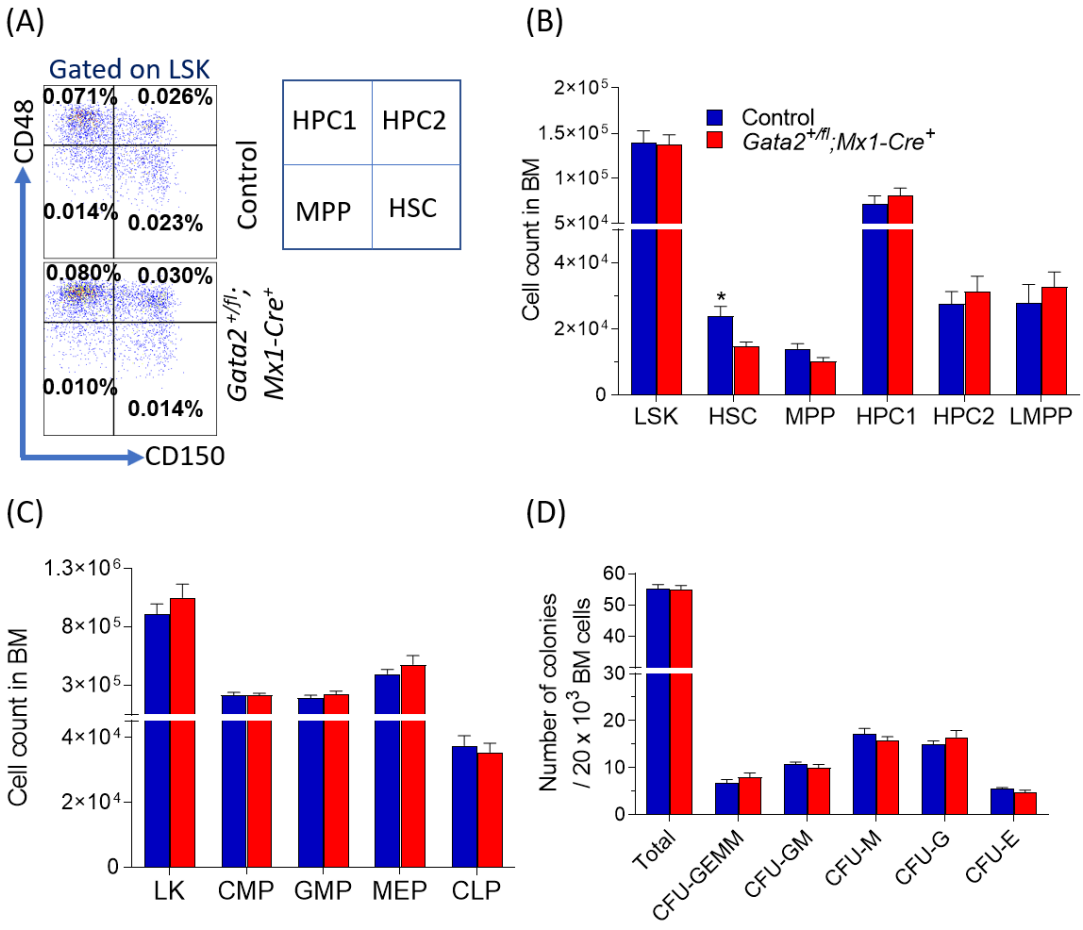

Figure 4-3: Acute induction of *Gata2* haploinsufficiency reduces HSC numbers.

(A) Representative FACS plots (Lift-hand) and gating method (Right) show the frequencies of primitive BM HSPCs of control (n=6) and *Gata2*$^{+/fl}$*; Mx1-Cre*$^{+}$ (n=6) mice from two independent experiments. (B and C) The absolute numbers of HSPCs (HSCs, HPC1, HPC2, MPPs, and LMPPs) (B) and committed myeloid/lymphoid progenitors (CMPs, GMPs, MEPs, and CLPs) (C) in the BM of control (n=6) and *Gata2*$^{+/fl}$*; Mx1-Cre*$^{+}$ (n=6) mice from two separate experiments. (D) The number of CFC colonies of *Gata2* heterozygote and control BM cells. 20x10^3 BM cells from both genotypes were plated in M3434 semisolid-methylcellulose media, and colonies were counted 12 days post plating. n=4 for each genotype from two independent experiments. CFU indicates colony-forming unit; CFU-GEMM, CFU_Granulocyte_Erythrocyte_Macrophage_Megakaryocyte; CFU-GM, CFU_ Granulocyte_ Macrophage; CFU-M, CFU_Macrophage; CFU-G, CFU_Granulocyte; and CFU-E, CFU_Erythroid. Data represent mean ± SEM. Statistical analysis: Mann-Whitney U test *, P < 0.05.

4.2.4 Acute induction of *Gata2* haploinsufficiency does not perturb HSPCs survival

To evaluate whether altered cellular survival of HSCs in acutely deleted *Gata2* haploinsufficient mice reduces the abundance of HSCs, the annexin V assay was performed (Wallberg et al., 2016). Flow cytometric analysis revealed that the frequencies of total apoptosis of BM LSK, HSCs, MPPs HPC1, and HPC2 were comparable in both *Gata2*$^{+/fl}$*; Mx1-Cre*$^{+}$ and control mice (Figure 4.4 A). These results demonstrate that cell survival of HSPCs is unimpaired in adult *Gata2* haploinsufficient mice following acute deletion.

4.2.5 Acute induction of *Gata2* haploinsufficiency promotes HSCs quiescence

Next, utilising Ki-67 assays, cellular proliferation in HSPCs of *Gata2* haploinsufficiency mice was assessed as another possible mechanism for reduced HSC abundance (Gerdes et al., 1984). Immunophenotypic analysis showed that the frequency of HSCs in the G0 stage was significantly higher in the BM of *Gata2*$^{+/fl}$*; Mx1-Cre*$^{+}$ when compared with control mice, while the frequency of HSCs in G1 and G2/S/M phases were similar in both littermates (Figure 4.4 B and C). No difference was noticed in the percentages of BM MPPs, HPC1, and HPC2 in G0, G1, and S/G2/M phases in both genotypes (Figure 4.4 C). These findings signify that acute induction of *Gata2* haploinsufficiency reduces HSC numbers in correlation with enhanced cellular quiescence.

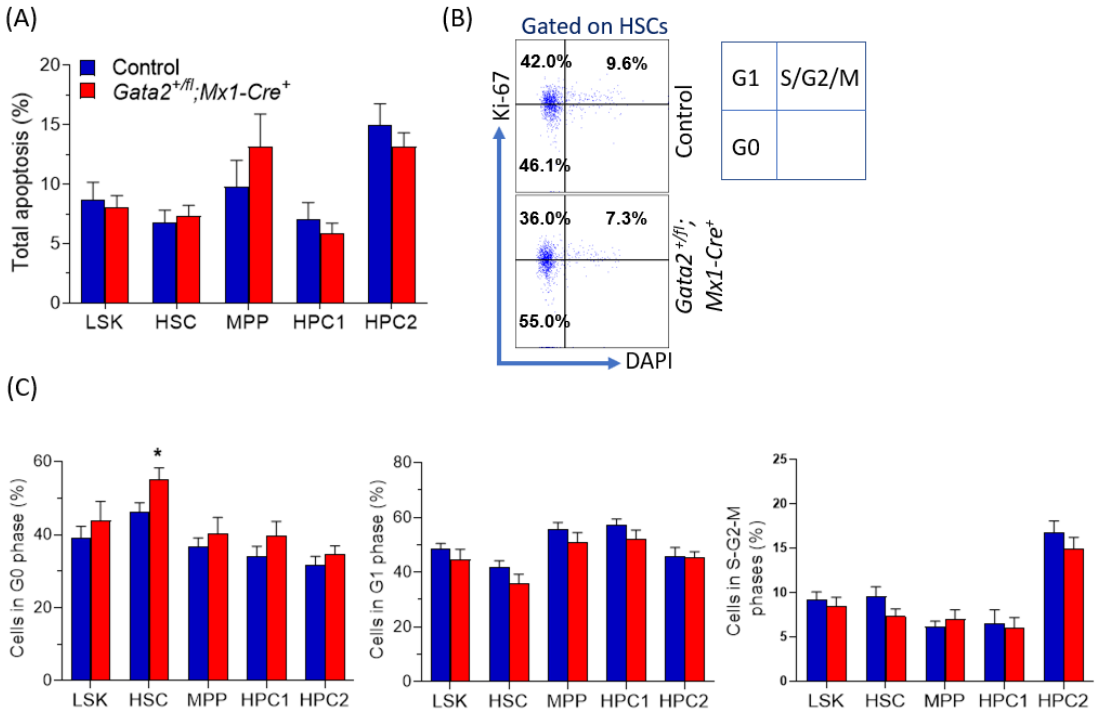

Figure 4-4: Acute induction of *Gata2* haploinsufficiency promotes BM HSCs quiescence.
(A) The percentages of total apoptotic cells in HSPCs (LSK, HPC1, HPC2, HSC, and MPP) of control (n=6) and *Gata2*$^{+/fl}$*; Mx1-Cre*$^{+}$ (n=6) mice from two independent experiments. Total apoptosis indicates the percentage of early (annexin V^{+}_DAPI^{-}) plus late apoptosis (annexin V^{+}_DAPI^{+}). (B) Representative FACS plots and gating strategy of BM HSCs in the cell cycle phases from control (n=6) and *Gata2*$^{+/fl}$*; Mx1-Cre*$^{+}$ (n=6) mice from two separate experiments. G0-phase indicates ki67^{-}_DAPI^{-}; G1-phase, ki67^{+}_DAPI^{-}; and S/G2/M phases, ki67^{+}_DAPI^{+}. (C) proportions of BM HSPCs in the cell cycle phases from control (n=6) and *Gata2*$^{+/fl}$*; Mx1-Cre*$^{+}$ (n=6) mice from two different experiments. Data represent mean ± SEM. Statistical analysis: Mann-Whitney U test *, P < 0.05.

4.3 Cell autonomous roles of *Gata2* following acute induction of *Gata2* haploinsufficiency in adult mouse haematopoietic compartments

4.3.1 Acute induction of *Gata2* haploinsufficiency autonomously perturbs the distribution of primitive HSPCs and committed progenitors

Since Mx1-Cre mediates recombination in both haematopoietic compartments and BM niches, we performed cell-autonomous experiments to assess the impact of the acute induction of *Gata2* haploinsufficiency in the adult haematopoietic compartments. To do this, unfractionated BM cells from either untreated *Gata2*$^{+/fl}$*; Mx1-Cre*$^{+}$ or control (*Gata2*$^{+/fl}$*; Mx1-Cre*$^{-}$) (CD45.2) mice together with competitor unfractionated CD45.1 BM cells were injected into lethally-irradiated recipient hosts (CD45.1). Subsequently, the recipient mice received 6 doses of pIpC over 10 days at week 8 post-transplantation to excise the floxed *Gata2* allele. PB, BM, and spleen were harvested at 14 days post the last dose to analyse donor contributions for HSPCs, committed progenitors, and multi-lineage (Figure 4.5 A).

Given the spontaneous activity of Mx1 promoter (Velasco-Hernandez et al., 2016), we firstly assessed the donor contribution at week 8 post-transplant before pIpC injections. No difference was observed in the total donor contribution and donor-derived myeloid/lymphoid cells in PB of both genotypes. Haematopoietic tissues were collected at 14 days after the last dose of pIpC to perform immunophenotypic analysis. The frequency of total CD45.2 donor contribution was significantly lower in PB (Figure 4.5 B) and BM (Figure 4.6 A) of *Gata2*$^{+/fl}$*; Mx1-Cre*$^{+}$ donor-cells as compared with control donor-cells. There was a significant diminution in the frequency of CD45.2 donor contribution for myeloid-cells (Mac1^{+}Gr1^{+} and Mac1^{+}Gr1^{-}) and T-cells (CD4^{+} and CD8^{+}) in PB of *Gata2*$^{+/fl}$*; Mx1-Cre*$^{+}$ donor-cells when compared with control donor-cells, whilst the donor contribution for B-cells (B220^{+}) was comparable in both donor genotypes (Figure 4.5 B). The proportion of donor contribution for myeloid and T-cells was diminished in BM and spleen of *Gata2*$^{+/fl}$*; Mx1-Cre*$^{+}$ donor-cells, whereas frequencies of donor cells for B-cells (B220^{+}) and erythroid-cells (Ter119^{+}) in BM and

spleen were similar in both *Gata2*$^{+/fl}$*; Mx1-Cre*$^{+}$ and control donor-cells (Figure 4.6 A and B).

Evaluating the donor contribution for primitive HSPCs and committed myeloid/lymphoid/erythroid/megakaryocyte progenitors revealed that the frequency of CD45.2 *Gata2*$^{+/fl}$*; Mx1-Cre*$^{+}$ donor-cells was significantly declined for BM LSK, HSC, MPPs, HPC1, HPC2, LK, CMPs, GMPs, MEPs, and CLPs when compared with control donor-cells (Figure 4.6 C and D). We next explored whether the cellular survival of HSPCs was affected in this setting. Annexin V assays showed that the frequency of total apoptosis was higher in BM HSCs and MPPs of *Gata2*$^{+/fl}$*; Mx1-Cre*$^{+}$ derived-cells, whilst decreased apoptosis in HPC2 was observed in *Gata2*$^{+/fl}$*; Mx1-Cre*$^{+}$ derived-cells as compared with control derived-cells, implying that increased apoptosis level was associated with decreased numbers of HSC derived-cells (Figure 4.6 E). Collectively, these results indicate that acute deletion of *Gata2* haploinsufficient HSCs fails to adequately reconstitute primitive HSPCs, myeloid/lymphoid restricted progenitors, and multi-lineage in a cell-autonomous manner.

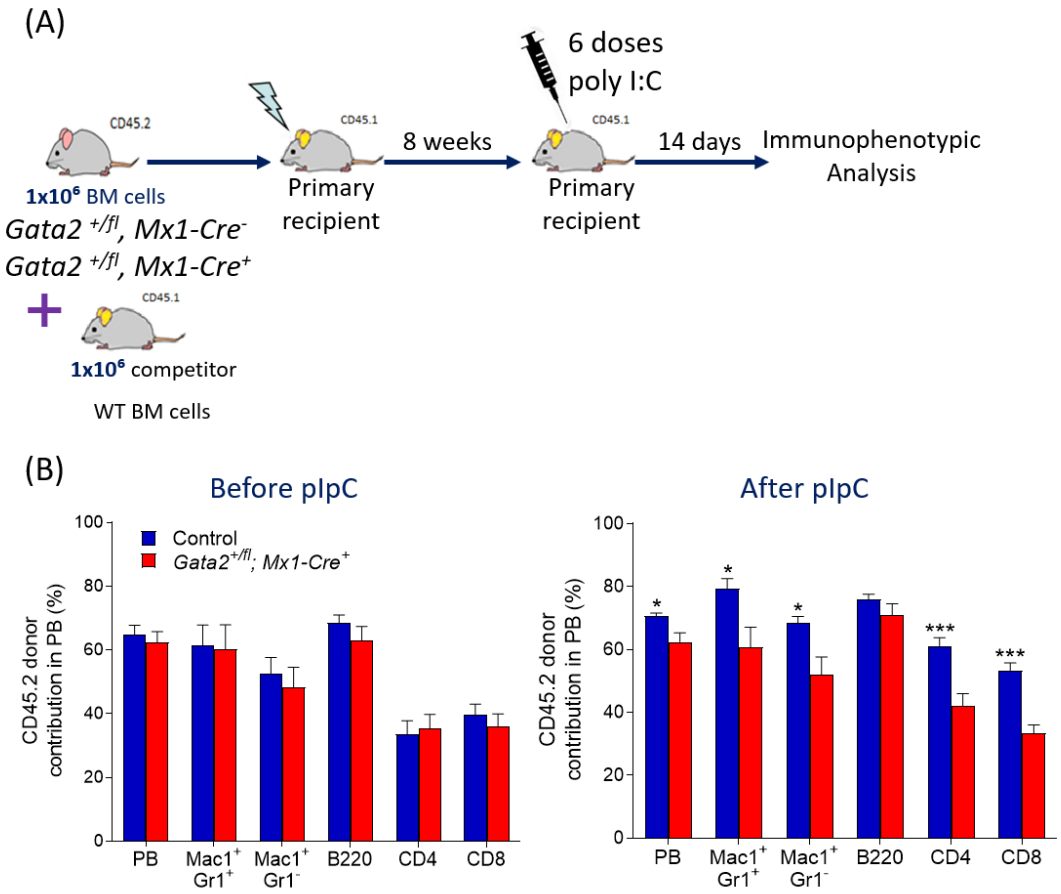

Figure 4-5: Acute induction of *Gata2* haploinsufficiency autonomously perturbs the distribution of peripheral mature cells.

(A) Experimental design of primary competitive transplant experiments, $1x10^6$ CD45.2 BM cells from untreated *Gata2*$^{+/fl}$*; Mx1-Cre*$^{+}$ and control mice alongside with $1x10^6$ CD45.1 support BM cells were transplanted into lethally-irradiated CD45.1 recipients by tail-vein injection. At week 8 post-transplant, primary recipient mice were injected with 6 doses of pIpC. 14 days after the last injection, PB, BM, and spleen cells were collected for FACS analysis. (B) Proportions of total CD45.2 cells and donor contribution for myeloid (Mac1^{+}Gr1^{+}, Mac1^{+}Gr1^{-}), B-cells (B220^{+}) and T-cells (CD4^{+}, CD8^{+}) in PB prior (Left-hand) and post (Right) pIpC injections from *Gata2*$^{+/fl}$*; Mx1-Cre*$^{+}$ (n=9) and control (n=9) donor-cells from two independent experiments. Four independent biological donors were used for each group. Data represent mean ± SEM. Statistical analysis: unpaired, 2-tailed t-test. *, $P < 0.05$; **, $P < 0.01$; ***, $P < 0.001$.

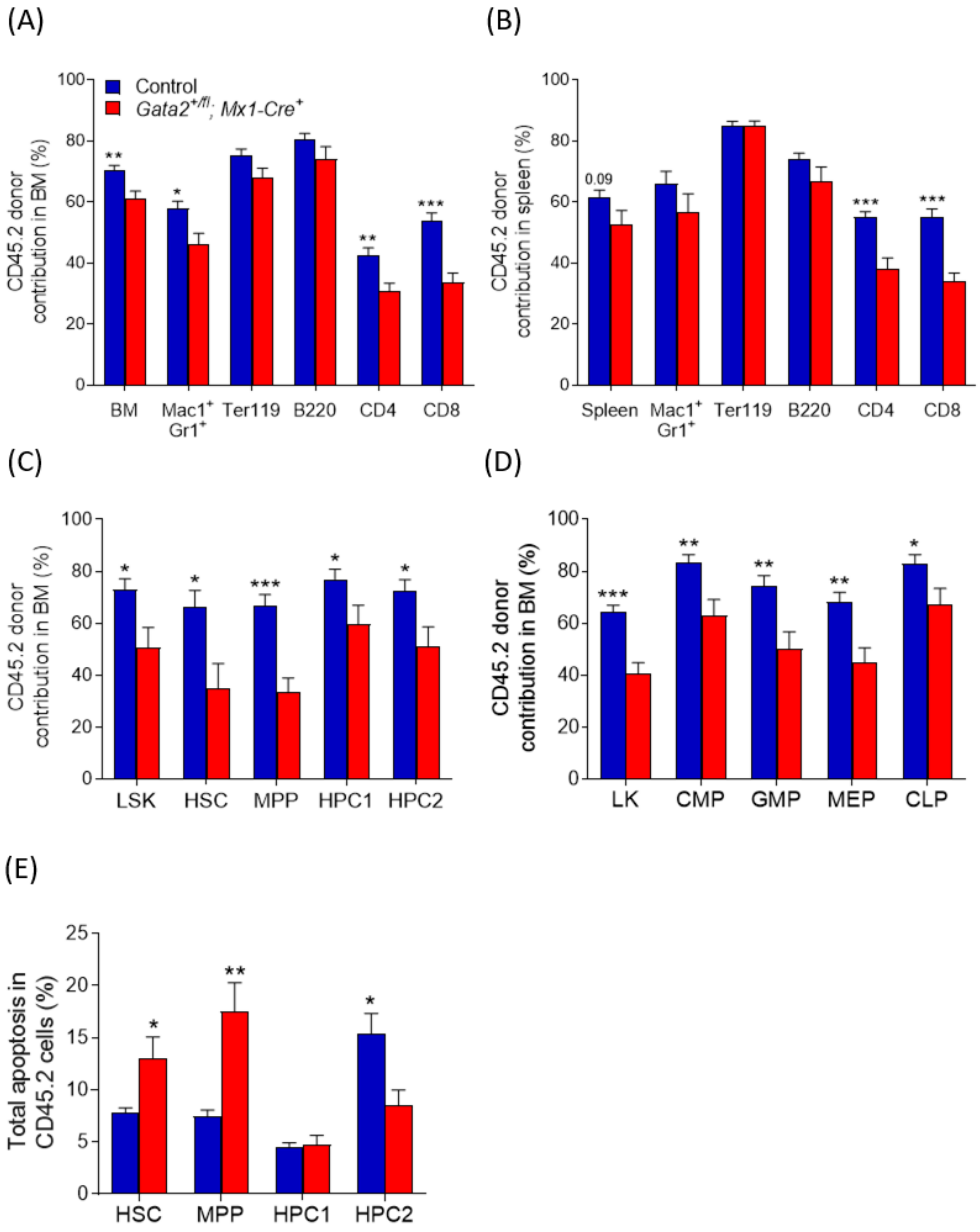

Figure 4-6: Acute induction of *Gata2* haploinsufficiency autonomously perturbs the distribution of primitive HSPCs and committed progenitors.

(A and B) Frequencies of total CD45.2 and donor contribution for myeloid ($Mac1^+Gr1^+$, $Mac1^+Gr1^-$), erythroid (Ter119), B-lymphoid (B220), and T-lymphoid (CD4, CD8) in BM (A) and spleen (B) from *Gata2*$^{+/fl}$*; Mx1-Cre*$^+$ (n=9) and control (n=9) donor-cells from two separate experiments. Unpaired, 2-tailed t-test. (C and D) Proportions of donor cells for BM HSPCs (HSCs, MPPs, HPC1, and HPC2) (C) and committed myeloid/lymphoid/erythroid /megakaryocytes progenitors (CMPs, GMPs, MEPs, and CLPs) (D) from control (n=9) and *Gata2*$^{+/fl}$*; Mx1-Cre*$^+$ (n=8) donor-cells from two independent experiments. Unpaired, 2-tailed t-test. (E) Percentages of total apoptosis in the BM HSPCs of control (n=6) and *Gata2*$^{+/fl}$*; Mx1-Cre*$^+$ (n=6) derived-cells from two separate experiments. Total apoptosis equals the percentage of early apoptosis (annexin V^+_$DAPI^-$) plus late apoptosis (annexin V^+_$DAPI^+$). Mann-Whitney U test. Four independent donors were used for each genotype. Data are mean ± SEM. *, $P < 0.05$; **, $P < 0.01$; ***, $P < 0.001$.

4.3.2 Acute deletion of *Gata2* haploinsufficiency autonomously impairs adult HSCs self-renewal capacity

In order to evaluate the self-renewal capability of acutely deleted *Gata2* haploinsufficient HSCs, we conducted serial transplant experiments. To this end, sorted CD45.2 HSCs (LSK_CD150^{+}CD48^{-}) from both *Gata2$^{+/fl}$; Mx1-Cre^{+}* and control donor derived-cells were mixed with CD45.1 support BM cells and injected into secondary CD45.1 recipient-hosts. PB was tested every month for donor cell chimerism until 4 months after transplantation. At week 16, BM and spleen were harvested for analysis at week 16 post-transplant (Figure 4.7 A).

The follow-up PB analysis post-transplant showed that CD45.2 cells severely dropped in PB of *Gata2$^{+/fl}$; Mx1-Cr^{+}* donor cells when compared to control donor cells during the whole period (Figure 4.7 B). The reduction of CD45.2 derived cells was reflected in reduced donor contribution for myeloid cells (Ma1^{+}Gr1^{+} and Ma1^{+}Gr1^{-}), T-cells (CD4 and CD8), and B-cells (B220) of *Gata2$^{+/fl}$; Mx1-Cr^{+}* donor cells (Figure 4.7 C). Likewise, there was a significant decrease in the frequency of CD45.2 derived cells in BM and spleen of *Gata2$^{+/fl}$; Mx1-Cre^{+}* donor cells when compared to control donor cells (Figure 4.7 D). These observations indicate that acute deletion of *Gata2* haploinsufficient HSCs is incapable of repopulating multilineage haematopoietic cells in serial transplant experiments. Thus, *Gata2* is a significant regulator of adult HSCs self-renewal.

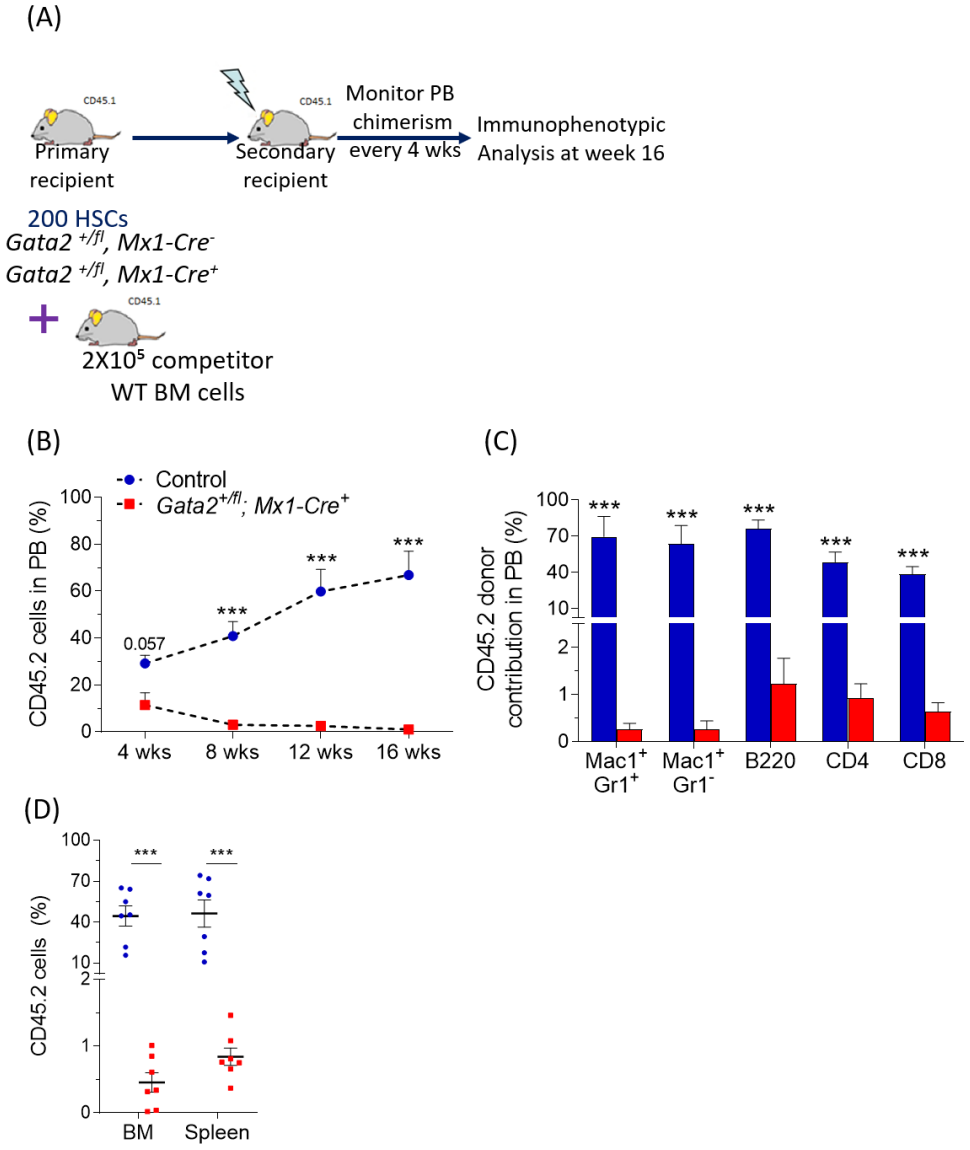

Figure 4-7: Acute induction of *Gata2* haploinsufficiency autonomously impairs adult HSCs self-renewal capacity.

(A) A scheme of secondary competitive transplant experiments, enriched 200 CD45.2 HSCs from *Gata2*$^{+/fl}$*; Mx1-Cre*$^{+}$ and control donor derived-cells from primary recipient mice at day 14 post the last pIpC dose together with 2x10^{5} CD45.1 support BM cells were transplanted to secondary lethally CD45.1-irradiated recipients. (B) Frequencies of total CD45.2^{+} cells during the whole experimental interval in PB of Gata*2*$^{+/fl}$*; Mx1-Cre*$^{+}$ (n=7) and control (n=7) donor cells from two independent experiments. (C) Proportions of CD45.2 donor contribution for myeloid-cells (Mac1^{+}Gr1^{+}, Mac1^{+}Gr1^{-}), T-cells (CD4 and CD8), and B-cells (B220) in PB at week 16 post-transplantation of Gata*2*$^{+/fl}$*; Mx1-Cre*$^{+}$ (n=7) and control (n=7) donor cells from two different experiments. (D) Frequencies of total CD45.2^{+} cells in BM and spleen at week 16 after-transplant from Gata*2*$^{+/fl}$*; Mx1-Cre*$^{+}$ (n=7) and control (n=7) donor cells from two separate experiments. Four different donors were used for each genotype. Data represent mean ± SEM. Statistical analysis: Mann-Whitney U test *, P < 0.05; **, P < 0.01; ***, P < 0.001.

4.4 Acute induction of *Gata2* haploinsufficiency in HSCs induces transcriptional alterations involved in proinflammatory signalling and ECM regulations

To identify transcriptomic changes in acutely deleted *Gata2* haploinsufficient HSCs, we carried out RNA-sequencing (RNA-seq) analysis. At day 14 post the last pIpC injection, HSCs (LSK_CD150^{+}CD48^{-}) were purified from both *Gata2$^{+/fl}$; Mx1-iCre^{+}* and control mice, and extracted RNA was used for RNA-seq. Analysis of RNA-Seq data utilising DEseq2 computing-software identified 79 significantly differentially regulated genes with FDR values less than 0.05 in *Gata2* haploinsufficient HSCs as compared to control HSCs, including 41 genes whose expression was up-regulated and 38 genes whose expression was down-regulated (Figure 4.8 A). Gene ontology (GO) analysis of differentially dysregulated genes utilising IPA database showed that molecular and biological processes were affected in *Gata2* haploinsufficient HSCs, including cellular proliferation, cellular maintenance, cell morphology, cellular assembly and organisation, and nervous system development and function (Figure 4.8 B). We employed ICP and GSEA molecular signatures database to investigate which biological pathways were changed in *Gata2* haploinsufficient HSCs. ICP analysis showed dysregulated pathways involved in cellular assembly and organisation (Paxillin signalling, Macropinocytosis signalling, Selenocysteine biosynthesis II, and Chondroitin sulfate degradation), and HSCs maintenance and proliferation (IL-4 signalling, and Prolactin signalling) (Figure 4.8 C). In GSEA analysis, we uncovered that downregulated genes were involved in IL-6 signalling and extracellular matrix (ECM) receptor interaction (Figure 4.8 D). Down-regulated ECM receptors were associated with dysregulated genes that were involved in cellular maintenance, cytoskeleton organisation and cell adhesion molecules (Figure 4.9). Consistent with the observed HSC phenotype after acute induction of *Gata2* haploinsufficiency, significantly dysregulated genes were involved in haematopoiesis and cell cycle regulation (Figure 4.9). Collectively, these data suggest that *Gata2* regulates the interaction between HSCs and ECM proteins/molecules to sustain HSCs development, differentiation and proliferation. Additionally, *Gata2* haploinsufficiency perturbs signalling pathways that participate in HSCs maintenance and proliferation such as IL6, IL-4, and prolactin signalling.

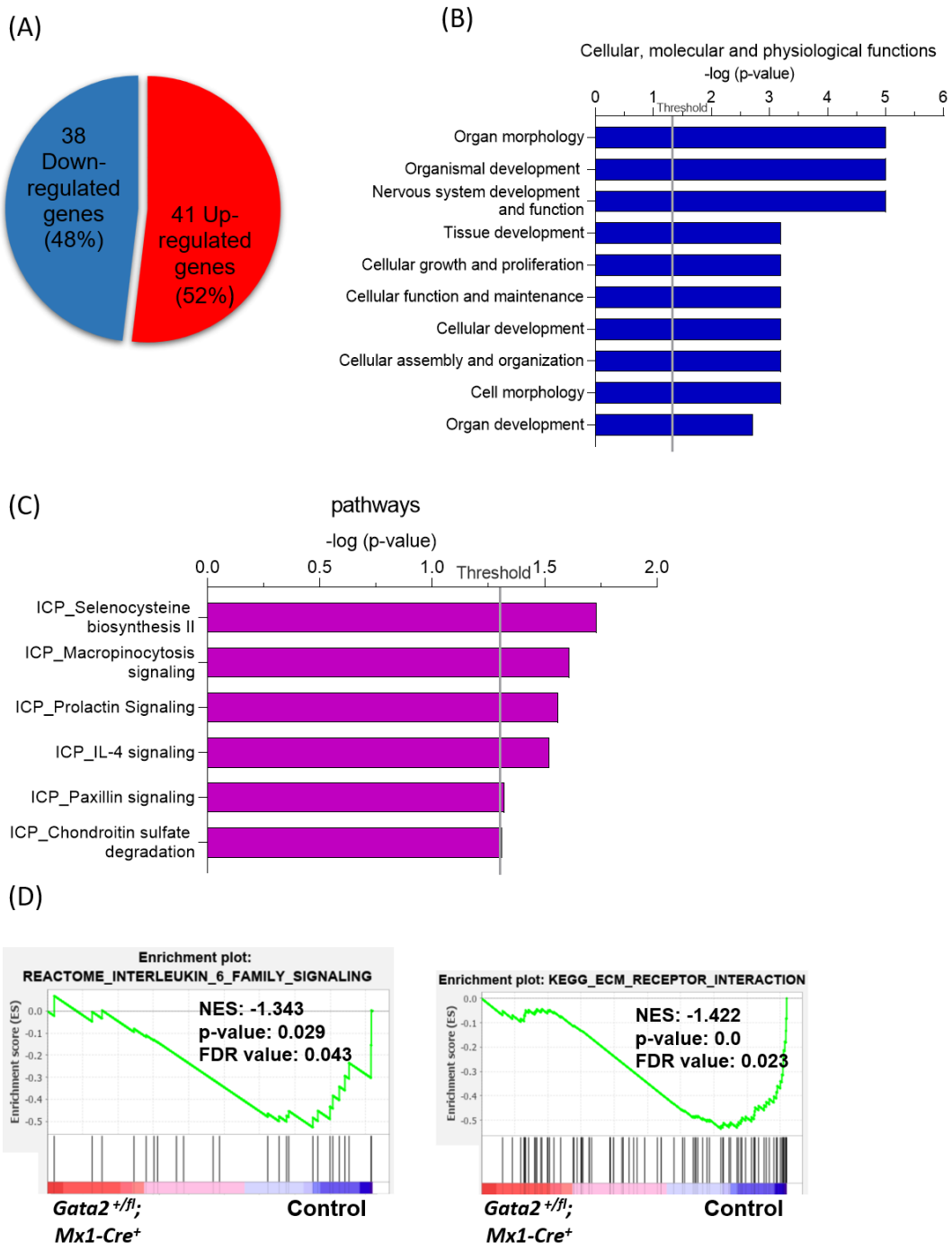

Figure 4-8: Acute loss of *Gata2* haploinsufficient HSCs induces transcriptional alterations. (A) The Venn graph shows the numbers of significantly differentiated genes in purified HSCs at 14 days following the administration of pIpC from *Gata2*$^{+/fl}$*; Mx1-Cre*$^{+}$ (n=4) and control (n=4) mice. Significant genes were determined using DEseq2 computing-software with p-values and FDR-values of <0.05. (B and C) Cellular and molecular processes (B) and potentially biological pathways of dysregulated genes in *Gata2* haploinsufficient HSCs. Data present as $-\log_{10}$ (p-value). Fischer's Exact Test was used to determine significant pathways. The grey colour represents the threshold of significant pathways with a p-value of <0.05. (D) GSEA plots display enriched pathways for down-regulated genes in *Gata2* haploinsufficient HSCs based on p-values and FDR-values of <0.05. NES indicates normalised enrichment score.

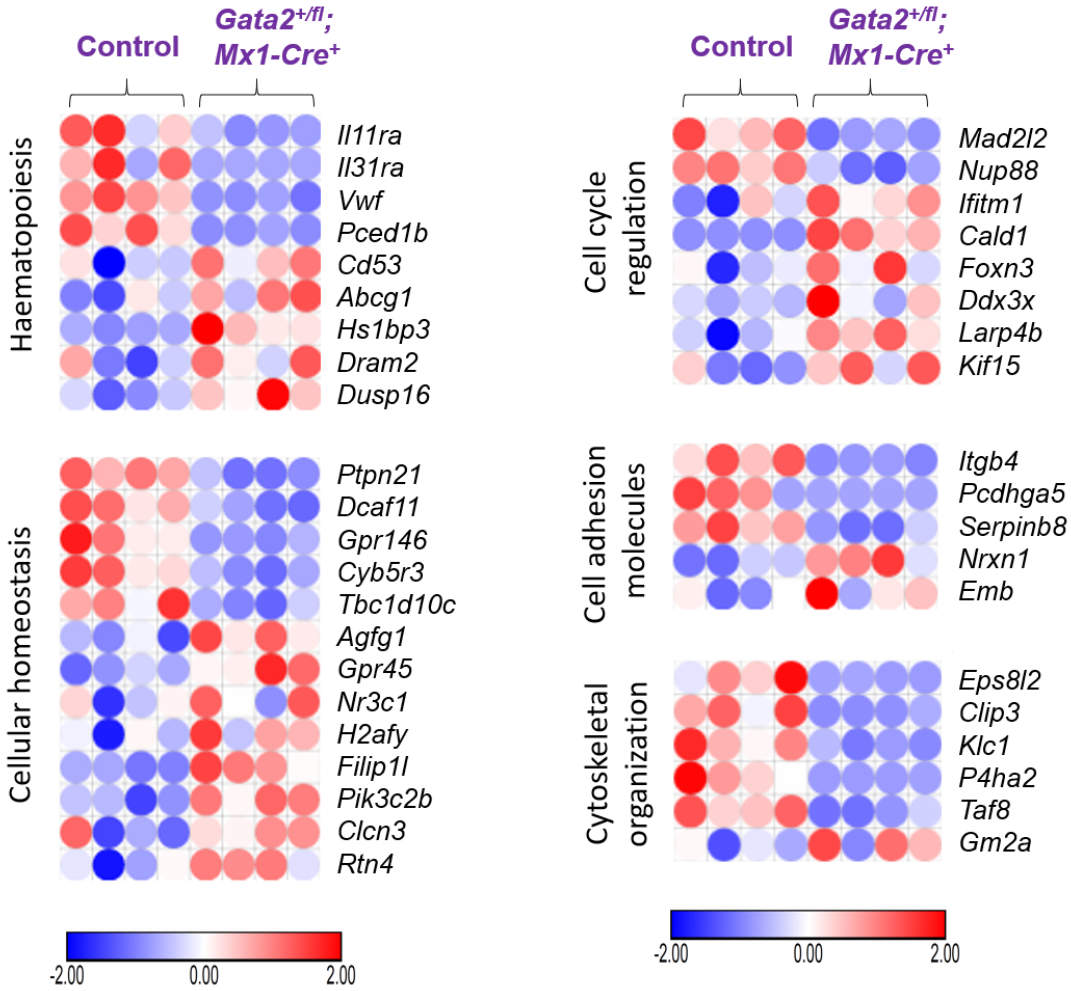

Figure 4-9: Heat maps of differentially expressed genes after acute induction of *Gata2* haploinsufficiency in HSCs.

Heat maps show differentially deregulated genes of purified HSCs at 14 days post the last dose of pIpC from *Gata2*$^{+/fl}$*; Mx1-Cre*$^{+}$ (n=4) and control (n=4) mice. Morpheus online software was used to prepare heatmaps showing a Z-score scale. The red colour indicates up-regulated genes, while the blue colour indicates down-regulated genes. The intensity of gene expression is reflected by the colour gradients.

4.5 Discussion

In this chapter, we aimed to clarify the influence of acute induction of *Gata2* haploinsufficiency on adult HSPCs and haematopoiesis employing Mx1-Cre mouse models. The inducible Mx1 promoter is stimulated by administration of interferon type 1 to conditionally delete *Gata2* heterozygote in the adult haematopoietic compartments and BM niches (Joseph et al., 2013, Kuhn et al., 1995). Previous reports have indicated that the acute lack of *Gata2* (*Gata2$^{fl/fl}$; ER-Cre^{+}* and *Gata2$^{fl/fl}$; Mx1-Cre^{+}*) produces profound exhaustion of adult HSPCs and committed haematopoietic progenitors (Li et al., 2016, Menendez-Gonzalez et al., 2019b). We employed *Gata2* heterozygote (*Gata2$^{+/fl}$; Mx1-Cre^{+}*) mouse models to find out the basis of HSPC defects that were detected in *Gata2$^{fl/fl}$; ER-Cre^{+}* and *Gata2$^{fl/fl}$; Mx1-Cre^{+}* mice. This model of *Gata2* haploinsufficiency may also be of critical relevance to understand how sporadic *GATA2* mutations observed in myeloid neoplasms impact HSPC behaviour (Zhang et al., 2008, Greif et al., 2012, Green et al., 2013).

We firstly induced the deletion of *Gata2* haploinsufficiency in both haematopoietic cells and the BM niche. There was a significant reduction in HSC numbers in *Gata2$^{+/fl}$; Mx1-Cre^{+}* mice, whilst no alterations were observed in frequencies of uncommitted progenitors, committed myeloid lymphoid progenitors, and lineage positive cells in BP and haematopoietic tissues of *Gata2$^{+/fl}$; Mx1-Cre^{+}* mice (Table 4.1). Consistent with constitutive deletion of *Gata2* haploinsufficiency models, *Gata2* is essential for HSCs development at the embryonic stage and later for adult HSCs maintenance (Menendez-Gonzalez et al., 2019b, Gao et al., 2013, Ling et al., 2004, Rodrigues et al., 2005, Li et al., 2016). The reduction of HSC numbers was accompanied by an increase of cellular quiescence with no difference in HSCs survival (Table 4.1). These results imply that HSCs become more quiescent upon acute deletion of *Gata2* haploinsufficiency without alterations in their cell survival status. RNA-Seq analysis demonstrated that dysregulated genes were involved in the regulation of cell cycle such as *Mad2l2, Nup88, Foxn3, Ddx3x, Kif15, Larp4b, Ifitm1,* and *Cald1* genes. For instance, the expression of Forkhead-box-N3 (*Foxn3*), also known as Checkpoint-suppressor-1 (*Ches1*), and Interferon-induced transmembrane-protein-1 (*Ifitm1*) were upregulated in RNA-Seq data. Upregulation of *Foxn3* and *Ifitm1* mediates arrest

of the cell cycle in G1 phase to protect HSCs integrity (Forsberg et al., 2005, Yang et al., 2007).

RNA-Seq analysis showed that there were cell-extrinsic mechanisms involved in the regulation of HSCs maintenance, which may reflect the deletion of a single Gata2 allele in the entire BM, including HSCs and also non-haematopoietic niche cells, where *Gata2* is expressed (Joseph et al., 2013). ECM is a scaffold of noncellular elements (proteins, polysaccharides, integrin molecules, and growth factors) that form a structural barrier for BM niches and enhances HSCs integrity, migration, proliferation, survival, adhesion, and differentiation (Kular et al., 2014, Zhang et al., 2019). This study found that the proteins of down-regulated genes in HSCs were required to interact with ECM components. In support of this observation, we found affected genes and pathways participated in cellular assembly and organisation as Paxillin signalling, Chondroitin sulfate degradation, Macropinocytosis signalling, cellular maintenance (*Ptpn21, Dcaf11, Gpr146, Cyb5r3, Tbc1d10c, Abcg1, Agfg1, Gpr45, H2afy, Nr3c1, Filip1l, Pik3c2b, Clcn3, Rtn4*), cytoskeleton organisation (*Clip3, Eps8l2, Klc1, P4ha2, Taf8,* and *Gm2a*), and cell adhesion molecules (*Itgb4, Pcdhga5, Serpinb8, Nrxn1,* and *Emb*). Paxillin signalling, a connective protein, enhances the binding of integrins to the actin cytoskeleton and mediates cellular migration and proliferation (López-Colomé et al., 2017). Integrins are a crucial component of ECM and regulate cellular interactions with ECM molecules and enhance cellular migration, homing, proliferation, and differentiation (Moreno-Layseca and Streuli, 2014). The expression of integrin subunit beta-4 (*Itgb4*) was down-regulated in our RNA-Seq data. We also noticed decreased CAP-Gly domain-containing linker-protein-3 (*Clip3*) expression. Linker proteins promote the expression of integrins (Kular et al., 2014). Together, these observations suggest that down-regulated ECM components are associated with decreased cellular proliferation and migration. Therefore, it is possible that down-regulated ECM receptors may explain increased quiescence in *Gata2* haploinsufficient HSCs.

Furthermore, RNA-Seq data showed downregulation of interleukin-6 (IL6) signalling in *Gata2* haploinsufficient HSCs. The proinflammatory IL6 has essential roles in the

acute-phase immune response to foreign infections through innate and adaptive mechanisms (Bernad et al., 1994, Tie et al., 2019). Retroviral overexpression of IL6 in BM mice showed myeloproliferative phenotypes within four weeks post-transplantation (Hawley et al., 1992). IL6 KO mice exhibited a reduction in numbers of pre-CFU-S and CFU-S colonies, and a defect in HSCs self-renewal competency in serial transplant experiments (Bernad et al., 1994). IL6 is also involved in HSCs emanation from haemogenic endothelium (Tie et al., 2019). These findings signify the role of IL6 signalling in HSCs specification, proliferation, self-renewal, and differentiation. Onodera et al. investigated the immune response in germline *Gata2* heterozygote mice by injecting endotoxin, a cell-wall module of Gram-negative bacteria, into adult mice (Onodera et al., 2016). Despite the normal distribution of peripheral mature cells, they detected a significant reduction in the IL6 expression in the BM of *Gata2* heterozygote mice. Remarkably, Notch signalling is an upstream regulator for both GATA2 and IL6 in HSCs generation (Robert-Moreno et al., 2005, Tie et al., 2019). Collectively, these observations suggest that the interaction between GATA2 and IL6 signalling may be required to sustain HSC functions.

To exclude the extrinsic influence of BM niches, we also performed cell-autonomous experiments in which *Gata2* heterozygote was only deleted within haematopoietic compartments. There was a reduction in frequencies of *Gata2*$^{+/fl}$*; Mx1-Cre*$^{+}$ donor-cells for HSPCs (HSCs, MPPs, HPC1, and HPC2) and committed myeloid/lymphoid/ erythroid/megakaryocyte progenitors (CMPs, GMPs, MEPs, and CLPs) (Table 4.1). The reduction of *Gata2*$^{+/fl}$*; Mx1-Cre*$^{+}$ derived HSCs was accompanied with increased apoptosis level. At lineage positive stage, the donor contribution of *Gata2*$^{+/fl}$*; Mx1-Cre*$^{+}$ derived-cells was decreased for myeloid and T-lymphoid cells in PB, BM, and spleen, whereas the distribution of B-cells and erythroid cells was similar to control derived-cells. These results indicate that cell-autonomous acute loss of *Gata2* haploinsufficiency disrupts the reconstitution of haematopoietic populations under proliferative stress conditions. We next implemented serial transplant experiments to assess the self-renewal ability of *Gata2* haploinsufficient HSCs. This study uncovered a multi-lineage deficiency of *Gata2*$^{+/fl}$*; Mx1-Cre*$^{+}$ donor-cells in secondary recipient hosts (Table 4.1). These observations imply that adult HSCs maintenance

and self-renewal are strictly managed by *Gata2* transcriptional factor. Altogether, therefore, *Gata2* regulates a stage-specific HSC functions in both non-cell- and cell-autonomous manners.

Table 4.1: Haematological phenotypes of acutely deleted *Gata2* haploinsufficiency in non-cell- and cell-autonomous manners.

	acute deletion of *Gata2* haploinsufficiency (*Gata2*$^{+/fl}$; *Mx1-Cre*$^{+}$)	
	Non-cell autonomous roles	**Cell autonomous roles**
HSPCs	↓HSCs	↓ HSCs, MPPs, HPC1, HPC2, LMPPs
Committed progenitors	No difference	↓ CMPs, GMPs, MEPs, CLPs
Mature cells in PB	No difference	↓ Myeloid, T-cell
Lineage positive cells in BM	No difference	↓ Myeloid, T-cells
Lineage positive cells in spleen	No difference	↓ T-cells
Cell cycle status	↑HSCs frequency in G0 phase	Not assessed
Apoptosis level	No difference	↑ HSCs and MPPs ↓ HPC2
HSCs self-renewal potential	Not assessed	A defect in HSCs self-renewal

CHAPTER 5 : The genetic interaction between *Gata2* and *Asxl1* in adult haematopoiesis

5.1 Introduction

Additional-sex-combs (*Asx*) gene was originally discovered in *Drosophila*, and the Additional Sex Combs Like-1 (*ASXL1*) gene is the human homologue of the ASX protein (Milne et al., 1999, Schuettengruber et al., 2017, Brock and Fisher, 2005, Asada et al., 2019, Katoh, 2013). The *Asx* gene is an epigenetic modifier and controls the expression of homeobox genes through regulating trithorax (*TrxG*) genes, which promote the expression of downstream target proteins, and polycomb (*PcG*) genes, which are involved in the suppression of expression of their target proteins. Human ASXL1 protein is involved in the regulation of *PcG* genes in haematopoiesis and haematological neoplasms. *Asxl1* mRNA is broadly expressed in primitive HSPCs, progenitors, and terminally differentiated blood cells (Abdel-Wahab et al., 2013, Wang et al., 2014, Fisher et al., 2010).

Constitutive deletion of *Asxl1* KO mice causes embryonic lethality with frequent developmental abnormalities such as dwarfism, cleft palates, microcephaly, weight loss, anophthalmia, and skeletal abnormalities (Wang et al., 2014, Abdel-Wahab et al., 2013). Conditional ablation of *Asxl1* in haematopoietic populations using *Vav-Cre* and inducible Mx1-Cre mouse models at 6-12 months old revealed that peripheral blood cytopenias, myeloid/erythroid dysplastic features, an increase in HSPC numbers, and impairment in HSCs self-renewal ability (Abdel-Wahab et al., 2013). Constitutive *Asxl1* heterozygote (*Asxl1*$^{+/-}$) mice displayed anaemia, leukopenia/ leucocytosis, thrombocytopenia, erythroid/myeloid dysplasia, a reduction in numbers of B-cells and neutrophils, an increase in peripheral monocyte numbers, normal distribution of primitive HSPCs and committed progenitors, and a self-renewal defect in serial transplant assays (Wang et al., 2014). A subsequent study utilising germline *Asxl1*$^{+/-}$ mice exhibited normal distribution of peripheral blood cells, normal HSPC numbers, and a repopulation deficiency in competitive transplantation

(Zhang et al., 2018). Collectively, *Asxl1*$^{-/-}$ and *Asxl1*$^{+/-}$ mice develop phenotypes comparable and consistent with features of human MDS/MPN with a latency of 12 months, although they demonstrate disparate haematological phenotypes. These findings indicate that deficient ASXL1 proteins act as loss-of-function mutations. Nevertheless, other studies have indicated that *ASXL1* mutations act as gain-of-function mutations that enhance transformation of myeloid cells (discussed in section 1.4.4). For instance, overexpression of mutant ASXL1 protein (p.G646TfsX12) utilising a retroviral vector in murine BM shows leukocytopenia, thrombocytopenia, anaemia, increased BM/spleen cellularity, myeloid/erythroid dysplasia, decreased levels of H3K27me3, and upregulated expression of *miR152a* and *Hoxa9* genes (Inoue et al., 2013). Mutant ASXL1 proteins develop MDS-like phenotypes at 12 months old.

Inherited heterozygote *ASXL1* mutations have been detected in developmental syndromes such as Bohring-Opitz disorder (Hoischen et al., 2011). Sporadic mutations of *ASXL1* heterozygote are frequently observed in myeloid malignancies involving MPN patients (around 45%), MDS cases (15–20%), and *de novo*/secondary AML patients (40-50%), (Paschka et al., 2015, Katoh, 2013, Gelsi-Boyer et al., 2012). In addition, somatic *ASXL1* mutations are a frequent lesion in clonal haematopoiesis of indeterminate potential (CHIP) and represent around 9.1% of healthy older people (Jaiswal et al., 2014). CHIP is characterised by acquired genetic mutations, clonal expansion of haematopoietic cells, normal peripheral blood indices, and normal morphology of blood cells (Jaiswal et al., 2014). Thus, acquired *ASXL1* mutations confer the transformation of haematopoietic cells during human aging. Of relevance to this study, germline *GATA2* mutations are frequently associated with secondary acquired genetic disorders as monosomy 7, trisomy 8, *ASXL1*, *EZH2*, *SETBP1*, *HECW2*, *GATA1*, *NPM1*, *NRAS*, and *WT1* in MDS/AML patients (Fujiwara et al., 2014, Luesink et al., 2012, West et al., 2014).

5.1.1 Aims of this chapter

Acquired *ASXL1* mutations have been detected in approximately 30% of MDS/AML cases with *GATA2* inherited mutations (Bödör et al., 2012, West et al., 2014). Given that *Gata2* haploinsufficient mice do not develop MDS/AML phenotypes, this study sought to explore whether the genetic interaction between *Gata2* and *Asxl1* would be sufficient to perturb haematopoiesis and induce MDS/AML transformation. To do this, we employed double heterozygote knockout mice (*Gata2*$^{+/fl}$, *Asxl1*$^{+/fl}$; *Vav-iCre*$^{+}$) and *in vitro* lentiviral knockdown of *Asxl1*-shRNA in *Gata2* haploinsufficient LSK cells to explore the impact of the genetic interaction between *Asxl1* and *Gata2* on haematopoiesis as well as cellular transformation by performing immunophenotypic, functional, and molecular experiments such as flow cytometric analysis, CFC assays, survival assays, proliferation assays, gene expression analysis, and *in vivo* HSCs transplantation experiments.

5.2 The production and validation of *Gata2*$^{+/fl}$; *Asxl1*$^{+/fl}$; *Vav-iCre*$^{+}$ mice

Transgenic *Gata2*$^{fl/fl}$ and *Asxl1*$^{fl/fl}$ strains were generated and maintained as previously described (Charles et al., 2006, Abdel-Wahab et al., 2013). To generate compound *Gata2/Asxl1* heterozygote mice, *Gata2*$^{+/fl}$, *Asxl1*$^{+/fl}$, *Vav-iCre*$^{-}$ males were intercrossed with *Gata2*$^{+/+}$; *Asxl1*$^{+/+}$; *Vav-iCre*$^{+}$ females to produce all experimental mice including *Gata2*$^{+/fl}$; *Asxl1*$^{+/fl}$; *Vav-iCre*$^{+}$ (double *Gata2/Asxl1* heterozygote mice), *Gata2*$^{+/fl}$; *Asxl1*$^{+/fl}$; *Vav-iCre*$^{-}$ (control mice), *Gata2*$^{+/fl}$; *Vav-iCre*$^{+}$ (single *Gata2* heterozygote), and *Asxl1*$^{+/fl}$; *Vav-iCre*$^{+}$ (single *Asxl1* heterozygote) (Figure 5.1 A). All littermates were born healthy in the predicted Mendelian proportions.

Conventional PCR analysis of both ear notch biopsies and BM cells revealed the complete excision of one allele of both *Gata2* and *Asxl1* genes (Figure 5.1 B). Sex and age-matched (8-12 weeks) mice were utilised for immunophenotypic and functional analysis (Figure 5.2 A). At the mRNA level, the qPCR analysis showed the expression of *Asxl1*-mRNA was diminished by two-fold in total BM cells in *Asxl1*$^{+/fl}$; *Vav-iCre*$^{+}$ mice when compared with control mice (Figure 5.2 B). A 40%-50% decrease of either *Asxl1* mRNA or *Gata2* mRNA was noted in BM c-kit^{+} cells of *Gata2*$^{+/fl}$; *Asxl1*$^{+/fl}$; *Vav-iCre*$^{+}$

mice as compared with the expression in control cells (Figure 5.2 C). We further evaluated the *Asxl1* expression in *Gata2*$^{+/fl}$*; Vav-iCre*$^{+}$ mice, and *Asxl1 mRNA* level in total BM cells was unaltered between *Gata2*$^{+/fl}$*; Vav-iCre*$^{+}$ mice and control littermates (Figure 5.2 D). Together, these results confirm the deletion of one allele of both *Gata2* and *Asxl1* genes before being utilised for analysis.

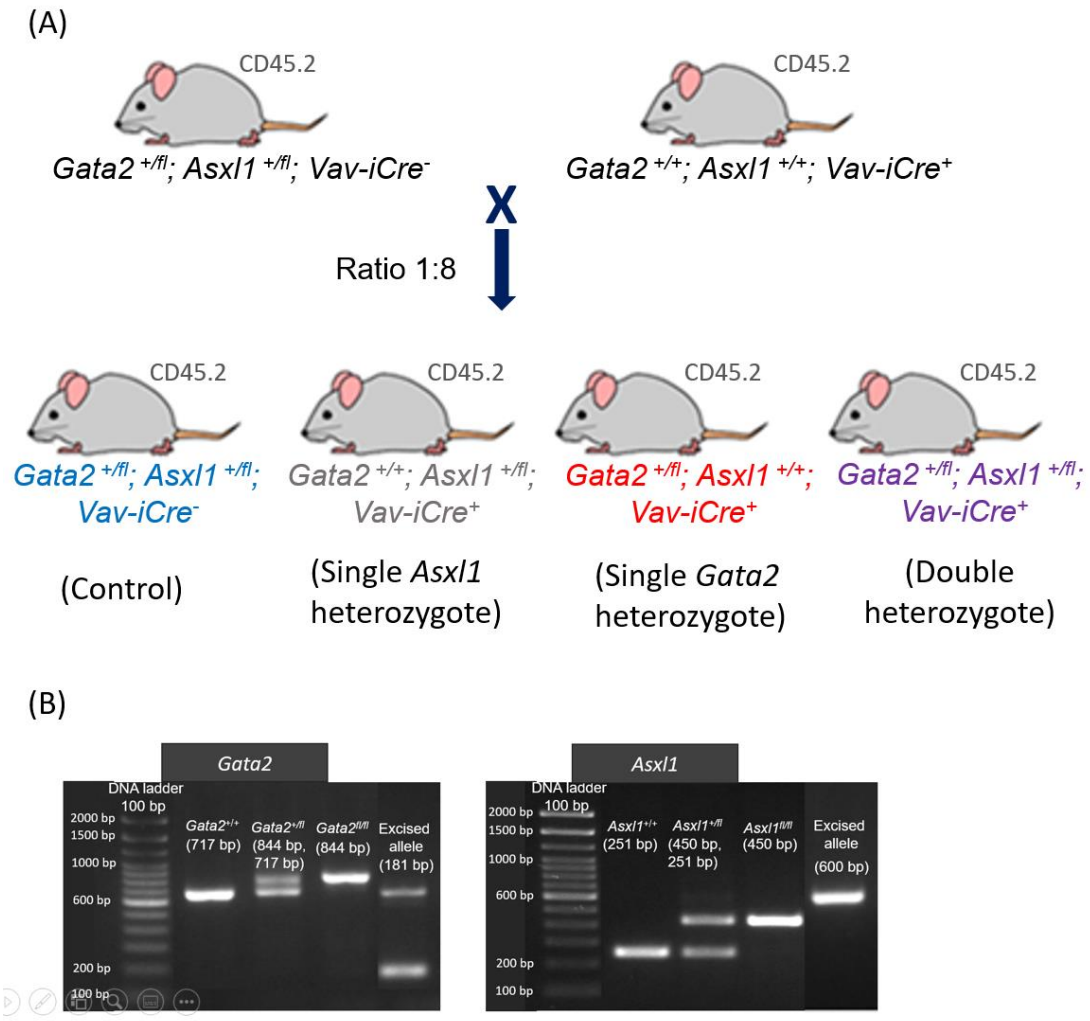

Figure 5-1: The production and validation of *Gata2*$^{+/fl}$*; Asxl1*$^{+/fl}$*; Vav-iCre*$^{+}$ mice.
(A) Scheme illustrating the generation of *Gata2*$^{+/fl}$*; Asxl1*$^{+/fl}$*; Vav-iCre*$^{-}$, *Asxl1*$^{+/fl}$*; Vav-iCre*$^{+}$, *Gata2*$^{+/fl}$*; Vav-iCre*$^{+}$, and *Gata2*$^{+/fl}$*; Asxl1*$^{+/fl}$*; Vav-iCre*$^{+}$ experimental mice. (B) Genomic DNA analysis for BM samples from *Gata2*$^{+/fl}$*; Vav-iCre*$^{+}$ (Left-hand) and *Vav-iCre*$^{-}$, *Asxl1*$^{+/fl}$ (Right-hand). For *Asxl1*, ($^{+}$) indicates wild type, 251 bp; (^{f}), floxed allele, 450 bp; and excised allele, 600 bp.

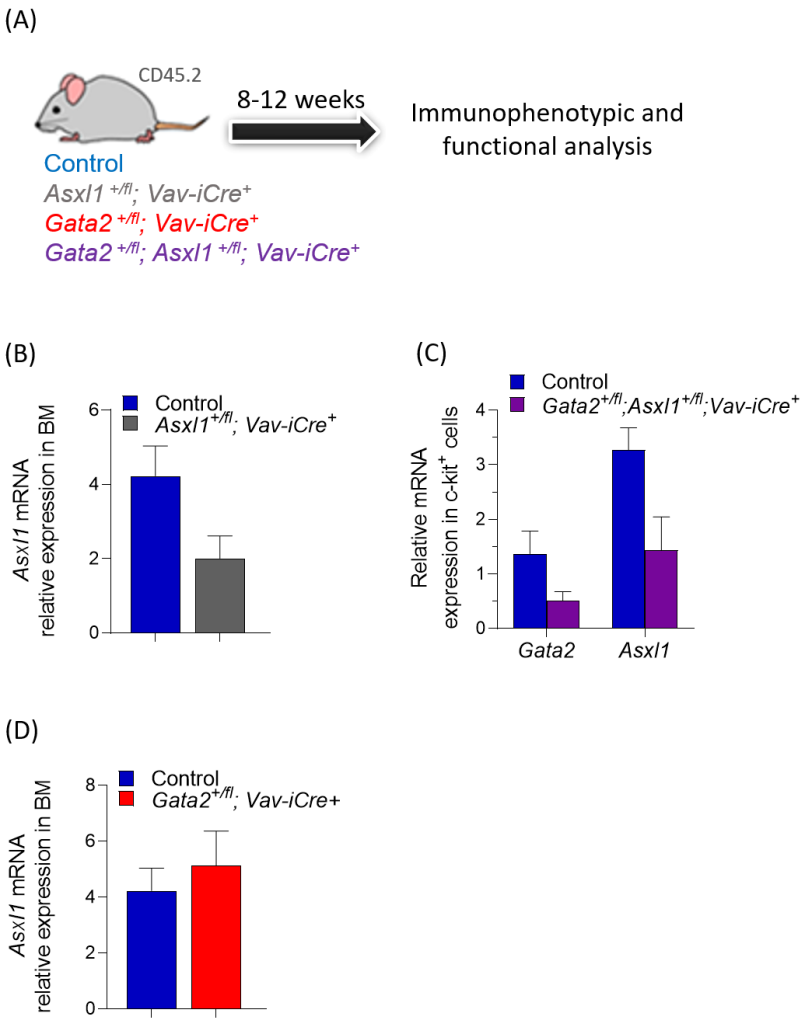

Figure 5-2: *Gata2* and *Asxl1* expression levels in *Gata2*$^{+/fl}$; *Asxl1*$^{+/fl}$; *Vav-iCre*$^{+}$ mice.
(A) The experimental design. *Gata2*$^{+/fl}$; *Asxl1*$^{+/fl}$; *Vav-iCre*$^{-}$, *Asxl1*$^{+/fl}$; *Vav-iCre*$^{+}$, *Gata2*$^{+/fl}$; *Vav-iCre*$^{+}$, and *Gata2*$^{+/fl}$; *Asxl1*$^{+/fl}$; *Vav-iCre*$^{+}$ mice were assessed at 8-12 weeks of age. (B) *Asxl1* mRNA expression in total BM cells from control (n=5) and *Asxl1*$^{+/fl}$; *Vav-iCre*$^{+}$ (n=3) mice relative to *Hprt* mRNA. (C) *Gata2* and *Asxl1* mRNA expression levels in BM c-kit^{+} cells from control (n=3) and *Gata2*$^{+/fl}$; *Asxl1*$^{+/fl}$; *Vav-iCre*$^{+}$ (n=2) littermates. (D) Expression of *Asxl1* mRNA in BM cells of *Gata2*$^{+/fl}$; *Vav-iCre*$^{+}$ (n=5) and control (n=5) mice. Data represent mean ± SEM. Mann-Whitney U test.

5.3 *Gata2* and *Asxl1* double haploinsufficient mice display normal distribution of terminal multi-lineage haematopoietic cells

To begin exploring the collaborative impact of *Gata2* and *Asxl1* haploinsufficiency on haematopoiesis, we performed CBC analysis for *Gata2$^{+/fl}$; Asxl1$^{+/fl}$; Vav-iCre^{-}*, *Asxl1$^{+/fl}$; Vav-iCre^{+}*, *Gata2$^{+/fl}$; Vav-iCre^{+}*, and *Gata2$^{+/fl}$; Asxl1$^{+/fl}$; Vav-iCre^{+}* mice. The absolute numbers of WBCs, RBCs, haemoglobin, and platelets were comparable between double haploinsufficient mice and the other littermates (Figure 5.3 A). Reduced platelet numbers were found in *Gata2$^{+/fl}$; Vav-iCre^{+}* mice at a p-value of 0.06 compared to control mice. Likewise, no significant alterations in frequencies of myeloid-cells (Mac1^{+}Gr1^{+} and Mac1^{+}Gr1^{-}), B-cells (B220^{+}) and T-cells (CD4^{+} and CD8^{+}) were noted in PB of all genotypes (Figure 5.3 B).

This study next evaluated the frequencies of lineage positive cells from BM and spleen of all 4 genotypes. The overall cellularity counts in BM and spleen were indistinguishable between all experimental genotypes (Figure 5.4 A and C). The proportions of myeloid (Mac1^{+}Gr1^{+}), erythroid (Ter119^{+}), and lymphoid (CD4^{+}, CD8^{+}, and B220^{+}) cells in BM and spleen of double haploinsufficient mice were similar to the other groups (Figure 5.4 B and D). Altogether, these results indicate that cooperative haploinsufficiency of *Gata2* and *Asxl1* does not disrupt the terminal differentiation of lineage positive haematopoietic blood cells.

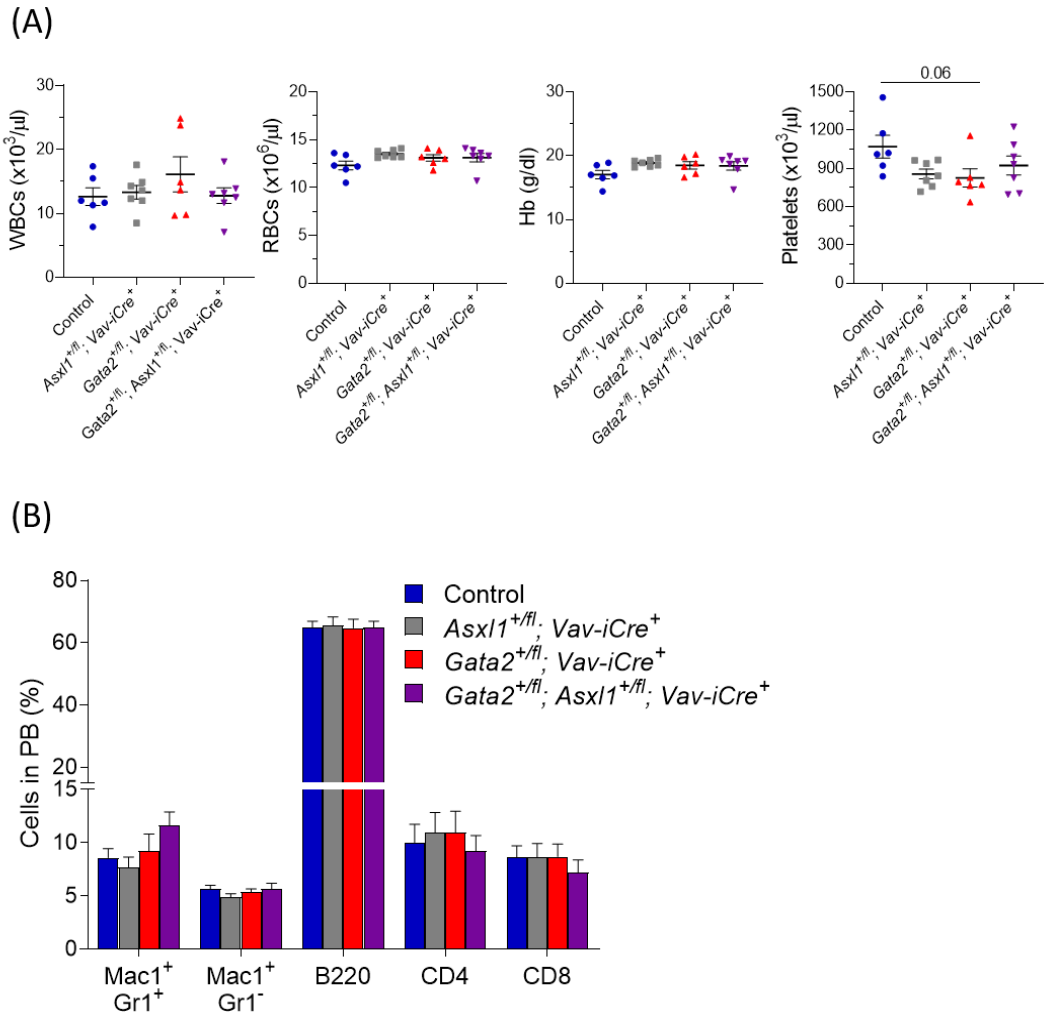

Figure 5-3: *Gata2* and *Asxl1* double haploinsufficient mice display normal distribution of peripheral mature haematopoietic cells.

(A) Absolute numbers of peripheral CBC indices (WBCs, RBC, haemoglobin, and platelets) in *Gata2*$^{+/fl}$*; Asxl1*$^{+/fl}$*; Vav-iCre*$^{-}$ (n=6), *Asxl1*$^{+/fl}$*; Vav-iCre*$^{+}$ (n=7), *Gata2*$^{+/fl}$*; Vav-iCre*$^{+}$ (n=6), and *Gata2*$^{+/fl}$*; Asxl1*$^{+/fl}$*; Vav-iCre*$^{+}$ (n=7) mice from two independent experiments. (B) The percentages of myeloid (Mac1^{+}Gr1^{+}, Mac1^{+}Gr1^{-}) and lymphoid (B220, CD4, CD8) cells in the PB of *Gata2*$^{+/fl}$*; Asxl1*$^{+/fl}$*; Vav-iCre*$^{-}$ (n=10), *Asxl1*$^{+/fl}$*; Vav-iCre*$^{+}$ (n=10), *Gata2*$^{+/fl}$*; Vav-iCre*$^{+}$ (n=10), and *Gata2*$^{+/fl}$*; Asxl1*$^{+/fl}$*; Vav-iCre*$^{+}$ (n=10) mice from three separate experiments. Presented data are mean ± SEM. Statistical analysis: One-Way ANOVA with Tukey's multiple comparisons test *, P < 0.05.

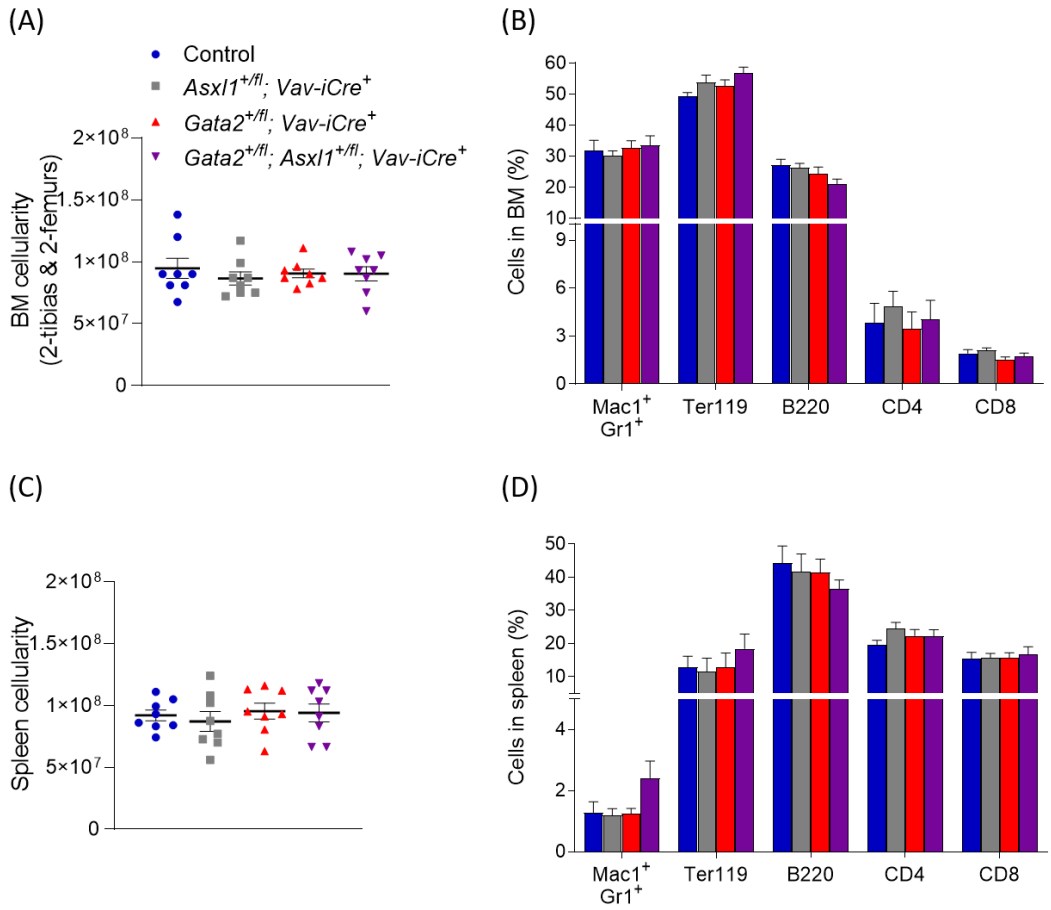

Figure 5-4: *Gata2* and *Asxl1* double haploinsufficient mice display normal distribution of multi-lineage haematopoietic cells in BM and spleen.

(A and C) Cellularity numbers in BM (cells/30mL) (A) and spleen (cells/7mL) (C) of *Gata2*$^{+/fl}$*; Asxl1*$^{+/fl}$*; Vav-iCre*$^{-}$ (n=8), *Asxl1*$^{+/fl}$*; Vav-iCre*$^{+}$ (n=8), *Gata2*$^{+/fl}$*; Vav-iCre*$^{+}$ (n=8), and *Gata2*$^{+/fl}$*; Asxl1*$^{+/fl}$*; Vav-iCre*$^{+}$ (n=8) mice from three independent experiments. (B and D) The proportions of myeloid (Mac1, Gr1), erythroid (Ter119) and lymphoid (B220, CD4, CD8) cells in BM (B) and spleen (D) from *Gata2*$^{+/fl}$*; Asxl1*$^{+/fl}$*; Vav-iCre*$^{-}$ (n=8), *Asxl1*$^{+/fl}$*; Vav-iCre*$^{+}$ (n=8), *Gata2*$^{+/fl}$*; Vav-iCre*$^{+}$ (n=8), and *Gata2*$^{+/fl}$*; Asxl1*$^{+/fl}$*; Vav-iCre*$^{+}$ (n=8) mice from three separate biological experiments. Data are mean ± SEM. Statistical analysis: One-Way ANOVA with Tukey's multiple comparisons test.

5.4 Cooperative haploinsufficiency of *Gata2* and *Asxl1* perturbs adult HSPCs and GMPs homeostasis

After observing no significant alterations in frequencies of terminally differentiated blood cells in haematopoietic tissues of double haploinsufficient mice, this study next analysed the proportions of primitive HSPCs (HSCs, MPPs, HPC1, HPC2, and LMPPs) and committed progenitors (CMPs, GMPs, MEPs, CLPs) in the BM cells of *Gata2*$^{+/fl}$*; Asxl1*$^{+/fl}$*; Vav-iCre*$^{-}$, *Asxl1*$^{+/fl}$*; Vav-iCre*$^{+}$, *Gata2*$^{+/fl}$*; Vav-iCre*$^{+}$, and *Gata2*$^{+/fl}$*; Asxl1*$^{+/fl}$*; Vav-iCre*$^{+}$ mice (Akashi et al., 2000, Kondo et al., 1997, Oguro et al., 2013, Kiel et al., 2005, Adolfsson et al., 2005). Phenocopying and directly equivalent to *Gata2* haploinsufficient mice, the frequencies of HSCs, MPPs, and LMPPs were significantly diminished in the BM of double haploinsufficient mice as compared to *Asxl1*$^{+/fl}$*; Vav-iCre*$^{+}$ or control littermates (Figure 5.5 A). At committed progenitor levels, flow cytometric analysis showed a significant decrease in the proportion of GMPs in the BM of both *Gata2*$^{+/fl}$*; Vav-iCre*$^{+}$, and *Gata2*$^{+/fl}$*; Asxl1*$^{+/fl}$*; Vav-iCre*$^{+}$ mice when compared with control mice, whilst no significant differences were observed in the percentages of CMPs, MEPs, and CLPs between all genotypes (Figure 5.5 B).

We next assessed the capacity of committed myeloid progenitors of double haploinsufficient BM cells to proliferate and differentiate by performing *in vitro* CFC assays (Figure 5.5 C). The total colony numbers were significantly reduced as well as CFU-GEMM and CFU-GM numbers in BM cells of double haploinsufficient mice relative to control BM cells. We additionally noticed a decrease in CFU-GM numbers in BM cells from *Asxl1*$^{+/fl}$*; Vav-iCre*$^{+}$ and *Gata2*$^{+/fl}$*; Vav-iCre*$^{+}$ compared to control cells. These results imply that the collaborative haploinsufficiency of *Gata2* and *Asxl1* disrupts adult BM HSCs, MPPs, LMPPs, and GMPs homeostasis. Collectively, the impacts of the double haploinsufficiency on HSPCs and haematopoiesis are extremely comparable to those of single *Gata2* haploinsufficiency.

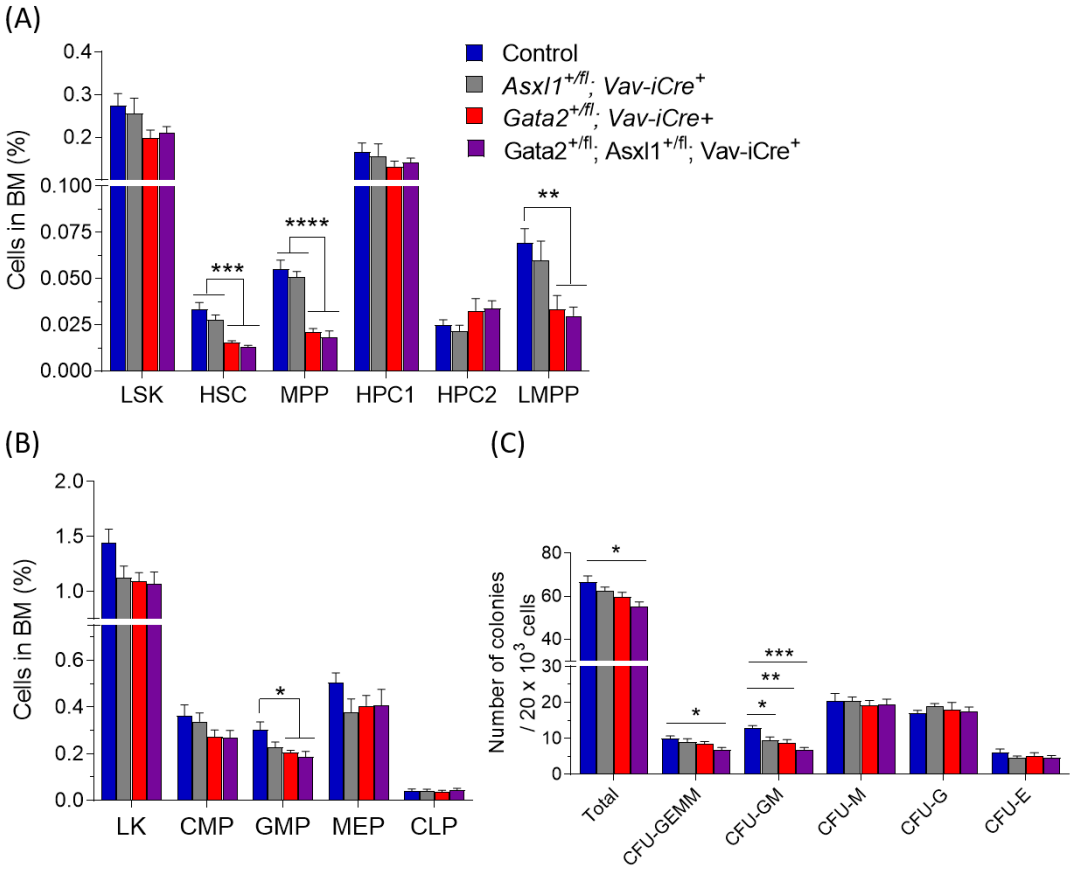

Figure 5-5: Double haploinsufficiency of *Gata2* and *Asxl1* perturbs adult HSPCs and GMPs homeostasis.

(A and B) The percentages of BM HSPCs (LSK, HSCs, MPPs, HPC1, HPC2, and LMPPs) (A) and committed myeloid/lymphoid/erythroid/megakaryocyte progenitors (LK, CMPs, GMPs, MEPs, and CLPs) (B) from control (n=6), *Asxl1$^{+/fl}$; Vav-iCre^{+}* (n=5), *Gata2$^{+/fl}$; Vav-iCre^{+}* (n=6), and *Gata2$^{+/fl}$; Asxl1$^{+/fl}$; Vav-iCre^{+}* (n=6) mice from two independent experiments. (C) CFC numbers of BM cells after 10-12 days plating in methylcellulose (M3434) media from control, *Asxl1$^{+/fl}$; Vav-iCre^{+}*, *Gata2$^{+/fl}$; Vav-iCre^{+}*, and *Gata2$^{+/fl}$; Asxl1$^{+/fl}$; Vav-iCre^{+}* mice. n=5 mice for each group from two separate experiments. CFU indicates Colony-Forming Unit; CFU-GEMM, CFU Granulocytes_Erythrocytes_Macrophages_Megakaryocytes; CFU-GM, CFU Granulocytes_Macrophages; CFU-M, CFU Macrophages; CFU-G, CFU Granulocytes; and CFU-E, CFU Erythrocytes. Presented data are mean ± SEM. Statistical analysis: One-Way ANOVA with Tukey's multiple comparisons test *, $P < 0.05$; **, $P < 0.01$; ***, $P < 0.001$; ****, $P < 0.0001$.

5.5 *Gata2* and *Asxl1* double haploinsufficient mice exhibit decreased survival rates in HSPC compartments

We next examined apoptosis using annexin V to investigate whether the decrease of HSPC numbers in double haploinsufficient mice correlated with cellular survival. A significant increase in total apoptosis was detected in BM HSCs and MPPs of *Gata2*$^{+/fl}$; *Vav-iCre*$^{+}$ and *Gata2*$^{+/fl}$; *Asxl1*$^{+/fl}$; *Vav-iCre*$^{+}$ mice when compared to control littermates, whereas the total apoptosis in BM HPC1 and HPC2 was identical among all genotypes (Figure 5.6). These findings disclose that the reduction in HSC and MPP numbers in both double haploinsufficient mice and single *Gata2* haploinsufficient genotypes is associated with increased cellular apoptosis levels.

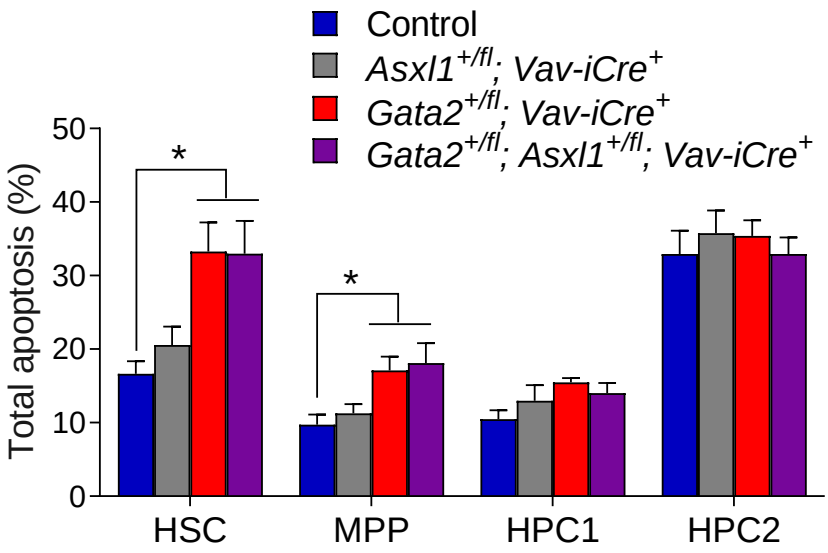

Figure 5-6: Decreased survival rates in primitive HSPCs of *Gata2* and *Asxl1* double haploinsufficient mice.
The bar graph shows proportions of total apoptosis in BM HSPCs (HSCs, MPPs, HPC1, and HPC2) from control (n=6), *Asxl1*$^{+/fl}$; *Vav-iCre*$^{+}$ (n=5), *Gata2*$^{+/fl}$; *Vav-iCre*$^{+}$ (n=6), and *Gata2*$^{+/fl}$; *Asxl1*$^{+/fl}$; *Vav-iCre*$^{+}$ (n=6) mice from two independent experiments. The apoptosis assay was carried out using annexin V and DAPI staining as follows: early-apoptosis, annexin V^{+} DAPI^{-}; late-apoptosis, annexin V^{+} DAPI^{+}; and total apoptosis, early-apoptosis plus late-apoptosis. Data are presented as mean ± SEM. Statistical analysis: One-Way ANOVA with Tukey's multiple comparisons test *, $P < 0.05$.

5.6 Increased proliferation potential in *Gata2* and *Asxl1* double haploinsufficient HSCs

Utilising Ki-67 assay, we next sought whether cellular proliferation was changed in double haploinsufficient HSPCs. Consistent with our previous results in chapter 3, increased frequency of BM HSCs in G0 phase was observed in *Gata2*$^{+/fl}$*; Vav-iCre*$^{+}$ mice as compared with *Asxl1*$^{+/fl}$*; Vav-iCre*$^{+}$ or control genotypes, and, importantly, not in *Gata2* and *Asxl1* double haploinsufficient HSCs (Figure 5.7). Remarkably, there was a significant increase in the percentages of HSCs in S/G2/M stages of *Gata2*$^{+/fl}$*; Asxl1*$^{+/fl}$*; Vav-iCre*$^{+}$ mice compared to *Gata2*$^{+/fl}$*; Vav-iCre*$^{+}$ or control littermates (Figure 5.7). These results signify that cooperative *Gata2* and *Asxl1* haploinsufficiency of HSCs causes more proliferation than single haploinsufficient HSCs of *Gata2* or *Asxl1*.

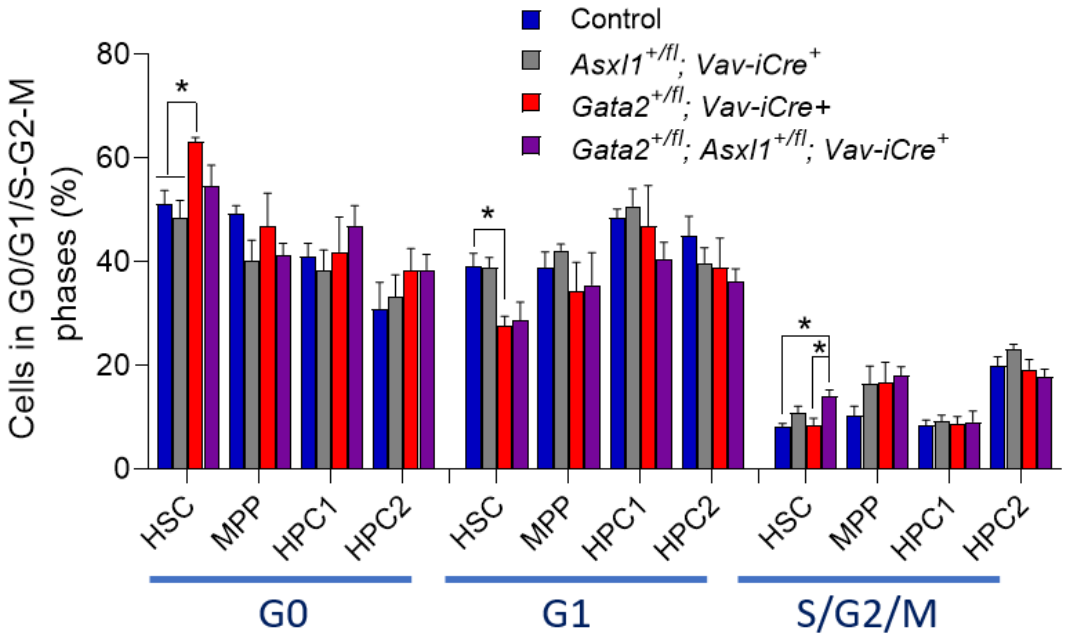

Figure 5-7: Increased proliferation potential in *Gata2* and *Asxl1* double haploinsufficient HSCs.

Frequencies of HSPCs (HSCs, MPPs, HPC1, and HPC2) in the cell cycle stages in the BM of control (n=4), *Asxl1*$^{+/fl}$*; Vav-iCre*$^{+}$ (n=4), *Gata2*$^{+/fl}$*; Vav-iCre*$^{+}$ (n=4), and *Gata2*$^{+/fl}$*; Asxl1*$^{+/fl}$*; Vav-iCre*$^{+}$ (n=4) mice from two independent experiments. The cell cycle status was assessed using Ki-67 and DAPI stains, in which G0 indicates ki67^{-}DAPI^{-}; G1, ki67^{+}DAPI^{-}; and S/G2/M, ki67^{+}DAPI^{+}. Presented data are mean ± SEM. Statistical analysis: One-Way ANOVA with Tukey's multiple comparisons test *, $P < 0.05$.

5.7 *Gata2* and *Asxl1* double haploinsufficient HSCs lose their repopulating potential in competitive transplant experiments

Apart from increased proliferation of HSCs, we observed no significant difference between *Gata2* haploinsufficient HSCs and the cooperative haploinsufficient HSCs of *Gata2* and *Asxl1* in steady-state haematopoiesis. This study next studied the capacity of double haploinsufficient HSCs of reconstituting multi-lineage haematopoietic populations under proliferative stress conditions by performing competitive transplantation experiments. We transplanted purified CD45.2 HSCs from control, *Asxl1$^{+/fl}$; Vav-iCre^{+}*, *Gata2$^{+/fl}$; Vav-iCre^{+}*, and *Gata2$^{+/fl}$; Asxl1$^{+/fl}$; Vav-iCre^{+}* mice alongside 2x10^{5} CD45.1 support BM cells into irradiated CD45.1-recipient mice. The donor contribution cells were monitored in PB every 4 weeks, and haematopoietic tissues of primary recipient hosts were evaluated for donor-derived cells in BM and spleen at week 16 post-transplant (Figure 5.8 A).

Analysis of chimerism in PB exhibited a steady decrease of CD45.2 double haploinsufficient donor-cells when compared to control CD45.2 donor-cells from week 8 through week 16 post-transplant, whilst insignificant reduction was noted in double haploinsufficient donor-cells compared to *Asxl1$^{+/fl}$; Vav-iCre^{+}* or *Gata2$^{+/fl}$; Vav-iCre^{+}* CD45.2 donor cells (Figure 5.8 B). Reduced CD45.2 cells in PB were also noticed from *Asxl1$^{+/fl}$; Vav-iCre^{+}* and *Gata2$^{+/fl}$; Vav-iCre^{+}* donor cells relative to WT donor-cells (Figure 5.8 B). Consistently, the percentage of CD45.2 donor cells for myeloid-cells (Mac1^{+}Gr1^{+} and Mac1^{+}Gr1^{-}) and B-cell (B220^{+}) was diminished in PB of transplanted cells from *Gata2$^{+/fl}$; Vav-iCre^{+}* and *Gata2$^{+/fl}$; Asxl1$^{+/fl}$; Vav-iCre^{+}* when compared with control derived-cells, whilst a decline in frequencies of donor cells for T-cell (CD4^{+} and CD8^{+}) was detected in the different genotypes relative to control donor-cells (Figure 5.8 C). Likewise, the donor contribution in BM and spleen was decreased for myeloid, erythroid, lymphoid, and total CD45.2^{+} cells in recipients receiving cells from *Gata2$^{+/fl}$; Vav-iCre^{+}* and *Gata2$^{+/fl}$; Asxl1$^{+/fl}$; Vav-iCre^{+}* when compared with control donor cells (Figure 5.9 A and B). Contrarily, no significant alteration was noted in *Asxl1$^{+/fl}$; Vav-iCre^{+}* donor cells for haematopoietic cells in BM and spleen compared with all groups (Figure 5.9 A and B). Interestingly, overall engraftment and myeloid

and lymphoid reconstitution displayed a trend reduction from HSCs of *Gata2*$^{+/fl}$*; Asxl1*$^{+/fl}$*; Vav-iCre*$^{+}$ when compared to their single haploinsufficient counterparts.

Within the BM HSPCs and committed haematopoietic populations, a significant decrease in proportions of CD45.2 donor contribution cells was observed in *Gata2*$^{+/fl}$*; Asxl1*$^{+/fl}$*; Vav-iCre*$^{+}$ donor cells for HSPCs (HSCs, MPPs, HPC1, HPC2, and LMPPs) and committed progenitors (CMPs, GMPs, MEPs, and CLPs) compared to control, *Asxl1*$^{+/fl}$*; Vav-iCre*$^{+}$, or *Gata2*$^{+/fl}$*; Vav-iCre*$^{+}$ derived cells (Figure 5.9 C and D). As anticipated, the frequencies of donor cells for HSPCs and haematopoietic progenitors in transplanted recipients with HSCs from *Gata2*$^{+/fl}$*; Vav-iCre*$^{+}$ mice were significantly lower than control derived cells, whereas recipients of *Asxl1*$^{+/fl}$*; Vav-iCre*$^{+}$ cells showed comparable repopulating potential to control cells (Figure 5.9 C and D). Cooperatively, *Asxl1* haploinsufficient HSCs causes a mild multi-lineage defect in competitive transplant experiments in agreement with published studies (Zhang et al., 2018, Abdel-Wahab et al., 2013, Wang et al., 2014, Fisher et al., 2010). Notably, overall engraftment of HSPC compartments from *Gata2*$^{+/fl}$*; Asxl1*$^{+/fl}$*; Vav-iCre*$^{+}$ recipients were markedly reduced when compared to their single haploinsufficient counterparts. Thus, collaborative haploinsufficient HSCs from *Gata2* and *Asxl1* fail to reconstitute HSPC compartments as well as multi-lineage haematopoiesis in proliferative stress assays.

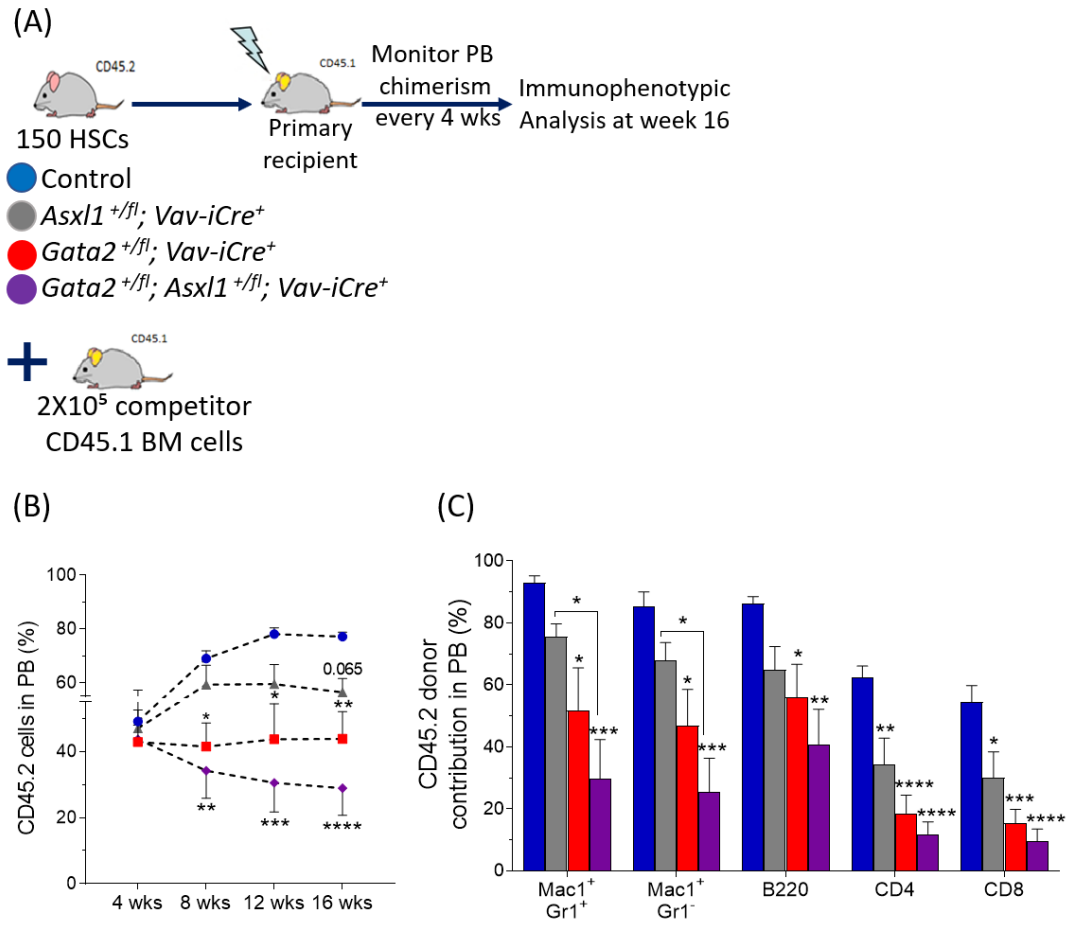

Figure 5-8: *Gata2* and *Asxl1* double haploinsufficient HSCs fail to repopulate peripheral multi-lineage haematopoietic cells.

(A) A scheme of competitive transplant experiments, lethally irradiated recipients (CD45.1) were injected with 150 enriched HSCs (CD45.2) from *Gata2*$^{+/fl}$*; Asxl1*$^{+/fl}$*; Vav-iCre*$^{-}$, *Asxl1*$^{+/fl}$*; Vav-iCre*$^{+}$, *Gata2*$^{+/fl}$*; Vav-iCre*$^{+}$, and *Gata2*$^{+/fl}$*; Asxl1*$^{+/fl}$*; Vav-iCre*$^{+}$ mice together with 2x10^{5} competitor CD45.1 BM cells. Three independent donor mice were used for each genotype. (B) follow-up analysis after-transplant of CD45.2^{+} cells in PB throughout the entire period from control (n=7), *Asxl1*$^{+/fl}$*; Vav-iCre*$^{+}$ (n=6), *Gata2*$^{+/fl}$*; Vav-iCre*$^{+}$ (n=6), and *Gata2*$^{+/fl}$*; Asxl1*$^{+/fl}$*; Vav-iCre*$^{+}$ (n=6) donor derived-cells from two independent experiments. (C) Proportions of CD45.2 donor cells at week 16 post-transplantation for myeloid (Mac1^{+}Gr1^{+}, Mac1^{+}Gr1^{-}) and lymphoid (B220^{+}, CD4^{+}, CD8^{+}) cells in PB of control (n=7), *Asxl1*$^{+/fl}$*; Vav-iCre*$^{+}$ (n=6), *Gata2*$^{+/fl}$*; Vav-iCre*$^{+}$ (n=6), and *Gata2*$^{+/fl}$*; Asxl1*$^{+/fl}$*; Vav-iCre*$^{+}$ (n=6) donor derived-cells from two separate experiments. Data are presented as mean ± SEM. Statistical analysis: One-Way ANOVA with Tukey's multiple comparisons test *, P < 0.05; **, P < 0.01; ***, P < 0.001; ****, P < 0.0001.

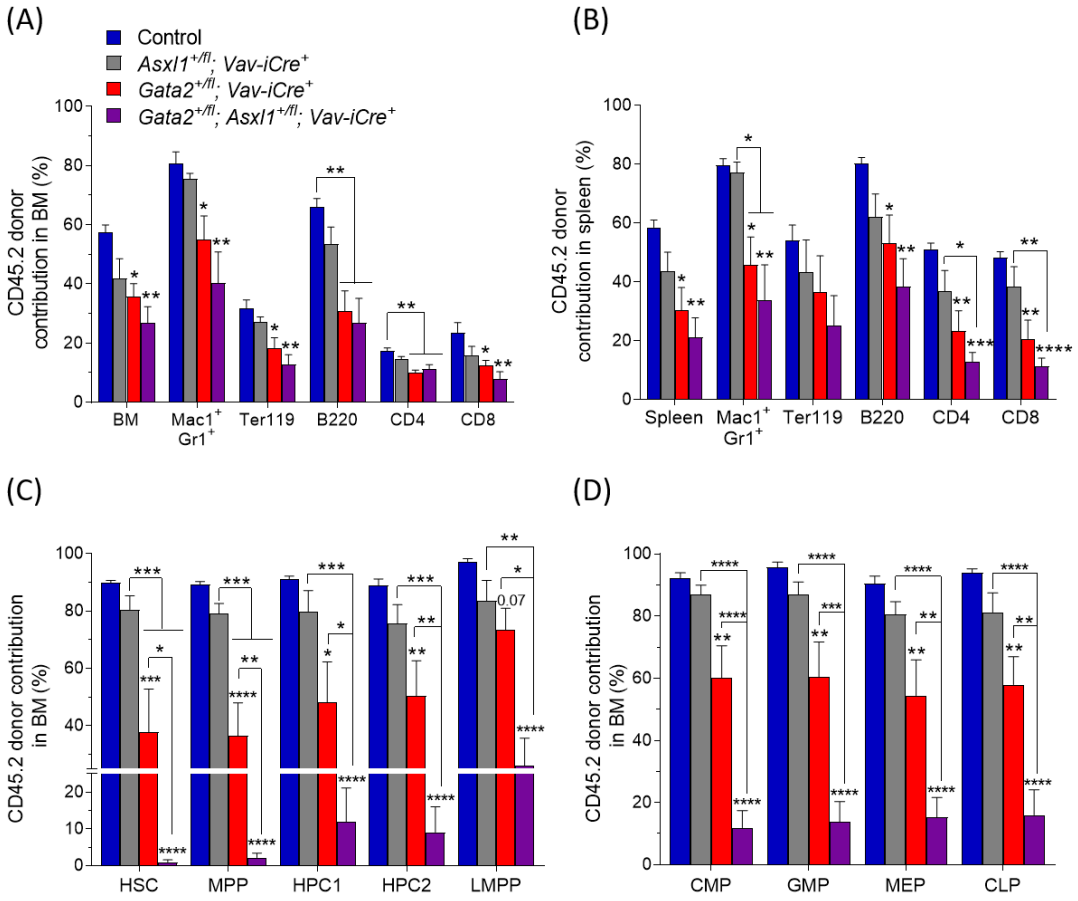

Figure 5-9: *Gata2* and *Asxl1* double haploinsufficient HSCs markedly lose their repopulating potential in competitive transplant experiments.

(A and B) Frequencies of CD45.2 donor contribution cells in BM (A) and spleen (B) for myeloid ($Mac1^+Gr1^+$, $Mac1^+Gr1^-$), erythroid ($Ter119^+$), lymphoid ($B220^+$, $CD4^+$, $CD8^+$), and total $CD45.2^+$ cells at week 16 after-transplantation in receipient mice harboring donor cells from control (n=7), *Asxl1*$^{+/fl}$*; Vav-iCre*$^+$ (n=6), *Gata2*$^{+/fl}$*; Vav-iCre*$^+$ (n=6), and *Gata2*$^{+/fl}$*; Asxl1*$^{+/fl}$*; Vav-iCre*$^+$ (n=6) from two different experiments. (C and D) Proportions of donor contribution at 16 weeks receiving CD45.2 transplant cells in BM HSPCs (HSCs, MPPs, HPC1, HPC2, LMPPs) and progenitors (CMPs, GMPs, MEPs, CLPs) from control (n=7), *Asxl1*$^{+/fl}$*; Vav-iCre*$^+$ (n=6), *Gata2*$^{+/fl}$*; Vav-iCre*$^+$ (n=6), and *Gata2*$^{+/fl}$*; Asxl1*$^{+/fl}$*; Vav-iCre*$^+$ (n=6) donor derived-cells from two independent experiments. We utilised three different donor mice per group. Data represent mean ± SEM. Statistical analysis: One-Way ANOVA with Tukey's multiple comparisons test *, $P < 0.05$; **, $P < 0.01$; ***, $P < 0.001$; ****, $P < 0.0001$.

5.8 Transcriptional signatures in double haploinsufficient HSCs

Gata2 and *Asxl1* double haploinsufficient HSCs display enhanced proliferation and functional defects in transplantation reconstitution beyond that observed in their single haploinsufficient counterparts, suggesting cooperative genetic interaction between *Gata2* and *Asxl1* pathways. To explore the transcriptional programmes underpinning genetic interaction between *Gata2* and *Asxl1* pathways, we conducted RNA-Seq of purified BM HSCs from control, *Asxl1*$^{+/fl}$*; Vav-iCre*$^{+}$, *Gata2*$^{+/fl}$*; Vav-iCre*$^{+}$, and *Gata2*$^{+/fl}$*; Asxl1*$^{+/fl}$*; Vav-iCre*$^{+}$ mice. In contrast to *Gata2* haploinsufficient HSCs (117 differentially expressed genes), the DEseq2 analysis showed that large numbers of significant differentially regulated genes in *Asxl1* haploinsufficient HSCs (4218 genes) and double haploinsufficient HSCs (2606 genes) with FDR values less than 0.05 as compared with WT HSCs (Figure 5.10 A). *Asxl1* haploinsufficient HSCs exhibited 2083 genes whose expression was down-regulated and 2135 up-regulated genes, whilst 1251 down-regulated genes and 1355 up-regulated genes were found in double haploinsufficient HSCs (Figure 5.10 A). The expression of most dysregulated genes was common between double haploinsufficient HSCs and *Asxl1* haploinsufficient HSCs (2139 genes), whereas there were 39 shared dysregulated genes common to *Gata2* and *Asxl1* single haploinsufficient HSCs and *Gata2* and *Asxl1* double haploinsufficient HSCs, confirming a common transcriptional signature between *Gata2* and *Asxl1* pathways. (Figure 5.10 B). Around 39% of dysregulated genes (46 genes) of *Gata2* haploinsufficient HSCs were shared with double haploinsufficient HSCs (Figure 5.10 B). Approximately 16% (421) of deregulated genes were unique to *Gata2 and Asxl1* double haploinsufficient HSCs, indicating that the collaborative impact of *Gata2 and Asxl1* haploinsufficiency induces a distinct transcriptional signature when compared to either *Gata2* or *Asxl1* haploinsufficiency alone.

Ingenuity canonical pathway (ICP) and Gene set enrichment (GSEA) software tools were used to inform the biological pathways operating in double *Gata2 and Asxl1* haploinsufficient HSCs. The shared affected biological pathways in double haploinsufficient HSCs, *Gata2* haploinsufficient HSCs, and *Asxl1* haploinsufficient

HSCs involved DNA repair pathways including dsDNA break repair by homologous recombination and base excision repair (Figure 5.10 C).

ICP and GSEA analysis for single *Gata2* haploinsufficient HSCs were discussed in-depth in chapter 3, section 3.2.10. In agreement with the notion that *ASXL1* mutations act as a preleukaemic initiator (Micol et al., 2017, Zhang et al., 2018, Abdel-Wahab et al., 2013), several affected pathways that are involved in haematopoiesis, cell cycling, DNA damage and repair, cellular survival, metabolic processes, and AML signalling were detected in *Asxl1* haploinsufficient HSCs (Figure 5.11 A and B).

Double haploinsufficient HSCs displayed up-regulated pathways that are associated with cellular proliferation (cyclins and cell cycle regulation, cell cycle control of chromosomal replication, estrogen-mediated S-phase entry, and mitotic roles of Polo-like kinase), DNA damage and repair (ATM signalling, G2/M DNA damage checkpoint regulation, and cell cycle regulation by B-cell translocation gene-1 (BTG1), protein synthesis (unfolded protein response, tRNA charging, endoplasmic reticulum stress pathway), apoptosis (death receptor signalling), metabolic pathways (sirtuin signalling pathway, folate polyglutamylation), and cytoskeletal organisation (Rho family GTPases signalling) (Figure 5.11 A). The unique up-regulated pathways in double haploinsufficient HSCs were mainly implicated in regulation of the cell cycle (cyclins regulation, estrogen-mediated S-phase entry, cell cycle regulation by BTG1, Rho family GTPases signalling) and apoptosis (death receptor signalling) when compared with *Asxl1* haploinsufficient HSCs. In contrast, down-regulated pathways in double haploinsufficient HSCs were involved in cellular metabolism (cholesterol biosynthesis, oxidative phosphorylation, urate biosynthesis, isoleucine degradation-I, ketogenesis, ketolysis, Glutaryl-coA degradation, and mevalonate pathway-I), cell cycle regulations (G1/S checkpoint regulation), and protein synthesis (eukaryotic Initiation factor 2 (EIF2) signalling) (Figure 5.11 B). In comparison with *Asxl1* haploinsufficient HSCs, double haploinsufficient HSCs uniquely exhibited down-regulated pathways implicated in G1/S checkpoint regulation and metabolic pathways (ketolysis and mevalonate pathway-I). The ICP and GSEA assessment of the 421 uniquely dysregulated genes in double haploinsufficient HSCs uncovered

distinctive biological pathways linked to cellular growth and proliferation (GADD45 signalling, MYC targets-v1, and mitotic spindle), apoptosis, mRNA spliceosomes (pre-mRNA splicing and assembly of RNA polymerase III complex), inflammatory responses (neutrophil degranulation, IFN-γ response, and Tnfα signalling via NF-κB), and metabolic processes (methionine degradation I, coenzyme-A biosynthesis, hypusine biosynthesis, and cysteine biosynthesis III) (Figure 5.12).

Congruent with the well-known roles of GATA2 and ASXL1 in haematopoiesis as well as in leukaemogenesis, double haploinsufficient HSCs exhibited a wide range of dysregulated genes related to haematopoietic cell regulations and haematological malignancies (Table 5.1). Consistently, double haploinsufficient HSCs showed a robust pattern of dysregulated genes that are associated with DNA repair processes, cell cycle regulations, spindle checkpoints, apoptosis, chromosomal organisation, spliceosomes, adipogenesis, mitochondrial regulations, membrane transport proteins, cytoskeleton regulations, and adhesion molecules (Table 5.1).

GSEA analysis further confirmed that up-regulated expressed genes in double haploinsufficient HSCs were enriched for cellular proliferation including G2M checkpoints, E2F target genes, mitotic spindle, and MYC target genes, and unfolded protein response (Figure 5.13 A). MYC target genes were further enriched in double haploinsufficient HSCs as compared with *Asxl1* haploinsufficient HSCs (Figure 5.13 B). Furthermore, double haploinsufficient HSCs exhibited upregulated biological pathways that were associated with G2M checkpoints, E2F target genes, mRNA splicing, mitotic spindle, MYC target genes, and adipogenesis comparative to *Gata2* haploinsufficient HSCs (Figure 5.13 C). Altogether, consistent with increased HSCs cycling and decreased HSCs survival in double haploinsufficient mice, these outcomes indicate that haploinsufficient HSCs of *Gata2* and *Asxl1* cooperate to induce alterations in transcriptional signatures that enrich in cellular proliferation, apoptosis, and DNA damage repair pathways.

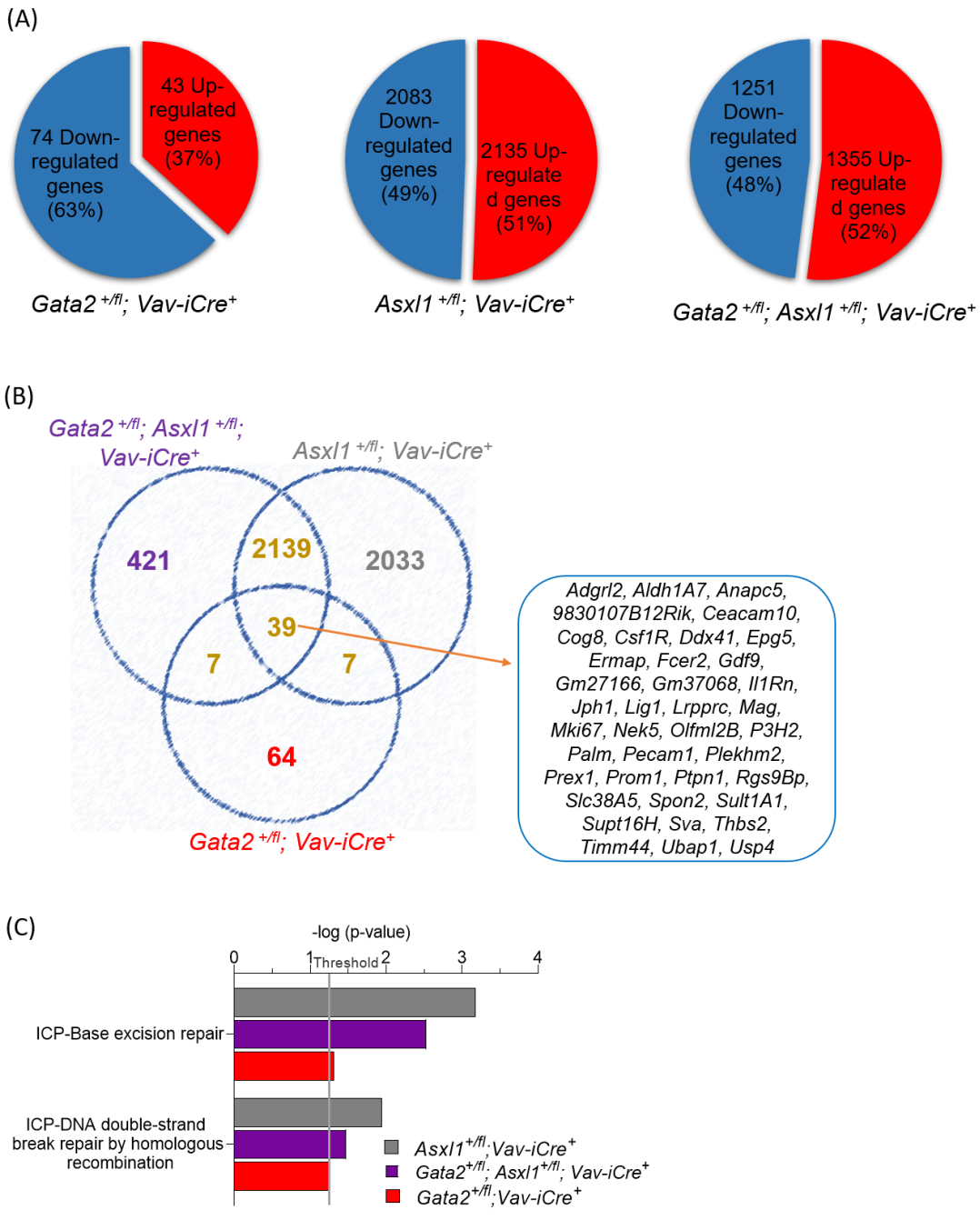

Figure 5-10: Transcriptional signatures in double haploinsufficient HSCs.
(A) Venn diagrams show the numbers of significant differentially regulated genes in *Gata2* haploinsufficient HSCs (Left-hand), *Asxl1* haploinsufficient HSCs (Middle), and double haploinsufficient HSCs (Right-hand) compared to control HSCs. n=4 for each genotype. The identification of expressed genes was achieved using DEseq2 computing-software based on p-values and FDR-values of <0.05 level. (B) Overlapping analysis of significantly expressed genes of *Gata2* haploinsufficient HSCs, *Asxl1* haploinsufficient HSCs, and double haploinsufficient HSCs. (C) The commonly dysregulated pathways in *Gata2* haploinsufficient HSCs, *Asxl1* haploinsufficient HSCs, and double haploinsufficient HSCs. Data are presented as $-\log_{10}$ (p-value), and the grey line represents the threshold at a p-value of 0.05. Statistical analysis: Fischer's Exact Test.

(A)


Up-regulated pathways
-log (p-value)
0
5
10
15
20
Threshold
ICP_Sirtuin signaling pathway
ICP_tRNA charging
ICP_Cell cycle control of chromosomal replication
ICP_Unfolded protein response
ICP_Mitotic roles of Polo-like kinase
ICP_ATM signaling
ICP_G2/M DNA damage checkpoint regulation
ICP_Endoplasmic reticulum stress pathway
ICP_Folate polyglutamylation
ICP_Cyclins and cell cycle regulation
ICP_Estrogen-mediated S-phase entry
ICP_Cell cycle regulation by BTG proteins
ICP_Death receptor signaling
ICP_Signaling by Rho family GTPases
ICP_Regulation of eIF4 and p70S6K signaling
ICP_mTOR signaling
ICP_Leukocyte extravasation signaling
ICP_Integrin signaling
ICP_IL-8 signaling
ICP_IL-7 signaling pathway
ICP_CD40 signaling
ICP_IL-3 signaling
ICP_VEGF signaling
ICP_p70S6K signaling
ICP_IL-2 signaling
ICP_Paxillin signaling
ICP_PI3K signaling in B-lymphocytes
ICP_JAK/Stat signaling
ICP_Heme biosynthesis II
ICP_PI3K/AKT signaling
ICP_B-cells receptor signaling
ICP_Acute Myeloid Leukemia signaling
ICP_ERK/MAPK signaling
ICP_Pentose phosphate pathway
ICP_IL-22 signaling
ICP_Senescence pathway
ICP_BAG2 signaling pathway
ICP_RANK signaling in osteoclasts
ICP_PFKFB4 signaling pathway
ICP_BRCA1 in DNA damage response
ICP_GM-CSF signaling
ICP_IL-9 signaling
ICP_Th2 pathway
ICP_CD28 signaling in T-helper cells
ICP_CXCR4 signaling
ICP_UVA-induced MAPK signaling
ICP_IL-6 signaling
ICP_Thioredoxin pathway
ICP_FLT3 signaling in haematopoietic progenitors
ICP_B-cells activating factor signaling
ICP_Prolactin signaling
Asxl1+/fl;Vav-iCre+
Gata2+/fl; Asxl1+/fl; Vav-iCre+

(B)

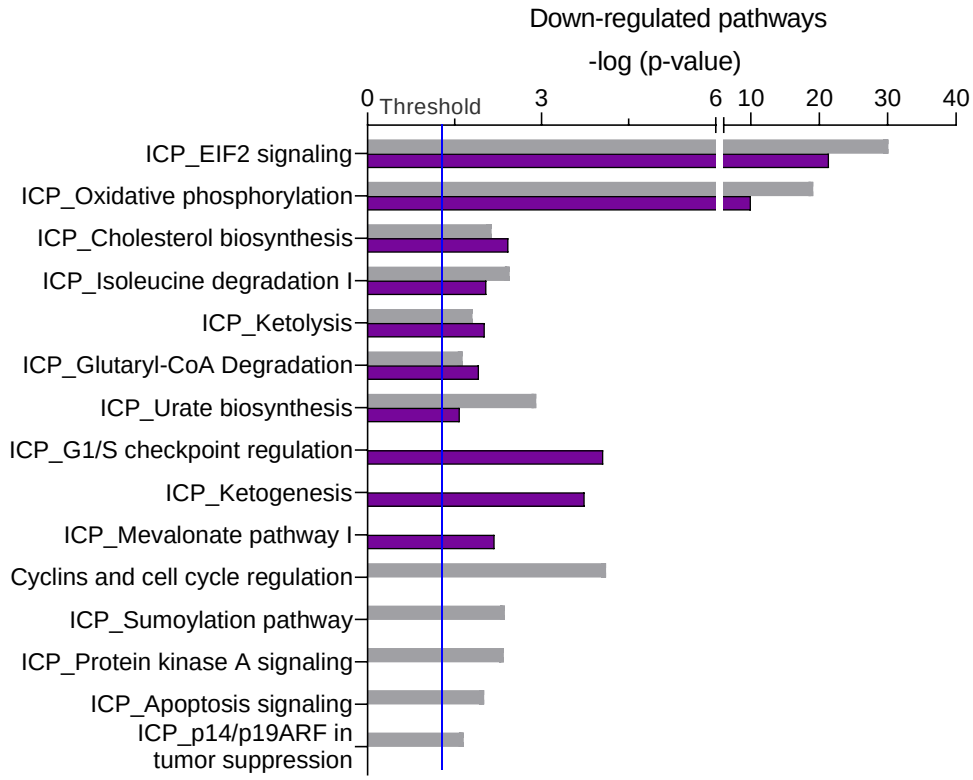

Figure 5-11: ICP analysis for transcriptional signatures in double haploinsufficient HSCs and *Asxl1* haploinsufficient HSCs.

(A and B) ICP analysis for up-regulated (A) and down-regulated (B) biological pathways for dysregulated genes in double haploinsufficient HSCs and *Asxl1* haploinsufficient HSCs. Data present as $-\log_{10}$ (p-value). The threshold line in blue shows a p-value at 0.05 ($-\log_{10}$ (p-value)). Statistical analysis: Fischer's Exact Test.

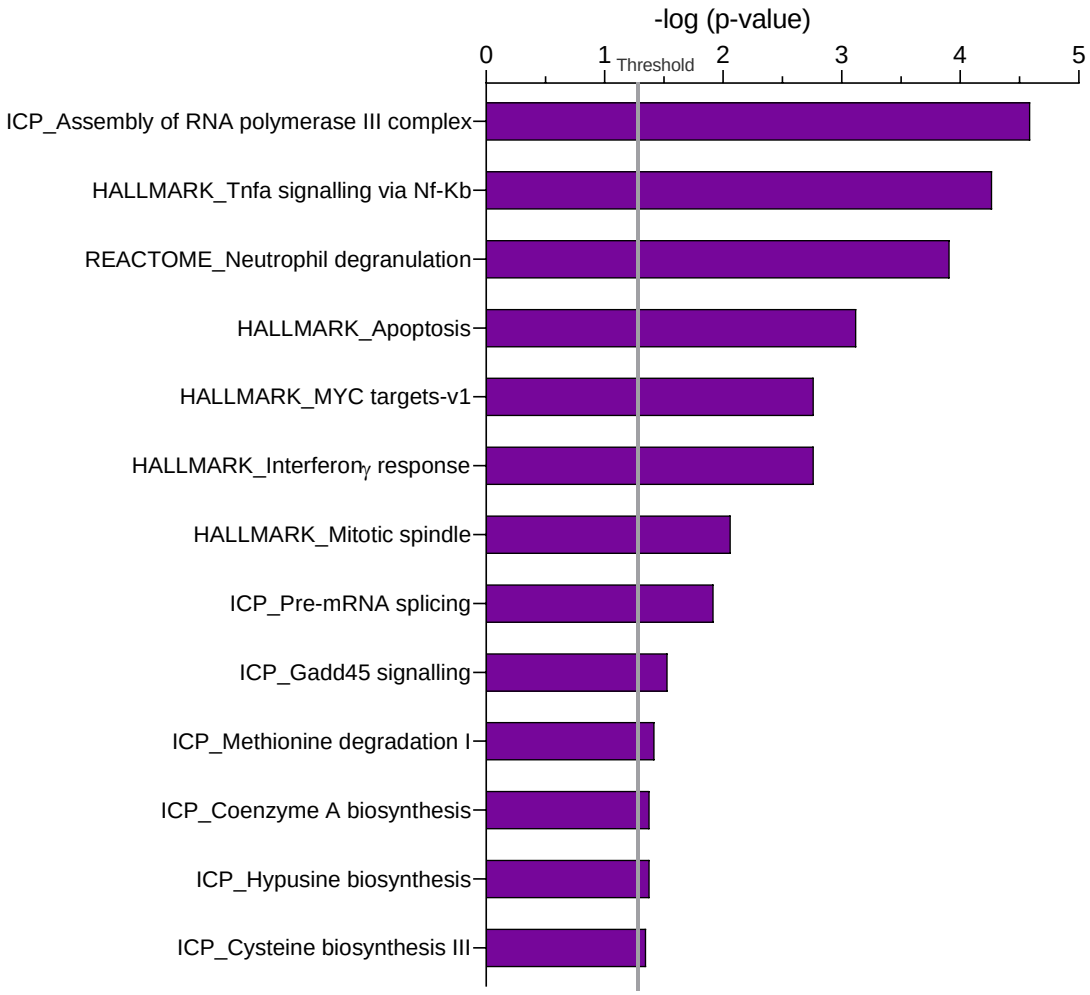

Figure 5-12: Unique dysregulated pathways in double haploinsufficient HSCs.
ICP and GSEA assessment for affected biological pathways for the 421 unique dysregulated genes in double haploinsufficient HSCs. Data are presented as $-\log_{10}$ (p-value). The threshold line in grey indicates the p-value at the 0.05 level. Statistical analysis: Fischer's Exact Test.

(A)

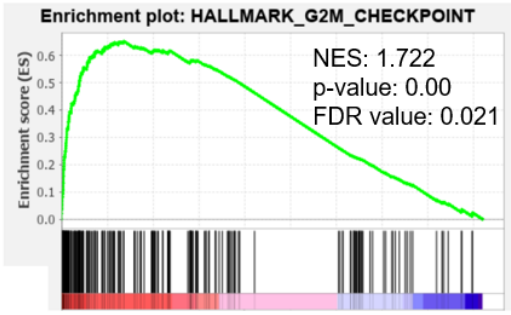

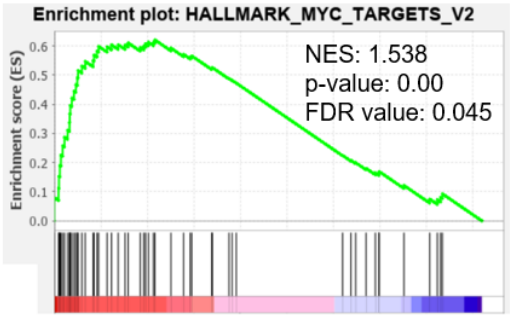

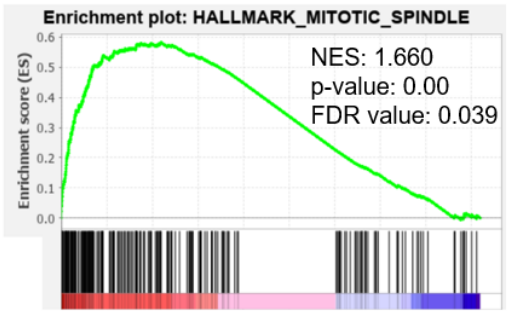

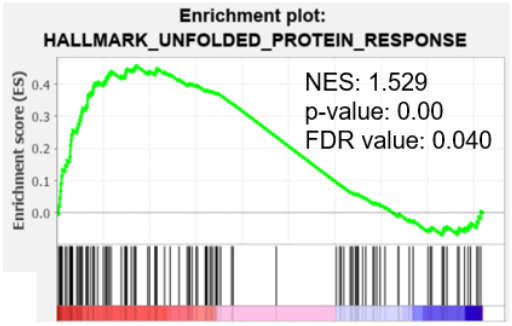

Gata2$^{+/fl}$*; Asxl1*$^{+/fl}$*; Vav-iCre*$^{+}$ Control

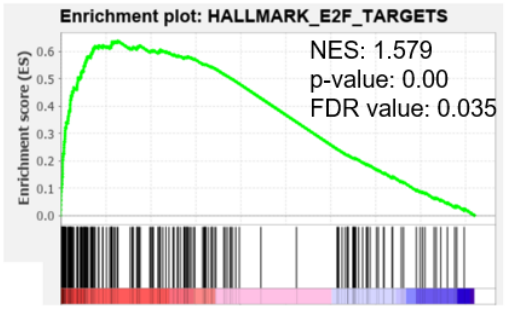

Gata2$^{+/fl}$*; Asxl1*$^{+/fl}$*; Vav-iCre*$^{+}$ Control

(B)

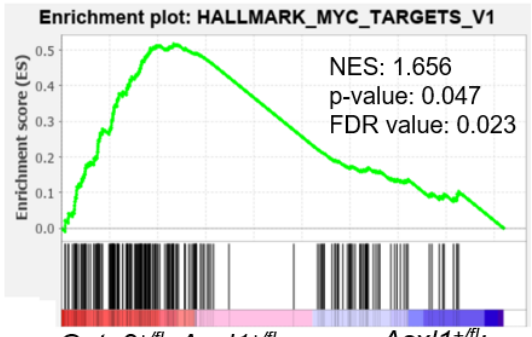

Gata2$^{+/fl}$*; Asxl1*$^{+/fl}$*; Vav-iCre*$^{+}$ *Asxl1*$^{+/fl}$*; Vav-iCre*$^{+}$

(C)

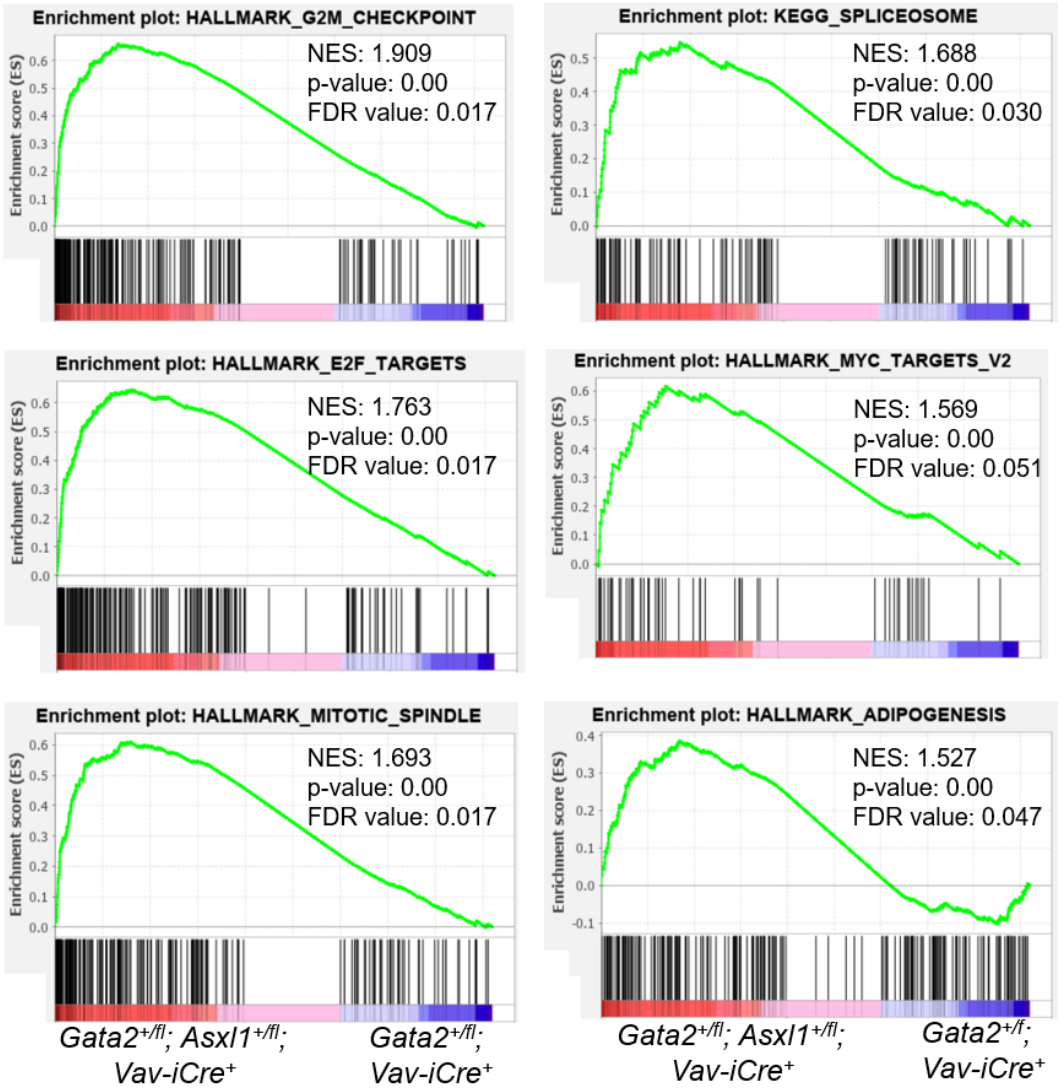

Figure 5-13: GSEA assessment for dysregulated pathways in *Gata2* and *Asxl1* double haploinsufficient HSCs.

(A) GSEA analysis of enriched pathways in double haploinsufficient HSCs related to control HSCs. (B and C) Enrichment plots for dysregulated pathways in double haploinsufficient HSCs versus *Asxl1* haploinsufficient HSCs (B) and haploinsufficient HSCs versus *Gata2* haploinsufficient HSCs (C). p-values and FDR-values of <0.05 were applied to determine enriched pathways.

Table 5.1: Biological processes of differentially dysregulated genes in double haploinsufficient HSCs.

Down-regulated genes	Categories	Up-regulated genes
Acvr2a, Cd34, Hoxa10, Il18, Tsc22d3	**Myelopoiesis**	*Arid4a, Cebpe, Csf1r, Cxcl12, Cxcl14, Dock8, Eif2ak1, Il1rn, Ly6d, Prex1, S100a8, Stat3, Stat5a, Stat5b, Spon2*
Cd1D, Cd23, Cd86, Cd200, Il15ra	**Lymphopoiesis**	*Atf4, Pax5, Blk, Cd2, Cd37, Cd40, Cd69, Cd74, Cd79a, Cd84, Cd180, Ighm, Ilf3, Palm, Rasgrp1, Runx3, Spib, Syk, Tcf3*
Cd63, Nfe2, Rps14, Rps19	**Erythropoiesis and megakaryopoiesis**	*Ankrd54, Calr, Ermap, Gata1, Gfi1b, Hspa9, Kat7, Klf1, Plek, Tfrc, Trim10, vWf, Zfpm1*
Acot9, Anxa4, Cd1d1, Ctsc, Extl2, Gbp2, Gemin2, Ggps1, Hlf, Idh1, Immp2l, Kdm6a, Klhl4, Lgals1, Mlf1, Mllt3, Nqo1, Phf6, Ppia, Psmb1, Psmb2, Psmd10, Rbm7, Rps6, S100a10, Tfpi, Tnfsf10, Vmp1, Xdh	**Haematological neoplasms**	*Add3, Chd2, Clec4a2, Crlf2, Ctsg, Dhx16, Dnmt1, Dnmt3b, Gdf15, Hectd1, Hsp90b1, Hspb1, Hsph1, Hvcn1, Impdh2, Jak3, Kif2c, Myd88, Msh6, Ms4a1, Ncor1, Nipbl, Nrp1, Nup214, Opa1, Patz1, Psmd2, Ptpn1, Ptpn11, Ranbp3, Rrm1, Rxrb, St6galnac3, Trim7, Tuba4a, Tuba8, Zfp36l2, Gpr183, Hnrnpa2b1, Ikbkb, Jarid2, Med12, Syncrip*
Cyclin B1, Cyclin G2, E2f3, Ptov1, Skp1a	**Cell Cycle**	*Atf5, Btg2, Cdc37, Cdc45, Cyclin A2, Cyclin D1, Cyclin E1, Cyclin Y, Cyclin D3, Cdk5rap2, Cdk5rap3, Cep57, Cep76, Cep78, Chfr, Donson, E2f2, E2f4, E2f8, Junb, Mki67, Mcm2, Mcm3, Mcm4, Mcm5, Mcm6, Mcm7, Mcm10, Nek2, Phlda1, P21, Taok3, Top2a, Uhrf1, Ube2c*
Mad2l1bp, Mzt1, Pttg1	**Spindle checkpoint and morphology**	*Aspm, Bub1, Bub1b, Cdc20, Cdt1, Cenpe, Cenpn, Dctn2, Dlgap5, Epn1, Hsf1, Kif11, Kif20a, Kif22, Mad1l1, Myh10, Plk1, Prpf4, Rcc1, Rest, Sac3d1, Sun1 Tpr, Tpx2, Tubg1*
H1f5, Pot1b	**Chromosomal organisation and morphology**	*Aurka, Aurkb, Cdca8, Ep400, Hdac2, Kif4a, Klf1, Lrwd1, Pelo, Sfpq, Smarca4, Smc2, Smc3, Smc4, Smc6, Smc1a, Smchd1, Suv39h1, Zbtb7a, Chaf1a, Hip1r, Kat6a, Kdm5b, Ncapd2, Ncapg2, Pds5b*
Bnip3l, Birc2, Gimap6, Pdcd5, Pdcd6, Pdcd10, Pycard, Sgms1	**Apoptosis**	*Acin1, Bak1, Bclaf1, Casp8ap2, Ccar1, Dusp1, Egr1, Htra2, Lmna, Ndrg1, Faim3, Immt, Pdcd11, Ppp1r13l, Prelid1, Tnfrsf21, Tnfrsf14, Tp53, Ubash3a*
Eif3a, Gtf2h5, Hmga2, Polr2d, Polr2g, Polr2j, Polr2k, Rbx1, Rps27a, Tcea1	**Excision repair of DNA**	*Atf3, Chaf1b, Ddb1, Exo1, Fen1, Hmgb1, Hnrnpu, Huwe1, Lig1, Lig3, Parp1, Pold1, Pold2, Polg, Polr2a, Polr2b, Rad23a, Rpa1, Ubc, Ung, Usp47*

Rps9	**Homologous recombination repair**	*Atrx, Rad50, Rad51d, Blm, Chd4, Eme1, Ewsr1, H2ax, Hsf1, Ipo5, Lsm2, Ncoa3, Ndc1, Pabpc1, Pcna, Prpf6, Prpf8, Rad54l, Rnf126, Spidr, Sf3b2, Sf3b3, Sf3b4, Xrcc3, Xrcc4, Zmynd8*
Sf3b6, Lsm1, Lsm3, Lsm7, Lsm10	**Spliceosome**	*Ddx39b, Ddx42, Ddx46, Dhx9, Dhx16, Eftud2, Prpf3, Prpf4, Prpf6, Prpf8, Prpf38b, Prpf4b, Sf1, Sf3a1, Sf3a2, Sf3b2, Sf3b3. Sf3b4, Snrnp35, Snrnp70, Snrnp200*
Cmpk1, Ddt, Dnajb9, Dnajc15, G3bp2, Gbe1, Ghitm, Jagn1, Nkiras1, Phyh, Rnf11, Sult1a1	**Adipocyte differentiation**	*Chchd10, Fabp4, Esyt1, Gpx3, Lpcat3, Nmt1, Rtn3, Sin3a, Stom, Tkt, Ucp2, Ywhag*
Atp5e, Atp5f1c, Atp5md, Atp5mf, Cox14, Cox16, Cox19, Cox4i1, Cox6b1, Cox6c, Cox7a2, Cox7a2l, Cox7b, Cox7c, Fis1, Hsd17b10, Maoa, Mterf1, Mterf2, Mterf3, Ndufa2, Ndufa4, Ndufa6, Ndufa7, Ndufa10, Ndufa11, Ndufab1, Ndufaf8, Ndufb3, Ndufb4, Ndufb6, Ndufb8, Ndufc1, Ndufb2, Ndufs4, Ndufs6, Ndufs8, Ndufv2, Sdhd, Uqcr10, Uqcr11, Uqcrb	**Mitochondrial regulations**	*Aco2, Atp13a1, Atp1a1, Atp2a3, Atp5f1a, Atp5f1b, Atp5f1d, Cox10, Cyc1, Htra2, Txn2*
Arhgap15, Arhgap15os, Arhgef11, Map1lc3b, Pdgfd, Ppp1cb, Rhoj, Trio	**Cytoskeleton regulations**	*Acta2, Actg1, Actn4, Arhgap11a, Arhgef2, Cfl1, Cit, Ckap5, Ckap2l, Clasp1, Clasp2, Cyfip1, Cyfip2, Ezr, F2r, Fgf3, Flii, Iqgap1, Iqgap3, Map1s, Rhob, Wasf2,*
F11r, Emcn, Itgb3bp, Itgbbp1, Mpzl1, Nrxn2, Ocln, Sdc4	**Cell adhesion molecules**	*Cercam, Icam4, Itga8, Itga2b, Itgb2, Itgb7, Mag, Pecam1, Psen1, Psen2, Prkca, Thbs2, Spn*
Slc6a15, Slc9b2, Slc16a12, Slc17a8, Slc22a21, Slc25a4, Slc25a30, Slc25a36, Slc39a1, Slc49a4, Slc50a1, Slc66a3, Slc35b3	**Membrane transport proteins (solute carrier)**	Slc4a1, Slc6a20, Slc7a5, Slc14a1, Slc15a4, Slc16a1, Slc16a6, Slc16a10, Slc20a1, Slc22a3, Slc25a38, Slc25a44, Slc26a1, Slc29a1, Slc38a1, Slc38a5, Slc38a10, Slc43a1, Slc43a3, Slc45a4, Slc35b1, Slc35c1, Slc35c2

5.9 *In vitro* knockdown of *Asxl1* in *Gata2* haploinsufficient BM cells

In order to mimic *GATA2* germline mutations with acquired *ASXL1* somatic mutations as human *GATA2* haploinsufficiency presenting with MDS/AML, this study employed lentiviral *Asxl1* shRNA to perform knockdown of *Asxl1* in *Gata2* haploinsufficient LSK cells. To do this, harvested LSK cells from *Gata2*$^{+/fl}$*; Vav-iCre*$^{+}$ and control mice were transduced with lentiviral shRNAs as previously described (Holmfeldt et al., 2016, Hosokawa et al., 2010). Two *Asxl1* shRNAs (*Asxl1*-sh1 and *Asxl1*-sh2) and empty vector (Scramble) were utilised to infect LSK cells with a multiplicity of infection (MOI) of 50 to transduce around 50%-60% of total infected cells for each genotype (Figure 5.14 A). Transduced LSK cells were maintained in liquid culture for four days. mCherry^{+} cells from control LSK cells were sorted to evaluate the transduction efficiency as well as the knockdown potency of *Asxl1*. Since all vectors co-expressed a red mCherry fluorochrome, we assessed the frequency of mCherry^{+} cells 4-days post-transduction. Flow cytometric assessment showed that the proportions of mCherry^{+} cells in empty vector (EV) and *Asxl1* hairpins were approximately 50%-60% in transduced control cells (Figure 5.14 B). We next measured the *Asxl1*-mRNA level in transduced WT LSK cells with EV or Asxl1 hairpins. Transduced LSK cells with *Asxl1*-sh1 displayed around a twofold reduction in *Asxl1*-mRNA as compared to transduced LSK cells with *Asxl1*-EV, whilst *Asxl1*-mRNA was fourfold decreased in *Asxl1*-sh2 transduced cells (Figure 5.14 C).

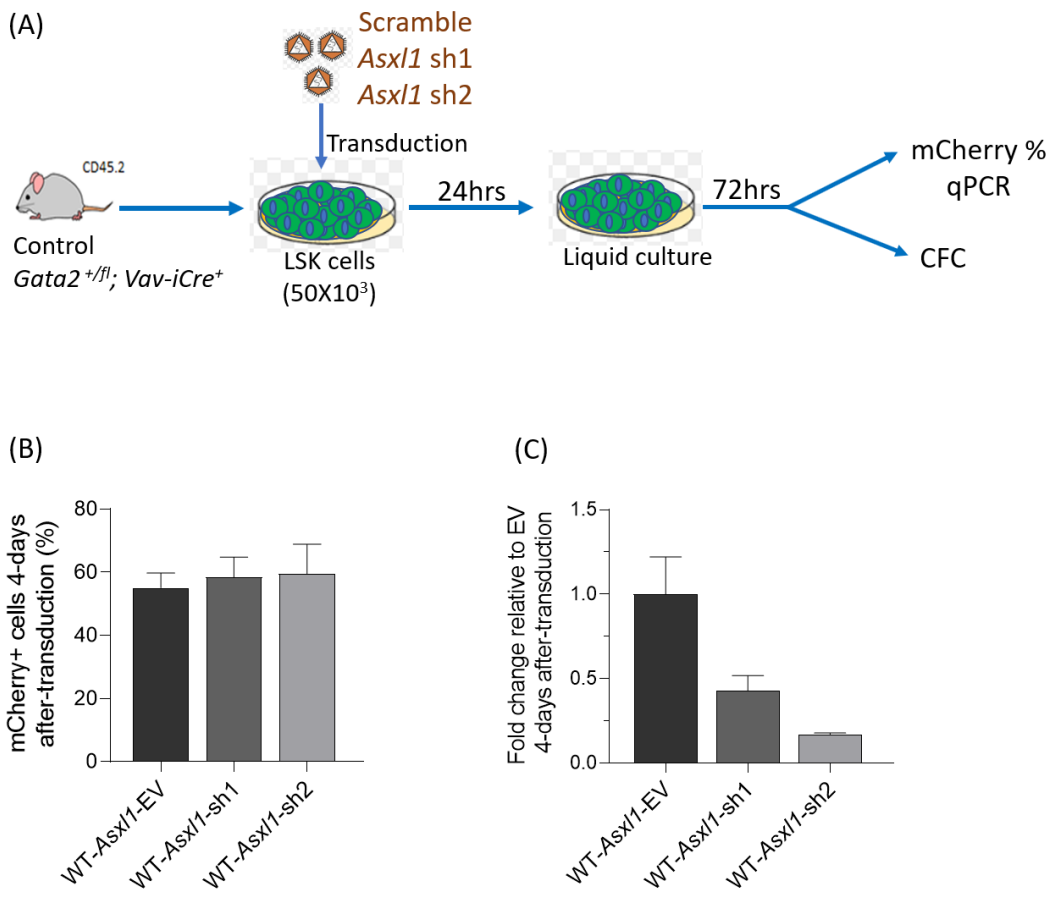

Figure 5-14: *In vitro* knockdown of *Asxl1* in *Gata2* haploinsufficient haematopoietic cells. (A) A scheme of *Asxl1* knockdown experiments. 50x10^3 freshly purified LSK cells from control or *Gata2*$^{+/fl}$*; Vav-iCre*$^+$ mice were transduced with *Asxl1*-EV, *Asxl1*-sh1, or *Asxl1*-sh2 at MOI of 50 and incubated overnight in IMDM media supplemented with 10% FBS, 1% L-glutamine, 1% Penicillin/Streptomycin, 100 ng/ml m-SCF, 100 ng/ml m-TPO, and 100 ng/ml m-Flt3L. Cells were then washed with PBS and cultured in IMDM media with 10% FBS, 1% L-glutamine, 1% Penicillin/Streptomycin, 100 ng/ml m-SCF, 100 ng/ml m-TPO, and 100 ng/ml m-Flt3L for 3 days. 4-days post-transduction, mCherry$^+$ cells were evaluated by FACS. mCherry$^+$ cells were collected by FACS-sorter for qPCR analysis and CFC assays. (B) The frequency of mCherry$^+$ cells 4-days after transduction in transduced control LSK cells (n=3) with EV and *Asxl1* hairpins from three independent experiments. (C) The expression level of *Asxl1*-mRNA in control LSK cells (n=2) that were transduced with EV, *Asxl1*-sh1, or *Asxl1*-sh2 from two separate experiments. Data are presented as mean ± SEM. One-Way ANOVA with Tukey's multiple comparisons test.

5.9.1 Decreased colony-forming potential in double haploinsufficient BM mCherry^{+} cells

In vitro CFC assay was performed to evaluate CFC-myeloid numbers in double haploinsufficient BM mCherry^{+} cells. To this end, mCherry^{+} cells were sorted 4-days after-transduction from WT or *Gata2*$^{+/fl}$*; Vav-iCre*$^{+}$ infected LSK cells with EV or *Asxl1*-hairpins and plated in methylcellulose medium (Figure 5.14 A). Although the total numbers of colonies were decreased in all different groups as compared to WT-EV, there was a two- to three-fold decline in the total colony number in *Gata2*$^{+/fl}$*; Vav-iCre*$^{+}$*-Asxl1*-sh1/sh2 BM cells compared to single haploinsufficient *Gata2* or *Asxl1* cells (Figure 5.15 A). Double haploinsufficient BM mCherry^{+} cells exhibited a reduction in numbers of CFU-GEMM and CFU-GM, CFU-M, CFU-G, and CFU-E when compared with control, *Asxl1* haploinsufficient cells, or *Gata2* haploinsufficient cells (Figure 5.15 B). There was a significant decrease in CFU-GEMM and CFU-GM, CFU-M, and CFU-E numbers in *Asxl1* haploinsufficient BM cells compared to control cells, whereas *Gata2* haploinsufficient BM cells displayed a significant decline in CFU-GM numbers compared to control BM cells. Collectively, these results suggest that knockdown of *Asxl1* in *Gata2* haploinsufficient LSK cells perturbs the differentiation capacity of BM myeloid progenitors in CFU assays *in vitro*.

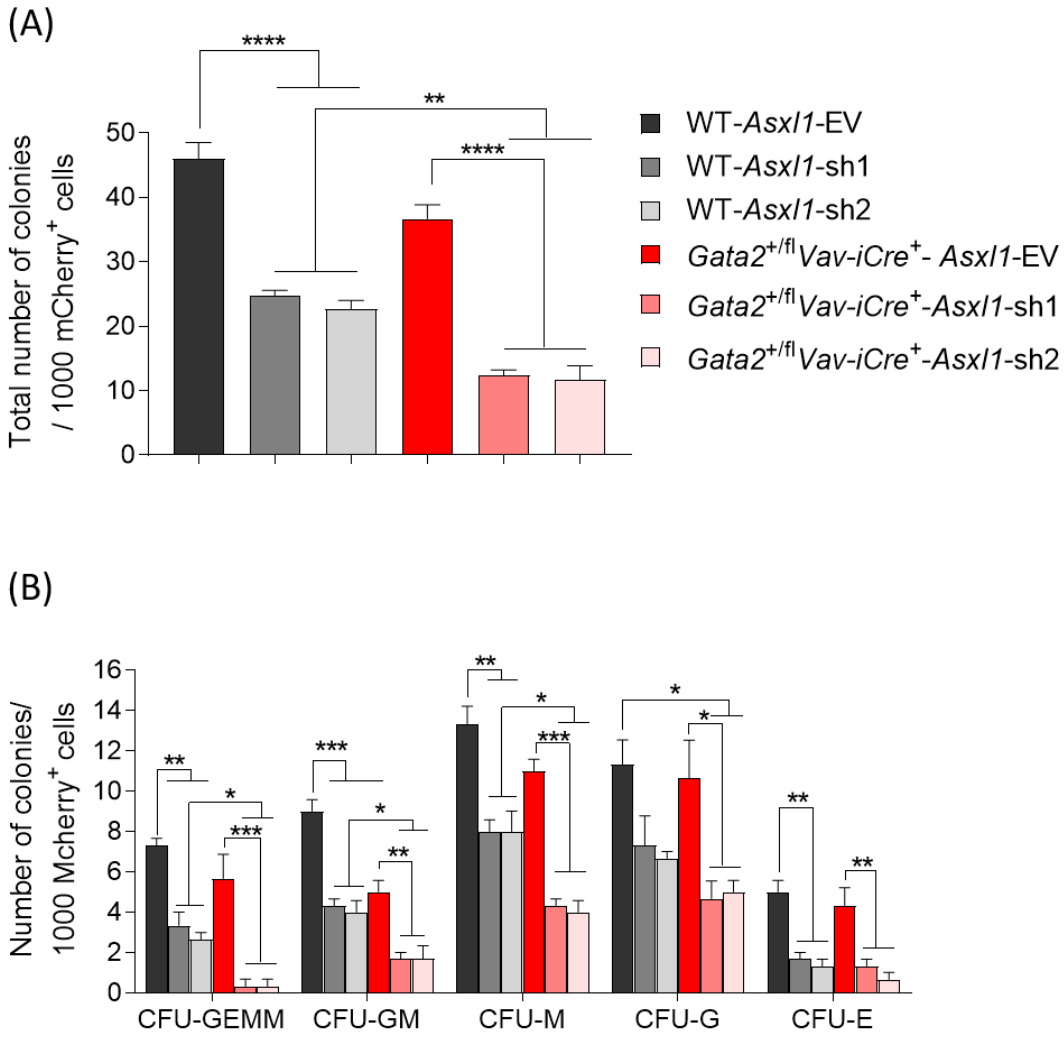

Figure 5-15: Decreased colony-forming potential in double haploinsufficient BM mCherry$^+$ cells.

(A and B) Total colony numbers (A) and differentiated myeloid colonies (B) 10-12 days post plating in methylcellulose media of sorted mCherry$^+$ BM cells 4-days post-transduction from WT-*Asxl1*-EV (control), WT-*Asxl1*-sh1, WT-*Asxl1*-sh2, *Gata2*$^{+/fl}$*; Vav-iCre -Asxl1*-EV, *Gata2*$^{+/fl}$*; Vav-iCre -Asxl1*-sh1, *Gata2*$^{+/fl}$*; Vav-iCre -Asxl1*-sh2 transduced cells. n=3 per genotype from 2 independent experiments. Data show as mean ± SEM. Statistical analysis: One-Way ANOVA with Tukey's multiple comparisons test *, P < 0.05; **, P < 0.01; ***, P < 0.001; ****, P < 0.0001.

5.10 Discussion

In line with the multi-step process of cancer development, the acquired monosomy 7, trisomy 8, *ASXL1*, *EZH2*, *SETBP1*, *HECW2*, *GATA1*, *NPM1*, *NRAS*, and *WT1* abnormalities are the most widespread secondary somatic mutations in patients with haploinsufficient GATA2 presenting with MDS/AML (Fujiwara et al., 2014, Luesink et al., 2012, West et al., 2014). Acquired *ASXL1* mutations exemplify the most common secondary somatic mutations in MDS/AML patients harbouring *GATA2* germline mutations and represent around 30% of all cases (Bödör et al., 2012, West et al., 2014). Acquired heterozygote somatic mutations of *ASXL1* are noticeably common in MDS, MPN, and AML patients (Paschka et al., 2015, Katoh, 2013, Gelsi-Boyer et al., 2012). Both conditional homozygote and heterozygote *Asxl1* KO mice exhibit haematological defects similar to human MDS/MPN phenotypes with a long-latency period of about 12 months of age (Abdel-Wahab et al., 2013, Wang et al., 2014). In this chapter, this study aimed to analyse the effect of the genetic cooperation between *Gata2* and *Asxl11* on haematopoiesis as well as the MDS/AML initiation by employing double conditional heterozygote knockout mice (*Gata2*$^{+/fl}$*; Asxl1*$^{+/fl}$*; Vav-iCre*$^{+}$) and lentiviral *Asxl1*-shRNA knockdown in *Gata2* haploinsufficient haematopoietic cells.

Double haploinsufficient mice showed no distinctive features of the distribution of lineage positive cells in PB, BM, and spleen relative to WT littermates (Table 5.2). The immunophenotypic assessment of primitive HSPCs and committed haematopoietic progenitors showed that the frequencies of HSCs, MPPs, LMPPs, and GMPs were significantly diminished in the BM of double haploinsufficient mice which largely phenocopied to what was observed in *Gata2* haploinsufficient mice (Table 5.2). Mechanistically, the reduced numbers of HSCs and MPPs were due to a decrease in cellular survival rates as demonstrated by the annexin V analysis (Figure 5.6). In remarkable contrast to *Gata2* haploinsufficient HSCs, the proliferative activity of double haploinsufficient HSCs was noticeably higher than *Gata2* haploinsufficient HSCs or control HSCs as indicated by the Ki-67 assay (Figure 5.7). Together, these results imply that *Gata2* and *Asxl1* double haploinsufficient HSCs genetically interact to increase proliferation. Functionally, double haploinsufficient HSCs were

inadequate of reconstituting long-term multi-lineage haematopoietic compartments in competitive transplant experiments. In particular, recipient mice transplanted with double haploinsufficient HSCs displayed a major decrease in frequencies of donor-derived cells for HSPCs when compared to *Gata2* haploinsufficient HSCs, *Asxl1* haploinsufficient HSCs, and WT derived cells (Table 5.2). Consistently, the assessment of *in vitro* colony-forming potential of double haploinsufficient BM cells revealed a decrease in total myeloid colonies and CFU-GEMM numbers relative to WT BM cells. In addition, *in vitro* knockdown of *Asxl1* in *Gata2* haploinsufficient LSK cells displayed efficient formation of myeloid colonies in the colony-forming assay of double haploinsufficient BM cells that was attenuated when compared to single haploinsufficiency of *Gata2* or *Asxl1* BM cells, indicating a defect in the differentiation capability induced cooperatively by *Gata2* and *Asxl1*. Collectively, double haploinsufficiency of *Gata2* and *Asxl1* perturbs the long-term repopulation capability and ultimately causes HSCs exhaustion after transplant. On the other hand, in accord with published data, young heterozygote *Asxl1* mice (8-12 weeks old) exhibit normal frequencies of haematopoietic compartments with a mild defect in the reconstitution capacity (Zhang et al., 2018, Wang et al., 2014).

Consistent with increased cycling of double haploinsufficient HSCs, RNA-Seq data showed a robust pattern of up-regulated biological pathways that are associated with regulations of cellular proliferation such as cyclins and cell cycle regulations, E2F target genes, G2M checkpoints, mitotic spindle checkpoints, mitotic roles of Polo-like kinase, cell cycle control of chromosomal replication, estrogen-mediated S-phase entry, and MYC target genes. Increased proliferation of HSCs was accompanied by upregulation of genes that are involved in G1/S stage transition including *E2F* transcription factors (*E2f2, E2f4, E2f8*), cyclins (*Cyclin D1, Cyclin D3, Cyclin E1, Cyclin A2, Cyclin Y*), and DNA replication initiators (*Cdc45, Mcm2, Mcm3, Mcm4, Mcm5, Mcm6, Mcm7, Mcm10*) (Ren et al., 2002, Pietras et al., 2011), that were coupled with down-regulation of G1/S checkpoints. GSEA analysis revealed upregulated target genes of E2F that are involved in several biological processes of the cell cycle involving G1/S phase, DNA replication, G2/M checkpoints, DNA damage checkpoints, DNA repair pathways, chromosomal segregation, mitotic regulations, and mitotic

spindle checkpoints (Table 5.2) (Ren et al., 2002). GSEA and IPA data further indicated enriched genes in double haploinsufficient HSCs that are involved in mitotic spindle checkpoints and chromosomal organisation required for mitotic spindle assembly (aurora kinase-A (*Aurka*) and aurora kinase-B (*Aurkb*)), mitotic checkpoints (Budding uninhibited by benzimidazoles-1 mitotic checkpoint serine/threonine kinase (*Bub1*), Bub1 mitotic checkpoint serine/threonine kinase-B (*Bub1b*), and mitotic arrest deficient-1 like-1 (*Mad1l1*)), spindle maintenance (polo-like kinase-1 (*Plk1*)), chromosome alignment (centromere protein-E (*Cenpe*) and centromere protein-N (*Cenpn*)) and others (Table 5.2) (Brown et al., 2017). GSEA investigation identified upregulated genes involved in MYC signalling. Although MYC target genes are implicated in different biological functions such as cellular growth and proliferation, cell cycle regulations, cellular metabolism, mitochondrial functions, and apoptosis, persistent expression of Myc targets is positively correlated with cellular transformation and tumorigenesis (Mannava et al., 2008, Dang et al., 2006). Together, analysis of transcriptional signatures provides clear evidence to conclude that double haploinsufficiency of *Gata2* and *Asxl1* cooperatively encourages HSCs cycling and proliferation.

In addition, ICP identified upregulated signalling of Rho-GTPases in double haploinsufficient HSCs, and transcriptional alterations related to cytoskeletal regulations and adhesion molecules. Ras homologous GTPases (Rho- GTPases) participate in several biological processes such as actin organisation, cellular migration, endocytosis, cellular adhesion, cellular polarity, and cell cycle (Mulloy et al., 2010, David et al., 2012). At HSCs level, Rho activity regulates HSCs homing, trafficking, survival, and proliferation (Mulloy et al., 2010). For example, RhoB is required for proper cell cycle cytokinesis (Mulloy et al., 2010). Furthermore, our data showed upregulation of integrin molecules involved in cell cycle regulations such as *Itga8, Itga2b, Itgb2,* and *Itgb7* (Moreno-Layseca and Streuli, 2014). Integrins encourage cellular migration, adhesion, proliferation, and differentiation (Moreno-Layseca and Streuli, 2014). Together, these data further support increased cycling capacity in double haploinsufficient HSCs.

Increased proliferative potential of double haploinsufficient HSCs was coupled with dysregulated DNA damage repair signatures (G2/M DNA damage checkpoint regulations, base excision repair, nucleotide excision repair, dsDNA break repair by homologous recombination, ATM signalling, and cell cycle regulation by BTG1 protein and GADD45 signalling) and activated cell death programmes, as shown by RNA-Seq data. Robust dysregulated genes associated with DNA damage repair processes were detected in double haploinsufficient HSCs (Table 5.1). The upregulation of G2/M DNA damage checkpoints was accompanied by up-regulated Trp53/p21 signalling. The tumour suppressor Trp53 plays different roles in the DNA damage response, cell cycle arrest, DNA repair, and apoptosis through activation of cyclin-dependent kinase inhibitor p21 to prevent cellular transformation (Agarwal et al., 1995, Taylor and Stark, 2001). Growth arrest DNA damage-45 (GADD45) signalling is triggered in response to physiological stressors and promotes either G1/S or G2/M arrest, DNA repair, cellular survival, and activation of apoptosis (Liebermann and Hoffman, 2008). GADD45 signalling mediates G2/M arrest by inhibiting the formation of cyclin-dependent kinase 1/cyclin B1 complex through Trp53/p21 activation (Liebermann and Hoffman, 2008). The tumour suppressor B-cell translocation gene-2 (BTG2), a downstream target of Trp53 signalling, has antiproliferative potential in response to cellular stress agents and involves in G2/M arrest, DNA repair, apoptosis, and mRNA stability (Yuniati et al., 2019). Additionally, RNA-Seq data revealed dysregulated biological mechanisms included in apoptosis signalling as death receptor signalling, endoplasmic reticulum stress, unfolded protein response, and mitochondrial dysfunction (Lavrik et al., 2005, Faitova et al., 2006, Papa et al., 2019). The death receptor (DR), a member of tumour necrosis factor receptor superfamily (TNFRS), is a cell surface receptor and possesses a cytoplasmic death-domain that initiates caspase activation and efficiently induces apoptosis (Lavrik et al., 2005). For instance, *Tnfrsf21* (DR6) and *Casp8* were upregulated in double haploinsufficient HSCs. Overall, these data indicate that the cooperative haploinsufficient HSCs of *Gata2* and *Asxl1* induce genomic instability that combines with activation of DNA damage repair and apoptosis pathways.

Additionally, our analysis showed that deregulation of mitochondrial genes associated with down-regulation of oxidative phosphorylation. Mitochondria acts as a regulator of cellular energy through oxidative phosphorylation (aerobic respiration) processes that fuel citric-acid cycle (Krebs-cycle) by converting pyruvate to acetyl-CoA and is further involved in several biological processes such as amino acid biosynthesis, cellular signalling, calcium homeostasis, inflammatory response, cellular differentiation, cell cycle regulations, and apoptosis (Papa et al., 2019, Bejarano-García et al., 2016). On the other hand, quiescent HSCs localise in the hypoxic environment within the BM niches and depend on glycolysis (anaerobic respiration), which occurs in the cellular cytoplasm, as the central supply of energy (Papa et al., 2019, Bejarano-García et al., 2016). Since the differentiation of HSCs requires a high level of energy, mitochondrial oxidative phosphorylation mediates the ATP generation in HSCs to meet their demands of energy (Papa et al., 2019, Bejarano-García et al., 2016). However, several reports have revealed that mitochondrial oxidative phosphorylation is essential to preserve the capacity of HSCs self-renewal and survival (Papa et al., 2019, Bejarano-García et al., 2016, Sarosiek et al., 2017). For instance, the deletion of succinate-dehydrogenase complex subunit-d (*Sdhd*, a component of mitochondrial complex-II), which was also down-regulated in our data, in the mouse BM perturbs the HSCs survival (Bejarano-García et al., 2016). One more example, in accordance with our data, the high expression of BCL2 homologous antagonist/killer (BAK1) promotes mitochondrial apoptosis (Sarosiek et al., 2017). Collectively, these data suggest that mitochondrial dysfunction may take part in decreased HSCs survival and differentiation capability in double haploinsufficient HSCs.

While HSPCs produce innate and adaptive immune cells to protect organism tissues from foreign pathogens, increased demands on HSPCs to generate immune effector cells drive HSCs exhaustion and BM failure syndromes (Schuettpelz and Link, 2013, de Bruin et al., 2014). Our analysis of double haploinsufficient HSCs indicated that affected biological pathways were involved in inflammatory responses such as IFN-γ response, neutrophil degranulation, TNF-α signalling by NF-κB, and adipogenesis. Congruous with what was noticed in *Gata2* haploinsufficient HSCs (chapter 3), double

haploinsufficient HSCs displayed dysregulation in IFN-γ signalling. Given that decreased expression of GATA2 or ASXL1 is required for adipocytes differentiation (Park et al., 2011, Tong et al., 2000), GSEA demonstrated enriched genes in double haploinsufficient HSCs were involved in adipogenesis. Adipocytes play important roles in inflammation responses, in which they secrete pro-inflammatory cytokines such as TNF-α, IL6, monocyte chemoattractant proteins, and macrophage inflammatory proteins to invade pathogens (Berg and Scherer, 2005). Additionally, our data revealed deregulation of TNF-α signalling by NF-κB signalling. Together, these data suggest that reduced HSC numbers in double haploinsufficient mice are combined with increased adipocyte formation that leads to fatty marrow replacement and induction of pro-inflammatory signalling, which impairs normal haematopoiesis (Xu et al., 2009, Berg and Scherer, 2005).

Analysis of unique dysregulated genes in double haploinsufficient HSCs indicated alterations in biological pathways implicated in leukaemogenesis such as spliceosomes assembly (pre-mRNA splicing complex, and assembly of RNA polymerase-III), death receptor signalling, and mitotic spindle checkpoints. Dysregulated expression of death receptor genes impairs apoptosis signalling in AML patients and results in worse clinical outcome (Schmohl et al., 2015). The adequate assembly of mitotic spindles during cell division is required for chromosomal segregation in order to avert chromosomal anomalies such as translocations or aneuploidy (Brown et al., 2017). Spliceosomes assembly is a process of formation of mature mRNA from precursor-mRNA by removing introns (noncoding sequences) and splicing exons (coding sequences) together through recruiting small nuclear ribonucleoproteins (snRNPs) and splicing factors (Will and Lührmann, 2011). RNA-Seq data identified dysregulated genes related to mRNA assembly including Pre-mRNA Processing Factors (*Prpf3, Prpf4, Prpf6, Prpf8, Prpf38b,* and *Prpf4b*), splicing factor (*Sf1, Sf3a1, Sf3a2, Sf3b2, Sf3b3. Sf3b4,* and *Sf3b6*), snRNPs (*Snrnp35, Snrnp70,* and *Snrnp200*), DEAD-Box-Helicase genes (*Ddx39b, Ddx42, Ddx46, Dhx9, and Dhx16*) and Sm-like genes (*Lsm1, Lsm3, Lsm7*, and *Lsm10*). Consistently, RNA polymerase-III is required for pre-mRNA splicing, tRNA, and 5S rRNA synthesis, and continual transcription of this enzyme is frequently observed in transformed leukaemic cells

(Han et al., 2018). Given that approximately 40% of MDS patients harbour mutations in the assembly of mRNA splicing (Figure 1.8) (Bejar and Steensma, 2014, Sperling et al., 2017), more than 70% of GATA2 deficiency patients develop MDS phenotypes (Wlodarski et al., 2017, Collin et al., 2015, Donadieu et al., 2018). Thus, deregulation of mRNA spliceosomes may explain the recurrent MDS phenotypes in GATA2 haploinsufficiency syndromes. To conclude, the present evidence in RNA-Seq data provides vital insights into the genetic interaction between *Gata2* and *Asxl1* and suggests that double haploinsufficient HSCs disturb biological pathways such as DNA damage repair pathways, mitotic spindle checkpoints, and mRNA spliceosomes, that impair the genomic stability and correlate with the development of haematological malignancies.

Table 5.2: Haematological phenotypes of adult *Asxl1$^{+/fl}$; Vav-iCre^{+}*, *Gata2$^{+/fl}$; Vav-iCre^{+}*, and *Gata2$^{+/fl}$; Asxl1$^{+/fl}$; Vav-iCre^{+}* mice.

	Asxl1$^{+/fl}$; Vav-iCre^{+}	*Gata2$^{+/fl}$; Vav-iCre^{+}*	*Gata2$^{+/fl}$; Asxl1$^{+/fl}$; Vav-iCre^{+}*
HSPCs	No difference	↓HSCs, MPPs, and LMPPs	↓HSCs, MPPs, and LMPPs
Committed progenitors	↓Insignificant GMPs	↓GMPs	↓GMPs
Colony-forming potential	↓CFU-GM	↓CFU-GM	↓CFU-GEMM, and CFU-GM
Mature cells (PB)	No difference	No difference	No difference
Lineage positive cells (BM and spleen)	No difference	No difference	No difference
Cell cycle status	No difference	↑HSCs frequency in G0 phase	↑HSCs frequency in S/G2/M phases
Apoptosis level	No difference	↑HSCs and MPPs	↑HSCs and MPPs
HSCs repopulation potential	A mild multi-lineage defect	A multi-lineage defect	A multi-lineage defect, especially in HSC populations

CHAPTER 6 : General discussion and future perspectives

HSCs are the only source of continuous replenishment of haematopoietic progenitors and mature blood cells for the period of the lifespan. HSCs architecture, quiescence, survival, self-renewal, and differentiation are regulated by complex regulatory processes, involving intrinsic (transcription factors) and extrinsic (BM niches) mechanisms (Rieger and Schroeder, 2012, Orkin and Zon, 2008, Seita and Weissman, 2010). GATA2, a zinc finger transcription factor, is one of heptad transcription factors (*SCL/TAL1, RUNX1, ERG, LYL1, LMO2, FLI1, and GATA2*) that are crucial regulators for HSCs development and differentiation (Wilson et al., 2010). The expression of GATA2 is found in distinct kinds of tissues such as the nervous system, endothelial cells, placenta, and BM cells (Vicente et al., 2012a, Lentjes et al., 2016). Haematopoietic cells such as HSCs, MPPs, HPCs, CMPs, MEPs, erythroid-precursors, mast cells and megakaryocytes highly express *Gata2* mRNA (Menendez-Gonzalez et al., 2019b, Orlic et al., 1995, Guo et al., 2013).

The emanation of HSCs from haemogenic endothelium is dependent on *Gata2* expression (de Pater et al., 2013). Germline ablation of *Gata2* (*Gata2*$^{-/-}$) is lethal at E10.5 with significant anaemic indicators (Tsai et al., 1994). Constitutive deletion of one allele of *Gata2* (*Gata2*$^{+/-}$) embryos reveals reduced numbers of AGM-HSCs and impairment in AGM-HSCs repopulating capacity and self-renewal capacity (Ling et al., 2004). Consistently, conditional deletion of one allele of *Gata2* after the HSCs generation (*Gata2*$^{+/fl}$*; Vav-Cre*$^{+}$) causes the number of HSCs to significantly diminish in the AGM region and foetal liver (de Pater et al., 2013). Adult *Gata2*$^{+/-}$ mice exhibit a reduction in HSCs pool size, increased quiescent HSCs, decreased HSCs survival, diminished numbers of GMPs and CFU-GM, and a repopulating defect in HSCs as evaluated by transplantation experiments (Rodrigues et al., 2008, Rodrigues et al., 2005). Acute ablation of *Gata2* in adult haematopoietic compartments (*Gata2*$^{fl/fl}$*; ER-Cre*$^{+}$ and *Gata2*$^{fl/fl}$*; Mx1-Cre*$^{+}$) causes nearly complete disappearance of BM HSPCs (Li et al., 2016, Menendez-Gonzalez et al., 2019b).

Since most MDS/AML cases occur sporadically, investigation of familial cases is beneficial to understand the molecular mechanisms triggering leukaemogenesis. To date, mutations of *GATA2, RUNX1*, *CEBPα, ETV6, ANKRD26,* and *DDX41* have been only detected in familial MDS/AML cases (Song et al., 1999, Arber et al., 2016). GATA2 haploinsufficiency disorders are several clinical immunodeficiency syndromes that can cause BM failure and eventually increased predisposition to develop MDS/AML (Dickinson et al., 2011, Hyde and Liu, 2011, Hahn et al., 2011, Hsu et al., 2011, Ostergaard et al., 2011). There is a lack of understanding about how specific haematopoietic compartments are impacted by GATA2 haploinsufficiency in these settings.

In order to uncover the requirement of *Gata2* heterozygote in the adult haematopoietic compartments, conditional *Gata2* heterozygote knockout mice models provide a convenient model to study these GATA2 haploinsufficiency syndromes. Vav and Mx1 promoters that utilise the Cre-Lox recombination system are specifically able to drive Cre-mediated recombination to excise floxed *Gata2* allele in the mouse haematopoietic system. The pan Vav-iCre promoter is spontaneously triggered at E11 in the developing embryo and provides a model to investigate the chronic deficiency of *Gata2* heterozygote in adult (8-12 weeks) and aged (18-20 Months) mice, whilst the inducible Mx1-Cre promoter acutely deletes *Gata2* heterozygote in the adult stage through the administration of pIpC doses (Stadtfeld and Graf, 2005, Kuhn et al., 1995). Therefore, both the Vav-Cre and Mx1-Cre mice models serve as tools to mimic hereditary and acquired GATA2 mutations, respectively. Since sporadic *ASXL1* mutations are the most frequent secondary genetic disorders in MDS/AML patients harbouring *GATA2* inherited mutations, we further assessed the impact of the genetic interaction between *Gata2* and *Asxl1* on the adult haematopoietic system by employing double heterozygote mouse models (*Gata2*$^{+/fl}$*, Asxl1*$^{+/fl}$*; Vav-iCre*$^{+}$) and knockdown of *Asxl1* in *Gata2* haploinsufficient haematopoietic cells (Bödör et al., 2012, West et al., 2014).

Congruous with previous reports (de Pater et al., 2013, Ling et al., 2004, Rodrigues et al., 2005), our data showed that either chronic (*Gata2*$^{+/fl}$*; Vav-iCre*$^{+}$) or acute

(*Gata2*$^{+/fl}$; *Mx1-Cre*$^{+}$) loss of *Gata2* haploinsufficiency perturbs adult HSCs homeostasis, and these findings signify that the biallelic expression of *Gata2* is necessary for ideal HSCs development and maintenance. Cooperative haploinsufficient HSCs from *Gata2* and *Asxl1* (*Gata2*$^{+/fl}$; *Asxl1*$^{+/fl}$; *Vav-iCre*$^{+}$) result in increased rates of HSCs proliferation and severe functional defects in transplantation settings as compared with single haploinsufficient counterparts, indicating collaborative transcriptional signatures between *Gata2* and *Asxl1*.

6.1 Proposed roles of *Gata2* in haematopoietic compartments

In order to unveil the impact of *Gata2* haploinsufficiency in the adult haematopoietic system, this study employed *Gata2*$^{+/fl}$; *Vav-iCre*$^{+}$ mouse models to mimic germline *GATA2* mutations that cause immunodeficiency syndromes. Immunophenotypic characterisations of *Gata2*$^{+/fl}$; *Vav-iCre*$^{+}$ mice were extensively examined using different staining protocols. Our analysis showed that diminished numbers of LT-HSCs, ST-HSCs (Known as MPP1 or MPPs) and MPP4/LMPPs (lymphoid/GMP-biased MPPs), normal distribution of MPP3 (GMP-biased-MPPs), and an increase in numbers of MPP2 (megakaryocyte/ erythroid-biased MPPs) (Figure 6.1 A). The expansion of uncommitted MPP2 progenitors affects the differentiation of downstream bipotent Pre-MegE progenitors that ultimately lead to decreasing numbers of committed megakaryocyte (MkPs) and erythrocyte (Pre-CFU-E) progenitors. The reduction of MkP numbers is reflected by declined numbers of mature megakaryocytes and peripheral platelets. In other respects, decreased MPP4/LMPP numbers disturb the differentiation capability of committed myeloid progenitors (Pre-GM and GMPs). Overall, these results highlight the requirement of *Gata2* in haematopoiesis and indicate that *Gata2* haploinsufficiency disorganises the normal differentiation of HSPC compartments, early erythroid/myeloid progenitors, and megakaryopoiesis. In support of this, single-cell RNA-Seq of purified BM CD34^{+} cells from human MDS patients harbouring GATA2 haploinsufficiency shows up-regulation of erythrocytes/megakaryocytes priming genes and down-regulation of lymphoid/ myeloid (MLPs) priming genes (Wu et al., 2020). Thus, the differentiation defects of MPP2 observed in this model may explain the recurrent megakaryoid/erythroid

dysplastic features (about 85%) and peripheral thrombocytopenia (around 20%), that have been reported in GATA2 haploinsufficient patients (Donadieu et al., 2018, Collin et al., 2015, Dickinson et al., 2014). The analysis of primitive haematopoietic progenitors undertaken in this study has extended our knowledge of the requirements for *Gata2* in specific MPP compartments during haematopoietic differentiation.

On the other hand, immunophenotypic analysis of GATA2 haploinsufficient patients with immunodeficiency phenotypes such as MonoMAC and DCML syndromes reveals a reduction in numbers of MPPs and MLP progenitors, which ultimately perturb the abundance of downstream haematopoietic cells such as GMPs, monocytes, dendritic cells, B-cells, NK-cells, and CD4/CD8 ratios, whilst the frequencies of granulocytes, erythrocytes, and megakaryocytes are unperturbed (Figure 6.1 B) (Collin et al., 2015, Dickinson et al., 2014, Calvo et al., 2011, Bigley et al., 2011). Thus, GATA2 expression is required for MLPs differentiation in the human hierarchy. Functionally, murine LMPPs are the closest population to human MLPs (Doulatov et al., 2012). In comparison to GATA2 haploinsufficient patients, *Gata2* haploinsufficient mice generate low numbers of MPPs, MPP4/LMPPs (human MLPs), and GMPs, but demonstrate normal distributions of peripheral myeloid and lymphoid lineages. Given that GATA2 haploinsufficient patients have normal haematological parameters at the time of diagnosis (before infections), additional research is required to investigate whether *Gata2* haploinsufficient mice will develop immunodeficiency phenotypes following injection with acute infection agents such as *Mycobacterium avium*, a causative agent of MonoMAC syndrome.

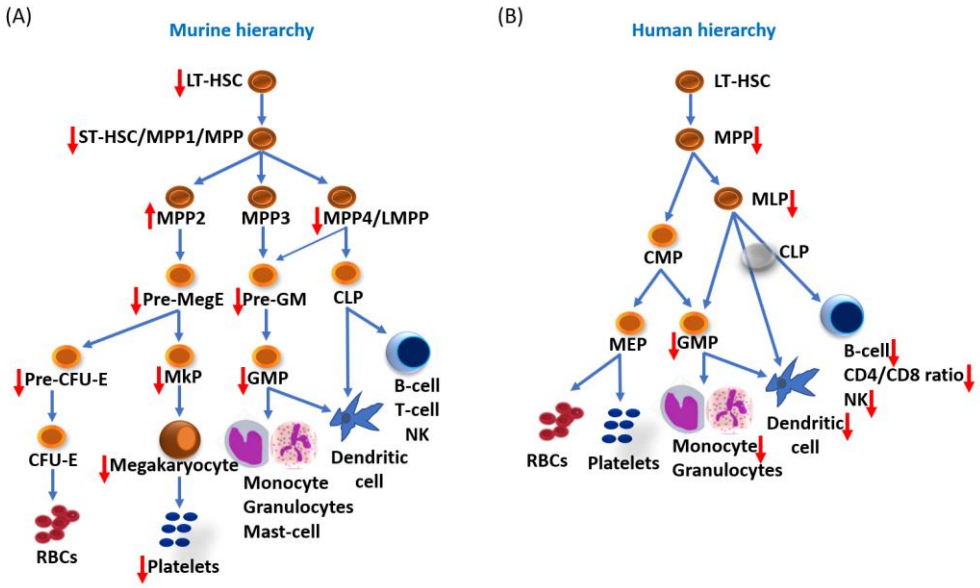

Figure 6-1: Immunophenotypic features of *GATA2* haploinsufficiency in human and murine haematopoietic compartments.
(A) Immunophenotypic abnormalities in *Gata2*$^{+/fl}$*; Vav-iCre*$^{+}$ mice. (B) Immunophenotypic features in GATA2 haploinsufficient patients with DCML syndromes.

6.2 The effect of chronic and acute loss of *Gata2* haploinsufficiency on the adult HSPCs and haematopoiesis

Acute and chronic mice models were employed to evaluate the impact of *Gata2* haploinsufficiency on haematopoiesis. The most prominent results were observed at the HSC level, in which both models demonstrate a decrease in HSCs pool size. Whereas *Gata2*$^{+/fl}$*; Mx1-Cre*$^{+}$ mice show no alterations in frequencies of primitive and committed progenitors, there is significant reduction in proportions of MPPs, HPC1, LMPPs, and GMPs in *Gata2*$^{+/fl}$*; Vav-iCre*$^{+}$ mice (Table 6.1). The reduction of HSC numbers in both models correlated with increased HSCs quiescence. Thus, *Gata2* haploinsufficiency promotes decreased HSCs cycling, perhaps to protect HSCs from exhaustion. Increased demands on HSCs to replenish haematopoietic progenitors lead to proliferative stress and eventually perturbs HSCs survival as shown in young *Gata2*$^{+/fl}$*; Vav-iCre*$^{+}$ mice. Continual proliferative stress on HSCs precedes to increased HSCs cycling, diminished survival rates, and persistent reduced HSC numbers as demonstrated in aged *Gata2*$^{+/fl}$*; Vav-iCre*$^{+}$ mice. Consistently, given that serial transplant experiments can imitate HSCs ageing and are commonly applied to assess the HSCs self-renewal potency (Rieger and Schroeder, 2012, Orkin and Zon, 2008, Seita and Weissman, 2010), HSCs from *Gata2*$^{+/fl}$*; Vav-iCre*$^{+}$ or *Gata2*$^{+/fl}$*; Mx1-Cre*$^{+}$

mice are ineffectual in reconstituting multi-lineage haematopoietic cells in serial transplantation settings. Altogether, these results signify that *Gata2* haploinsufficiency disrupts adult HSCs survival, differentiation, self-renewal, and maintenance.

Transcriptome analysis of purified HSCs from both models displayed that 117 differentially expressed genes were dysregulated in *Gata2*$^{+/fl}$*; Vav-iCre*$^{+}$ HSCs, whilst 79 dysregulated genes were detected in HSCs from *Gata2*$^{+/fl}$*; Mx1-Cre*$^{+}$ mice. Only one expressed gene (*Armh4*) was shared between acute and chronic *Gata2* haploinsufficient HSCs (Figure 6.2 A). The function of *Armh4* in haematopoiesis is largely undetermined. Consistent with HSCs phenotypes, gene ontology evaluation of cellular and molecular processes revealed that dysregulated genes in acutely deleted haploinsufficient HSCs were implicated in cellular homeostasis and maintenance, whereas chronically deleted haploinsufficient HSCs showed alterations in the proliferation of blood cells, apoptosis, and myeloid cells migration and accumulation (Figure 6.2 B). Our bioinformatic analysis using IPA software indicated no shared pathways amongst dysregulated genes in both groups. A possible explanation for these results is that dysregulated transcriptional signatures in Vav-iCre (developmental deletion) and Mx1-Cre (acute deletion) models may reflect stage-specific transcriptional functions for GATA2 during haematopoietic ontogeny, indicating that GATA2 has different regulatory pathways for HSCs development and maintenance. Another possibility is that long-term (Vav-iCre) GATA2 deficiency may reflect long-term pre-leukaemia potential such as deregulated DNA repair genes, whereas short-term (Mx-Cre) deletion model may reflect initial transcriptional changes (homeostatic alterations) after GATA2 function is lost in adult, as evidenced by RNA-Seq data.

Although our results in both models indicated *Gata2* haploinsufficiency autonomously perturbed HSCs quiescence, self-renewal, and maintenance, RNA-Seq data exhibited dysregulated pathways associated with ECM signalling in HSCs from *Gata2*$^{+/fl}$*; Mx1-Cre*$^{+}$ mice that had an acute deletion of one allele of *Gata2* in both haematopoietic populations and BM niches (Chapter 3 and 4). ECM provides BM

niches with essential substances that regulate several biological functions of HSCs such as adhesion, migration, integrity, survival, proliferation, and differentiation (Kular et al., 2014, Zhang et al., 2019). Therefore, it seems possible that *Gata2* haploinsufficiency may have effects on HSC niches. Further investigation with more focus on the adult *Gata2* haploinsufficient niches utilising *Mx1* mouse models by transplanting WT BM cells into *Gata2*$^{+/fl}$*; Mx1-Cre*$^{+}$ hosts or employing niche-specific Cre models such as VE-Cadherin-CreER^{T2}, Prx1-Cre, or LepR-Cre might explore whether *Gata2* haploinsufficiency could affect HSCs microenvironment.

Table 6.1: Immunophenotypic comparison between *Gata2*$^{+/fl}$*; Vav-iCre*$^{+}$ and *Gata2*$^{+/fl}$*; Mx1-Cre*$^{+}$ mice.

	Young *Gata2*$^{+/fl}$*; Vav-iCre*$^{+}$	Young *Gata2*$^{+/fl}$*; Mx1-Cre*$^{+}$
HSPCs	↓ HSCs, MPPs, HPC1, and LMPPs ↑ HPC2	↓ HSCs
Committed progenitors	↓ GMPs	No difference
Colony-forming potential	↓ CFU-GM	No difference
Lineage positive cells (PB, BM and spleen)	↓ Megakaryocytes, Platelets No difference in myeloid, lymphoid, and erythroid lineages	No difference in myeloid, lymphoid, and erythroid lineages
Cell cycle status	↑ HSCs frequency in G0 phase	↑ HSCs frequency in G0 phase
Apoptosis level	↑ HSCs and MPPs	No difference
HSCs repopulation potential	A multi-lineage defect	A multi-lineage defect
HSCs self-renewal potential	A defect in HSCs self-renewal	A defect in HSCs self-renewal

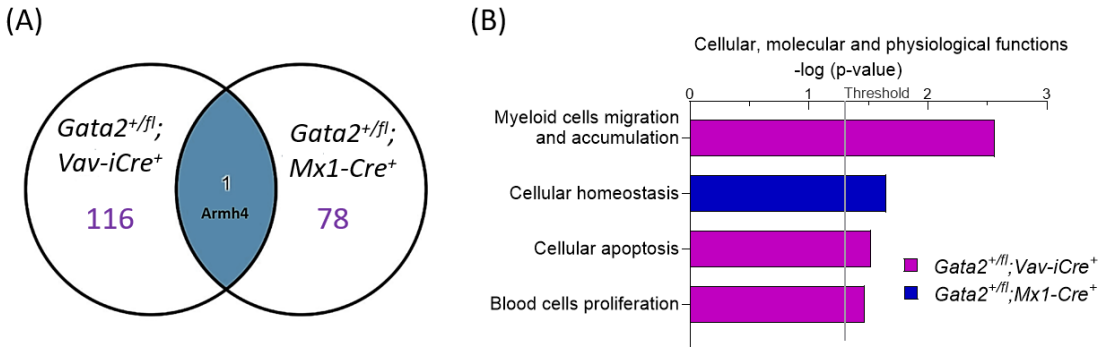

Figure 6-2: Transcriptome changes in of *Gata2*$^{+/fl}$*; Vav-iCre*$^{+}$ and *Gata2*$^{+/fl}$*; Mx1-Cre*$^{+}$ mice. (A) The Venn diagram describes dysregulated gene numbers (p-values and FDR-values <0.05) in sorted HSCs from both *Gata2*$^{+/fl}$*; Vav-iCre*$^{+}$ mice (n=4) *and Gata2*$^{+/fl}$*; Mx1-Cre*$^{+}$ mice (n=4) relative to their controls. (B) Biological processes of significant differentially regulated genes in both models. Data are presented as $-\log_{10}$ (p-value). The threshold line in grey shows significant processes with a p-value at 0.05 using Fischer's Exact Test.

6.3 *Gata2* haploinsufficiency impairs HSCs self-renewal through dysregulation of proinflammatory signalling

Self-renewal impairment in *Gata2* haploinsufficient HSCs is a novel finding in this thesis. Proinflammatory cytokines have indispensable roles in regulating adult HSCs survival, proliferation, and differentiation under homeostatic circumstances (Schuettpelz and Link, 2013, de Bruin et al., 2014). Given that HSPCs provide the blood circulation with innate and adaptive immune cells to invade pathogen, chronic inflammatory stimulation of HSCs to adequately repopulate immune effector cells leads to HSCs exhaustion and eventually produces BM failure and cellular transformation (Schuettpelz and Link, 2013, de Bruin et al., 2014). Congruent with the existing knowledge that GATA2 haploinsufficiency gives rise to immunodeficiency disorders, HSCs from *Gata2*$^{+/fl}$*; Vav-iCre*$^{+}$ and *Gata2*$^{+/fl}$*; Mx1-Cre*$^{+}$ mice disclosed dysregulated biological pathways engaged in cellular immune responses such as up-regulation of IFN-γ signalling, down-regulation of IL-6 signalling, IL-4 signalling, IL-10 signalling, Toll-like receptor signalling, humoral immune response, and immune cell trafficking, as demonstrated by RNA-Seq data.

Dysregulation of IFN-γ or IL-6 signalling perturbs HSCs specification, self-renewal, and differentiation (de Bruin et al., 2013, Bernad et al., 1994, Tie et al., 2019). Up-regulation of IFN-γ signalling disturbs the capacity of HSCs self-renewal via increased expression of suppressor of cytokine-signalling-1 (*Socs1*) that ultimately restrains signal transducer and activator of transcription-5 (STAT5) phosphorylation in response to thrombopoietin (*Tpo*) (*IFNγ-Socs1-Tpo-Stat5* signalling) (de Bruin et al., 2013). On the other hand, down-regulation of IL-6 signalling results in a decline in interleukin-6 signal transducer (*Il6st*) expression that inhibits STAT3 phosphorylation and ultimately disrupts HSCs self-renewal ability (*Il6-Il6st-Stat3* signalling) (Lee et al., 2016). It is broadly well-known that *Stat3* and *Stat5* have a positive impact on HSCs self-renewal effectiveness (Kato et al., 2005, Chung et al., 2006). Interestingly, the expression level of *Stat3* and *Stat5* was insignificantly reduced in our RNA-Seq data. Collectively, these observations suggest that proinflammatory signalling could be a key factor triggering a self-renewal defect in *Gata2* haploinsufficient HSCs. Further work is therefore needed to validate the expression level of *Stat3* and *Stat5* in *Gata2*

haploinsufficient HSCs for establishing these observations. Moreover, it would be noteworthy to evaluate whether the physiological response of *Gata2* haploinsufficient HSCs to proinflammatory agents such as IFN-γ could enhance cellular transformation.

6.4 *Gata2* haploinsufficient HSCs display increased DNA damage repair responses

Our data signify that HSC functions are broadly affected by *Gata2* haploinsufficiency, including HSCs cycling, survival, multi-lineage reconstitution, and self-renewal potential. In contrast to haematopoietic progenitors, HSCs are the main exporter of genetic alterations in the haematopoietic system for several reasons: the long lifespan of HSCs; a multi-linage differentiation capability; an infinite ability for cycling and proliferation; and a resistant capacity of quiescent HSCs to chemotherapy and targeted treatments (Moehrle and Geiger, 2016, Niedernhofer, 2008, Biechonski et al., 2017). DNA-damage response (DDR) processes play vital functions in safeguarding HSCs genomic integrity. There are four distinct categories of DDR processes, which are recognition of DNA damage, recruitment of DNA signal transducers, DNA repair effectors, and cell cycle arrest or apoptosis effectors (Moehrle and Geiger, 2016, Niedernhofer, 2008, Biechonski et al., 2017). DNA signal transducers include DNA-damage checkpoints ATM (Ataxia telangiectasia mutated) and ATR (Ataxia-telangiectasia and rad3-related protein), that repress the expression of Cell division cycle-25a (CDC25A) and ultimately halt the cell cycle progression during DNA repairs (Moehrle and Geiger, 2016, Niedernhofer, 2008, Biechonski et al., 2017). Inefficient DDR mechanisms trigger apoptosis signalling, premature differentiation, and senescence (Moehrle and Geiger, 2016, Niedernhofer, 2008, Biechonski et al., 2017). A consequence of accumulated DNA damage can result in reduced HSCs pool size as well as impaired HSCs repopulating and self-renewal capacity (Moehrle and Geiger, 2016, Niedernhofer, 2008, Biechonski et al., 2017). A defect in DDR activities can lead to BM failure, immunodeficiency, and haematological disorders (Moehrle and Geiger, 2016, Niedernhofer, 2008, Biechonski et al., 2017).

Acquired genetic alterations are required to trigger leukaemogenesis in germline *GATA2* haploinsufficient patients such as *ASXL1*, *EZH2*, *SETBP1*, *HECW2*, *GATA1*, *NPM1*, *NRAS*, *WT1,* monosomy 7, and trisomy 8 (Fujiwara et al., 2014, Luesink et al., 2012, West et al., 2014). HSCs from young and aged *Gata2*$^{+/fl}$*; Vav-iCre*$^{+}$ mice exhibited an increased level of γH2AX, a DNA-damage marker. Consistently, up-regulation of DNA repair pathways such as dsDNA break repair by homologous-recombination and base excision repair was detected in young *Gata2* haploinsufficient HSCs. Additionally, RNA-Seq data showed an insignificant reduction of the DNA-damage checkpoint *Atr* (p-value: 0.0006; FDR-value: 0.07) and its downstream target Checkpoint kinase-1(*Chek1*) (p-value: 0.008; FDR-value: 0.2). Thus, elevated DNA-damage level in *Gata2* haploinsufficient HSCs was accompanied by activation of DNA repair processes and diminished expression of DNA-damage checkpoints. Together, these observations provide vital insights into how *Gata2* haploinsufficiency causes genomic instability of HSCs and forces the development of acquired genetic abnormalities. Further assessment is required to confirm the expression level of *Atr-Check1-Cdc25a* genes in *Gata2* haploinsufficient HSCs.

6.5 Cooperative haploinsufficient HSCs of *Gata2* and *Asxl1* act as a reservoir of preleukaemic initiators

Combined haploinsufficient mice of *Gata2* and *Asxl1* result in increased HSCs cycling. Upon transplantation, double haploinsufficient HSCs display compromised HSCs reconstitution capacity and exhausted HSCs pool size under stress haematopoiesis much more profoundly than their *Gata2* or *Asxl1* single haploinsufficient counterparts. Likewise, acquired knockdown of *Asxl1* in *Gata2* haploinsufficient primitive cells specifically impairs the differentiation efficiency of myeloid progenitors in the colony-forming assay. These findings indicate collaborative genetic interaction between *Gata2* and *Asxl1* pathways. Although double haploinsufficient mice do not display malignant haematological phenotypes, double haploinsufficient HSCs show alterations in biological pathways that may have implications for the subsequent emergence of haematological disorders such as cyclins and cell cycle regulations, cell cycle control of chromosomal replication, mitotic spindle

checkpoints, DNA damage repair signalling, and mRNA spliceosomes. Together these conclusions may help to understand the molecular mechanisms that underlie the malignant transformation in GATA2 haploinsufficiency syndromes. Consequently, additional investigations with more focus on the integrated analysis of RNA-Seq data with previously published chromatin immunoprecipitation sequencing (ChiP-seq) reports are recommended to further identify exclusive and combinatorial *Gata2/Asxl1* direct and indirect target genes potentially contributing to pathogenesis in clinical GATA2 syndromes. In addition, given that the latency period of *Asxl1* KO mice to develop MDS/MPN phenotypes is more than 12 months of age (Abdel-Wahab et al., 2013, Wang et al., 2014), further experiments will be necessary to be undertaken to evaluate the impacts of the long-term loss of double haploinsufficiency on HSPCs and haematopoiesis to determine whether double haploinsufficient mice would develop myeloid malignancies.

GATA2 haploinsufficient patients with somatic *ASXL1* mutations have a rapid onset of MDS/AML, poor prognosis, and decreased survival rates (West et al., 2014, Bödör et al., 2012). Analysis of gene expression data in double haploinsufficient HSCs indicated up-regulation of DNA methyltransferase genes (*Dnmt1* and *Dnmt3b*) and ATP-binding cassette (ABC) transporters (*Abcb8, Abcc9, Abcf1, Abcg4*). DNA methylation genes regulate essential biological mechanisms involving gene expression and silencing, inactivation of the X-chromosome, haematopoiesis, and tumorigenesis (Gore and Weinstein, 2016, Wong et al., 2019). Oncogenic roles of DNA methylation genes have been previously described in the pathogenesis of MDS/AML patients, in which up-regulation of *DNMT1* and *DNMT3B* represses tumour suppressor genes and eventually promotes cellular proliferation (Gore and Weinstein, 2016, Wong et al., 2019). Thus, impaired expression of DNA methylation genes results in aggressive malignancies. Similarly, membrane ABC proteins are broadly existent in HSCs and act as export transporters to protect cells from undesirable metabolites and toxins, as well as anticancer drugs (Raaijmakers, 2007, Chigaev, 2015). High expression of ABC proteins perturbs the chemotherapy effectiveness in cancerous cells through the diminished cellular accumulation of chemotherapeutic agents and conferring multidrug resistance in several malignant

cells (Raaijmakers, 2007, Chigaev, 2015). Pharmacological inhibitors have been applied to restrain the expression of ABC transporters (such as ABCB1 and ABCG2) in leukaemic stem cells in AML patients (Raaijmakers, 2007, Chigaev, 2015). Therefore, increased expression of ABC transporters is poorly correlated with clinical outcomes. Furthermore, our data showed deregulation of the solute carrier (SLC) membrane transport proteins (Table 5.1). SLC transporters import substrates across cellular membranes, involving a myriad of nutrients and anticancer agents (Chigaev, 2015). SLC transporters enhance delivering of anticancer drugs into malignant cells and confer chemotherapeutic efficacy. SLC proteins also import metabolic nutrients to cancer cells conferring their survival rates. For example, AML and B-ALL patients have high expression of SLC2A1 (GLUT1, glucose transporter-1) with poor clinical outcome (Chigaev, 2015). Thus, SLC members boost either chemosensitivity or chemoresistance. Collectively, DNA methylation as well as ABC and SLC transporters highly affect the disease progression and overall clinical outcomes. These data may assist in understanding the worse prognosis in clinical MDS/AML patients harbouring inherited *GATA2* mutations and acquired *ASXL1* mutations.

REFERENCES

Abdel-Wahab, O., Adli, M., Lafave, L. M., Gao, J., Hricik, T., Shih, A. H., Pandey, S., Patel, J. P., Chung, Y. R. & Koche, R. 2012. ASXL1 mutations promote myeloid transformation through loss of PRC2-mediated gene repression. *Cancer Cell,* 22**,** 180-193.

Abdel-Wahab, O., Gao, J., Adli, M., Dey, A., Trimarchi, T., Chung, Y. R., Kuscu, C., Hricik, T., Ndiaye-Lobry, D. & Lafave, L. M. 2013. Deletion of Asxl1 results in myelodysplasia and severe developmental defects in vivoConditional deletion of Asxl1 results in MDS. *The Journal of Experimental Medicine,* 210**,** 2641-2659.

Adolfsson, J., Borge, O. J., Bryder, D., Theilgaard-Mönch, K., Åstrand-Grundström, I., Sitnicka, E., Sasaki, Y. & Jacobsen, S. E. 2001. Upregulation of Flt3 expression within the bone marrow Lin− Sca1+ c-kit+ stem cell compartment is accompanied by loss of self-renewal capacity. *Immunity,* 15**,** 659-669.

Adolfsson, J., Månsson, R., Buza-Vidas, N., Hultquist, A., Liuba, K., Jensen, C. T., Bryder, D., Yang, L., Borge, O.-J. & Thoren, L. A. 2005. Identification of Flt3+ lympho-myeloid stem cells lacking erythro-megakaryocytic potential: a revised road map for adult blood lineage commitment. *Cell,* 121**,** 295-306.

Agarwal, M. L., Agarwal, A., Taylor, W. R. & Stark, G. R. 1995. p53 controls both the G2/M and the G1 cell cycle checkpoints and mediates reversible growth arrest in human fibroblasts. *Proceedings of the National Academy of Sciences,* 92**,** 8493-8497.

Akashi, K., Traver, D., Miyamoto, T. & Weissman, I. L. 2000. A clonogenic common myeloid progenitor that gives rise to all myeloid lineages. *Nature,* 404**,** 193-197.

Allsopp, R. C., Cheshier, S. & Weissman, I. L. 2001. Telomere shortening accompanies increased cell cycle activity during serial transplantation of hematopoietic stem cells. *The Journal of Experimental Medicine,* 193**,** 917-924.

Antonchuk, J., Sauvageau, G. & Humphries, R. K. 2002. HOXB4-induced expansion of adult hematopoietic stem cells ex vivo. *Cell,* 109**,** 39-45.

Arai, F., Hirao, A., Ohmura, M., Sato, H., Matsuoka, S., Takubo, K., Ito, K., Koh, G. Y. & Suda, T. 2004. Tie2/angiopoietin-1 signaling regulates hematopoietic stem cell quiescence in the bone marrow niche. *Cell,* 118**,** 149-161.

Arber, D. A., Orazi, A., Hasserjian, R., Thiele, J., Borowitz, M. J., Le Beau, M. M., Bloomfield, C. D., Cazzola, M. & Vardiman, J. W. 2016. The 2016 revision to the World Health Organization classification of myeloid neoplasms and acute leukemia. *Blood,* 127**,** 2391-2405.

Arinobu, Y., Mizuno, S.-I., Chong, Y., Shigematsu, H., Iino, T., Iwasaki, H., Graf, T., Mayfield, R., Chan, S. & Kastner, P. 2007. Reciprocal activation of GATA-1 and PU. 1 marks initial specification of hematopoietic stem cells into myeloerythroid and myelolymphoid lineages. *Cell Stem Cell,* 1**,** 416-427.

Asada, S., Fujino, T., Goyama, S. & Kitamura, T. 2019. The role of ASXL1 in hematopoiesis and myeloid malignancies. *Cellular and Molecular Life Sciences***,** 1-13.

Baldridge, M. T., King, K. Y., Boles, N. C., Weksberg, D. C. & Goodell, M. A. 2010. Quiescent haematopoietic stem cells are activated by IFN-γ in response to chronic infection. *Nature,* 465**,** 793-797.

Beerman, I., Bhattacharya, D., Zandi, S., Sigvardsson, M., Weissman, I. L., Bryder, D. & Rossi, D. J. 2010. Functionally distinct hematopoietic stem cells modulate hematopoietic lineage potential during aging by a mechanism of clonal expansion. *Proceedings of the National Academy of Sciences,* 107**,** 5465-5470.

Bejar, R., Levine, R. & Ebert, B. L. 2011. Unraveling the molecular pathophysiology of myelodysplastic syndromes. *Journal of Clinical Oncology,* 29**,** 504.

Bejar, R. & Steensma, D. P. 2014. Recent developments in myelodysplastic syndromes. *Blood, The Journal of the American Society of Hematology,* 124**,** 2793-2803.

Bejarano-García, J. A., Millán-Uclés, Á., Rosado, I. V., Sánchez-Abarca, L. I., Caballero-Velázquez, T., Durán-Galván, M. J., Pérez-Simón, J. A. & Piruat, J. I. 2016. Sensitivity of hematopoietic stem cells to mitochondrial dysfunction by SdhD gene deletion. *Cell Death & Disease,* 7**,** e2516.

Benjamini, Y. & Hochberg, Y. 1995. Controlling the false discovery rate: a practical and powerful approach to multiple testing. *Journal of the Royal Statistical Society: series B (Methodological),* 57**,** 289-300.

Bennett, J. M., Catovsky, D., Daniel, M., Flandrin, G., Galton, D., Gralnick, H. & Sultan, C. 1982. Proposals for the classification of the myelodysplastic syndromes. *British Journal of Haematology,* 51**,** 189-199.

Bennett, J. M., Catovsky, D., Daniel, M. T., Flandrin, G., Galton, D. A., Gralnick, H. R. & Sultan, C. 1976. Proposals for the classification of the acute leukaemias French‐American‐British (FAB) co‐operative group. *British Journal of Haematology,* 33**,** 451-458.

Berg, A. H. & Scherer, P. E. 2005. Adipose tissue, inflammation, and cardiovascular disease. *Circulation Research,* 96**,** 939-949.

Bernad, A., Kopf, M., Kulbacki, R., Weich, N., Koehler, G. & Gutierrez-Ramos, J. C. 1994. Interleukin-6 is required in vivo for the regulation of stem cells and committed progenitors of the hematopoietic system. *Immunity,* 1**,** 725-731.

Biechonski, S., Yassin, M. & Milyavsky, M. 2017. DNA-damage response in hematopoietic stem cells: an evolutionary trade-off between blood regeneration and leukemia suppression. *Carcinogenesis,* 38**,** 367-377.

Bigley, V., Haniffa, M., Doulatov, S., Wang, X.-N., Dickinson, R., Mcgovern, N., Jardine, L., Pagan, S., Dimmick, I. & Chua, I. 2011. The human syndrome of dendritic cell, monocyte, B and NK lymphoid deficiencyHuman DC deficiency. *The Journal of Experimental Medicine,* 208**,** 227-234.

Björnsson, J. M., Larsson, N., Brun, A. C., Magnusson, M., Andersson, E., Lundström, P., Larsson, J., Repetowska, E., Ehinger, M. & Humphries, R. K. 2003. Reduced proliferative capacity of hematopoietic stem cells deficient in Hoxb3 and Hoxb4. *Molecular and Cellular Biology,* 23**,** 3872-3883.

Bödör, C., Renneville, A., Smith, M., Charazac, A., Iqbal, S., Etancelin, P., Cavenagh, J., Barnett, M. J., Kramarzova, K. & Krishnan, B. 2012. Germ-line GATA2 p. THR354MET mutation in familial myelodysplastic syndrome with acquired monosomy 7 and ASXL1 mutation demonstrating rapid onset and poor survival. *Haematologica,* 97**,** 890-894.

Borghesi, L., Aites, J., Nelson, S., Lefterov, P., James, P. & Gerstein, R. 2005. E47 is required for V (D) J recombinase activity in common lymphoid progenitors. *The Journal of Experimental Medicine,* 202**,** 1669-1677.

Boyd, A. S. & Rodrigues, N. P. 2018. Stem Cells Cycle toward Immune Surveillance. *Immunity,* 48**,** 187-190.

Brock, H. W. & Fisher, C. L. 2005. Maintenance of gene expression patterns. *Developmental dynamics: an official publication of the American Association of Anatomists,* 232**,** 633-655.

Brown, A., Pospiech, J., Eiwen, K., Baker, D. J., Moehrle, B., Sakk, V., Nattamai, K., Vogel, M., Grigoryan, A. & Geiger, H. 2017. The spindle assembly checkpoint is required for hematopoietic progenitor cell engraftment. *Stem Cell Reports,* 9**,** 1359-1368.

Bruns, I., Lucas, D., Pinho, S., Ahmed, J., Lambert, M. P., Kunisaki, Y., Scheiermann, C., Schiff, L., Poncz, M. & Bergman, A. 2014. Megakaryocytes regulate hematopoietic stem cell quiescence through CXCL4 secretion. *Nature Medicine,* 20**,** 1315.

Butko, E., Distel, M., Pouget, C., Weijts, B., Kobayashi, I., Ng, K., Mosimann, C., Poulain, F. E., Mcpherson, A. & Ni, C.-W. 2015. Gata2b is a restricted early regulator of hemogenic endothelium in the zebrafish embryo. *Development,* 142**,** 1050-1061.

Calvo, K. R., Vinh, D. C., Maric, I., Wang, W., Noel, P., Stetler-Stevenson, M., Arthur, D. C., Raffeld, M., Dutra, A. & Pak, E. 2011. Myelodysplasia in autosomal dominant and sporadic monocytopenia immunodeficiency syndrome: diagnostic features and clinical implications. *Haematologica***,** 2011.041152.

Cantor, A. B., Iwasaki, H., Arinobu, Y., Moran, T. B., Shigematsu, H., Sullivan, M. R., Akashi, K. & Orkin, S. H. 2008. Antagonism of FOG-1 and GATA factors in fate choice for the mast cell lineage. *The Journal of Experimental Medicine,* 205**,** 611-624.

Chambers, S. M., Shaw, C. A., Gatza, C., Fisk, C. J., Donehower, L. A. & Goodell, M. A. 2007. Aging hematopoietic stem cells decline in function and exhibit epigenetic dysregulation. *PLoS Biology,* 5.

Charles, M. A., Saunders, T. L., Wood, W. M., Owens, K., Parlow, A., Camper, S. A., Ridgway, E. & Gordon, D. F. 2006. Pituitary-specific Gata2 knockout: effects on gonadotrope and thyrotrope function. *Molecular Endocrinology,* 20**,** 1366-1377.

Chen, M. J., Yokomizo, T., Zeigler, B. M., Dzierzak, E. & Speck, N. A. 2009. Runx1 is required for the endothelial to haematopoietic cell transition but not thereafter. *Nature,* 457**,** 887-891.

Cheng, H., Liang, P. H. & Cheng, T. 2013. Mouse hematopoietic stem cell transplantation. *Stem Cells and Aging.* Springer.

Cheshier, S. H., Morrison, S. J., Liao, X. & Weissman, I. L. 1999. In vivo proliferation and cell cycle kinetics of long-term self-renewing hematopoietic stem cells. *Proceedings of the National Academy of Sciences,* 96**,** 3120-3125.

Chigaev, A. 2015. Does aberrant membrane transport contribute to poor outcome in adult acute myeloid leukemia?. *Frontiers in Pharmacology,* 6**,** 134.

Cho, H. J., Lee, J., Yoon, S. R., Lee, H. G. & Jung, H. 2020. Regulation of Hematopoietic Stem Cell Fate and Malignancy. *International Journal of Molecular Sciences,* 21**,** 4780.

Chou, S. T., Khandros, E., Bailey, L. C., Nichols, K. E., Vakoc, C. R., Yao, Y., Huang, Z., Crispino, J. D., Hardison, R. C. & Blobel, G. A. 2009. Graded repression of PU. 1/Sfpi1 gene transcription by GATA factors regulates hematopoietic cell fate. *Blood, The Journal of the American Society of Hematology,* 114**,** 983-994.

Christensen, J. L. & Weissman, I. L. 2001. Flk-2 is a marker in hematopoietic stem cell differentiation: a simple method to isolate long-term stem cells. *Proceedings of the National Academy of Sciences,* 98**,** 14541-14546.

Christensen, J. L., Wright, D. E., Wagers, A. J. & Weissman, I. L. 2004. Circulation and chemotaxis of fetal hematopoietic stem cells. *PLoS Biology,* 2.

Chun, T.-H., Itoh, H., Subramanian, L., Iñiguez-Lluhí, J. A. & Nakao, K. 2003. Modification of GATA-2 transcriptional activity in endothelial cells by the SUMO E3 ligase PIASy. *Circulation Research,* 92**,** 1201-1208.

Chung, Y.-J., Park, B.-B., Kang, Y.-J., Kim, T.-M., Eaves, C. J. & Oh, I.-H. 2006. Unique effects of Stat3 on the early phase of hematopoietic stem cell regeneration. *Blood,* 108**,** 1208-1215.

Collin, M., Dickinson, R. & Bigley, V. 2015. Haematopoietic and immune defects associated with GATA2 mutation. *British Journal of Haematology,* 169**,** 173-187.

Crane, G. M., Jeffery, E. & Morrison, S. J. 2017. Adult haematopoietic stem cell niches. *Nature Reviews Immunology,* 17**,** 573.

Dang, C. V., O'donnell, K. A., Zeller, K. I., Nguyen, T., Osthus, R. C. & Li, F. 2006. The c-Myc target gene network. Seminars in Cancer Biology. Elsevier, 253-264.

Dash, A. & Gilliland, D. G. 2001. Molecular genetics of acute myeloid leukaemia. *Best practice & research. Clinical Haematology,* 14**,** 49-64.

David, M., Petit, D. & Bertoglio, J. 2012. Cell cycle regulation of Rho signaling pathways. *Cell Cycle,* 11**,** 3003-3010.

De Bruijn, M. F., Speck, N. A., Peeters, M. C. & Dzierzak, E. 2000. Definitive hematopoietic stem cells first develop within the major arterial regions of the mouse embryo. *The EMBO Journal,* 19**,** 2465-2474.

De Bruin, A. M., Demirel, Ö., Hooibrink, B., Brandts, C. H. & Nolte, M. A. 2013. Interferon-γ impairs proliferation of hematopoietic stem cells in mice. *Blood, The Journal of the American Society of Hematology,* 121**,** 3578-3585.

De Bruin, A. M., Voermans, C. & Nolte, M. A. 2014. Impact of interferon-γ on hematopoiesis. *Blood, The Journal of the American Society of Hematology,* 124**,** 2479-2486.

De Pater, E., Kaimakis, P., Vink, C. S., Yokomizo, T., Yamada-Inagawa, T., Van Der Linden, R., Kartalaei, P. S., Camper, S. A., Speck, N. & Dzierzak, E. 2013. Gata2 is required for HSC generation and survival. *Journal of Experimental Medicine,* 210**,** 2843-2850.

Deguchi, K. & Gilliland, D. 2002. Cooperativity between mutations in tyrosine kinases and in hematopoietic transcription factors in AML. *Leukemia,* 16**,** 740-744.

Delogu, A., Schebesta, A., Sun, Q., Aschenbrenner, K., Perlot, T. & Busslinger, M. 2006. Gene repression by Pax5 in B cells is essential for blood cell homeostasis and is reversed in plasma cells. *Immunity,* 24**,** 269-281.

Dickinson, R. E., Griffin, H., Bigley, V., Reynard, L. N., Hussain, R., Haniffa, M., Lakey, J. H., Rahman, T., Wang, X.-N. & Mcgovern, N. 2011. Exome sequencing identifies GATA-2 mutation as the cause of dendritic cell, monocyte, B and NK lymphoid deficiency. *Blood,* 118**,** 2656-2658.

Dickinson, R. E., Milne, P., Jardine, L., Zandi, S., Swierczek, S. I., Mcgovern, N., Cookson, S., Ferozepurwalla, Z., Langridge, A. & Pagan, S. 2014. The evolution of cellular deficiency in GATA2 mutation. *Blood,* 123**,** 863-874.

Ding, L. & Morrison, S. J. 2013. Haematopoietic stem cells and early lymphoid progenitors occupy distinct bone marrow niches. *Nature,* 495**,** 231-235.

Ding, L., Saunders, T. L., Enikolopov, G. & Morrison, S. J. 2012. Endothelial and perivascular cells maintain haematopoietic stem cells. *Nature,* 481**,** 457.

Donadieu, J., Lamant, M., Fieschi, C., De Fontbrune, F. S., Caye, A., Ouachee, M., Beaupain, B., Bustamante, J., Poirel, H. A. & Isidor, B. 2018. Natural history of GATA2 deficiency in a survey of 79 French and Belgian patients. *Haematologica,* 103**,** 1278-1287.

Doulatov, S., Notta, F., Eppert, K., Nguyen, L. T., Ohashi, P. S. & Dick, J. E. 2010. Revised map of the human progenitor hierarchy shows the origin of macrophages and dendritic cells in early lymphoid development. *Nature Immunology,* 11**,** 585.

Doulatov, S., Notta, F., Laurenti, E. & Dick, J. E. 2012. Hematopoiesis: a human perspective. *Cell Stem Cell,* 10**,** 120-136.

Duran-Struuck, R. & Dysko, R. C. 2009. Principles of bone marrow transplantation (BMT): providing optimal veterinary and husbandry care to irradiated mice in BMT studies. *Journal of the American Association for Laboratory Animal Science,* 48**,** 11-22.

Eilken, H. M., Nishikawa, S.-I. & Schroeder, T. 2009. Continuous single-cell imaging of blood generation from haemogenic endothelium. *Nature,* 457**,** 896-900.

Emberger, J., Navarro, M., Dejean, M. & Izarn, P. 1979. Deaf-mutism, lymphedema of the lower limbs and hematological abnormalities (acute leukemia, cytopenia) with autosomal dominant transmission. *Journal De Genetique Humaine,* 27**,** 237-245.

Ergen, A. V., Boles, N. C. & Goodell, M. A. 2012. Rantes/Ccl5 influences hematopoietic stem cell subtypes and causes myeloid skewing. *Blood, The Journal of the American Society of Hematology,* 119**,** 2500-2509.

Ernst, P., Fisher, J. K., Avery, W., Wade, S., Foy, D. & Korsmeyer, S. J. 2004. Definitive hematopoiesis requires the mixed-lineage leukemia gene. *Developmental Cell,* 6**,** 437-443.

Ezoe, S., Matsumura, I., Nakata, S., Gale, K., Ishihara, K., Minegishi, N., Machii, T., Kitamura, T., Yamamoto, M. & Enver, T. 2002. GATA-2/estrogen receptor chimera regulates cytokine-dependent growth of hematopoietic cells through accumulation of p21WAF1 and p27Kip1 proteins. *Blood, The Journal of the American Society of Hematology,* 100**,** 3512-3520.

Ezoe, S., Matsumura, I., Satoh, Y., Tanaka, H. & Kanakura, Y. 2004. Cell cycle regulation in hematopoietic stem/progenitor cells. *Cell Cycle,* 3**,** 312-316.

Faitova, J., Krekac, D., Hrstka, R. & Vojtesek, B. 2006. Endoplasmic reticulum stress and apoptosis. *Cellular & Molecular Biology Letters,* 11**,** 488-505.

Fata, J. E., Leco, K. J., Voura, E. B., Hoi-Ying, E. Y., Waterhouse, P., Murphy, G., Moorehead, R. A. & Khokha, R. 2001. Accelerated apoptosis in the Timp-3–deficient mammary gland. *The Journal of Clinical Investigation,* 108**,** 831-841.

Fehse, B., Kustikova, O., Bubenheim, M. & Baum, C. 2004. Pois (s) on–it's a question of dose. *Gene Therapy,* 11**,** 879-881.

Ficara, F., Murphy, M. J., Lin, M. & Cleary, M. L. 2008. Pbx1 regulates self-renewal of long-term hematopoietic stem cells by maintaining their quiescence. *Cell Stem Cell,* 2**,** 484-496.

Fisher, C. L., Pineault, N., Brookes, C., Helgason, C. D., Ohta, H., Bodner, C., Hess, J. L., Humphries, R. K. & Brock, H. W. 2010. Loss-of-function Additional sex combs like 1 mutations disrupt hematopoiesis but do not cause severe myelodysplasia or leukemia. *Blood, The Journal of the American Society of Hematology,* 115**,** 38-46.

Florian, M. C., Dörr, K., Niebel, A., Daria, D., Schrezenmeier, H., Rojewski, M., Filippi, M.-D., Hasenberg, A., Gunzer, M. & Scharffetter-Kochanek, K. 2012. Cdc42 activity regulates hematopoietic stem cell aging and rejuvenation. *Cell Stem Cell,* 10**,** 520-530.

Forsberg, E. C., Prohaska, S. S., Katzman, S., Heffner, G. C., Stuart, J. M. & Weissman, I. L. 2005. Differential expression of novel potential regulators in hematopoietic stem cells. *PLoS Genetics,* 1.

Fujiwara, T., Fukuhara, N., Funayama, R., Nariai, N., Kamata, M., Nagashima, T., Kojima, K., Onishi, Y., Sasahara, Y. & Ishizawa, K. 2014. Identification of acquired mutations by whole-genome sequencing in GATA-2 deficiency evolving into myelodysplasia and acute leukemia. *Annals of Hematology,* 93**,** 1515-1522.

Fujiwara, T., Yokoyama, H., Okitsu, Y., Kamata, M., Fukuhara, N., Onishi, Y., Fujimaki, S., Takahashi, S., Ishizawa, K. & Bresnick, E. H. 2012. Gene expression profiling identifies HOXB4 as a direct downstream target of GATA-2 in human CD34+ hematopoietic cells. *PloS One,* 7.

Fujiwara, Y., Browne, C. P., Cunniff, K., Goff, S. C. & Orkin, S. H. 1996. Arrested development of embryonic red cell precursors in mouse embryos lacking transcription factor GATA-1. *Proceedings of the National Academy of Sciences,* 93**,** 12355-12358.

Galy, A., Travis, M., Cen, D. & Chen, B. 1995. Human T, B, natural killer, and dendritic cells arise from a common bone marrow progenitor cell subset. *Immunity,* 3**,** 459-473.

Gao, X., Johnson, K. D., Chang, Y.-I., Boyer, M. E., Dewey, C. N., Zhang, J. & Bresnick, E. H. 2013. Gata2 cis-element is required for hematopoietic stem cell generation in the mammalian embryo. *Journal of Experimental Medicine,* 210**,** 2833-2842.

Gelsi-Boyer, V., Brecqueville, M., Devillier, R., Murati, A., Mozziconacci, M.-J. & Birnbaum, D. 2012. Mutations in ASXL1 are associated with poor prognosis across the spectrum of malignant myeloid diseases. *Journal of Hematology & Oncology,* 5**,** 12.

Georgopoulos, K., Bigby, M., Wang, J.-H., Molnar, A., Wu, P., Winandy, S. & Sharpe, A. 1994. The Ikaros gene is required for the development of all lymphoid lineages. *Cell,* 79**,** 143-156.

Gerdes, J., Lemke, H., Baisch, H., Wacker, H.-H., Schwab, U. & Stein, H. 1984. Cell cycle analysis of a cell proliferation-associated human nuclear antigen defined by the monoclonal antibody Ki-67. *The Journal of Immunology,* 133**,** 1710-1715.

Ghanem, H., Tank, N. & Tabbara, I. A. 2012. Prognostic implications of genetic aberrations in acute myelogenous leukemia with normal cytogenetics. *American Journal of Hematology,* 87**,** 69-77.

Giacinti, C. & Giordano, A. 2006. RB and cell cycle progression. *Oncogene,* 25**,** 5220-5227.

Gore, A. V. & Weinstein, B. M. 2016. DNA methylation in hematopoietic development and disease. *Experimental Hematology,* 44**,** 783-790.

Goyama, S., Yamamoto, G., Shimabe, M., Sato, T., Ichikawa, M., Ogawa, S., Chiba, S. & Kurokawa, M. 2008. Evi-1 is a critical regulator for hematopoietic stem cells and transformed leukemic cells. *Cell Stem Cell,* 3**,** 207-220.

Grass, J. A., Jing, H., Kim, S.-I., Martowicz, M. L., Pal, S., Blobel, G. A. & Bresnick, E. H. 2006. Distinct functions of dispersed GATA factor complexes at an endogenous gene locus. *Molecular and Cellular Biology,* 26**,** 7056-7067.

Green, C. L., Tawana, K., Hills, R. K., Bödör, C., Fitzgibbon, J., Inglott, S., Ancliff, P., Burnett, A. K., Linch, D. C. & Gale, R. E. 2013. GATA 2 mutations in sporadic and familial acute myeloid leukaemia patients with CEBPA mutations. *British Journal of Haematology,* 161**,** 701-705.

Greenberg, P., Cox, C., Lebeau, M. M., Fenaux, P., Morel, P., Sanz, G., Sanz, M., Vallespi, T., Hamblin, T. & Oscier, D. 1997. International scoring system for evaluating prognosis in myelodysplastic syndromes. *Blood, The Journal of the American Society of Hematology,* 89**,** 2079-2088.

Greif, P. A., Dufour, A., Konstandin, N. P., Ksienzyk, B., Zellmeier, E., Tizazu, B., Sturm, J., Benthaus, T., Herold, T. & Yaghmaie, M. 2012. GATA2 zinc finger 1 mutations associated with biallelic CEBPA mutations define a unique genetic entity of acute myeloid leukemia. *Blood***,** 2012-01-403220.

Guo, G., Luc, S., Marco, E., Lin, T.-W., Peng, C., Kerenyi, M. A., Beyaz, S., Kim, W., Xu, J. & Das, P. P. 2013. Mapping cellular hierarchy by single-cell analysis of the cell surface repertoire. *Cell Stem Cell,* 13**,** 492-505.

Guo, Y., Fu, X., Huo, B., Wang, Y., Sun, J., Meng, L., Hao, T., Zhao, Z. J. & Hu, X. 2016. GATA2 regulates GATA1 expression through LSD1-mediated histone modification. *American Journal of Translational Research,* 8**,** 2265.

Hahn, C. N., Chong, C.-E., Carmichael, C. L., Wilkins, E. J., Brautigan, P. J., Li, X.-C., Babic, M., Lin, M., Carmagnac, A. & Lee, Y. K. 2011. Heritable GATA2 mutations associated with familial myelodysplastic syndrome and acute myeloid leukemia. *Nature Genetics,* 43**,** 1012.

Han, Y., Yan, C., Fishbain, S., Ivanov, I. & He, Y. 2018. Structural visualization of RNA polymerase III transcription machineries. *Cell Discovery,* 4**,** 1-15.

Harada, N., Hasegawa, A., Hirano, I., Yamamoto, M. & Shimizu, R. 2019. GATA 2 hypomorphism induces chronic myelomonocytic leukemia in mice. *Cancer Science,* 110**,** 1183-1193.

Harrison, D., Zhong, R., Jordan, C., Lemischka, I. & Astle, C. 1997. Relative to adult marrow, fetal liver repopulates nearly five times more effectively long-term than short-term. *Experimental Hematology,* 25**,** 293-297.

Harrison, D. E., Jordan, C., Zhong, R. & Astle, C. 1993. Primitive hemopoietic stem cells: direct assay of most productive populations by competitive repopulation with simple binomial, correlation and covariance calculations. *Experimental Hematology,* 21**,** 206-219.

Hawley, R. G., Fong, A., Burns, B. F. & Hawley, T. S. 1992. Transplantable myeloproliferative disease induced in mice by an interleukin 6 retrovirus. *The Journal of Experimental Medicine,* 176**,** 1149-1163.

Hayakawa, F., Towatari, M., Ozawa, Y., Tomita, A., Privalsky, M. L. & Saito, H. 2004. Functional regulation of GATA‐2 by acetylation. *Journal of Leukocyte Biology,* 75**,** 529-540.

Hirabayashi, S., Wlodarski, M. W., Kozyra, E. & Niemeyer, C. M. 2017. Heterogeneity of GATA2-related myeloid neoplasms. *International Journal of Hematology,* 106**,** 175-182.

Ho, A. & Dowdy, S. F. 2002. Regulation of G1 cell-cycle progression by oncogenes and tumor suppressor genes. *Current Opinion in Genetics & Development,* 12**,** 47-52.

Hock, H., Hamblen, M. J., Rooke, H. M., Schindler, J. W., Saleque, S., Fujiwara, Y. & Orkin, S. H. 2004a. Gfi-1 restricts proliferation and preserves functional integrity of haematopoietic stem cells. *Nature,* 431**,** 1002-1007.

Hock, H., Meade, E., Medeiros, S., Schindler, J. W., Valk, P. J., Fujiwara, Y. & Orkin, S. H. 2004b. Tel/Etv6 is an essential and selective regulator of adult hematopoietic stem cell survival. *Genes & Development,* 18**,** 2336-2341.

Hoischen, A., Van Bon, B. W., Rodríguez-Santiago, B., Gilissen, C., Vissers, L. E., De Vries, P., Janssen, I., Van Lier, B., Hastings, R. & Smithson, S. F. 2011. De novo nonsense mutations in ASXL1 cause Bohring-Opitz syndrome. *Nature Genetics,* 43**,** 729-731.

Holmfeldt, P., Ganuza, M., Marathe, H., He, B., Hall, T., Kang, G., Moen, J., Pardieck, J., Saulsberry, A. C. & Cico, A. 2016. Functional screen identifies regulators of murine hematopoietic stem cell repopulation. *Journal of Experimental Medicine,* 213**,** 433-449.

Hosokawa, K., Arai, F., Yoshihara, H., Iwasaki, H., Nakamura, Y., Gomei, Y. & Suda, T. 2010. Knockdown of N-cadherin suppresses the long-term engraftment of hematopoietic stem cells. *Blood, The Journal of the American Society of Hematology,* 116**,** 554-563.

Hossfeld, D. 2002. World Health Organization classification of tumours: pathology and genetics of tumours of haematopoietic and lymphoid tissues. *Annals of Oncology,* 13**,** 490.

Hsu, A. P., Johnson, K. D., Falcone, E. L., Sanalkumar, R., Sanchez, L., Hickstein, D. D., Cuellar-Rodriguez, J., Lemieux, J. E., Zerbe, C. S. & Bresnick, E. H. 2013. GATA2 haploinsufficiency caused by mutations in a conserved intronic element leads to MonoMAC syndrome. *Blood, The Journal of the American Society of Hematology,* 121**,** 3830-3837.

Hsu, A. P., Sampaio, E. P., Khan, J., Calvo, K. R., Lemieux, J. E., Patel, S. Y., Frucht, D. M., Vinh, D. C., Auth, R. D. & Freeman, A. F. 2011. Mutations in GATA2 are associated with the autosomal dominant and sporadic monocytopenia and mycobacterial infection (MonoMAC) syndrome. *Blood,* 118**,** 2653-2655.

Hsu, Y.-C., Chiu, Y.-C., Lin, C.-C., Kuo, Y.-Y., Hou, H.-A., Tzeng, Y.-S., Kao, C.-J., Chuang, P.-H., Tseng, M.-H. & Hsiao, T.-H. 2017. The distinct biological implications of Asxl1 mutation and its roles in leukemogenesis revealed by a knock-in mouse model. *Journal of Hematology & Oncology,* 10**,** 139.

Huang, Z., Dore, L. C., Li, Z., Orkin, S. H., Feng, G., Lin, S. & Crispino, J. D. 2009. GATA-2 reinforces megakaryocyte development in the absence of GATA-1. *Molecular and Cellular Biology,* 29**,** 5168-5180.

Hyde, R. K. & Liu, P. P. 2011. GATA2 mutations lead to MDS and AML. *Nature Genetics,* 43**,** 926.

Ikuta, K. & Weissman, I. L. 1992. Evidence that hematopoietic stem cells express mouse c-kit but do not depend on steel factor for their generation. *Proceedings of the National Academy of Sciences,* 89**,** 1502-1506.

Imagawa, S., Yamamoto, M. & Miura, Y. 1997. Negative regulation of the erythropoietin gene expression by the GATA transcription factors. *Blood, The Journal of the American Society of Hematology,* 89**,** 1430-1439.

Inoue, D., Kitaura, J., Togami, K., Nishimura, K., Enomoto, Y., Uchida, T., Kagiyama, Y., Kawabata, K. C., Nakahara, F. & Izawa, K. 2013. Myelodysplastic syndromes are induced by histone methylation–altering ASXL1 mutations. *The Journal of Clinical Investigation,* 123**,** 4627-4640.

Iwasaki, H. & Akashi, K. 2007. Myeloid lineage commitment from the hematopoietic stem cell. *Immunity,* 26**,** 726-740.

Iwasaki, H., Somoza, C., Shigematsu, H., Duprez, E. A., Iwasaki-Arai, J., Mizuno, S.-I., Arinobu, Y., Geary, K., Zhang, P. & Dayaram, T. 2005. Distinctive and indispensable roles of PU. 1 in maintenance of hematopoietic stem cells and their differentiation. *Blood,* 106**,** 1590-1600.

Jackson, S. J., Andrews, N., Ball, D., Bellantuono, I., Gray, J., Hachoumi, L., Holmes, A., Latcham, J., Petrie, A. & Potter, P. 2017. Does age matter? The impact of rodent age on study outcomes. *Laboratory Animals,* 51**,** 160-169.

Jaiswal, S., Fontanillas, P., Flannick, J., Manning, A., Grauman, P. V., Mar, B. G., Lindsley, R. C., Mermel, C. H., Burtt, N. & Chavez, A. 2014. Age-related clonal hematopoiesis associated with adverse outcomes. *New England Journal of Medicine,* 371**,** 2488-2498.

Johnson, K. D., Kong, G., Gao, X., Chang, Y.-I., Hewitt, K. J., Sanalkumar, R., Prathibha, R., Ranheim, E. A., Dewey, C. N. & Zhang, J. 2015. Cis-regulatory mechanisms governing stem and progenitor cell transitions. *Science Advances,* 1**,** e1500503.

Joseph, C., Quach, J. M., Walkley, C. R., Lane, S. W., Celso, C. L. & Purton, L. E. 2013. Deciphering hematopoietic stem cells in their niches: a critical appraisal of genetic models, lineage tracing, and imaging strategies. *Cell Stem Cell,* 13**,** 520-533.

Kaimakis, P., De Pater, E., Eich, C., Solaimani Kartalaei, P., Kauts, M.-L., Vink, C. S., Van Der Linden, R., Jaegle, M., Yokomizo, T. & Meijer, D. 2016. Functional and molecular characterization of mouse Gata2-independent hematopoietic progenitors. *Blood, The Journal of the American Society of Hematology,* 127**,** 1426-1437.

Karsunky, H., Inlay, M. A., Serwold, T., Bhattacharya, D. & Weissman, I. L. 2008. Flk2+ common lymphoid progenitors possess equivalent differentiation potential

for the B and T lineages. *Blood, The Journal of the American Society of Hematology,* 111**,** 5562-5570.

Kataoka, K., Sato, T., Yoshimi, A., Goyama, S., Tsuruta, T., Kobayashi, H., Shimabe, M., Arai, S., Nakagawa, M. & Imai, Y. 2011. Evi1 is essential for hematopoietic stem cell self-renewal, and its expression marks hematopoietic cells with long-term multilineage repopulating activity. *Journal of Experimental Medicine,* 208**,** 2403-2416.

Katayama, S., Suzuki, M., Yamaoka, A., Keleku-Lukwete, N., Katsuoka, F., Otsuki, A., Kure, S., Engel, J. D. & Yamamoto, M. 2017. GATA2 haploinsufficiency accelerates EVI1-driven leukemogenesis. *Blood, The Journal of the American Society of Hematology,* 130**,** 908-919.

Kato, Y., Iwama, A., Tadokoro, Y., Shimoda, K., Minoguchi, M., Akira, S., Tanaka, M., Miyajima, A., Kitamura, T. & Nakauchi, H. 2005. Selective activation of STAT5 unveils its role in stem cell self-renewal in normal and leukemic hematopoiesis. *The Journal of Experimental Medicine,* 202**,** 169-179.

Katoh, M. 2013. Functional and cancer genomics of ASXL family members. *British Journal of Cancer,* 109**,** 299-306.

Katsumura, K. R., Mehta, C., Hewitt, K. J., Soukup, A. A., De Andrade, I. F., Ranheim, E. A., Johnson, K. D. & Bresnick, E. H. 2018. Human leukemia mutations corrupt but do not abrogate GATA-2 function. *Proceedings of the National Academy of Sciences,* 115**,** E10109-E10118.

Katsumura, K. R., Ong, I. M., Devilbiss, A. W., Sanalkumar, R. & Bresnick, E. H. 2016. GATA factor-dependent positive-feedback circuit in acute myeloid leukemia cells. *Cell Reports,* 16**,** 2428-2441.

Kaushansky, K. 2006. Lineage-specific hematopoietic growth factors. *New England Journal of Medicine,* 354**,** 2034-2045.

Kazenwadel, J., Betterman, K. L., Chong, C.-E., Stokes, P. H., Lee, Y. K., Secker, G. A., Agalarov, Y., Demir, C. S., Lawrence, D. M. & Sutton, D. L. 2015. GATA2 is required for lymphatic vessel valve development and maintenance. *The Journal of Clinical Investigation,* 125**,** 2979-2994.

Kiel, M. J., Yilmaz, Ö. H., Iwashita, T., Yilmaz, O. H., Terhorst, C. & Morrison, S. J. 2005. SLAM family receptors distinguish hematopoietic stem and progenitor cells and reveal endothelial niches for stem cells. *Cell,* 121**,** 1109-1121.

Kim, I., Saunders, T. L. & Morrison, S. J. 2007. Sox17 dependence distinguishes the transcriptional regulation of fetal from adult hematopoietic stem cells. *Cell,* 130**,** 470-483.

Kim, M., Moon, H. B. & Spangrude, G. J. 2003. Major age‐related changes of mouse hematopoietic stem/progenitor cells. *Annals of the New York Academy of Sciences,* 996**,** 195-208.

Kimizuku, F., Taguchi, Y., Ohdate, Y., Kawase, Y., Shimojo, T., Hashino, K., Kato, I., Sekiguchi, K. & Titani, K. 1991. Production and characterization of functional domains of human fibronectin expressed in Escherichia coli. *The Journal of Biochemistry,* 110**,** 284-291.

Kimura, S., Roberts, A. W., Metcalf, D. & Alexander, W. S. 1998. Hematopoietic stem cell deficiencies in mice lacking c-Mpl, the receptor for thrombopoietin. *Proceedings of the National Academy of Sciences,* 95**,** 1195-1200.

Kingston, R. E., Chen, C. A. & Rose, J. K. 2003. Calcium phosphate transfection. *Current Protocols in Molecular Biology,* 63**,** 9.1. 1-9.1. 11.

Koegel, A. K., Hofmann, I., Moffitt, K., Degar, B., Duncan, C. & Tubman, V. N. 2016. Acute lymphoblastic leukemia in a patient with MonoMAC syndrome/GATA2 haploinsufficiency. *Pediatric Blood & Cancer,* 63**,** 1844-1847.

Koga, S., Yamaguchi, N., Abe, T., Minegishi, M., Tsuchiya, S., Yamamoto, M. & Minegishi, N. 2007. Cell-cycle–dependent oscillation of GATA2 expression in hematopoietic cells. *Blood,* 109**,** 4200-4208.

Kondo, M., Weissman, I. L. & Akashi, K. 1997. Identification of clonogenic common lymphoid progenitors in mouse bone marrow. *Cell,* 91**,** 661-672.

Koutsourakis, M., Langeveld, A., Patient, R., Beddington, R. & Grosveld, F. 1999. The transcription factor GATA6 is essential for early extraembryonic development. *Development,* 126**,** 723-732.

Kozar, K., Ciemerych, M. A., Rebel, V. I., Shigematsu, H., Zagozdzon, A., Sicinska, E., Geng, Y., Yu, Q., Bhattacharya, S. & Bronson, R. T. 2004. Mouse development and cell proliferation in the absence of D-cyclins. *Cell,* 118**,** 477-491.

Kranc, K. R., Schepers, H., Rodrigues, N. P., Bamforth, S., Villadsen, E., Ferry, H., Bouriez-Jones, T., Sigvardsson, M., Bhattacharya, S. & Jacobsen, S. E. 2009. Cited2 is an essential regulator of adult hematopoietic stem cells. *Cell Stem Cell,* 5**,** 659-665.

Kuhn, R., Schwenk, F., Aguet, M. & Rajewsky, K. 1995. Inducible gene targeting in mice. *Science,* 269**,** 1427-1429.

Kular, J. K., Basu, S. & Sharma, R. I. 2014. The extracellular matrix: Structure, composition, age-related differences, tools for analysis and applications for tissue engineering. *Journal of Tissue Engineering,* 5**,** 2041731414557112.

Kumano, K., Chiba, S., Shimizu, K., Yamagata, T., Hosoya, N., Saito, T., Takahashi, T., Hamada, Y. & Hirai, H. 2001. Notch1 inhibits differentiation of hematopoietic cells by sustaining GATA-2 expression. *Blood, The Journal of the American Society of Hematology,* 98**,** 3283-3289.

Kuo, C. T., Morrisey, E. E., Anandappa, R., Sigrist, K., Lu, M. M., Parmacek, M. S., Soudais, C. & Leiden, J. M. 1997. GATA4 transcription factor is required for ventral morphogenesis and heart tube formation. *Genes & Development,* 11**,** 1048-1060.

Larochelle, A., Vormoor, J., Hanenberg, H., Wang, J. C., Bhatia, M., Lapidot, T., Moritz, T., Murdoch, B., Xiao, X. L. & Kato, I. 1996. Identification of primitive human hematopoietic cells capable of repopulating NOD/SCID mouse bone marrow: implications for gene therapy. *Nature Medicine,* 2**,** 1329-1337.

Laurenti, E., Doulatov, S., Zandi, S., Plumb, I., Chen, J., April, C., Fan, J.-B. & Dick, J. E. 2013. The transcriptional architecture of early human hematopoiesis identifies multilevel control of lymphoid commitment. *Nature Immunology,* 14**,** 756.

Laverriere, A. C., Macneill, C., Mueller, C., Poelmann, R. E., Burch, J. & Evans, T. 1994. GATA-4/5/6, a subfamily of three transcription factors transcribed in developing heart and gut. *Journal of Biological Chemistry,* 269**,** 23177-23184.

Lavrik, I., Golks, A. & Krammer, P. H. 2005. Death receptor signaling. *Journal of Cell Science,* 118**,** 265-267.

Lee, D., Wang, Y.-H., Kalaitzidis, D., Ramachandran, J., Eda, H., Sykes, D. B., Raje, N. & Scadden, D. T. 2016. Endogenous transmembrane protein UT2 inhibits pSTAT3 and suppresses hematological malignancy. *The Journal of Clinical Investigation,* 126**,** 1300-1310.

Lee, M.-E., Temizer, D. H., Clifford, J. A. & Quertermous, T. 1991. Cloning of the GATA-binding protein that regulates endothelin-1 gene expression in endothelial cells. *Journal of Biological Chemistry,* 266**,** 16188-16192.

Lentjes, M. H., Niessen, H. E., Akiyama, Y., De Bruine, A. P., Melotte, V. & Van Engeland, M. 2016. The emerging role of GATA transcription factors in development and disease. *Expert Reviews in Molecular Medicine,* 18.

Li, H. S., Jin, J., Liang, X., Matatall, K. A., Ma, Y., Zhang, H., Ullrich, S. E., King, K. Y., Sun, S. C. & Watowich, S. S. 2016. Loss of c‐Kit and bone marrow failure upon conditional removal of the GATA‐2 C‐terminal zinc finger domain in adult mice. *European Journal of Haematology,* 97**,** 261-270.

Li, Y., Qi, X., Liu, B. & Huang, H. 2015. The STAT5–GATA2 pathway is critical in basophil and mast cell differentiation and maintenance. *The Journal of Immunology,* 194**,** 4328-4338.

Liang, Y., Van Zant, G. & Szilvassy, S. J. 2005. Effects of aging on the homing and engraftment of murine hematopoietic stem and progenitor cells. *Blood,* 106**,** 1479-1487.

Liao, Q., Shen, J., Liu, J., Sun, X., Zhao, G., Chang, Y., Xu, L., Li, X., Zhao, Y. & Zheng, H. 2014. Genome-wide identification and functional annotation of Plasmodium falciparum long noncoding RNAs from RNA-seq data. *Parasitology Research,* 113**,** 1269-1281.

Liebermann, D. A. & Hoffman, B. 2008. Gadd45 in stress signaling. *Journal of Molecular Signaling,* 3**,** 1-8.

Lim, K.-C., Hosoya, T., Brandt, W., Ku, C.-J., Hosoya-Ohmura, S., Camper, S. A., Yamamoto, M. & Engel, J. D. 2012. Conditional Gata2 inactivation results in HSC loss and lymphatic mispatterning. *The Journal of Clinical Investigation,* 122**,** 3705-3717.

Lindsley, R. C., Mar, B. G., Mazzola, E., Grauman, P. V., Shareef, S., Allen, S. L., Pigneux, A., Wetzler, M., Stuart, R. K. & Erba, H. P. 2015. Acute myeloid leukemia ontogeny is defined by distinct somatic mutations. *Blood, The Journal of the American Society of Hematology,* 125**,** 1367-1376.

Ling, K.-W., Ottersbach, K., Van Hamburg, J. P., Oziemlak, A., Tsai, F.-Y., Orkin, S. H., Ploemacher, R., Hendriks, R. W. & Dzierzak, E. 2004. GATA-2 Plays Two Functionally Distinct Roles during the Ontogeny of Hematopoietic Stem Cells. *The Journal of Experimental Medicine,* 200**,** 871-882.

López-Colomé, A. M., Lee-Rivera, I., Benavides-Hidalgo, R. & López, E. 2017. Paxillin: a crossroad in pathological cell migration. *Journal of Hematology & Oncology,* 10**,** 50.

Love, M. I., Huber, W. & Anders, S. 2014. Moderated estimation of fold change and dispersion for RNA-seq data with DESeq2. *Genome Biology,* 15**,** 550.

Luesink, M., Hollink, I. H., Van Der Velden, V. H., Knops, R. H., Boezeman, J. B., De Haas, V., Trka, J., Baruchel, A., Reinhardt, D. & Van Der Reijden, B. A. 2012. High GATA2 expression is a poor prognostic marker in pediatric acute myeloid

leukemia. *Blood, The Journal of the American Society of Hematology,* 120**,** 2064-2075.

Lugus, J. J., Chung, Y. S., Mills, J. C., Kim, S.-I., Grass, J. A., Kyba, M., Doherty, J. M., Bresnick, E. H. & Choi, K. 2007. GATA2 functions at multiple steps in hemangioblast development and differentiation. *Development,* 134**,** 393-405.

Lulli, V., Romania, P., Morsilli, O., Gabbianelli, M., Pagliuca, A., Mazzeo, S., Testa, U., Peschle, C. & Marziali, G. 2006. Overexpression of Ets-1 in human hematopoietic progenitor cells blocks erythroid and promotes megakaryocytic differentiation. *Cell Death & Differentiation,* 13**,** 1064-1074.

Mah, L., El-Osta, A. & Karagiannis, T. 2010. γH2AX: a sensitive molecular marker of DNA damage and repair. *Leukemia,* 24**,** 679-686.

Malumbres, M., Sotillo, R. O., Santamaría, D., Galán, J., Cerezo, A., Ortega, S., Dubus, P. & Barbacid, M. 2004. Mammalian cells cycle without the D-type cyclin-dependent kinases Cdk4 and Cdk6. *Cell,* 118**,** 493-504.

Mannava, S., Grachtchouk, V., Wheeler, L. J., Im, M., Zhuang, D., Slavina, E. G., Mathews, C. K., Shewach, D. S. & Nikiforov, M. A. 2008. Direct role of nucleotide metabolism in C-MYC-dependent proliferation of melanoma cells. *Cell Cycle,* 7**,** 2392-2400.

Manz, M. G., Miyamoto, T., Akashi, K. & Weissman, I. L. 2002. Prospective isolation of human clonogenic common myeloid progenitors. *Proceedings of the National Academy of Sciences,* 99**,** 11872-11877.

Matsumoto, A., Takeishi, S., Kanie, T., Susaki, E., Onoyama, I., Tateishi, Y., Nakayama, K. & Nakayama, K. I. 2011. p57 is required for quiescence and maintenance of adult hematopoietic stem cells. *Cell Stem Cell,* 9**,** 262-271.

Medvinsky, A. & Dzierzak, E. 1996. Definitive hematopoiesis is autonomously initiated by the AGM region. *Cell,* 86**,** 897-906.

Menendez-Gonzalez, J. B., Sinnadurai, S., Gibbs, A., Thomas, L.-A., Konstantinou, M., Garcia-Valverde, A., Boyer, M., Wang, Z., Boyd, A. S., Blair, A. & Rodrigues, N. P. 2019a. Inhibition of GATA2 restrains cell proliferation and enhances apoptosis and chemotherapy mediated apoptosis in human GATA2 overexpressing AML cells. *Scientific Reports,* 9**,** 1-8.

Menendez-Gonzalez, J. B., Vukovic, M., Abdelfattah, A., Saleh, L., Almotiri, A., Thomas, L.-A., Agirre-Lizaso, A., Azevedo, A., Menezes, A. C., Tornillo, G. & Rodrigues, N. P. 2019b. Gata2 as a Crucial Regulator of Stem Cells in Adult Hematopoiesis and Acute Myeloid Leukemia. *Stem Cell Reports,* 13**,** 291-306.

Mercier, F. E., Sykes, D. B. & Scadden, D. T. 2016. Single targeted exon mutation creates a true congenic mouse for competitive hematopoietic stem cell transplantation: The C57BL/6-CD45. 1STEM mouse. *Stem Cell Reports,* 6**,** 985-992.

Merika, M. & Orkin, S. H. 1993. DNA-binding specificity of GATA family transcription factors. *Molecular and Cellular Biology,* 13**,** 3999-4010.

Metzeler, K. H., Herold, T., Rothenberg-Thurley, M., Amler, S., Sauerland, M. C., Görlich, D., Schneider, S., Konstandin, N. P., Dufour, A. & Bräundl, K. 2016. Spectrum and prognostic relevance of driver gene mutations in acute myeloid leukemia. *Blood,* 128**,** 686-698.

Micol, J.-B., Pastore, A., Inoue, D., Duployez, N., Kim, E., Lee, S. C.-W., Durham, B. H., Chung, Y. R., Cho, H. & Zhang, X. J. 2017. ASXL2 is essential for haematopoiesis

and acts as a haploinsufficient tumour suppressor in leukemia. *Nature Communications,* 8**,** 1-13.

Migliaccio, A. R., Rana, R. A., Sanchez, M., Lorenzini, R., Centurione, L., Bianchi, L., Vannucchi, A. M., Migliaccio, G. & Orkin, S. H. 2003. GATA-1 as a regulator of mast cell differentiation revealed by the phenotype of the GATA-1 low mouse mutant. *The Journal of Experimental Medicine,* 197**,** 281-296.

Mikkola, H. K., Klintman, J., Yang, H., Hock, H., Schlaeger, T. M., Fujiwara, Y. & Orkin, S. H. 2003. Haematopoietic stem cells retain long-term repopulating activity and multipotency in the absence of stem-cell leukaemia SCL/tal-1 gene. *Nature,* 421**,** 547-551.

Milne, T., Sinclair, D. & Brock, H. 1999. The Additional sex combs gene of Drosophila is required for activation and repression of homeotic loci, and interacts specifically with Polycomb and super sex combs. *Molecular and General Genetics MGG,* 261**,** 753-761.

Minegishi, N., Ohta, J., Suwabe, N., Nakauchi, H., Ishihara, H., Hayashi, N. & Yamamoto, M. 1998. Alternative promoters regulate transcription of the mouse GATA-2 gene. *Journal of Biological Chemistry,* 273**,** 3625-3634.

Minegishi, N., Suzuki, N., Kawatani, Y., Shimizu, R. & Yamamoto, M. 2005. Rapid turnover of GATA‐2 via ubiquitin‐proteasome protein degradation pathway. *Genes to Cells,* 10**,** 693-704.

Minegishi, N., Suzuki, N., Yokomizo, T., Pan, X., Fujimoto, T., Takahashi, S., Hara, T., Miyajima, A., Nishikawa, S.-I. & Yamamoto, M. 2003. Expression and domain-specific function of GATA-2 during differentiation of the hematopoietic precursor cells in midgestation mouse embryos. *Blood,* 102**,** 896-905.

Miyawaki, K., Arinobu, Y., Iwasaki, H., Kohno, K., Tsuzuki, H., Iino, T., Shima, T., Kikushige, Y., Takenaka, K. & Miyamoto, T. 2015. CD41 marks the initial myelo‐erythroid lineage specification in adult mouse hematopoiesis: Redefinition of murine common myeloid progenitor. *Stem Cells,* 33**,** 976-987.

Moehrle, B. M. & Geiger, H. 2016. Aging of hematopoietic stem cells: DNA damage and mutations? *Experimental Hematology,* 44**,** 895-901.

Mohrin, M., Bourke, E., Alexander, D., Warr, M. R., Barry-Holson, K., Le Beau, M. M., Morrison, C. G. & Passegué, E. 2010. Hematopoietic stem cell quiescence promotes error-prone DNA repair and mutagenesis. *Cell Stem Cell,* 7**,** 174-185.

Molkentin, J. D., Tymitz, K. M., Richardson, J. A. & Olson, E. N. 2000. Abnormalities of the genitourinary tract in female mice lacking GATA5. *Molecular and Cellular Biology,* 20**,** 5256-5260.

Moreno-Layseca, P. & Streuli, C. H. 2014. Signalling pathways linking integrins with cell cycle progression. *Matrix Biology,* 34**,** 144-153.

Morgan, D. O. 1997. Cyclin-dependent kinases: engines, clocks, and microprocessors. *Annual Review of Cell and Developmental Biology,* 13**,** 261-291.

Morita, Y., Ema, H. & Nakauchi, H. 2010. Heterogeneity and hierarchy within the most primitive hematopoietic stem cell compartment. *Journal of Experimental Medicine,* 207**,** 1173-1182.

Morrison, S. J. & Scadden, D. T. 2014. The bone marrow niche for haematopoietic stem cells. *Nature,* 505**,** 327-334.

Morrison, S. J., Wandycz, A. M., Akashi, K., Globerson, A. & Weissman, I. L. 1996. The aging of hematopoietic stem cells. *Nature Medicine,* 2**,** 1011-1016.

Morrison, S. J., Wandycz, A. M., Hemmati, H. D., Wright, D. E. & Weissman, I. L. 1997. Identification of a lineage of multipotent hematopoietic progenitors. *Development,* 124**,** 1929-1939.

Mozziconacci, M. J. & Birnbaum, D. 2011. ASXL1 (additional sex combs like 1 (Drosophila)). *Atlas of Genetics and Cytogenetics in Oncology and Haematology*.

Mrozek, K., Heerema, N. A. & Bloomfield, C. D. 2004. Cytogenetics in acute leukemia. *Blood Reviews,* 18**,** 115-136.

Mufti, G. J. 2004. Pathobiology, classification, and diagnosis of myelodysplastic syndrome. *Best Practice & Research Clinical Haematology,* 17**,** 543-557.

Mufti, G. J., Bennett, J. M., Goasguen, J., Bain, B. J., Baumann, I., Brunning, R., Cazzola, M., Fenaux, P., Germing, U. & Hellström-Lindberg, E. 2008. Diagnosis and classification of myelodysplastic syndrome: International Working Group on Morphology of myelodysplastic syndrome (IWGM-MDS) consensus proposals for the definition and enumeration of myeloblasts and ring sideroblasts. *Haematologica,* 93**,** 1712-1717.

Müller, A. M., Medvinsky, A., Strouboulis, J., Grosveld, F. & Dzierzakt, E. 1994. Development of hematopoietic stem cell activity in the mouse embryo. *Immunity,* 1**,** 291-301.

Mulloy, J. C., Cancelas, J. A., Filippi, M.-D., Kalfa, T. A., Guo, F. & Zheng, Y. 2010. Rho GTPases in hematopoiesis and hemopathies. *Blood, The Journal of the American Society of Hematology,* 115**,** 936-947.

Nagase, R., Inoue, D., Pastore, A., Fujino, T., Hou, H.-A., Yamasaki, N., Goyama, S., Saika, M., Kanai, A. & Sera, Y. 2018. Expression of mutant Asxl1 perturbs hematopoiesis and promotes susceptibility to leukemic transformation. *Journal of Experimental Medicine,* 215**,** 1729-1747.

Nagy, A. 2000. Cre recombinase: the universal reagent for genome tailoring. *Genesis,* 26**,** 99-109.

Nakamura-Ishizu, A., Takizawa, H. & Suda, T. 2014a. The analysis, roles and regulation of quiescence in hematopoietic stem cells. *Development,* 141**,** 4656-4666.

Nakamura-Ishizu, A., Takubo, K., Fujioka, M. & Suda, T. 2014b. Megakaryocytes are essential for HSC quiescence through the production of thrombopoietin. *Biochemical and Biophysical Research Communications,* 454**,** 353-357.

Nandakumar, S. K., Johnson, K., Throm, S. L., Pestina, T. I., Neale, G. & Persons, D. A. 2015. Low-level GATA2 overexpression promotes myeloid progenitor self-renewal and blocks lymphoid differentiation in mice. *Experimental Hematology,* 43**,** 565-577. e10.

Nerlov, C., Querfurth, E., Kulessa, H. & Graf, T. 2000. GATA-1 interacts with the myeloid PU. 1 transcription factor and represses PU. 1-dependent transcription. *Blood, The Journal of the American Society of Hematology,* 95**,** 2543-2551.

Niedernhofer, L. J. 2008. DNA repair is crucial for maintaining hematopoietic stem cell function. *DNA Repair,* 7**,** 523-529.

Notta, F., Doulatov, S., Laurenti, E., Poeppl, A., Jurisica, I. & Dick, J. E. 2011. Isolation of single human hematopoietic stem cells capable of long-term multilineage engraftment. *Science,* 333**,** 218-221.

Notta, F., Zandi, S., Takayama, N., Dobson, S., Gan, O. I., Wilson, G., Kaufmann, K. B., Mcleod, J., Laurenti, E. & Dunant, C. F. 2016. Distinct routes of lineage development reshape the human blood hierarchy across ontogeny. *Science,* 351**,** aab2116.

Novakova, M., Žaliová, M., Sukova, M., Wlodarski, M., Janda, A., Froňková, E., Campr, V., Lejhancová, K., Zapletal, O. & Pospíšilová, D. 2016. Loss of B cells and their precursors is the most constant feature of GATA-2 deficiency in childhood myelodysplastic syndrome. *Haematologica,* 101**,** 707-716.

Nygren, J. M., Bryder, D. & Jacobsen, S. E. W. 2006. Prolonged cell cycle transit is a defining and developmentally conserved hemopoietic stem cell property. *The Journal of Immunology,* 177**,** 201-208.

Oguro, H., Ding, L. & Morrison, S. J. 2013. SLAM family markers resolve functionally distinct subpopulations of hematopoietic stem cells and multipotent progenitors. *Cell Stem Cell,* 13**,** 102-116.

Okada, S., Nakauchi, H., Nagayoshi, K., Nishikawa, S.-L., Miura, Y. & Suda, T. 1992. In vivo and in vitro stem cell function of c-kit-and Sca-1-positive murine hematopoietic cells. *Blood,* 80, 3044-3050.

Onodera, K., Fujiwara, T., Onishi, Y., Itoh-Nakadai, A., Okitsu, Y., Fukuhara, N., Ishizawa, K., Shimizu, R., Yamamoto, M. & Harigae, H. 2016. GATA2 regulates dendritic cell differentiation. *Blood, The Journal of the American Society of Hematology,* 128**,** 508-518.

Orkin, S. H. 2000. Diversification of haematopoietic stem cells to specific lineages. *Nature Reviews Genetics,* 1**,** 57-64.

Orkin, S. H. & Zon, L. I. 2008. Hematopoiesis: an evolving paradigm for stem cell biology. *Cell,* 132**,** 631-644.

Orlic, D., Anderson, S., Biesecker, L. G., Sorrentino, B. P. & Bodine, D. M. 1995. Pluripotent hematopoietic stem cells contain high levels of mRNA for c-kit, GATA-2, p45 NF-E2, and c-myb and low levels or no mRNA for c-fms and the receptors for granulocyte colony-stimulating factor and interleukins 5 and 7. *Proceedings of the National Academy of Sciences,* 92**,** 4601-4605.

Ostergaard, P., Simpson, M. A., Connell, F. C., Steward, C. G., Brice, G., Woollard, W. J., Dafou, D., Kilo, T., Smithson, S. & Lunt, P. 2011. Mutations in GATA2 cause primary lymphedema associated with a predisposition to acute myeloid leukemia (Emberger syndrome). *Nature Genetics,* 43**,** 929.

Owen, C., Barnett, M. & Fitzgibbon, J. 2008. Familial myelodysplasia and acute myeloid leukaemia–a review. *British Journal of Haematology,* 140**,** 123-132.

Palis, J., Robertson, S., Kennedy, M., Wall, C. & Keller, G. 1999. Development of erythroid and myeloid progenitors in the yolk sac and embryo proper of the mouse. *Development,* 126**,** 5073-5084.

Pandolfi, P. P., Roth, M. E., Karis, A., Leonard, M. W., Dzierzak, E., Grosveld, F. G., Engel, J. D. & Lindenbaum, M. H. 1995. Targeted disruption of the GATA3 gene causes severe abnormalities in the nervous system and in fetal liver haematopoiesis. *Nature Genetics,* 11**,** 40-44.

Papa, L., Djedaini, M. & Hoffman, R. 2019. Mitochondrial role in stemness and differentiation of hematopoietic stem cells. *Stem Cells International,* 4067162.

Pardee, A. B. 1974. A restriction point for control of normal animal cell proliferation. *Proceedings of the National Academy of Sciences,* 71**,** 1286-1290.

Park, I.-K., Qian, D., Kiel, M., Becker, M. W., Pihalja, M., Weissman, I. L., Morrison, S. J. & Clarke, M. F. 2003. Bmi-1 is required for maintenance of adult self-renewing haematopoietic stem cells. *Nature,* 423**,** 302-305.

Park, U.-H., Yoon, S. K., Park, T., Kim, E. J. & Um, S.-J. 2011. Additional sex comb-like (ASXL) proteins 1 and 2 play opposite roles in adipogenesis via reciprocal regulation of peroxisome proliferator-activated receptor γ. *Journal of Biological Chemistry,* 286**,** 1354-1363.

Parmar, K., Mauch, P., Vergilio, J. A., Sackstein, R. & Down, J. D. 2007. Distribution of hematopoietic stem cells in the bone marrow according to regional hypoxia. *Proceedings of the National Academy of Sciences,* 104**,** 5431-5436.

Paschka, P., Schlenk, R. F., Gaidzik, V. I., Herzig, J. K., Aulitzky, T., Bullinger, L., Späth, D., Teleanu, V., Kündgen, A. & Köhne, C.-H. 2015. ASXL1 mutations in younger adult patients with acute myeloid leukemia: a study by the German-Austrian Acute Myeloid Leukemia Study Group. *Haematologica,* 100**,** 324-330.

Pasquet, M., Bellanné-Chantelot, C., Tavitian, S., Prade, N., Beaupain, B., Larochelle, O., Petit, A., Rohrlich, P., Ferrand, C. & Van Den Neste, E. 2013. High frequency of GATA2 mutations in patients with mild chronic neutropenia evolving to MonoMac syndrome, myelodysplasia, and acute myeloid leukemia. *Blood,* 121**,** 822-829.

Patel, J. P., Gönen, M., Figueroa, M. E., Fernandez, H., Sun, Z., Racevskis, J., Van Vlierberghe, P., Dolgalev, I., Thomas, S. & Aminova, O. 2012. Prognostic relevance of integrated genetic profiling in acute myeloid leukemia. *New England Journal of Medicine,* 366**,** 1079-1089.

Pathania, S., Jayaram, M. & Voziyanov, Y. 1999. A general model for site-specific recombination by the integrase family recombinases. *Nucleic Acids Research,* 27**,** 930-941.

Pearce, D. J., Anjos-Afonso, F., Ridler, C. M., Eddaoudi, A. & Bonnet, D. 2007. Age-dependent increase in side population distribution within hematopoiesis: implications for our understanding of the mechanism of aging. *Stem Cells,* 25**,** 828-835.

Persons, D. A., Allay, J. A., Allay, E. R., Ashmun, R. A., Orlic, D., Jane, S. M., Cunningham, J. M. & Nienhuis, A. W. 1999. Enforced expression of the GATA-2 transcription factor blocks normal hematopoiesis. *Blood, The Journal of the American Society of Hematology,* 93**,** 488-499.

Pietras, E. M., Reynaud, D., Kang, Y.-A., Carlin, D., Calero-Nieto, F. J., Leavitt, A. D., Stuart, J. M., Göttgens, B. & Passegué, E. 2015. Functionally distinct subsets of lineage-biased multipotent progenitors control blood production in normal and regenerative conditions. *Cell Stem Cell,* 17**,** 35-46.

Pietras, E. M., Warr, M. R. & Passegué, E. 2011. Cell cycle regulation in hematopoietic stem cells. *Journal of Cell Biology,* 195**,** 709-720.

Pimanda, J. E., Ottersbach, K., Knezevic, K., Kinston, S., Chan, W. Y., Wilson, N. K., Landry, J.-R., Wood, A. D., Kolb-Kokocinski, A. & Green, A. R. 2007. Gata2, Fli1,

and Scl form a recursively wired gene-regulatory circuit during early hematopoietic development. *Proceedings of the National Academy of Sciences,* 104**,** 17692-17697.

Pronk, C. J., Rossi, D. J., Månsson, R., Attema, J. L., Norddahl, G. L., Chan, C. K. F., Sigvardsson, M., Weissman, I. L. & Bryder, D. 2007. Elucidation of the phenotypic, functional, and molecular topography of a myeloerythroid progenitor cell hierarchy. *Cell Stem Cell,* 1**,** 428-442.

Pui, J. C., Allman, D., Xu, L., Derocco, S., Karnell, F. G., Bakkour, S., Lee, J. Y., Kadesch, T., Hardy, R. R. & Aster, J. C. 1999. Notch1 expression in early lymphopoiesis influences B versus T lineage determination. *Immunity,* 11**,** 299-308.

Raaijmakers, M. 2007. ATP-binding-cassette transporters in hematopoietic stem cells and their utility as therapeutical targets in acute and chronic myeloid leukemia. *Leukemia,* 21**,** 2094-2102.

Radomska, H. S., Huettner, C. S., Zhang, P., Cheng, T., Scadden, D. T. & Tenen, D. G. 1998. CCAAT/enhancer binding protein α is a regulatory switch sufficient for induction of granulocytic development from bipotential myeloid progenitors. *Molecular and Cellular Biology,* 18**,** 4301-4314.

Randall, T. D., Lund, F. E., Howard, M. C. & Weissman, I. L. 1996. Expression of murine CD38 defines a population of long-term reconstituting hematopoietic stem cells. *Blood,* 87, 4057-4067.

Ren, B., Cam, H., Takahashi, Y., Volkert, T., Terragni, J., Young, R. A. & Dynlacht, B. D. 2002. E2F integrates cell cycle progression with DNA repair, replication, and G2/M checkpoints. *Genes & Development,* 16**,** 245-256.

Rieger, M. A. & Schroeder, T. 2012. Hematopoiesis. *Cold Spring Harbor Perspectives in Biology,* 4**,** a008250.

Robb, L., Lyons, I., Li, R., Hartley, L., Köntgen, F., Harvey, R. P., Metcalf, D. & Begley, C. G. 1995. Absence of yolk sac hematopoiesis from mice with a targeted disruption of the scl gene. *Proceedings of the National Academy of Sciences,* 92**,** 7075-7079.

Robert-Moreno, À., Espinosa, L., De La Pompa, J. L. & Bigas, A. 2005. RBPjκ-dependent Notch function regulates Gata2 and is essential for the formation of intra-embryonic hematopoietic cells. *Development,* 132**,** 1117-1126.

Rodak, B. F., Keohane, E. M. & Fritsma, G. A. 2013. *Hematology-E-Book: Clinical Principles and Applications*, Elsevier Health Sciences.

Rodrigues, N. P., Boyd, A. S., Fugazza, C., May, G. E., Guo, Y., Tipping, A. J., Scadden, D. T., Vyas, P. & Enver, T. 2008. GATA-2 regulates granulocyte-macrophage progenitor cell function. *Blood, The Journal of the American Society of Hematology,* 112**,** 4862-4873.

Rodrigues, N. P., Janzen, V., Forkert, R., Dombkowski, D. M., Boyd, A. S., Orkin, S. H., Enver, T., Vyas, P. & Scadden, D. T. 2005. Haploinsufficiency of GATA-2 perturbs adult hematopoietic stem-cell homeostasis. *Blood,* 106**,** 477-484.

Rodrigues, N. P., Tipping, A. J., Wang, Z. & Enver, T. 2012. GATA-2 mediated regulation of normal hematopoietic stem/progenitor cell function, myelodysplasia and myeloid leukemia. *The International Journal of Biochemistry & Cell Biology,* 44**,** 457-460.

Rodriguez-Fraticelli, A. E., Wolock, S. L., Weinreb, C. S., Panero, R., Patel, S. H., Jankovic, M., Sun, J., Calogero, R. A., Klein, A. M. & Camargo, F. D. 2018. Clonal analysis of lineage fate in native haematopoiesis. *Nature,* 553**,** 212-216.

Rossi, D. J., Bryder, D., Seita, J., Nussenzweig, A., Hoeijmakers, J. & Weissman, I. L. 2007. Deficiencies in DNA damage repair limit the function of haematopoietic stem cells with age. *Nature,* 447**,** 725-729.

Rossi, D. J., Bryder, D., Zahn, J. M., Ahlenius, H., Sonu, R., Wagers, A. J. & Weissman, I. L. 2005. Cell intrinsic alterations underlie hematopoietic stem cell aging. *Proceedings of the National Academy of Sciences,* 102**,** 9194-9199.

Saida, S., Zhen, T., Kim, E., Yu, K., Lopez, G., Mcreynolds, L. J. & Liu, P. P. 2020. Gata2 deficiency delays leukemogenesis while contributing to aggressive leukemia phenotype in Cbfb-MYH11 knockin mice. *Leukemia,* 34**,** 759-770.

Sanjuan-Pla, A., Macaulay, I. C., Jensen, C. T., Woll, P. S., Luis, T. C., Mead, A., Moore, S., Carella, C., Matsuoka, S. & Jones, T. B. 2013. Platelet-biased stem cells reside at the apex of the haematopoietic stem-cell hierarchy. *Nature,* 502**,** 232-236.

Sarosiek, K. A., Fraser, C., Muthalagu, N., Bhola, P. D., Chang, W., Mcbrayer, S. K., Cantlon, A., Fisch, S., Golomb-Mello, G. & Ryan, J. A. 2017. Developmental regulation of mitochondrial apoptosis by c-Myc governs age-and tissue-specific sensitivity to cancer therapeutics. *Cancer Cell,* 31**,** 142-156.

Schlaeger, T. M., Mikkola, H. K., Gekas, C., Helgadottir, H. B. & Orkin, S. H. 2005. Tie2Cre-mediated gene ablation defines the stem-cell leukemia gene (SCL/tal1)–dependent window during hematopoietic stem-cell development. *Blood,* 105**,** 3871-3874.

Schmittgen, T. D. & Livak, K. J. 2008. Analyzing real-time PCR data by the comparative C T method. *Nature Protocols,* 3**,** 1101.

Schmohl, J. U., Nuebling, T., Wild, J., Jung, J., Kroell, T., Kanz, L., Salih, H. R. & Schmetzer, H. 2015. Death receptor expression on blasts in AML is associated with unfavorable prognosis. *Anticancer Research,* 35**,** 4043-4052.

Schuettengruber, B., Bourbon, H.-M., Di Croce, L. & Cavalli, G. 2017. Genome regulation by polycomb and trithorax: 70 years and counting. *Cell,* 171**,** 34-57.

Schuettpelz, L. & Link, D. 2013. Regulation of hematopoietic stem cell activity by inflammation. *Frontiers in Immunology,* 4**,** 204.

Seita, J. & Weissman, I. L. 2010. Hematopoietic stem cell: self‐renewal versus differentiation. *Wiley Interdisciplinary Reviews: Systems Biology and Medicine,* 2**,** 640-653.

Shi, H., Yamamoto, S., Sheng, M., Bai, J., Zhang, P., Chen, R., Chen, S., Shi, L., Abdel-Wahab, O. & Xu, M. 2016. ASXL1 plays an important role in erythropoiesis. *Scientific Reports,* 6**,** 28789.

Shimshek, D. R., Kim, J., Hübner, M. R., Spergel, D. J., Buchholz, F., Casanova, E., Stewart, A. F., Seeburg, P. H. & Sprengel, R. 2002. Codon‐improved Cre recombinase (iCre) expression in the mouse. *Genesis,* 32**,** 19-26.

Signer, R. A., Montecino-Rodriguez, E., Witte, O. N., Mclaughlin, J. & Dorshkind, K. 2007. Age-related defects in B lymphopoiesis underlie the myeloid dominance of adult leukemia. *Blood, The Journal of the American Society of Hematology,* 110**,** 1831-1839.

Siminovitch, L., Mcculloch, E. A. & Till, J. E. 1963. The distribution of colony‐forming cells among spleen colonies. *Journal of Cellular and Comparative Physiology,* 62**,** 327-336.

Smith, J. N., Kanwar, V. S. & Macnamara, K. C. 2016. Hematopoietic stem cell regulation by type I and II interferons in the pathogenesis of acquired aplastic anemia. *Frontiers in Immunology,* 7**,** 330.

Song, W.-J., Sullivan, M. G., Legare, R. D., Hutchings, S., Tan, X., Kufrin, D., Ratajczak, J., Resende, I. C., Haworth, C. & Hock, R. 1999. Haploinsufficiency of CBFA2 causes familial thrombocytopenia with propensity to develop acute myelogenous leukaemia. *Nature Genetics,* 23**,** 166-175.

Spangrude, G. J., Heimfeld, S. & Weissman, I. L. 1988. Purification and characterization of mouse hematopoietic stem cells. *Science,* 241**,** 58-62.

Sperling, A. S., Gibson, C. J. & Ebert, B. L. 2017. The genetics of myelodysplastic syndrome: from clonal haematopoiesis to secondary leukaemia. *Nature Reviews Cancer,* 17**,** 5.

Spyropoulos, D. D., Pharr, P. N., Lavenburg, K. R., Jackers, P., Papas, T. S., Ogawa, M. & Watson, D. K. 2000. Hemorrhage, Impaired Hematopoiesis, and Lethality in Mouse Embryos Carrying a Targeted Disruption of the Fli1Transcription Factor. *Molecular and Cellular Biology,* 20**,** 5643-5652.

Stadtfeld, M. & Graf, T. 2005. Assessing the role of hematopoietic plasticity for endothelial and hepatocyte development by non-invasive lineage tracing. *Development,* 132**,** 203-213.

Subramanian, A., Tamayo, P., Mootha, V. K., Mukherjee, S., Ebert, B. L., Gillette, M. A., Paulovich, A., Pomeroy, S. L., Golub, T. R. & Lander, E. S. 2005. Gene set enrichment analysis: a knowledge-based approach for interpreting genome-wide expression profiles. *Proceedings of the National Academy of Sciences,* 102**,** 15545-15550.

Sugiyama, T., Kohara, H., Noda, M. & Nagasawa, T. 2006. Maintenance of the hematopoietic stem cell pool by CXCL12-CXCR4 chemokine signaling in bone marrow stromal cell niches. *Immunity,* 25**,** 977-988.

Sumide, K., Matsuoka, Y., Kawamura, H., Nakatsuka, R., Fujioka, T., Asano, H., Takihara, Y. & Sonoda, Y. 2018. A revised road map for the commitment of human cord blood CD34-negative hematopoietic stem cells. *Nature Communications,* 9**,** 1-17.

Sun, J., Ramos, A., Chapman, B., Johnnidis, J. B., Le, L., Ho, Y.-J., Klein, A., Hofmann, O. & Camargo, F. D. 2014. Clonal dynamics of native haematopoiesis. *Nature,* 514**,** 322-327.

Takahashi, S., Komeno, T., Suwabe, N., Yoh, K., Nakajima, O., Nishimura, S., Kuroha, T., Nagasawa, T. & Yamamoto, M. 1998. Role of GATA-1 in proliferation and differentiation of definitive erythroid and megakaryocytic cells in vivo. *Blood, The Journal of the American Society of Hematology,* 92**,** 434-442.

Taylor, W. R. & Stark, G. R. 2001. Regulation of the G2/M transition by p53. *Oncogene,* 20**,** 1803-1815.

Tie, R., Li, H., Cai, S., Liang, Z., Shan, W., Wang, B., Tan, Y., Zheng, W. & Huang, H. 2019. Interleukin-6 signaling regulates hematopoietic stem cell emergence. *Experimental & Molecular Medicine,* 51**,** 1-12.

Till, J. E. & Mcculloch, E. A. 1961. A direct measurement of the radiation sensitivity of normal mouse bone marrow cells. *Radiation Research,* 14**,** 213-222.

Ting, C.-N., Olson, M. C., Barton, K. P. & Leiden, J. M. 1996. Transcription factor GATA-3 is required for development of the T-cell lineage. *Nature,* 384**,** 474-478.

Tipping, A. J., Pina, C., Castor, A., Hong, D., Rodrigues, N. P., Lazzari, L., May, G. E., Jacobsen, S. E. W. & Enver, T. 2009. High GATA-2 expression inhibits human hematopoietic stem and progenitor cell function by effects on cell cycle. *Blood, The Journal of the American Society of Hematology,* 113**,** 2661-2672.

Tong, Q., Dalgin, G., Xu, H., Ting, C.-N., Leiden, J. M. & Hotamisligil, G. S. 2000. Function of GATA transcription factors in preadipocyte-adipocyte transition. *Science,* 290**,** 134-138.

Tong, Q., Tsai, J., Tan, G., Dalgin, G. & Hotamisligil, G. S. 2005. Interaction between GATA and the C/EBP family of transcription factors is critical in GATA-mediated suppression of adipocyte differentiation. *Molecular and Cellular Biology,* 25**,** 706-715.

Towatari, M., May, G. E., Marais, R., Perkins, G. R., Marshall, C. J., Cowley, S. & Enver, T. 1995. Regulation of GATA-2 phosphorylation by mitogen-activated protein kinase and interleukin-3. *Journal of Biological Chemistry,* 270**,** 4101-4107.

Trainor, C. D., Ghirlando, R. & Simpson, M. A. 2000. GATA zinc finger interactions modulate DNA binding and transactivation. *Journal of Biological Chemistry,* 275**,** 28157-28166.

Tsai, F.-Y., Keller, G., Kuo, F. C., Weiss, M., Chen, J., Rosenblatt, M., Alt, F. W. & Orkin, S. H. 1994. An early haematopoietic defect in mice lacking the transcription factor GATA-2. *Nature,* 371**,** 221-226.

Tsai, F.-Y. & Orkin, S. H. 1997. Transcription factor GATA-2 is required for proliferation/survival of early hematopoietic cells and mast cell formation, but not for erythroid and myeloid terminal differentiation. *Blood, The Journal of the American Society of Hematology,* 89**,** 3636-3643.

Tsai, S.-F., Martin, D. I., Zon, L. I., D'andrea, A. D., Wong, G. G. & Orkin, S. H. 1989. Cloning of cDNA for the major DNA-binding protein of the erythroid lineage through expression in mammalian cells. *Nature,* 339**,** 446-451.

Tsang, A. P., Visvader, J. E., Turner, C. A., Fujiwara, Y., Yu, C., Weiss, M. J., Crossley, M. & Orkin, S. H. 1997. FOG, a multitype zinc finger protein, acts as a cofactor for transcription factor GATA-1 in erythroid and megakaryocytic differentiation. *Cell,* 90**,** 109-119.

Velasco-Hernandez, T., Säwén, P., Bryder, D. & Cammenga, J. 2016. Potential pitfalls of the Mx1-Cre system: implications for experimental modeling of normal and malignant hematopoiesis. *Stem Cell Reports,* 7**,** 11-18.

Viatour, P., Somervaille, T. C., Venkatasubrahmanyam, S., Kogan, S., Mclaughlin, M. E., Weissman, I. L., Butte, A. J., Passegué, E. & Sage, J. 2008. Hematopoietic stem cell quiescence is maintained by compound contributions of the retinoblastoma gene family. *Cell Stem Cell,* 3**,** 416-428.

Vicente, C., Conchillo, A., García-Sánchez, M. A. & Odero, M. D. 2012a. The role of the GATA2 transcription factor in normal and malignant hematopoiesis. *Critical Reviews in Oncology/Hematology,* 82**,** 1-17.

Vicente, C., Vazquez, I., Conchillo, A., Garcia-Sanchez, M., Marcotegui, N., Fuster, O., Gonzalez, M., Calasanz, M., Lahortiga, I. & Odero, M. 2012b. Overexpression

of GATA2 predicts an adverse prognosis for patients with acute myeloid leukemia and it is associated with distinct molecular abnormalities. *Leukemia,* 26**,** 550-554.

Vinh, D. C., Patel, S. Y., Uzel, G., Anderson, V. L., Freeman, A. F., Olivier, K. N., Spalding, C., Hughes, S., Pittaluga, S. & Raffeld, M. 2010. Autosomal dominant and sporadic monocytopenia with susceptibility to mycobacteria, fungi, papillomaviruses, and myelodysplasia. *Blood,* 115**,** 1519-1529.

Wadman, I. A., Osada, H., Grütz, G. G., Agulnick, A. D., Westphal, H., Forster, A. & Rabbitts, T. H. 1997. The LIM‐only protein Lmo2 is a bridging molecule assembling an erythroid, DNA‐binding complex which includes the TAL1, E47, GATA‐1 and Ldb1/NLI proteins. *The EMBO Journal,* 16**,** 3145-3157.

Wallberg, F., Tenev, T. & Meier, P. 2016. Analysis of apoptosis and necroptosis by fluorescence-activated cell sorting. *Cold Spring Harbor Protocols,* pdb. prot087387.

Walsh, J. C., Dekoter, R. P., Lee, H.-J., Smith, E. D., Lancki, D. W., Gurish, M. F., Friend, D. S., Stevens, R. L., Anastasi, J. & Singh, H. 2002. Cooperative and antagonistic interplay between PU. 1 and GATA-2 in the specification of myeloid cell fates. *Immunity,* 17**,** 665-676.

Wang, J., Li, Z., He, Y., Pan, F., Chen, S., Rhodes, S., Nguyen, L., Yuan, J., Jiang, L. & Yang, X. 2014. Loss of Asxl1 leads to myelodysplastic syndrome–like disease in mice. *Blood, The Journal of the American Society of Hematology,* 123**,** 541-553.

Warren, A. J., Colledge, W. H., Carlton, M. B., Evans, M. J., Smith, A. J. & Rabbitts, T. H. 1994. The oncogenic cysteine-rich LIM domain protein rbtn2 is essential for erythroid development. *Cell,* 78**,** 45-57.

West, R. R., Hsu, A. P., Holland, S. M., Cuellar-Rodriguez, J. & Hickstein, D. D. 2014. Acquired ASXL1 mutations are common in patients with inherited GATA2 mutations and correlate with myeloid transformation. *Haematologica,* 99**,** 276-281.

Will, C. L. & Lührmann, R. 2011. Spliceosome structure and function. *Cold Spring Harbor Perspectives in Biology,* 3**,** a003707.

Wilson, A., Murphy, M. J., Oskarsson, T., Kaloulis, K., Bettess, M. D., Oser, G. M., Pasche, A.-C., Knabenhans, C., Macdonald, H. R. & Trumpp, A. 2004. c-Myc controls the balance between hematopoietic stem cell self-renewal and differentiation. *Genes & Development,* 18**,** 2747-2763.

Wilson, N. K., Foster, S. D., Wang, X., Knezevic, K., Schütte, J., Kaimakis, P., Chilarska, P. M., Kinston, S., Ouwehand, W. H. & Dzierzak, E. 2010. Combinatorial transcriptional control in blood stem/progenitor cells: genome-wide analysis of ten major transcriptional regulators. *Cell Stem Cell,* 7**,** 532-544.

Wlodarski, M. W., Collin, M. & Horwitz, M. S. 2017. GATA2 deficiency and related myeloid neoplasms. Seminars in Hematology, 81-86.

Wong, K. K., Lawrie, C. H. & Green, T. M. 2019. Oncogenic roles and inhibitors of DNMT1, DNMT3A, and DNMT3B in acute myeloid leukaemia. *Biomarker Insights,* 14**,** 1177271919846454.

Wright, D. E., Bowman, E. P., Wagers, A. J., Butcher, E. C. & Weissman, I. L. 2002. Hematopoietic stem cells are uniquely selective in their migratory response to chemokines. *The Journal of Experimental Medicine,* 195**,** 1145-1154.

Wu, A. M., Till, J. E., Siminovitch, L. & Mcculloch, E. A. 1968. Cytological evidence for a relationship between normal hematopoietic colony-forming cells and cells of the lymphoid system. *The Journal of Experimental Medicine,* 127**,** 455-464.

Wu, Z., Gao, S., Diamond, C., Kajigaya, S., Chen, J., Shi, R., Palmer, C., Hsu, A. P., Calvo, K. R. & Hickstein, D. D. 2020. Sequencing of RNA in single cells reveals a distinct transcriptome signature of hematopoiesis in GATA2 deficiency. *Blood Advances,* 4**,** 2702-2716.

Xu, Y., Takahashi, Y., Wang, Y., Hama, A., Nishio, N., Muramatsu, H., Tanaka, M., Yoshida, N., Villalobos, I. B. & Yagasaki, H. 2009. Downregulation of GATA-2 and overexpression of adipogenic gene-PPARγ in mesenchymal stem cells from patients with aplastic anemia. *Experimental Hematology,* 37**,** 1393-1399.

Yamamoto, R., Morita, Y., Ooehara, J., Hamanaka, S., Onodera, M., Rudolph, K. L., Ema, H. & Nakauchi, H. 2013. Clonal analysis unveils self-renewing lineage-restricted progenitors generated directly from hematopoietic stem cells. *Cell,* 154**,** 1112-1126.

Yamazaki, H., Suzuki, M., Otsuki, A., Shimizu, R., Bresnick, E. H., Engel, J. D. & Yamamoto, M. 2014. A remote GATA2 hematopoietic enhancer drives leukemogenesis in inv (3)(q21; q26) by activating EVI1 expression. *Cancer Cell,* 25**,** 415-427.

Yang, G., Xu, Y., Chen, X. & Hu, G. 2007. IFITM1 plays an essential role in the antiproliferative action of interferon-γ. *Oncogene,* 26**,** 594-603.

Yang, L., Dybedal, I., Bryder, D., Nilsson, L., Sitnicka, E., Sasaki, Y. & Jacobsen, S. E. W. 2005. IFN-γ negatively modulates self-renewal of repopulating human hemopoietic stem cells. *The Journal of Immunology,* 174**,** 752-757.

Yang, L., Sun, H., Cao, Y., Xuan, B., Fan, Y., Sheng, H. & Zhuang, W. 2017. GATA2 Inhibition Sensitizes Acute Myeloid Leukemia Cells to Chemotherapy. *PloS One,* 12**,** e0170630.

Ye, M., Zhang, H., Amabile, G., Yang, H., Staber, P. B., Zhang, P., Levantini, E., Alberich-Jordà, M., Zhang, J. & Kawasaki, A. 2013. C/EBPa controls acquisition and maintenance of adult haematopoietic stem cell quiescence. *Nature Cell Biology,* 15**,** 385-394.

Yoshida, T., Ng, S. Y.-M., Zuniga-Pflucker, J. C. & Georgopoulos, K. 2006. Early hematopoietic lineage restrictions directed by Ikaros. *Nature Immunology,* 7**,** 382-391.

Yoshimi, A., Goyama, S., Watanabe-Okochi, N., Yoshiki, Y., Nannya, Y., Nitta, E., Arai, S., Sato, T., Shimabe, M. & Nakagawa, M. 2011. Evi1 represses PTEN expression and activates PI3K/AKT/mTOR via interactions with polycomb proteins. *Blood, The Journal of the American Society of Hematology,* 117**,** 3617-3628.

Yuan, Y., Shen, H., Franklin, D. S., Scadden, D. T. & Cheng, T. 2004. In vivo self-renewing divisions of haematopoietic stem cells are increased in the absence of the early G1-phase inhibitor, p18 INK4C. *Nature Cell Biology,* 6**,** 436-442.

Yuasa, H., Oike, Y., Iwama, A., Nishikata, I., Sugiyama, D., Perkins, A., Mucenski, M. L., Suda, T. & Morishita, K. 2005. Oncogenic transcription factor Evi1 regulates hematopoietic stem cell proliferation through GATA‐2 expression. *The EMBO Journal,* 24**,** 1976-1987.

Yuniati, L., Scheijen, B., Van Der Meer, L. T. & Van Leeuwen, F. N. 2019. Tumor suppressors BTG1 and BTG2: Beyond growth control. *Journal of Cellular Physiology,* 234**,** 5379-5389.

Zhang, P., Behre, G., Pan, J., Iwama, A., Wara-Aswapati, N., Radomska, H. S., Auron, P. E., Tenen, D. G. & Sun, Z. 1999. Negative cross-talk between hematopoietic regulators: GATA proteins repress PU. 1. *Proceedings of the National Academy of Sciences,* 96**,** 8705-8710.

Zhang, P., He, F., Bai, J., Yamamoto, S., Chen, S., Zhang, L., Sheng, M., Zhang, L., Guo, Y. & Man, N. 2018. Chromatin regulator Asxl1 loss and Nf1 haploinsufficiency cooperate to accelerate myeloid malignancy. *The Journal of Clinical Investigation,* 128**,** 5383-5398.

Zhang, P., Iwasaki-Arai, J., Iwasaki, H., Fenyus, M. L., Dayaram, T., Owens, B. M., Shigematsu, H., Levantini, E., Huettner, C. S. & Lekstrom-Himes, J. A. 2004. Enhancement of hematopoietic stem cell repopulating capacity and self-renewal in the absence of the transcription factor C/EBPα. *Immunity,* 21**,** 853-863.

Zhang, P., Zhang, C., Li, J., Han, J., Liu, X. & Yang, H. 2019. The physical microenvironment of hematopoietic stem cells and its emerging roles in engineering applications. *Stem Cell Research & Therapy,* 10**,** 1-13.

Zhang, S.-J., Ma, L. Y., Huang, Q.-H., Li, G., Gu, B.-W., Gao, X.-D., Shi, J.-Y., Wang, Y.-Y., Gao, L. & Cai, X. 2008. Gain-of-function mutation of GATA-2 in acute myeloid transformation of chronic myeloid leukemia. *Proceedings of the National Academy of Sciences,* 105**,** 2076-2081.

Zhao, M., Perry, J. M., Marshall, H., Venkatraman, A., Qian, P., He, X. C., Ahamed, J. & Li, L. 2014. Megakaryocytes maintain homeostatic quiescence and promote post-injury regeneration of hematopoietic stem cells. *Nature Medicine,* 20**,** 1321.

Zoumbos, N. C., Gascon, P., Djeu, J. Y. & Young, N. S. 1985. Interferon is a mediator of hematopoietic suppression in aplastic anemia in vitro and possibly in vivo. *Proceedings of the National Academy of Sciences,* 82**,** 188-192.